Journal of Structural Chemistry
Vol. 2 No. 3

JOURNAL OF STRUCTURAL
CHEMISTRY
VOLUME 2 NUMBER 3 1961

ANALYSIS OF THE PRECISION OF ELECTRON-DIFFRACTION DETERMINATION OF THE STRUCTURAL PARAMETERS OF MOLECULES IN THE GAS PHASE

N. G. Rambidi and P. A. Akishin

M. V. Lomonosov Moscow State University
Translated from Zhurnal Strukturnoi Khimii, Vol. 2, No. 3, pp. 251-259, May-June, 1961
Original article submitted May 6, 1960

The precision of determination of the geometric parameters of molecules in the gas phase by the consecutive approximation and radial-distribution methods is examined. Formulas are derived for estimation of random errors in the parameters of a given molecule.

Developments of experimental techniques and theoretical principles of gas-phase electron diffraction have extended its potentialities in recent years and have given rise to objective methods [1-4] whereby precise data on the geometric parameters of complex molecules can be obtained and internal rotation and oscillations in such molecules can be studied. Workers engaged on these problems [3-4] devoted considerable attention to estimates of the accuracy of modern variants of the electron-diffraction method. Nevertheless, the literature lacks generally accepted formulas for objective calculation of errors in determinations of a required structural parameter in every concrete instance.

As the number of electron-diffraction patterns examined in the course of structure investigation is usually small, it is impossible to perform a reliable statistical anlysis and to find an objective characteristic of the experimental precision (for example, the mean value of the experimental distribution of electron scattering intensity and its standard deviation). Therefore for estimation of errors in structure determinations it is desirable to derive equations which correlate the precision of values measured by direct experiment, which can be examined statistically (stability of the diffraction camera feed circuit, distance between the evaporator nozzle and the plate, etc.), with the precision of experimental determinations of intensity distribution and the geometric parameters of the molecule in question.

Preliminary Comments

We start with the expression for the molecular component of electron scattering intensity

$$M_r(s) = \frac{1}{\sum_i z_i^2 + z_i} \sum_{ij} z_i z_j \exp(-l_{ij}^2 s^2/2) \frac{\sin s r_{ij}}{s r_{ij}}, \quad (1)$$

where

$$s = \frac{4\pi}{\lambda} \sin \frac{\Phi}{2},$$

Φ is the scattering angle, λ is the electron wavelength, z_i, z_j are the nuclear charges of the i-th and j-th atoms, at distance r_{ij} apart; l_{ij} is the projection of the root mean square vibration amplitude of the nuclei of the i-th and j-th atoms on the line connecting them.

We assume that, in accordance with [1], corrections for electron scattering at the electron shells of the atom are introduced into the experimental distribution of scattering intensity. As the radial-distribution function we use

$$f(r) = \int_0^{s_{max}} s M_e(s) \exp(-as^2) \sin sr \, ds, \quad (2)$$

where the constant in the modifying function g is chosen so as to smooth out as much as possible the termination wave of the experimental intensity distribution at $s = s_{max}$. We denote the absolute and relative error of the parameter x by Δx and δx respectively, and the relative value of the standard deviation by $\sigma(x)$*

The sources of error in determination of geometric parameters of molecules can be divided into three main groups [5]: 1) errors introduced by the equipment (instrumental errors) and imperfections of experimental technique (experimental error); 2) errors associated with the approximate character of the calculation or with lack of correspondence between the calculation and the diffraction pattern (calculation error); and 3) inadequacy of the theoretical approximation used (theoretical error).

In this communication we consider errors in determination of the structural parameters of a molecule caused by experimental errors. We assume that all the variety of experimental errors gives rise to two types of deviation of the intensity distribution from the true distribution: a) random shifts of the whole diffraction pattern without a change in the character of the intensity distribution; and b) random local deviations $\Delta M(s)$ in the individual regions of the diffraction pattern.

a) Random shifts of the diffraction pattern as a whole are primarily associated with errors in measurement of the wavelength λ of the scattered electrons. If λ is calculated from the accelerating voltage measured in the experiment, then the measurement circuit introduces a certain error $\delta\lambda_c$; if the electron diffraction patterns are obtained and measured at different times, there is an additional error $\delta\lambda_0$, which is due to instability of the feed circuit of the electron-diffraction apparatus:

$$\delta\lambda = \delta\lambda_0 + \delta\lambda_c. \tag{3}$$

If λ is calculated from the electron-diffraction patterns of a crystalline standard, the error is the sum of $\delta\lambda_0$ and the inaccuracy in determination of λ with the crystalline standard. The latter in accuracy can be found from the simplified Bragg – Vulf equation

$$\lambda = \frac{2d}{n}\sin\theta \approx \frac{d}{n}\cdot\frac{D_c}{l}, \tag{4}$$

where θ is the scattering angle, d is the interplanar spacing, D_c is the corresponding diameter of the diffraction ring, and l is the distance between the standard and the photographic plate.

With the aid of (3) and (4), we have by the usual methods of the theory of errors**:

$$\delta\lambda = \delta\lambda_0 + \delta l + \delta D_c. \tag{5}$$

Each point in the diffraction pattern is correlated with the value of the scattering angle in the units

$$s = \frac{4\pi}{\lambda}\sin\frac{\theta}{2} \approx \frac{2\pi n}{d}\cdot\frac{lD}{LD_c}, \tag{6}$$

* The symbol $\sigma(x)$ is used to represent $\frac{[s_x^2]^{\frac{1}{2}}}{\bar{x}}$, which tends to $\frac{[\sigma_x^2]^{\frac{1}{2}}}{\mu_x}$ with increase of the number of measurements; here s_x^2 is the root mean square deviation, $\bar{x}$ is the mean value, σ_x^2 is the dispersion, and μ_x is the mathematical expectation of the measured quantity.

** It is evident that when λ is found from electron-diffraction patterns of a crystalline standard a certain systematic error in the determination of molecular structure parameters is introduced by the inaccuracy of the Bragg – Vulf equation (4) and by experimental data on the interplanar spacings of the crystal. We do not consider these errors, on the assumption that the values of d for the standard are known with a high degree of accuracy and that appropriate corrections can be introduced into Eq. (4).

where L is the distance between the evaporator nozzle and the photographic plate; D/2 is the position of the point relative to the center of the diffraction pattern. It follows from Eq. (6) that the magnitude of the shift δs caused by errors in measurement of L and λ is

$$\delta s = \delta\lambda + \delta L. \tag{7}$$

In addition to these factors, a random shift δs_{vap} of the diffraction pattern is caused by delocalization of the vapor stream during exposure. Without going into the theory of this effect, we may note that with a perfected evaporation technique the error δs_{vap} is $\sim 0.001 - 0.005$ A [6].

We assume further that the errors in measurement of all the experimental values conform to a normal distribution. We then have for the random shift $\sigma(s)$:

$$\sigma(s) = [\sigma^2(\lambda) + \sigma^2(L) + \sigma^2(s)_{vap}]^{\frac{1}{2}}; \tag{8}$$

where

$$\sigma(\lambda) = [\sigma^2(\lambda_0) + \sigma^2(\lambda_c)]^{1/2} \quad \text{or} \quad \sigma(\lambda) = [\sigma^2(\lambda_0) + \sigma^2(l) + \sigma^2(D_c)]^{1/2}.$$

b) Deviations of the scattering-intensity distribution in individual regions of the diffraction pattern are caused by: scattering of electrons at parts of the evaporator and the sector device, inaccurate adjustment of the sector, defects in the photographic emulsion, errors in microphotometric measurement and further analysis of the electron-diffraction patterns (mainly in calculations of scattering intensity from blackening of the emulsion), etc. A considerable error is introduced by inaccuracy in drawing the background line on the microphotogram. An important feature of these errors is their local character, i.e., limitation of the regions in which the scattering-intensity distribution deviates from the exact distribution. Therefore the Fourier transform of the experimental scattering-intensity distribution

$$f(r) = \int_0^{s_{max}} s\,[M(s) + \Delta M(s)] \exp(-as^2) \sin sr\, ds \tag{9}$$

differs from the exact by the magnitude of the error wave

$$\Delta f(r) = \int_0^{s_{max}} s\Delta M(s) \exp(-as^2) \sin sr\, ds. \tag{10}$$

The frequencies of the complex converging periodic function $\Delta f(r)$ are determined by the position of the error regions on the experimental $M_e(s)$ curve, and the amplitudes, by the magnitude of the deviations $\Delta M(s)$. With the aid of the principle of the positive character of the radial-distribution function [7,8], it is possible to correct to a considerable extent the experimental scattering-intensity distribution and to reduce $\Delta M(s)$ to a minimum.

We now estimate the displacement of the extremals of the experimental scattering-intensity distribution due to local deviations of $\Delta M(s)$, which lead to appearance of the error wave (10) on the radial-distribution curve.

Since the function $s\Delta M(s) \exp(-as^2)$ diminishes, we replace the upper integration limit in Eq. (10) by ∞. Then

$$\delta M(s) = \frac{2}{\pi} \cdot \frac{1}{sM(s) \exp(-as^2)} \int_0^{\infty} \Delta f(r) \sin sr\, dr. \tag{11}$$

Here, since the function $\Delta f/(r)$ is convergent, we can put

$$\int_0^{\infty} \Delta f(r) \sin sr\, dr = \int_0^{r_{max}} \Delta f(r) \sin sr\, dr, \tag{12}$$

where r_{max} can be chosen in accordance with the particular form of the $i(r)$ curve. Using (11), we can easily find the magnitude of the standard deviation $\sigma[M(s)]$, due to the error wave:

$$\sigma[M(s)] = \{\overline{|\delta M(s)|^2}\}^{1/2} = \left\{\frac{1}{s_{max}} \int_0^{s_{max}} |\delta M(s)|^2 ds\right\}^{1/2}. \tag{13}$$

The function $\Delta f(r)$ required for calculation of $\sigma[M(s)]$ can be found by subtraction of the theoretical radial-distribution curve calculated for the values found for the interatomic distances and vibration amplitudes from the experimental curve.

The deviations $\Delta M(s)$ displace the k-th maximum (or minimum) on the M(s) curve; the magnitude of the displacement can be estimated as

$$\Delta s_k = \left|\frac{\overline{\partial \Delta M(s)}}{\partial s}\right| \Big/ \left|\frac{\partial^2 M(s)}{\partial s^2}\right|_{s=s_k}. \tag{14}$$

Approximating the form of the extremals by the expression

$$M(s) = K \cos C(s - s_k), \tag{15}$$

where K and C are constants determined from the M(s) curve, and assuming that

$$\Delta M(s) = \sigma[M(s)]\, M(s), \tag{16}$$

we find the magnitude of the displacement of the extremal caused by the error wave

$$\{\overline{|\Delta s_k|^2}\}^{1/2} = \sigma[M(s)]/C\sqrt{2} \tag{17}$$

or

$$\tilde{\sigma}_k(s) = \sigma[M(s)]/Cs_k\sqrt{2}. \tag{18}$$

According to (8) and (18), the total displacement of the k-th extremal $\sigma_k(s)$ is:

$$\sigma_k(s) = \{\sigma^2(s) + \tilde{\sigma}_k^2(s)\}^{1/2}. \tag{19}$$

Accuracy of Determination of Geometric Parameters of Molecules in the Gas Phase by the Method of Successive Approximation (Trial and Error)

Suppose that, as the result of refinement by successive approximation, a final configuration of a given molecule had been found such that the theoretical $M_T(s)$ curve gives the best agreement with the experimental intensity distribution. It is evident that uncertainty in the position of each extremal in the experimental diffraction pattern corresponds to some degree of uncertainty in the parameters of the model found for the given molecule. As the sensitivities of different extremals on the theoretical $M_T(s)$ curve to variations of particular parameters of the model

may, in general, differ, it follows that deviations of the parameters differing in magnitude may correspond to different extremals. We assume that the least of the deviations of the parameters of the model correspond to the error in determination of the geometrical configuratin of the given molecule by the method of successive approximations.

By the usual methods of the theory of errors, the absolute error of a parameter r_{mn} of the selected model of the given molecule, corresponding to Δs_k, is

$$\Delta r_{m,n}^{(k)} = \left|\frac{\partial r_{mn}}{\partial s}\right|_{s=s_k} \Delta s_k = \frac{\left|\frac{\partial M_\tau(s)}{\partial s}\right|_{s=s_k}}{\left|\frac{\partial M_\tau(s)}{\partial r_{mn}}\right|_{s=s_k}} \Delta s_k \tag{20}$$

From Eq. (1) it is easily found that

$$\left|\frac{\partial M_\tau(s)}{\partial s}\right|_{s=s_k} = \frac{1}{\sum_i z_i^2 + z_i}\left|\sum_{ij} z_i z_j \exp(-l_{ij}^2 s_k^2/2) \times \right.$$
$$\left. \times \frac{s_k r_{ij}\cos s_k r_{ij} - \sin s_k r_{ij}}{s_k^2 r_{ij}} - \sum_{ij} z_i z_j l_{ij}^2 s_k \exp(-l_{ij}^2 s_k^2/2) \frac{\sin s_k r_{ij}}{s_k r_{ij}}\right|. \tag{21}$$

Since l_{ij}^2 is small, the second term in (21) may be neglected. Putting

$$\frac{s_k r_{ij}\cos s_k r_{ij} - \sin s_k r_{ij}}{s_k r_{ij}} = A_{ij}^{(k)},$$

we have

$$\left|\frac{\partial M_\tau(s)}{\partial s}\right|_{s=s_k} = \frac{1}{\sum_i z_i^2 + z_i}\left|\sum_{ij} z_i z_j \exp(-l_{ij}^2 s_k^2/2)\, A_{ij}^{(k)}/s_k\right|. \tag{22}$$

Analogously we find

$$\left|\frac{\partial M_\tau(s)}{\partial r_{mn}}\right|_{s=s_k} = \frac{1}{\sum_i z_i^2 + z_i}\left|\sum_{ij} z_i z_j \exp(-l_{ij}^2 s_k^2/2) \frac{A_{ij}^{(k)}}{r_{ij}} \frac{\partial r_{ij}}{\partial r_{mn}}\right|. \tag{23}$$

Substituting (22) and (23) into (20) and passing to the standard deviation r_{mn} we have

$$\sigma(r_{mn}) = \sigma_k(s) \frac{\left|\sum_{ij} z_i z_j \exp(-l_{ij}^2 s_k^2/2)\, A_{ij}^{(k)}\right|}{\left|\sum_{ij} z_i z_j \frac{r_{mn}}{r_{ij}} \exp(-l_{ij}^2 s_k^2/2)\, A_{ij}^{(k)} \frac{\partial r_{ij}}{\partial r_{mn}}\right|}. \tag{24}$$

Here $\sigma_k(r_{mn})$ is the relative standard deviation r_{mn} corresponding to the standard deviation of the position of the k-th extremal $\sigma_k(s)$.

Expression (24) can be reduced to a more convenient form by means of Bessel functions of half-integral order:

$$\sigma_k(r_{mn}) = \sigma_k(s) \frac{\left|\sum_{ij} G_{ij} \exp(-l_{ij}^2 s_k^2/2)\, J_{n/2}(s_k r_{ij})\right|}{\left|\sum_{ij} G_{ij}^{mn} \exp(-l_{ij}^2 s_k^2/2)\, J_{n/2}(s_k r_{ij}) \frac{\partial r_{ij}}{\partial r_{mn}}\right|}, \tag{25}$$

where $J_{3/2}(s_k r_{ij})$ is a Bessel function of the order 3/2, and

$$G_{ij} = z_i z_j r_{ij}^{-4}; \quad G_{ij}^{mn} = z_i z_j r_{mn} / r_{ij}^{5}.$$

The form of expression (25) leads to the following conclusions.

For the simplest case (diatomic molecules) the accuracy in determination of the interatomic distance is $\sigma_k(s)$, which is the relative accuracy in determination of the position of the extremals in the diffraction pattern.

The error in determination of parameter r_{mn} in a complex molecule cannot be less than $\sigma_k(s)$. If a complex molecule contains an interatomic distance with scattering power $z_m z_n / r_{mn}$ considerably greater than all the others, the error in its determination is close to $\sigma_k(s)$.

If with variation of parameter r_{mn} the geometrical configuration of a complex molecule alters similarly, i.e.,

$$r_{ij} = k_{ij} r_{mn},$$

where k_{ij} is a proportionality factor, then the following is also true:

$$\sigma_k(r_{mn}) = \sigma_k(s).$$

We now consider another specific source of error in structure determinations, which arises if the method of successive approximations is used. In interpretation of electron-diffraction patterns of complex molecules with large numbers of interatomic distances it is often impossible in practice to select every parameter without exception. Therefore certain interatomic distances are assumed equal to the corresponding distances in known similar molecules. It is evident that inaccuracies in these assumed values introduce additional errors into the parameters determined by successive approximation. Suppose that in a complex molecule, an assumed parameter r_{pq} differs from the true value by Δr_{pq}. From the obvious relationship

$$\Delta s = \left|\frac{\partial s}{\partial r_{mn}}\right| \Delta r_{mn} + \left|\frac{\partial s}{\partial r_{pq}}\right| \Delta r_{pq} \tag{26}$$

it follows that

$$\Delta r_{mn} = \left|\frac{\partial r_{mn}}{\partial s}\right| \Delta s + \left|\frac{\partial s}{\partial r_{pq}}\right| \left|\frac{\partial r_{mn}}{\partial s}\right| \Delta r_{pq}. \tag{27}$$

Using Eqs. (22) and (23) to find $\partial r_{mn}/\partial s$ and $\partial r_{pq}/\partial s$, we have

$$\sigma_k(r_{mn}) = \left\{ \sigma_k^2(s) \frac{\left|\sum_{ij} G_{ij} \exp(-l_{ij}^2 s_k^2/2) J_{5/2}(s_k r_{ij})\right|^2}{\left|\sum_{ij} G_{ij}^{mn} \exp(-l_{ij}^2 s_k^2/2) J_{5/2}(s_k r_{ij}) \frac{\partial r_{ij}}{\partial r_{mn}}\right|^2} + \right.$$
$$\left. + \sigma^2(r_{pq}) \frac{\left|\sum_{ij} G_{ij}^{pq} \exp(-l_{ij}^2 s_k^2/2) J_{5/2}(s_k r_{ij}) \frac{\partial r_{ij}}{\partial r_{pq}}\right|^2}{\left|\sum_{ij} G_{ij}^{mn} \exp(-l_{ij}^2 s_k^2/2) J_{5/2}(s_k r_{ij}) \frac{\partial r_{ij}}{\partial r_{mn}}\right|^2} \right\}^{1/2}. \tag{28}$$

If the values of several parameters are assumed in the interpretation, Eq. (28) naturally becomes

$$\sigma_k(r_{mn}) = \left\{ \sigma_k^2(s) \frac{\left| \sum_{ij} G_{ij} \exp(-l_{ij}^2 s_k^2/2) J_{\nu_{ij}}(s_k r_{ij}) \right|^2}{\left| \sum_{ij} G_{ij}^{mn} \exp(-l_{ij}^2 s_k^2/2) J_{\nu_{ij}}(s_k r_{ij}) \frac{\partial r_{ij}}{\partial r_{mn}} \right|^2} + \right.$$

$$\left. + \sum_{pq} \sigma^2(r_{pq}) \frac{\left| \sum_{ij} G_{ij}^{pq} \exp(-l_{ij}^2 s_k^2/2) J_{\nu_{ij}}(s_k r_{ij}) \frac{\partial r_{ij}}{\partial r_{pq}} \right|^2}{\left| \sum_{ij} G_{ij}^{mn} \exp(-l_{ij}^2 s_k^2/2) J_{\nu_{ij}}(s_k r_{ij}) \frac{\partial r_{ij}}{\partial r_{mn}} \right|^2} \right\}^{1/2}. \quad (29)$$

Accuracy of Determination of Geometric Parameters of Molecules in the Gas Phase by the Radial Distribution Method

a) Effect of a Shift of the Diffraction Pattern on the Position of the Maximum on the f(r) Curve

It follows from Eq. (1) that a displacement of the experimental intensity distribution by a value $\delta(s)$ without a change in the character of the intensity distribution should correspond to a similar transformation of the geometrical configuration of the molecule (i.e., to a simultaneous proportional change of all the interatomic distances in the model without distortion of the valence angles). It follows that a random shift of the diffraction pattern should displace the extremal points of all the peaks on the f(r) curve by certain values Δr_{mn}, which can evidently be estimated from the expression

$$\delta r_{mn}^{\circ} = \frac{\partial r_{mn}}{\partial s} \delta s. \quad (30)$$

Here δr_{mn}° is the relative error of the parameter r_{mn} caused by a shift of the experimental intensity distribution. According to (25), the standard deviation corresponding to δr_{mn}° is

$$\sigma(r_{mn})^{\circ} = \sigma(s). \quad (31)$$

b) Displacement of the Maximum of the Peak on the f(r) Curve Caused by Local Deviations $\Delta M(s)$

We use the method proposed by Cruickshank and Viervoll [5] for calculating the error in the position of the peak on the f(r) curve caused by the error wave of the experimental intensity distribution. According to [5], this error is

$$\tilde{\Delta} r_{mn} = \frac{\left| \frac{\partial \Delta f(r)}{\partial r} \right|}{\left| \frac{\partial^2 f(r)}{\partial r^2} \right|_{r=r_{mn}}}. \quad (32)$$

Suppose that the final model of the given molecule has been chosen. Then the expression (10) can be rewritten in the form:

$$\Delta f(r) = \int_0^{s_{max}} s [M_e(s) - M_T(s)] \exp(-as^2) \sin sr \, ds. \quad (33)$$

We then have

$$\left| \frac{\partial \Delta f(r)}{\partial r} \right|^2 = \left| \int_0^{s_{max}} s^2 [M_e(s) - M_T(s)] \exp(-as^2) \cos sr \, ds \right|^2. \quad (34)$$

Further use of Eq. (32) involves its simplification. To estimate the curvature of the peak we represent, in accordance with [7,8], the function f(r) in the form

$$f(r) = \sum_{ij} \frac{c_{ij}(\pi H_{ij})^{3/2}}{2r_{ij}} \exp[-H_{ij}(r - r_{ij})^2], \tag{35}$$

where

$$H_{ij} = h_{ij}/4\bar{a}h_{ij} + 1;\ h_{ij} = 1/2l_{ij}^2$$

c_{ij} is a quantity proportional to the product of the charges and the number of pairs of nuclei i and j under consideration. From (35) we have

$$\left|\frac{\partial^2 f(r)}{\partial r^2}\right|_{r=r_{mn}} = \frac{c_{mn}\pi^{3/2}H_{mn}^{5/2}}{r_{mn}}. \tag{36}$$

For practical utilization of (32) we have to know the root mean square value of the derivative of the error wave (34). The use of Eq. (34) in accordance with Cruickshank and Viervoll [5] involves cumbersome calculations. We start with Eq. (35) for the radial-distribution function and represent $\Delta f(r)$ in the form

$$\Delta f(r) = \overline{\delta f(r)} f(r), \tag{37}$$

where $\overline{\delta f(r)}$ is the relative magnitude of the mean value of the function $\Delta f(r)$. Then

$$\frac{\partial \Delta f(r)}{\partial r} = \frac{\overline{\delta f(r)}\,\pi^{3/2} c_{mn} H_{mn}^{5/2}(r - r_{mn}) \exp[-H_{mn}(r - r_{mn})^2]}{r_{mn}} \tag{38}$$

and

$$\left\{\left|\overline{\frac{\partial \Delta f(r)}{\partial r}}\right|^2\right\}^{1/2} = \frac{\sigma[f(r)]\,\pi^{3/2} c_{mn} H_{mn}^{5/2}}{r_{mn}} \{|(r - r_{mn}) \exp[-H_{mn}(r - r_{mn})^2]|^2\}^{1/2}. \tag{39}$$

Since the function $\exp[-H_{mn}(r - r_{mn})^2]$ tends rapidly to zero in the region at a distance of $\approx \Delta_{mn}$ from the maximum (Δ_{mn} is the half width of the maximum corresponding to r_{mn}), we average out Eq. (39) over the range $r_{mn} - \Delta_{mn}$, $r_{mn} + \Delta_{mn}$. For the same reason we can put

$$\int_{r_{mn}-\Delta_{mn}}^{r_{mn}+\Delta_{mn}} |(r - r_{mn}) \exp[-H_{mn}(r - r_{mn})^2]|^2 dr = \int_0^\infty |(r - r_{mn}) \exp[-H_{mn}(r - r_{mn})^2]|^2 dr. \tag{40}$$

Calculating (40) and putting its value into (39), we have

$$\left\{\left|\overline{\frac{\partial \Delta f(r)}{\partial r}}\right|^2\right\}^{1/2} = \frac{0.43393\,\sigma[f(r)]\,\pi^{3/2} c_{mn} H_{mn}^{5/2}}{r_{mn}}. \tag{41}$$

Hence, using (36), we find the standard deviation of the interatomic distance r_{mn} attributable to the error wave,

$$\tilde{\sigma}(r_{mn}) = 0{,}4339\,\frac{\sigma[f(r)]}{r_{mn}\,H_{mn}^{1/2}} = 0{,}6136\,\sigma[f(r)]\,\frac{(a+l_{mn}^2)^{1/2}}{r_{mn}}. \qquad (42)$$

We thus have an expression which connects the error in determination of interatomic distances with the structure of the given molecule.

The value of

$$\sigma[f(r)] = \frac{\overline{[\Delta f(r)]^2}^{1/2}}{f(r)_{r=r_{mn}}} = \frac{\overline{[\Delta f(r)]^2}^{1/2}}{e_{mn}\,H_{mn}^{1/2}} \qquad (43)$$

depends on the nuclear charges and vibration amplitudes of atoms m and n at distance r_{mn}, and the whole expression (42) also depends on the magnitude of the experimentally found region of scattering angles (a is a constant calculated from the condition $1.67\sqrt{a} = 2.5/s_{max}$ [9]). Equation (42) for the magnitude of the error in the interatomic distance caused by the error wave of the experimental intensity distribution coincides to an accuracy down to the constant factor with the expression derived recently in [4] by a somewhat different method; the difference between the coefficients is probably due to different selection of the magnitude of $\sigma[f(r)]$. According to Bonham and Bartell [4], $\sigma[f(r)]$ is defined as the root mean square value of the difference between the experimental and theoretical radial-distribution functions in the region $r_{ij}(\min) < r < r_{ij}(\max)$.

The total error in determinations of interatomic distances by the radial-distribution method is

$$\sigma(r_{mn}) = \{\sigma^2(r_{mn})^* + \tilde{\sigma}^2(r_{mn})\}^{1/2} = \{\sigma^2(s) + \tilde{\sigma}^2(r_{mn})\}^{1/2}. \qquad (44)$$

It should be noted that Eq. (44) is applicable only in absence of overlapping of the peaks in the radial-distribution curve and cannot be used in the general case. We therefore consider that Eq. (25), which refers to the method of successive approximations, may in some instances serve as an important supplement to the simpler Eq. (44), which is of limited applicability.

The authors are deeply grateful to L. V. Vilkov and V. B. Spiridonov for valuable advice in the course of discussions.

LITERATURE CITED

1. L. S. Bartell, L. O. Brockway, R. H. Schwendeman. J. Chem. Phys. 23, 1854 (1955).
2. O. Bastiansen, O. Hassel, E. Risberg. Acta chem. scand. 9, 232 (1955).
3. O. Bastiansen, L. Hedberg, K. Hedberg. J. Chem. Phys. 27, 1311 (1957).
4. R. A. Bonham, L. S. Bartell. J. Chem. Phys. 31, 702 (1959).
5. D. W. J. Cruickshank, H. Viervoll. Acta chem. scand. 3, 560 (1949).
6. L. S. Bartell. J. Appl. Phys. 31, 252 (1960).
7. I. L. Karle, J. Karle. J. Chem. Phys. 17, 1052 (1949).
8. J. Karle, I. L. Karle. J. Chem. Phys. 18, 957 (1950).
9. J. Waser, V. Schomaker. Rev. mod. phys. 25, 671 (1953).

EFFECT OF STRUCTURE ON THE THERMODYNAMIC PROPERTIES OF SOLUTIONS OF STRONG ELECTROLYTES

A. I. Gorbanev, Yu. M. Kessler, and V. V. Krylov

Institute of Electrochemistry, Academy of Sciences USSR
Translated from Zhurnal Strukturnoi Khimii, Vol. 2, No. 3, pp. 260-267,
May-June, 1961
Original article submitted December 30, 1960

A modified form of the Guggenheim equation, containing a correlation term and an empirical correction for "binding" of the solvent by the ions, is considered. It is shown that with the right correction for "binding" of water experimental data on activity coefficients may be represented by a one-parameter equation. Energies of short-range interaction of ions are estimated; for alkali chlorides these energies are negative and increase in absolute magnitude with increasing cation radius. In aqueous solutions of uni-univalent electrolytes the energy of short-range ion interaction changes appreciably when the distance of closest approach of the ions is about 3 A.

In earlier papers [2-4] we attempted to investigate the cause of the deviations of the Debye and Hückel theory [1] from experimental data. It was found that the main cause of the deviation is short-range ("specific") interaction between ions. It was formally described by means of the Guggenheim equation [5]:

$$\Delta F = \Delta F_D^I - bc^2 \left\{ \int_0^\infty [\exp(-v_{ab}/\theta)] r^2 dr - \int_0^\infty r^2 dr \right\}, \qquad (1)$$

where ΔF is the free energy of the solution; ΔF_D^I is the free energy in accordance with theory [1]; b is a coefficient which depends on temperature; $v_{ab} = v_{ab}(r)$ is the potential energy of short-range interaction of the ions; $\theta = kT$; r is the distance between the centers of the ions; c is the volume concentration. Our principal aim was to consider the physical nature of the function v_{ab} and to correlate it with solution structure.

By introducing the concepts of solvation sphere and desolvation energy, and by deriving the definition of an ion pair from these concepts, we were able to offer qualitative explanations for certain experimental data and to predict certain effects. In particular, experimental data on the heats of dilution of alkali chloride solutions in hydrogen peroxide and in concentrated mixtures of hydrogen peroxide with water were explained; it was shown that deviations from the Debye and Hückel theory, of either sign, are possible in principle; it was predicted that the less stable the structure of a pure solvent with respect to temperature the greater the deviation between theoretical and experimental heats of dilution [4]; the existence of a correlation between the deviations between theory [1] and experiment and the magnitude of the least approach of the ions r_0 was predicted [6]. The solution model is considered in finer detail in this paper.

Equation (1) contains two significant simplifications. First, the first approximation ΔF_D^I of the theory [1] was used for ΔF_D. Moreover, correlation [7] was disregarded in the second term. The simplification is not especially important for qualitative purposes, but it becomes significant in estimation of numerical values of v_{ab}. Furthermore, several effects (multiple ion collisions, changes of the macroscopic dielectric constant, variations of the amount of "free" solvent, etc.) are ignored in Eq. (1). Of these effects, the most significant from the quantitative standpoint is the change in the amount of "free" solvent caused by "binding" of solvent by the ions. This effect is of integral character in principle. However, the interaction of solvent molecules at long distances is virtually the same with ions of equal charge. Individuality is introduced only by interaction of ions with nearest molecules, which is influenced by differences of ionic radii. Therefore it is important to consider close-range interaction in examining differences in the behavior of solutions of different salts. This effect can be considered as a change in the effective electrolyte concentration [8] so that no contradictions are introduced if it is included in Eq. (1). It can be calculated

from the Bjerrum or the Stokes and Robinson equations [8]. However, these equations include the activity of water, which complicates the calculations technically. We therefore used the Glueckauf equation [9], derived on different considerations and different in form, but giving numerical results almost indentical with those of calculations based on the Stokes and Robinson equation. With these refinements Eq. (1) is modified, and the expression derived from it for activity coefficients on the molality scale is of the form

$$\lg \gamma_{\pm} = \lg f_{\pm}^{II} - \frac{h}{\nu} \lg (1 - 0{,}018\, mh) + \\ + \frac{h - \nu}{\nu} \lg [1 - 0{,}018\, m (h - \nu)] + B_0 c. \qquad (2)$$

Here

$$B_0 = -b \int_{r_0}^{r_c} \left[\exp\left(-\frac{v_{ab}}{\theta}\right) - \exp\left(-\frac{e^2 z_a z_b}{D_0 \theta r}\right) \right] r^2 dr, \qquad (3)$$

$\log f_I^{II}$ is the second approximation to theory [1], m is the molality, ν is the number of ions formed by dissociation of one electrolyte molecule, $b = 1.6437 \cdot 10^{21}$, r_c is the sum of the radii of the cation and anion solvation spheres, and h is the effective number of "bound" solvent molecules, defined by the equation derived earlier [10]:

$$h = \sum_i \nu_i n_i \frac{(\tau_i^0/\tau^0) \exp(\Delta E_i / RT) - 1}{(\tau_i^0/\tau^0) \exp(\Delta E_i / RT) + 1} \qquad (4)$$

The remaining symbols have their usual meanings.

Values of the preexponential factors from [11] and values of n_i and ΔE_i from [12] were used for calculation of h by means of Eq. (4). Therefore the values of r_0, which also enter the Debye term, and the coefficient of the last term remain unknown in Eq. (2). For determination of r_0 we can either take a definite reasonable value or estimate it from experimental data. In either case the estimation of r_0 is to some extent arbitrary, as the second method involves the tacit assumption that the equation used accurately describes the experimental data; this is, of course, untrue because of the approximate character of the formulas used (if only certain, though perhaps small, effects are neglected). Apart from some individual cases (for example, when r_0 estimated from experimental data is found to be appreciably smaller than the sum of the crystallographic ion radii $r_+ + r_-$) it is difficult to assess which method leads to the greater inaccuracy. We therefore preferred, as before, to assume in the first approximation that $r_0 = r_+ + r_-$. For weakly hydrated ions this probably corresponds to reality. In this case only the coefficient B_0, which can be found from experimental data, remains unknown in Eq. (2).

Calculations of this type were carried out for lithium, sodium, potassium, and rubidium chlorides. Values of B_0 were found by averages for concentrations up to and including 0.1 M. Figure 1 shows activity coefficient–concentration curves calculated from the values so found for B_0. The graphs show quite satisfactory agreement between calculated and experimental data up to $c = 0.1$. Above this concentration agreement cannot be expected, because in the region of moderate concentrations Eq. (2) is inapplicable, although it is possible, purely formally, to improve the agreement at moderate concentrations. To do this we must include the corresponding concentrations in calculations of B_0. As an example, Fig. 1d (curve 3) shows the result of such a calculation for cesium chloride. It is then found that although the deviations are considerably less at moderate concentrations they increase noticeably at low concentrations; this is an objective indication of the inapplicability of Eq. (2) at moderate concentrations.

The agreement between calculated and experimental data for LiCl, NaCl, and KCl can be improved still further if it is assumed that $r_0 > r_+ + r_-$. Since nothing is known in general about the value of r_0, we attempted to estimate it. Evaluation of r_0 from the apparent ionic volumes carried out by Stokes and Robinson [8] gave values greater by 0.7 A than r_0 found experimentally for alkali halides. In general, absolute calculation of r_0 is difficult at the present time. Comparative calculations appear to be more promising.

The increase of the effective ionic radii in comparison with the crystal radii in solution is due to the presence of solvation layers of varying stability. Under otherwise equal conditions it may be assumed that the effective

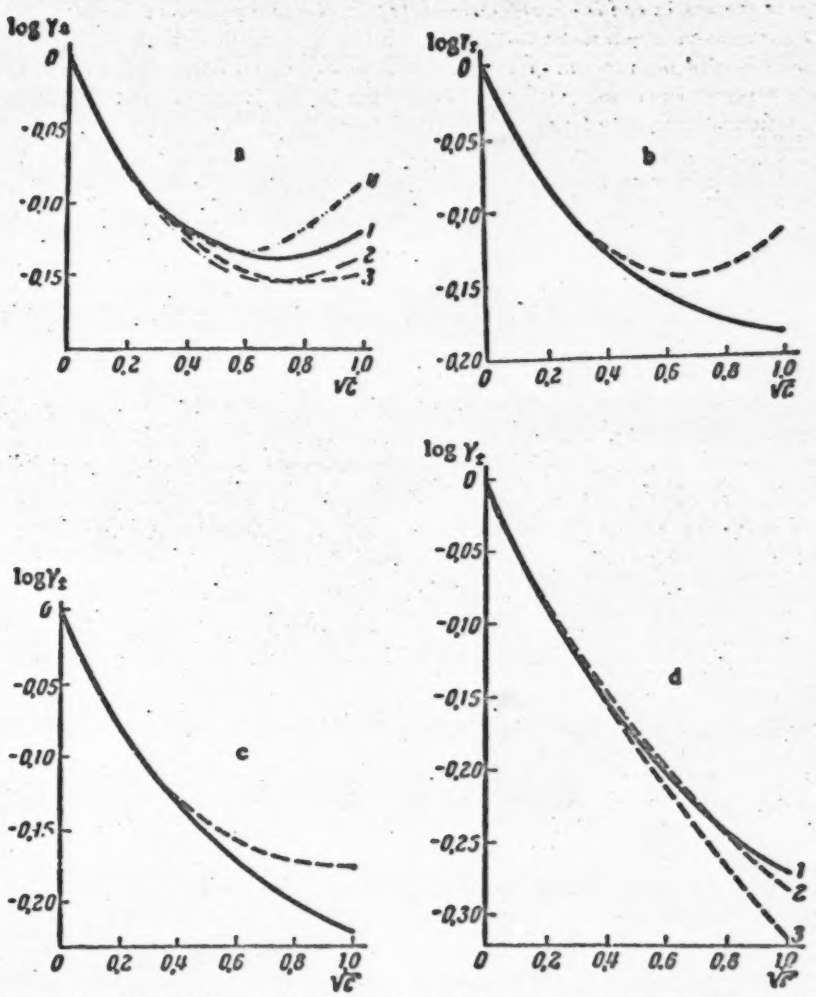

Fig. 1. Activity coefficents of uni-univalent electrolytes in water at 25°. Continuous curves – experimental; dash lines – calculated. a) LiCl (curve 2, r_0 = 2.59 A, h ≠ 0; curve 3, r_0 = 3.59 A, h ≠ 0; curve 4, r_0 = 2.59 A, h = 0); b) NaCl; c) KCl; d) CsCl (in calculations of B_0 experimental data were taken into account up to the following concentrations: Curve 2, 1.0 M; curve 3, 0.1 M).

adius of an ion is proportional to the energy of its interaction with the solvent molecules in the layer nearest to the ion and to the probability of entry of solvent molecules into this layer. This probability, in its turn, is proportional to the volume of the spherical layer, one water molecule thick, adjacent to the ion. Then, assuming that the interaction between the ion and the solvent molecules in this layer is of the ion–dipole type, we have as a very rough approximation

$$r_{eff} = k\frac{(r_i + 2r_s)^3 - r_i^3}{(r_i + r_s)^2}, \qquad (5)$$

where k is a proportionality factor, r_i is the crystal radius of the ion, and r_s is the radius of a solvent molecule. Since the value of k is in general unknown, the most objective approach is to estimate the variations of r_{eff} in series of similar ions from changes in the r_{eff}/k ratio. It was found, in agreement with experiment, that r_{eff} diminishes from lithium to cesium and from chloride to iodide. Further, in view of the fact that in the case of cesium chloride deviations between calculations based on Eq.(2) and experimental data do not exceed the experimental error, and in view of the low degree of hydration of cesium and chloride ions, it may be assumed that in aqueous solutions of this

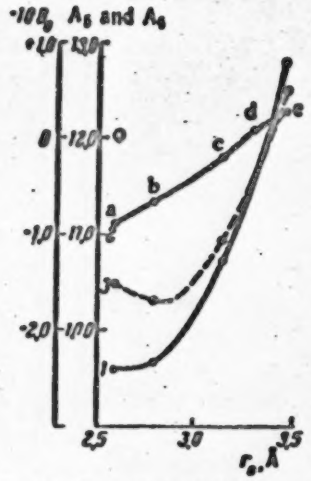

Fig. 2. Variations of A_s, A_s, and B_0 in Eqs. (2), (6), and (8) with r_0. 1) A_s; 2) A_s; 3) $(-10)B_0$. a) LiCl; b) NaCl; c) KCl; d) RbCl; e) CsCl.

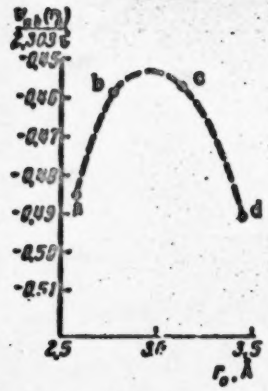

Fig. 3. Variation of the average value of $v_{ab}(r_k)$ with r_0: a) LiCl; b) NaCl; c) KCl; d) CsCl.

salt $r_0 = r_+ + r_-$. Hence we can determine $\underline{k}$ and calculate r_0 for other salts. For example, for lithium chloride we find $r_0 = 3.59$ A. Results of calculations with this value of r_0 are shown in Fig. 1; the agreement with experimental data is better than is obtained with $r_0 = r_+ + r_-$. For comparison, the same graph shows a curve found from Eq. (2) at $h = 0$; agreement with experimental data is worse in this case, which is evidence in favor of introducing a correction for "binding" of water.

Recalculations with r_{eff} in accordance with Eq. (5) were not performed for two reasons. First, the proposed estimation of r_{eff} in the form described is an illustration of the idea rather than a calculation method. For practical application, this method requires substantial improvement. Second, as will be shown later, the choice of r_0 has little effect on the main conclusions.

Values of B_0 found experimentally are shown as a function of r_0 in Fig. 2; this shows the minimum discovered earlier in calculations with the aid of the simplified Eq. (1) [6]. The cause of this can be analyzed to some extent by means of Eq. (2).

We may assume [2-4] that $r_0 \approx r_0 + 4\,r_{H_2O}$. Then Eq. (2) can be used for finding

$$A_s = a_1 \int_{r_a}^{r_c} [\exp(-v_{ab}/\theta)] r^2\,dr \tag{6}$$

and

$$-\frac{v_{ab}(r_k)}{2{,}303\,\theta} = \lg\frac{3}{a_1} + \lg\frac{10B_0 + A_s}{r_c^3 - r_a^3}, \tag{7}$$

where

$$A_s = a_2 \int_{r_a}^{r_a} \left[\exp\left(-\frac{e^2 z_a z_b}{D_0 \theta_r}\right)\right] r^2\,dr, \tag{8}$$

$$r_0 < r_k < r_c. \tag{9}$$

and a_1 and a_2 are numerical factors. The integral A_6 was calculated graphically after the following transformation [8]:

$$A_6 = a_2\left(\frac{e^2 z_a z_b}{D_0 \theta}\right)^6 \int_{Y_2}^{Y_1} [\exp(Y)] Y^{-6} dY,$$
$$Y_1 = \frac{e^2 z_a z_b}{D_0 \theta r_c}, \quad Y_2 = \frac{e^2 z_a z_b}{D_0 \theta r_0}. \tag{10}$$

Variations of A_5 and A_6 with r_0 are plotted in Fig. 2. The curves are connected by the relationship $A_5 = 10B_0 + A_6$. As was to be expected, A_5 increases smoothly with r_0. Because of this and of the nature of the variation of B_0 the slope of the A_5 curve increases sharply in the region $r_0 \approx 3$ A. The increase of A_5 with r_0 indicates increased attraction between the ions with increasing crystal radii, i.e., with decreasing energy of hydration of the free ions, which is in full agreement with the model. It must be emphasized that in accordance with the electrostatic theory [1] the reverse should be found.

In Fig. 3 average values of $v_{ab}(r_k)$ are plotted against r_0, in accordance with Eq. (7). Correspondingly to the course of the curves in Fig.2, the extremal on the $v_{ab}(r_k)$ curve is found at $r_0 \approx 3$A.

Similar calculations were also performed with the aid of Hamed and Owen's data [8] in order to find the extent to which the assumptions on which the calculation is based (in particular, the choice of r_0) influence the form of the curves. These authors used Eq. (2) at $h = 0$ and determined both r_0 and B_0 as empirical parameters. Their values of r_0, in contrast to those accepted in this paper, diminish in the LiCl – CsCl series, which must be accepted as reasonable from the qualitative standpoint. However, in the case of CsCl their value for r_0 was less by 0.46 A than the sum of the crystal radii, which is untrue and which indicates that their values of r_0 and B_0 are incorrect. This is because the equation used in [8], being approximate, cannot be used as a basis for calculation of r_0. Moreover, Hamed and Owen included experimental data for excessively high concentrations (1 M and higher) in the calculations.

The results of calculations based on data from [8] are plotted in Figs. 4 and 5. It is seen that B_0 does not have a minimum, but the slope changes sharply, again in the 3 A region, while the A_5 curve has an inflection point. The curve for $v_{ab}(r_k)$ (Fig. 5) does not have an extremal either, but it has a sharp break in the 3 A region, and this persists regardless of which r_0 is taken as the argument: $r_0 = r_+ + r_-$ or r_0 from [8]. Preliminary calculations show that r_{eff} calculated from Eq. (5) gives results close to those shown in Fig. 5.

Calculation of $\underline{h}$ introduces a certain error into calculations with Eq. (2), as the quantities in Eq. (4) are apparently not known with sufficient accuracy. Glueckauf [9] plotted h_{ion} against r_{ion} and against the entropy of hydration ΔS^{ion}_{hydr} in order to confirm the accuracy of the values found for $\underline{h}$, which he determined as an empirical parameter from experimental data with the aid of an equation of type (2) without the last term. He obtained linear plots in both cases and took this as confirmation of the validity of his values of $\underline{h}$. Similar plots for our values of h_{ion} are given in Figs. 6 and 7. These are also linear, but in Glueckauf's plot the point for Cs^+ is far from the $h_{ion} = f(r_+)$ line, while in ours it fits satisfactorily on the line, and the deviation of the point for Cs from the $h_{ion} = f(\Delta S^{ion}_{hydr})$ line is appreciably less in our case. However, we do not think that the existence of linear relationships is a criterion of the validity of the values found for h_{ion}: our h_{ion} values differ from the data in [9] even in sign, but the relationship is nevertheless linear. Therefore it cannot be guaranteed that our h_{ion} values are absolutely correct. However, the existence of linear relationships undoubtedly shows that no crude errors which might have a significant influence on the final results were introduced in our calculations of $\underline{h}$.

Thus, comparison of the results of three calculations (from Eq. (1) [4], from Eq. (2), and from data of [8]) leads to the conclusion that v_{ab} undergoes definite changes at $r_0 \approx 3$ A. In accordance with the reasoning detailed earlier [4] we may claim that this is associated with some as yet unknown peculiarities of hydration of ion pairs as a whole. A manifestation of these peculiarities is that near $r_0 = 3$ A the solvation energy of an ion pair diminishes sharply. It should be noted that the diameter of a water molecule is also close to 3 A. Of course, if only one solvent is considered there is always the risk that a random combination of circumstances is mistaken for a regular relationship. However, something similar is observed in the case of hydrogen peroxide.

From Eq. (1) it is easy to derive an expression for the integral heat of dilution, which is:

$$\Delta W = \Delta W^I_D + Kc, \tag{11}$$

where

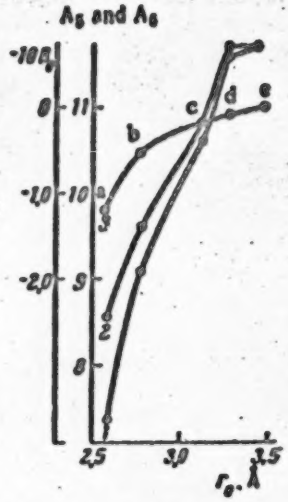

Fig. 4. Variations of A_δ, A_θ, and B_θ with r_θ according to [8]. For symbols, see caption to Fig. 2.

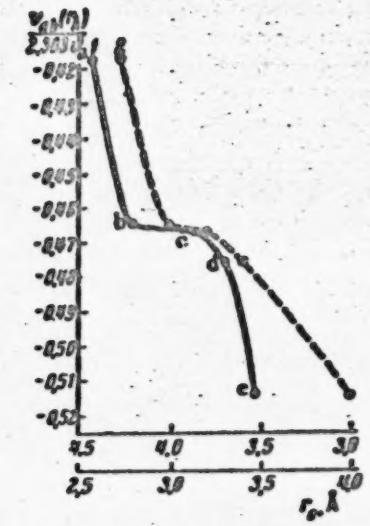

Fig. 5. Variations of the average value of $v_{ab}(r_k)$ with r_θ according to [8]; 1) abscissa corresponds to our r_θ (lower scale); 2) abscissa corresponds to r_θ from [8] (upper scale); for other symbols, see caption to Fig. 2.

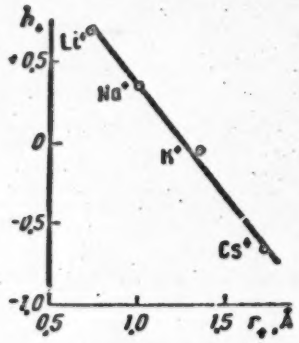

Fig. 6. Variation of h_+ [Eq. (4)] with r_+.

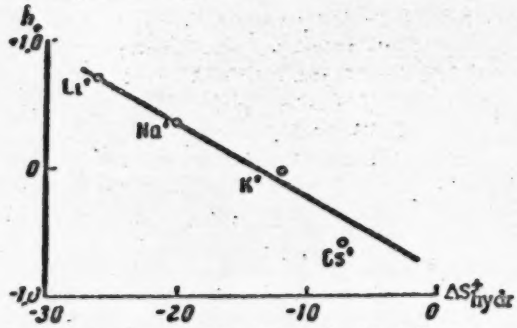

Fig. 7. Variation of h_+ [Eq. (4)] with $\Delta S^{\uparrow}_{hydr}$.

$$K = RT^2 N \cdot 10^{-3}\left(4\pi r_\theta^2 \frac{\partial r_\theta}{\partial T} - \frac{4}{3}\pi r_\theta^3 \varphi + \beta\varphi - \frac{\partial \beta}{\partial T}\right), \tag{12}$$

$$\beta = \int_{r_\theta}^{r_c} [\exp(-v_{ab}/\theta) - 1]\, 4\pi r^2 dr, \tag{13}$$

$$\varphi = \frac{1}{V}\frac{\partial V}{\partial T}; \tag{14}$$

N is the Avogadro number, and V is the solution volume. It is easy to show by a simple calculation that $\partial E/\partial T$ is greater by at least two tenth-powers than any of the other terms in parentheses in Eq. (12), and $B\varphi$ is greater by a tenth-power than the first two terms. Therefore the value of K is determined by the last two terms. The following values were found for K for alkali chlorides in hydrogen peroxide at 0°:

	NaCl	KCl	RbCl	CsCl
$K \cdot 10^{-4}$	6,04	—0,324	2,72	3,06

The absence of a monotonic relationship between K and r_0 is evident; here again the break comes at $r_0 \approx 3$ A. This value is close to the diameter of the OH group in hydrogen peroxide HO – OH, since $r_{OH} = 1.49 \pm 0.01$ A [13]. At the same time, pure liquid H_2O and H_2O_2 differ significantly in structure [14]. These facts support the view that the observed effects are associated with short-range interaction of the ion pair as a whole with the solvent molecules in the nearest layer. The true state of affairs can be revealed only by further investigations.

The results (Figs. 3 and 5) indicate that the average potential energy of interaction for alkali metal chlorides is $v_{ab}(r_k) < 0$ when $r_0 < r_k < r_0$, i.e., in this range of distances ions of opposite charges attract one another. Nevertheless, the last term in Eq. (2) introduces a correction which increases the activity coefficients. This is because $A_3/a_1 < A_0/a_2$ [see also Eq. (3)]. In order that $B_0 < 0$ when $v_{ab} < 0$, v_{ab} must be negative and of large enough absolute value. This in its turn, requires either a low (in the algebraic sense) energy of solvation of the ion pair, or a high (also in the algebraic sense) energy of solvation of the free ions. The difference between these energies determines v_{ab}. The solvation energy of the free ions is high enough in the algebraic sense (small in absolute magnitude) in the case of cesium chloride, and therefore $B_3 < 0$ for this salt. For the salts considered in this paper the average value of $v_{ab}(r_k)$ is in the range of 500-700 cal/mole. Such values are quite reasonable in order of magnitude. At 25°, $RT \approx 600$ cal/mole, and consequently $v_{ab}(r_k)\,RT \approx 1$, which is consistent with absence of any appreciable dissociation in solutions of strong electrolytes.

LITERATURE CITED

1. P. Debye, E. Hückel. Phys. Z. 24, 185, 305 (1923).
2. Yu. M. Kessler, A. I. Gorbanev. Izv. Vostochnykh filialov AN SSSR, 4-5, 75 (1957).
3. Yu. M. Kessler, A. I. Gorbanev. Izv. Vostochnykh filialov AN SSSR, 6, 50 (1957).
4. Yu. M. Kessler, A. I. Gorbanev. Dokl. AN SSSR 117, 3, 437 (1957).
5. E. A. Guggenheim. Phil. Mag. 19, 588 (1935).
6. A. I. Gorbanev, Yu. M. Kessler, Yu. M. Povarov, É. S. Sevast'yanov. Dokl. AN SSSR 125, 6, 1281 (1959).
7. R. H. Fowler and E. A. Guggenheim. Statistical Thermodynamics [Russian translation] (IL, Moscow, 1949).
8. H. S. Harned and B. B. Owen. Physical Chemistry of Electrolytic Solutions [Russian translation] (IL, Moscow 1952).
9. E. Glueckauf. Trans. Faraday Soc. 51, 1235 (1955).
10. A. I. Gorbanev, Yu. M. Kessler, Yu. M. Povarov, É. S. Sevast'yanov, V. V. Krylov. Izv. AN SSSR, Otd. Khim. n., 3, 570 (1960).
11. O. Ya. Samoilov, Zh. strukt. khimii 1, 1, 35 (1960).
12. O. Ya. Samoilov, Structure of Aqueous Electrolyte Solutions and Hydration of Ions [in Russian] (Izd. AN SSSR, Moscow, 1957).
13. P. A. Giguère. Bull. soc. chim. France, 720 (1954).
14. J. T. Randall. Proc. Roy. Soc. (London) A159, 83 (1937).

All abbreviations of periodicals in the above bibliography are letter-by-letter transliterations of the abbreviations as given in the original Russian journal. *Some or all of this periodical literature may well be available in English translation.* A complete list of the cover-to-cover English translations appears at the back of this issue.

DIELECTRIC CONSTANTS AND STRUCTURAL CHARACTERISTICS OF AQUEOUS ELECTROLYTE SOLUTIONS

P. S. Yastremskii

Stalingrad Pedagogic Institute
Translated from Zhurnal Strukturnoi Khimii, Vol. 2, No. 3, pp. 268-270, May-June, 1961
Original article submitted December 30, 1960

The dependence of the dielectric constants of aqueous electrolyte solutions on concentration, ionic radii of the dissolved electrolytes, and characteristics of ion hydration was studied. An attempt is made to explain the results in the light of modern concepts of the structure of water and aqueous electrolyte solutions.

With the development of radiophysical methods for investigation of matter it is now possible to measure the dielectric constants (DC) of polar liquids of low viscosity at frequencies close to the characteristic frequencies of the molecules of these liquids (the super-high-frequency region). Such measurements also provide new possibilities for studying the structure of aqueous electrolyte solutions.

It is known that hydration of ions in aqueous solutions consists primarily of changes in the mobility (and therefore ability to undergo orientation in an external electric field) of the water molecules nearest to the ions, in comparison to the mobility of the molecules in water [1]. Moreover, structural changes take place in aqueous solutions under the influence of the ionic field, leading to a displacement of the equilibrium between ice-like and close-packed structures and changes in the solvent polarizability. The close-packed structure corresponds to the state of water molecules contained in the voids of the ice-like structure [1-3]. The ice-like structure, where the molecules are linked by directed hydrogen bonds, and the close-packed structure with molecules in voids, where the directed nature of the bonds is weaker, differ in polarizability [1, 4]. In considering polarizability it is necessary to take into account the extensive redistribution of the electron density of the water molecules which undoubtedly accompanies the formation (and cleavage) of hydrogen bonds [5].

Direct measurements of the polarizability of aqueous electrolyte solutions in super-high-frequency fields provide additional information on the nature of hydrations of cations and anions in dissolved electrolytes, make it possible to determine the effects of concentration and temperature on the relaxation time in polarization, and throw light on a number of other problems associated with the structure of aqueous electrolyte solutions.

This paper contains the results of measurements of the DC of aqueous LiCl, NaCl, NaI, KCl, and KI solutions over a wide range of concentrations (from 0.05 to 5 N) at temperatures from −5 to +40° at a frequency of 9400 Mc/sec. The DC measurements were performed by a wave-guide method [6,7], which is fairly sensitive to temperature and concentration changes in solutions. Thin-walled glass test tubes 0.5-0.7 mm in internal diameter were used. The error in the measurements did not exceed 2.6%.

Results of the Measurements

The results of measurements of the real component of the complex DC of solutions as a function of concentration at various temperatures are given in Figs. 1-6 and Table 1.

These results show that the magnitude and nature of the changes of the DP of solutions depend to a considerable extent on temperature, ionic radii, and characteristics of ion hydration in the dissolved electrolytes.

At low temperatures (Figs. 1, 2) the DC values of the solutions form the following diminishing sequence: $\epsilon_{KI} > \epsilon_{KCl} > \epsilon_{NaI} > \epsilon_{NaCl} > \epsilon_{LiCl}$; i.e., iodide solutions have higher DC than chloride solutions. At temperatures above 20° the DC of the same solutions are in a somewhat different sequence, namely: $\epsilon_{KCl} > \epsilon_{KI} > \epsilon_{NaCl} > \epsilon_{NaI} > \epsilon_{LiCl}$. In this case chloride solutions have higher DC than iodide solutions. Aqueous LiCl solutions have the lowest DC at all temperatures at a given concentration.

TABLE 1. Experimental Values of ε' and ε°

c	$t = -5°C$										$t = 0°C$			
	LiCl		NaCl		NaI		KCl		KI		LiCl		NaCl	
	ε'	ε°	ε'	ε°	ε'	ε°	ε'	ε°	ε'	ε°	ε'	ε°	ε'	ε°
0,05											45	42,6	45,4	42,4
0,2											44,8	42,7	44,9	42,9
0,5											43,4	42,6	44,0	43,2
1											41,4	42,5	43,5	44,0
1,5											39,1	42,0	41,8	44,2
2	32,6	40,5	37,5	44	39,9	44,8	42,5	53,8	43,4	54,2	36,4	41,2	40,2	45,2
2,5	31,3	39,6	36	43,8	38,5	45,4	41,6	55,6	42,6	56,5	34,8	40,6	38,3	44,9
3	29,3	38	34,4	43,2	37,3	45,3	40,8	58,5	41,5	60,3	32,9	40,3	36,5	44,6
3,5	28,4	37,6	33,3	42,8	35,2	44,8		59,9	40,9	61,8	31,2	39,1	35,1	44,6
4	27,1	36,4	31,7	42,4	33,7	44			39,8	64,6	29,1	38,6	33,5	44,3
4,5	25,7	35,6	31,0	40,9	32,1	43,1			39	66,9	27,8	37,2	32,1	43,2
5	24,3	34,0	29,9	40,3	30,6	42,2			37,6	69,1	26,3	36,0	30,5	42,3
6	22,3	32,14												

c	$t = 10°C$										$t = 20°C$				
	LiCl		NaCl		NaI		KCl		KI		LiCl		NaCl		NaI
	ε'	ε°	ε'	ε°	ε'	ε°	ε'	ε°	ε'	ε°	ε'	ε°	ε'	ε°	ε'
55,0	37,7	55,5	38,5	55,6	38,2	55,6	39,0	55,8	39,2	61,7	31,3	61,9	31,5	61,96	
53,7	38,0	54,5	39,3	54,8	39,4	55,1	40,1	55,4	40,0	60,0	33,3	60,7	32,7	61,0	
51,2	39,1	53,4	40,8	54,1	40,9	54,7	42,1	55,0	42,5	57,7	34,5	58,4	35,6	58,8	
48,0	39,9	50,5	42,5	51,6	42,7	53,6	46,0	54,0	46,6	54,0	37,5	55,2	38,8	55,6	
45,2	41,1	48,1	44,5	49,3	45,3	52,0	51,5	52,6	52,0	50,1	40,0	52,4	42,5	52,2	
42,0	42,0	45,9	46,1	46,6	47,2	51,2	55,9	51,2	56,8	47,1	41,6	49,8	45,8	49,5	
39,6	42,5	43,7	47,8	44,3	49,0	50,0	59,1	49,6	61,6	44,2	43,0	47,5	48,5	46,8	
37,0	42,7	41,2	48,4	42,0	50,5	48,8	64,4	48,0	67,2	41,3	44,8	45,2	51,0	44,0	
34,6	42,2	39,7	48,9	39,9	51,6			46,9	70,4	39,1	45,5	42,9	53,0	41,5	
32,5	41,8	37,6	49,1	37,5	52,5			45,7	74,4	36,6	46,2	40,5	53,5	39,6	
31,2	40,9	35,8	49,3	35,3	52,8			44,6	77,6	35,0	46,5	38,5	54,5	37,4	
29,3	40,1	33,8	48,8	33,2	52,8			43,7	80,4	33,2	46,5	36,6	55,4	35,5	
25,5	38,5														

*ε° is given for 3,4 N concentration at $-5°$.

TABLE 1 (continued)

t = 0°C						t = 0°C									
NaI		KCl		KI		LiCl		NaCl		NaI		KCl		KI	
c'	c''	c'	c''	c'	c''	c'	c''	c'	c''	c'	c''	c'	c''	c'	c''
45,3	42,6	45,5	42,9	45,7	43,1	52,5	40,0	52,7	40,1	52,7	40,2	53,2	40,6	53,6	40,7
45,4	42,8	45,4	43,7	45,8	43,8	50,3	40,4	52,1	40,6	52,6	40,8	52,7	41,5	53,1	41,5
44,9	44,0	45,4	45,0	46,3	44,8	48,6	41,0	51,3	41,8	52,2	42,0	52,4	43,7	52,9	43,6
44,5	44,8	45,3	47,6	46,6	47,9	45,5	41,4	49,5	43,0	50,1	43,4	51,5	46,0	52,3	47,2
43,7	45,2	44,8	51,3	45,8	51,5	42,9	41,7	46,7	43,7	48,1	45,0	50,2	50,8	50,8	51,0
42,2	45,7	44,3	53,8	45,2	54,5	40,2	42,0	44,5	45,4	45,4	46,1	48,6	54,8	48,9	55,8
40,5	45,9	43,7	57,0	44,4	58,7	38,0	41,7	42,3	46,9	43,5	47,4	48,2	58,8	48,0	60,0
38,5	46,7	43,2	60,0	43,6	62,5	35,5	41,3	40,4	46,4	41,3	48,0	47,2	62,9	46,8	64,8
36,4	46,4			42,5	65,2	33,4	40,7	38,4	46,4	39,0	48,8		65,0	45,5	68,4
34,9	46,4			41,5	68,3	31,2	39,8	36,3	46,9	36,8	49,4			44,6	72,0
32,9	45,9			40,0	70,4	29,5	38,8	34,8	46,6	34,5	49,5			43,3	75,1
31,4	45,6			39,3	72,8	27,8	38,0	33,3	45,6	32,6	49,2			42,0	78,2

t = 20°C						t = 40°C									
NaI		KCl		KI		LiCl		NaCl		NaI		KCl		KI	
c'	c''	c'	c''	c'	c''	c'	c''	c'	c''	c'	c''	c'	c''	c'	c''
31,4	62,3	31,4	62,2	31,4		64,5	22,3	64,6	22,8	64,5	21,9	64,4	22,0	64,5	22,1
32,7	61,2	33,5	61,3	33,6		62,1	24,6			62,5	25,5	62,4	25,4	62,1	25,7
35,2	59,6	37,5	59,4	37,7		59,3	28,7	58,8	29,9	59,8	31,4	60,9	33,0	60,5	32,7
39,4	57,2	44,1	57,0	44,0		55,3	34,5	56,1	37,8	55,7	39,3	58,3	43,8	57,5	43,5
43,5	55,4	49,7	55,3	50,5		51,3	39,3	53,3	44,6	52,6	47,1	56,6	53,5	55,4	54,0
47,5	53,9	57,0	53,7	57,6		48,4	43,7	50,6	51,5	49,6	54,0	55,7	63,5	53,5	64,9
50,4	52,9	62,3	52,1	63,8		45,6	47,0	48,5	57,2	47,2	60,1	54,9	72,0	52,5	73,5
53,3	52,0	67,9	50,7	70,0		43,25	50,1	46,4	60,8	45,0	64,9	54,0	79,6	51,4	81,7
55,7	—	—	49,5	75,5		40,9	52,7	44,7	64,6	43,2	68,4	53,1	86,1	50,8	88,3
57,6	—	—	48,5	80,3		38,6	53,8	43,0	67,2	41,3	72,0	—		49,6	94,3
58,3	—	—	47,4	84,0		37,0	54,5	41,4	68,4	39,5	73,1	—		48,8	98,9
59,0	—	—	46,4	87,2		35,5	55,2	39,8	70,7	38,4	74,6	—		48,0	103,0

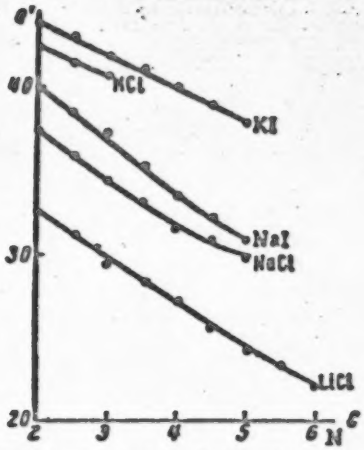

Fig. 1. Variation of ϵ' with concentration at − 5°.

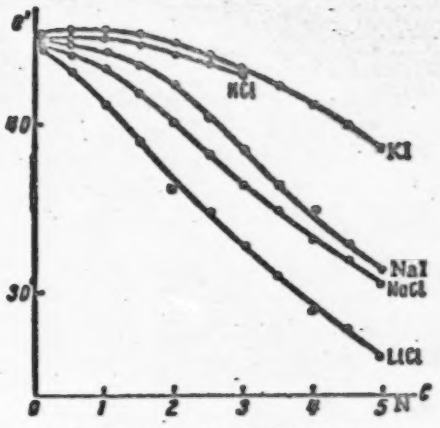

Fig. 2. Variation of ϵ' with concentration at 0°.

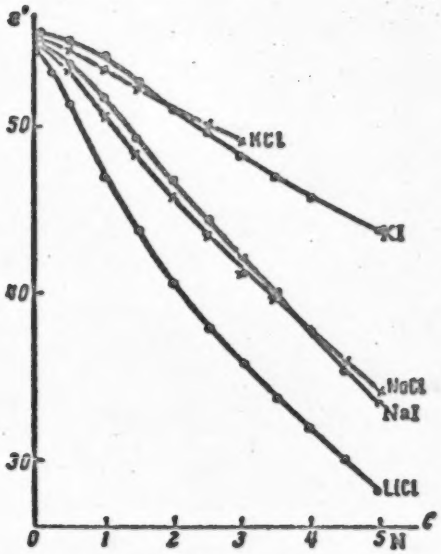

Fig. 3. Variation of ϵ' with concentration at 6°.

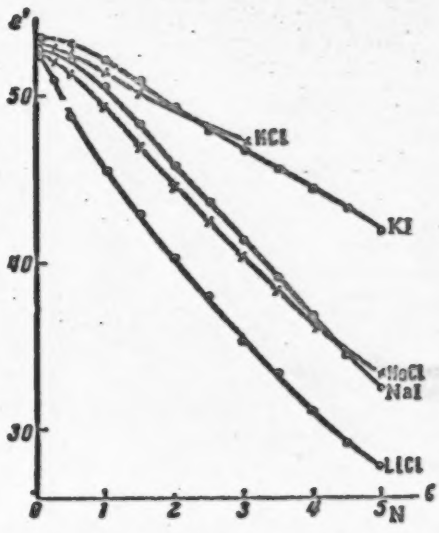

Fig. 4. Variation of ϵ' with concentration at 10°.

In the 5-20° temperature range the course of the DC − concentration relationship for iodides and chlorides undergoes inversion (Figs. 3-5). The point of intersection of the DC − concentration curves for these solutions is found at lower concentrations with increase of temperature. For example, the point of intersection of the $\epsilon' = f(C)$ curves for aqueous NaCl and NaI solutions corresponds to 4.3 N concentration at 6°, 3.8 N at 10°, and approximately 1.6 N at 20°. Similar results are obtained for KCl and KI solutions. The intersection of the $\epsilon' = f(C)$ curves corresponds to 2.5 N at 6°, 2 N at 10°, and at 20° the curves coincide over the 0.05 -1.1 N concentration range (here the DC differences are within the limits of experimental error).

Variations of ϵ'' (associated with dielectric losses) with concentration are given in Figs. 7-10 and Table 1.

The figures show that the values of ϵ'' (sum of the ionic conductivity and dipole relaxation losses) differ for solutions of different electrolytes and form the following sequence: $\epsilon''_{KI} > \epsilon''_{KCl} > \epsilon''_{NaI} > \epsilon''_{NaCl} > \epsilon''_{LiCl}$. This sequence holds over the entire temperature range studied. It corresponds to the low-frequency conductivities of these solutions.

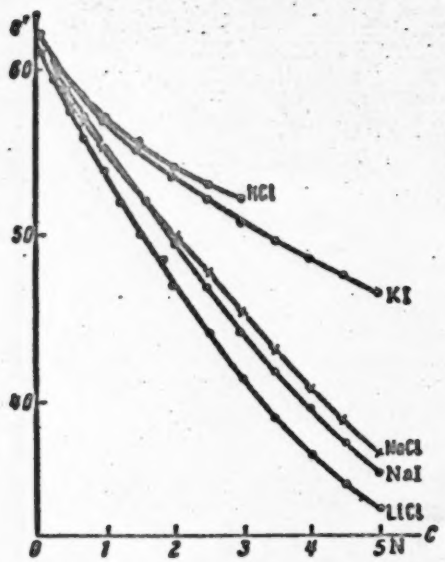

Fig. 5. Variation of ϵ' with concentration at 20°.

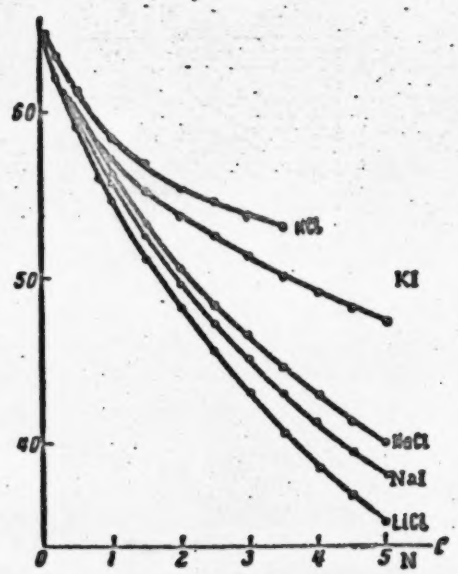

Fig. 6. Variation of ϵ' with concentration at 40°.

Calculations of the Relaxation Time

The relaxation time and the associated static DC ϵ_s were calculated by means of the modified Debye equations:

$$\varepsilon' = \varepsilon_\infty + \frac{\varepsilon_s - \varepsilon_\infty}{1 + \omega^2 \tau^2} \tag{1}$$

and

$$\varepsilon'' = \frac{(\varepsilon_s - \varepsilon_\infty)\,\omega\tau}{1 + \omega^2 \tau^2}, \tag{2}$$

where ϵ_∞ is the high-frequency DC which combines electronic and atomic polarization, ϵ_s is the static DC, τ is the relaxation time, and ω is the angular frequency.

The values of ϵ_∞, in accordance with Hasted and El Saben [8], were taken as 5.0 at 0° and 5.2 at 20°. In Eq. (2), for calculation of τ only the dipole component ϵ''_d of the imaginary part of the DC was used; this was calculated from the expression:

$$\varepsilon''_d = \varepsilon'' - 2\sigma_l / f,$$

where σ_l is the low-frequency conductance of the solution and f is the frequency of the external field. This approach is necessary because ϵ'' for solutions consists of two components: ϵ''_d, dielectric losses caused by dipole relaxation of molecules in rapidly alternating fields, and the losses $2\sigma_l/f$, associated with ionic conductance of the solutions. Naturally, only ϵ''_d is used in Eqs. (1) and (2) for calculation of τ.

For dilute solutions, ϵ''_d may be taken as approximately equal to ϵ'' for water [9]. However, as the solution concentration increases, the effect is tantamount to formation of new solvents with τ, ϵ_s and ϵ''_d differing from those of pure water. For example, the difference between ϵ''_d of aqueous NaCl solutions at 0° and ϵ'' of pure water is 1.2% at 0.05 N concentration, and 26% at 2 N concentration.

With regard to the applicability of Eqs. (1) and (2) for calculation of τ of aqueous electrolyte solutions at high concentrations, according to [8, 10, 11, 12] there is no reason for introducing any additional corrections.

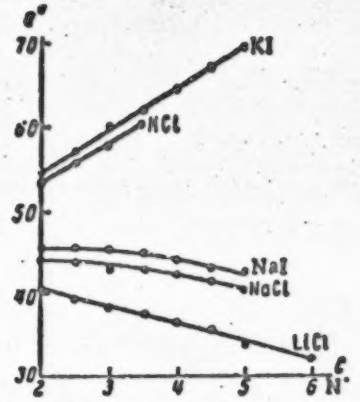

Fig. 7. Variation of ϵ° with concentration at -5°.

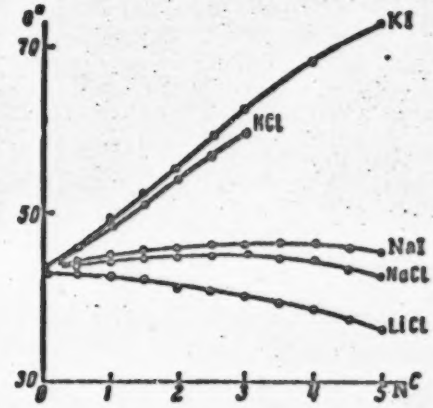

Fig. 8. Variation of ϵ° with concentration at 0°.

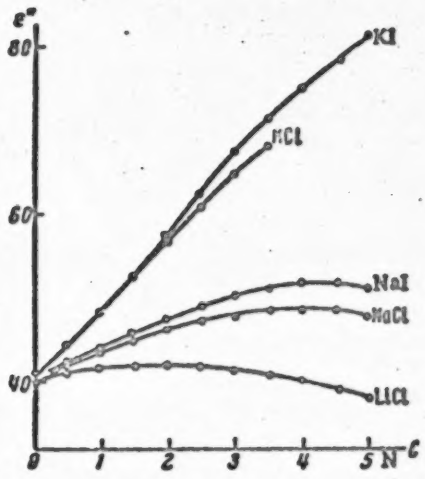

Fig. 9. Variation of ϵ° with concentration at 6°.

The calculated relaxation times (with the relevant experimental data) for different concentrations at 0° are given in Table 2.

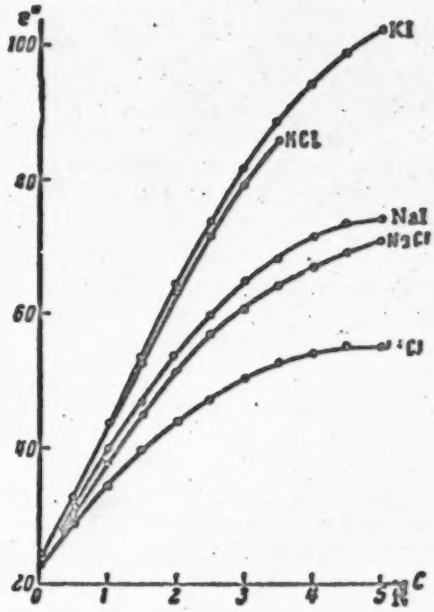

Fig. 10. Variation of ϵ° with concentration at 40°.

Discussion of Results

According to Hückel [13], ϵ° of aqueous electrolyte solutions falls with increasing concentration because the ions of the dissolved electrolyte penetrate into the water structure and cause orientation and polarization of the nearest solvent molecules. Therefore the influence of an external electric field on these molecules is considerably weakened, and polarization by an external field of a solvent containing ions is less than polarization of the pure solvent. Therefore the DC of the solution is less than the DC of the solvent and should decrease further with increasing concentration.

Hasted, Ritson and Collie [10] attempted to calculate the change of DC as a function of concentration by means of the following empirical relationship:

$$\varepsilon_s = \varepsilon_{s_0} - 2\delta C,$$

TABLE 2*

C	LiCl				NaCl				KCl				KI			
	ε_0	ε'_d	$2\alpha_E/l$	$\tau\times10^{-8}$	ε_0	ε'_d	$2\alpha_E/l$	$\tau\times10^{-8}$	ε_0	ε'_d	$2\alpha_E/l$	$\tau\times10^{-8}$	ε_0	ε'_d	$2\alpha_E/l$	$\tau\times10^{-8}$
0,05	89,0	42,0	0,51	18,4	87,0	41,8	0,57	17,4	89,3	42,2	0,7	17,8	90,1	42,4	0,72	18,0
0,2	86,3	40,8	1,85	17,3	85,0	40,8	2,12	16,8	86,6	41,0	2,65	17,0	86,4	41,0	2,75	17,0
0,5	81,4	38,4	4,2	16,9	81,0	38,2	4,96	16,1	82,4	39,6	6,4	15,9	82,0	38,1	6,7	15,7
1	74,8	34,9	7,63	16,2	74,7	35,0	9,0	15,5	76,4	35,2	12,5	15,0	76,0	34,5	13,4	14,3
2	61,6	28,1	12,8	15,2	64,0	29,4	15,6	14,0	66,6	29,5	24,3	12,6	65,2	27,7	26,8	11,5
3	53,3	23,9	16,4	14,5	55,0	23,6	21,0	13,2	58,1	24,3	35,7	11,0	57,3	23,0	39,5	10,0
4	45,2	19,7	18,9	13,8	48,0	20,2	24,1	11,7	—	—	—	—	50,1	17,7	50,6	8,1
5	38,9	16,4	20,2	13,0	41,7	16,6	25,7	11,0	—	—	—	—	44,4	13,5	59,3	6,9
6	35,3	14,5	20,5	12,6												

* Data for t = 0°.

where ϵ_s is the static DC of the solution, ϵ_{s_0} is the static DC of the solvent (water), $\delta = (\delta^+ + \delta^-)/2$, δ^+ and δ^- are coefficients representing polarization of the surrounding water volumes due to the positive and negative ions of the dissolved electrolyte, and C is the concentration in moles/liter.

These workers empirically found the following coefficients for aqueous NaCl solutions: $\delta^+ = -8$, $\delta^- = -3$. These values agree with experimental data only at concentrations up to 2 N. In the experimental selection of δ^+ and δ^- it is assumed that cations bind (saturate with their electric field) surrounding water molecules to a greater extent than do anions.

Figure 11 represents a model of the mutual orientation of cations (a) and anions (b and c) with their nearest water molecules. The positive charge of a cation is held more firmly (Fig. 11, a) by the two negative charges of a water molecule than the negative charge of an anion, which interacts mainly with one neighboring proton of a water molecule (Fig. 11, b). Therefore cations have a greater lowering effect on DC. It is assumed in [10] that if large anions are present in solution they interact simultaneously with pairs of protons in water molecules (Fig. 11, c). In this case the anions, despite their size, have a stronger orientating and polarizing effect on the surrounding water molecules than do smaller anions interacting with single nearest protons in water molecules (Fig. 11, b). It follows that solutions containing large anions (I^-) should have lower DC at a given concentration than solutions with smaller anions (Cl^-). This model appears to give a correct picture of the interaction of cations and anions in dissolved electrolytes with water molecules, and is in agreement with our experimental results (with the exception of measurements at low temperatures).

As already stated, at low temperatures chlorides have lower ϵ' than iodides, and the course of changes of ϵ' for iodides and chlorides was found to undergo inversion in the 5-20° range. These low-temperature results require some modification of the Hasted, Ritson, and Collie model described above. If it is assumed that at low temperatures or low concentrations anions are incapable of overcoming completely the hydrogen bonds in the ice-like structure and of causing reorientation (rotation) of the molecules at the coordination tetrahedrons of water, then anions of large and of small radius interact only with single nearest positive charges in water molecules. By this hypothesis, anions of small radius must evidently saturate (bind) water molecules to a greater extent than large anions. The same conclusion may be reached from the results of DC measurements of aqueous electrolyte solutions carried out by Carrelli and Della Caggia [14] by another method and in a different frequency range (8 Mc/sec). In the case of dilute solutions at room temperature they found that DC decreased with increasing concentration, and the DC values for different electrolyte solutions were in the following sequence: $\epsilon'_{KI} > \epsilon'_{KBr} > \epsilon'_{KCl} > \epsilon'_{KF}$. This result corresponds to our low-temperature measurements of DC of concentrated solutions.

At higher temperatures and concentrations, when considerable numbers of molecules are present in the structure voids, the orientating effect of large anions becomes greater, because under these conditions the molecules undergo reorientation more freely and interact with large anions to the same extent by both their positive charges (Fig. 11, c).

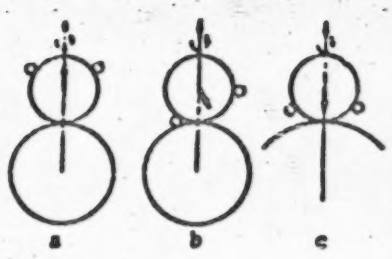

Fig. 11. Hydration models: a) Cations; b and c) anions.

Symikov [15] refers to the relatively weak orientating and polarizing action of anions on surrounding water molecules. He showed by a spectroscopic investigation that the bonds between water molecules and anions are similar in type to the bonds between molecules in pure water.

The existence of fourfold coordination in the structure of highly concentrated aqueous solutions of strong electrolytes has been confirmed by a number of experimental and theoretical investigations [1, 16, 17, 18]. Shakhparonov [16, 17] showed that in addition to concentration, density, and orientation fluctuations in solutions, a nonuniform distribution of matter exists in solutions at certain temperatures, and is relatively stable. Smolilov [1] concluded that the structures of aqueous electrolyte solutions at low temperatures probably remain similar to the structure of the components: the structure of a dilute solution is similar to that of water, and that of a concentrated solution resembles the structure of a solid hydrate. Further, Danilov and Neimark [18] showed experimentally that decrease of temperature restores the second maximum on the curves for the intensity of x-ray scattering by aqueous LiCl and NaCl solutions at concentrations above 4 N. This maximum is characteristic of fourfold coordination of molecules in the structure of water.

The variation of ϵ' of solutions in the 5-20° range, the observed inversion of the course of ϵ' for iodides and chlorides in that range (Figs. 3-5), and the displacement of the intersection point of the $\epsilon' = f(C)$ curves for iodides and chlorides toward lower concentrations with increase of temperature are consistent with the view put forward above that at relatively low temperatures orientational polarization of surrounding water molecules by large anions is weakened.

It follows from the work of Samoilov [1] and Stewart [19] that increase of concentration produces changes in the solvent structure which are similar to the changes taking place on rise of temperature (anions are considered here). In our case as the temperature rises an increasing number of large anions interact with two protons of the nearest H_2O^* molecules, thereby diminishing polarization of the solvent by the external field. This results in a sharper decrease of ϵ' in solutions containing large anions. Since temperature and concentration increases act in the same direction, weakening intermolecular bonding in the solvent, it is natural to expect that with increase of temperature the point of intersection of the $\epsilon' = f(C)$ curves for chloride and iodide solutions would be shifted toward lower concentrations. This is an example of the "structural temperature" concept introduced by Bernal and Fowler [20].

Let us consider in more detail the character of the ϵ' – concentration curves at temperatures close to 0°. These curves differ from the corresponding curves for higher temperatures by a lesser slope relative to the abscissa axis and the absence of a decrease of ϵ' for KI and KCl solutions in the concentration range from 0.05 to 1.5 N. To account for this result we must take into account the relationship between the relaxation time and the half period of the external alternating field. Calculation shows that in a field of the given frequency (9400 Mc/sec) the relaxation time at temperature close to 0° is greater than the half period of the applied field. Under these conditions orientational polarization is not completed during one half periodand ϵ' has relatively low values. Addition of ions, like increase of temperature, shortens the relaxation time and thereby favors polarization of the solvent, because polarization proceeds to a greater extent during one half periodof the external field.

The orientation effect on the ion fields on the neighboring molecules, which opposes polarization of the solution may in some cases be almost completely compensated by increased polarizability of the remaining water, less bonded by ions. This occurs because of more complete development of polarization during one half period of the applied field, with a corresponding decrease of the relaxation time. In such cases ϵ' of solutions may remain unchanged or may even increase with increasing concentration. In the range of higher temperatures the change of relaxation time with increasing concentration is less (the structure is close packed), and the orientating effect of the ion fields on the surrounding water molecules predominates, causing a corresponding decrease of DC.

The difference in the course of the $\epsilon' = f(C)$ curves for aqueous solutions of KI, KCl and NaCl, LiCl (ϵ' for NaI solutions occupies an intermediate position) is explained by unequal changes of the relaxation time due to these electrolytes. The greatest change of the relaxation time as a function of concentration was found for KI and KCl solutions. These are followed, in order of decreasing $\Delta\tau$, by NaI, NaCl, and LiCl solutions (Figs. 12, and 13). Apparently the large K^+ and I^- ions change the relaxation time and at the same time break down the solvent structure to a greater extent than the relatively small Li^+, Na^+, and Cl^- ions. Neverthless, cations play the predominant role in

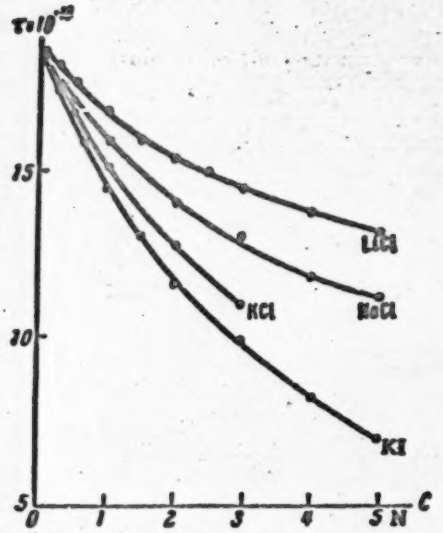

Fig. 12. Variation of τ with concentration at 0°.

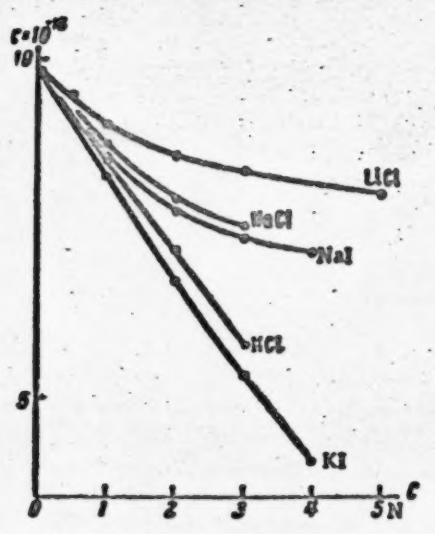

Fig. 13. Variation of τ with concentration at 18°.

this process. Solutions containing K^+ cations differ very sharply from the other solutions investigated not only by the magnitude of the change in the relaxation time but also by the magnitude of the dielectric losses (Figs. 7-10). Losses due to dipole relaxation are of almost the same magnitude for all the solutions studied, and decrease with increasing concentration. The total losses ϵ'' in LiCl, NaCl, and NaI solutions at low temperature also decrease (Fig. 7) or increase slowly (Figs. 8, 9) with increasing concentration, passing through a flat maximum. This maximum is shifted toward higher concentrations with rise of temperature. Evidently ϵ_d for such solutions are comparable with the losses due to ionic conductivity and even exceed them (ϵ'' decreases). Conversely, the considerable increase of ϵ'' with concentration observed for KI and KCl solutions over the entire temperature range studied is probably attributable to the higher conductivity due to the K^+ cation when shielding of its charge by the surrounding molecules is weakened; i.e., it may be attributed to a difference in the character of the hydration of this cation – negative hydration [1].

SUMMARY

1. The DC of aqueous electrolyte solutions at high concentrations are lower than the DC of water and decrease with increasing concentration.

2. The changes of DC of solutions with concentration and temperature differ for different aqueous electrolyte solutions and are determined to a considerable extent by the radii of the ions (especially cations) of the dissolved electrolytes and by the nature of their hydration.

3. The change of DC of solutions as a function of anion radius is not the same at low as at high temperatures. At low temperatures solutions containing small anions have lower DC than solutions containing large anions. At higher temperatures the reverse is true; in the 5-20° range the course of DC variations for iodides and chlorides undergoes inversion, accompanied by a shift of the point of intersection of the respective curves toward lower concentrations with rise of temperature.

4. Increase of concentration, like rise of temperature, shortens the relaxation time for solvent polarization in solutions.

5. Solutions containing potassium cations exhibit the greatest changes of relaxation time with concentration and the greatest dielectric losses; this is probably due to the negative hydration of these cations.

I am deeply grateful to Prof. P. V. Golubkov and Dr. Chem. Sci. O. Ya. Samoilov for discussion and valuable advice.

LITERATURE CITED

1. O. Ya. Samoilov, Structure of Aqueous Electrolyte Solutions and Hydration of Ions [in Russian] (Izd. AN SSSR, Moscow, 1957).
2. O. Ya. Samoilov, Zh. Fiz. khimii, 20, 12, 1411 (1946).
3. L. Holl, Phys. Rev. 73, 7, 775 (1948).
4. I. G. Mikhailov, Yu. P. Syrnikov, Zh. strukt. khimii 1, 1, 12 (1960).
5. Yu. V. Gurikov, Zh. strukt. khimii 1 3, 286 (1960).
6. Le Bot, Le Montagner, Compt. rend. 236, 469 (1953).
7. Yu. P. Radin, Izv. vyssh. uch. zav., Radiofizika 1, 5-6, 177 (1958).
8. J. B. Hasted, S. H. M. El Saben, Trans. Faraday Soc. 49, 9 (1953).
9. M. Divil'kovskii, D. Mash, Zh. éksperim i teor. fiziki 10, 520 (1940).
10. J. B. Hasted, D. M. Ritson, C. H. Collie, J. Chem. Phys 16, 1 (1948).
11. A. Saxton, J. Lane, Wireless Engr. 29, 269 (1952).
12. J. A. Lane, J. A. Saxton, Proc. Roy. Soc. 214, 1119 (1952).
13. P. Debye, E. Hückel, Phys. Z. 24, 185 (1923).
14. A. Carrelli, L. Della Caggia, Nuovo cimento 14, 1, 161 (1959).
15. Yu. P. Syrnikov, Dokl. AN SSSR 118, 4, 760 (1958).
16. M. I. Shakhparonov, Introduction to the Molecular Theory of Solutions [in Russian] (Izd. tekhn.-teor. lit., Moscow, 1956).
17. M. I. Sharkparunov, N. T. Shlenkina, Dokl. AN SSSR 96, 55 (1954); Zh. fiz. khimii 28, 1910 (1954).
18. V. I. Danilov, Structure and Crystallization of Liquids [in Russian] (Izd. AN UkrSSR, Kiev, 1956).
19. G. W. Stewart, Phys. Rev. 35, 1462 (1930).
20. J. D. Bernal, R. H. Fowler, J. Chem. Phys. 1, 515 (1933); Usp. fiz. nauk 14, 586 (1934).

All abbreviations of periodicals in the above bibliography are letter-by-letter transliterations of the abbreviations as given in the original Russian journal. *Some or all of this periodical literature may well be available in English translation.* A complete list of the cover-to-cover English translations appears at the back of this issue.

STRUCTURAL PRESSURE OF AQUEOUS ELECTROLYTE SOLUTIONS

A. V. Kopeliovich

Geological Institute, Academy of Sciences, USSR
Translated from Zhurnal Strukturnoi Khimii, Vol. 2, No. 3, pp. 279-281,
May-June, 1961
Original article submitted February 2, 1961

The influence of ions on translational motion of nearest water molecules is compared with the influence of pressure. The concept of structural pressure is introduced. The structural pressure of a solution is raised by ions with positive hydration and lowered by ions with negative hydration. These changes are manifested in the different stabilities of a number of minerals in the upper and lower zones of the sedimentary layers of the earth's crust and in the vertical hydrochemical zonality of subterranean waters.

The classic work of Bernal and Fowler [1] has had a great influence on the development of modern theories of the structure of water and aqueous solutions. They considered that many properties of water and aqueous electrolyte solutions can be satisfactorily explained on the hypothesis that water has an internal structure with three main forms of molecular arrangement: water I with structure of the ice (tridymite) type which is relatively rare and which is present in certain amounts at temperatures below 4°; water II with structure of the quartz type, predominant at room temperatures, and water III with a close-packed structue, predominant at high temperatures over a certain range below the critical point (374°).

The state of water, according to Bernal and Fowler, is determined by the equilibrium between these three types of structure. The equilibrium shifts in the direction I → II → III, i.e., toward close packing, with rise of temperature. According to these authors, ions in dilute aqueous solutions shift the equilibrium between structures I, II, and III either in the direction of the close-packed structue (water III) or in the direction of the ice tridymite structure (water I); i.e., their effects on water are analogous to increase or decrease of temperature.

Bernal and Fowler examined the effects of various ions on the structure of water in dilute solutions and put forward the concept of the structural temperature of solutions. This is defined by them as the temperature at which pure water has an internal structure and properties dependent on it corresponding to the structure and properties of the ionic solution the structural temperature of which is being defined. Changes in the structural temperature of the solvent have a distinct influence on viscosity, temperature of maximum density, and a number of other properties [1].

Ions may either raise or lower the structural temperature of a solution in accordance with their influence on the structure of water. According to Bernal and Fowler, ions which lower the structural temperature include Mg^{2+} Ca^{2+}, Li^{+}, and ions which raise it include Cs^{+}, Rb^{+}, Cl^{-}, and I^{-}.

The existence of an equilibrium between three types of structure in water was not confirmed by subsequent x-r. y investigations [2]. In the modern theory [3], short-range order in water corresponds to a tetrahedral ice structure, partially disordered by thermal motion of the molecules. This, according to Samoilov [3,4], is accompanied by filling of the voids in the tetrahedral structue, which intensifies with rise of temperature.

According to Samoilov, hydration of ions in aqueous solutions does not consist of binding of a certain number of water molecules by each ion; it consists primarily of a change, under the influence of the ions, of the potential barriers separating neighboring equilibrium positions of the water molecules. The translational motion (frequency of activated transitions) of water molecules in the solution nearest to the ions alters correspondingly. Multivalent and small univalent cations weaken the translational motion of the nearest water molecules; large univalent ions intensify it. The former case represents positive and the latter, negative hydration. Cations with positive hydration include Mg^{2+}, Ca^{2+} and other multivalent ions, Li^{+}, and to a lesser extent Na^{+}. Negative hydration is characteristic of K^{+}, Rb^{+}, and Cs^{+} cations. The anions Cl^{-}, Br^{-}, I^{-}, HSO_4^{-} have negative hydration, and the anions CO_3^{2-}, HCO_3^{-} SO_4^{2-} have positive hydration.

Thus, hydration is a change in the mobility of water molecules under the influence of ions. Since the mobility of water molecules is also changed with change of temperature, it is evident that the concept of structural temperature introduced by Bernal and Fowler is fully consistent with Samoilov's views on the structure of aqueous electrolyte solutions and ion hydration, and retains its significance.

The concept of structural temperature may be extended to problems associated with the influence of pressure on the thermal motion of particles in solution. External pressure influences the translational motion of the particles in a liquid. If the structure of the liquid is fairly dense, increase of pressure weakens the translational motion of its particles. One effect of this is the increase of liquid viscosity with pressure. This type of viscosity change is observed in nearly all liquids. In the case of water, which has tetrahedral structure, increase of pressure leads to increased mobility of the molecules, since its open structure breaks down under increased pressure, filling of the voids with molecules increases, and the bonds between the molecules break down. This accounts for the anomalous viscosity of water: between 0 and 20-30° its viscosity decreases steadily with rise of pressure. It was also shown that the dependence of the coefficient of self-diffusion of water on pressure is likewise anomalous: the coefficient of self-diffusion of water increases with pressure over certain temperature and pressure ranges [3].

As regards the molecules of water in solution which are nearest to the ions and are in their electrostatic fields, which, of course, are nondirectional in character, the conditions of their translational motion are such that increase of pressure merely weakens their translational motion, i.e., its effect on them is the same as on the translational motion of molecules of most other liquids. Therefore increase of external pressure weakens the translational motion of water molecules nearest to the ions, and, conversely, decrease of external pressure intensifies this motion.

Comparison of the effects of external pressure and of ions on the translational motion of water molecules nearest to the ions in solution shows that the effect of ions with positive hydration on these molecules is similar to the effect of increased pressure, i.e., the translational motion is weakened, whereas ions with negative hydration have the same effect as decreased pressure and intensify translational motion.

We thus have the concept of structural pressure of ionic solution, analogous to the Bernal and Fowler concept of structural temperature. The structural pressure is determined by the external pressure at which the magnitudes of the potential barrier separating neighboring equilibrium positions of water molecules in pure water and of water molecules nearest to the ions in a given ionic solution are equal, and the frequency of the translations is correspondingly the same in both cases. This leads to the conclusion that ions with positive hydration raise the structural pressure of a solution whereas ions with negative hydration lower it. If the consideration is confined to translational motion of water molecules nearest to the ions in solution, then increase of structural pressure corresponds to a decrease of structural temperature, and vice versa.

The concept of structural pressure may prove useful in clarification of certain problems associated with the effects of pressure on the solubilities of various substances and on ion mobilities in aqueous solutions. Let us consider the equilibrium between a solid phase containing different ions and a solution with these ions. In accordance with the Le Chatelier principle, increase of pressure should cause ions which lower the structural pressure of the solution, i.e., ions with negative hydration, such as K^+, Rb^+, Cs^+, Cl^-, Br^-, I^-, to pass into solution. Conversely, if the external pressure is decreased ions with positive hydration, Mg^{2+}, Ca^{2+}, HCO_3^-, CO_3^{2-}, SO_4^{2-}, etc., are preferentially dissolved.

Geological data indicate that this is precisely the state of affairs under natural conditions. It is known that in zones near the surface, carbonate and sulfate minerals and rocks have low stability and pass into solution fairly readily, whereas in deep zones of the sedimentary layer carbonates and sulfates are very resistant to the action of subterranean waters. At the same time, new formations of carbonates (calcite, dolomite, ankerite, siderite) and sulfates (anhydrite, celestine, baryte) are common in deep zones.

The concept of structural pressure provides a ready explanation of the well-known vertical hydrochemical zonality of subterranean waters in artesian wells, with replacement of hydrocarbonate waters by sulfate and then chloride waters, and enrichment of the latter with Br^- and I^- with increasing depth. This zonality corresponds to increasing negative hydration of the anions commonly present in natural waters, in the sequence HCO_3^-, SO_4^{2-}, Cl^-, Br^-, I^-. The structural pressure of a solution progressively diminishes with increasing negative hydration of a given anion, so that under the influence of a pressure gradient ions with negative hydration are displaced in solution, in accordance with the Le Chatelier principle, in the direction of increasing pressure. An analogous tendency is observed in the distribution of cations between hydrochemical zones in accordance with decreasing positive hydration

in the series Mg^{2+}, Ca^{2+}, Na^{+}, Sr^{2+}, Ba^{2+}, K^{+}. The greater the positive hydration of a cation, the more does it increase the structural pressure of the solution. The potassium ion has negative hydration. The low content of this ion in waters of the chloride zone is due to predominant absorption of potassium ions by clay minerals; this also follows from the modern views on the hydration of ionic solutions [5]. It should be noted that the vertical hydrochemical zonality of underground waters was considered earlier on a similar basis by Samoilov and Sokolov [6].

LITERATURE CITED

1. J. D. Bernal, R. H. Fowler, J. Chem. Phys. 1, 515 (1933); Usp. fiz. nauk 14, 586 (1934).
2. J. Morgan, B. E. Warren, J. Chem. Phys. 6, 666 (1938).
3. O. Ya. Samoilov, Structure of Aqueous Solutions and Ion Hydration [in Russian] (Izd. AN SSSR, Moscow, 1957).
4. O. Ya. Samoilov, Zh. fiz. khimii 20, 12, 1411 (1946).
5. O. Ya. Samoilov, Izv. AN SSSR. Otd. khim. n. 5, 931 (1959).
6. O. Ya. Samoilov and D. S. Sokolov, Izv. AN SSSR. Otd. khim. n. 3, 257 (1957).

All abbreviations of periodicals in the above bibliography are letter-by-letter transliterations of the abbreviations as given in the original Russian journal. *Some or all of this periodical literature may well be available in English translation.* A complete list of the cover-to-cover English translations appears at the back of this issue.

INVESTIGATION OF NEGATIVE IONS OF CERTAIN AROMATIC COMPOUNDS BY THE ELECTRON PARAMAGNETIC RESONANCE METHOD

S. P. Solodovnikov

Institute of Chemical Physics, Academy of Sciences, USSR
Translated from Zhurnal Strukturnoi Khimii, Vol.2, No. 3, pp. 282-292, May-June, 1961
Original article submitted March 5, 1960

The spectra of 26 aromatic anions were obtained and analyzed. In monoalkyl benzene derivatives the unpaired electron density is considerably less at the para-carbon atom than at the others. It is shown that electron transfer can occur not only along systems of conjugated double bonds but also along chains of single bonds (diphenylmethane and dibenzyl anions). Nitrogen-containing heterocycles can form stable anions. The relative stabilities of different aromatic anions were investigated, and the kinetics of decay of these anions was studied.

Solutions of alkali metals in ammonia, amines, and certain ethers have been studied repeatedly [1], because such solutions are being increasingly used as media for reduction of aromatic and unsaturated hydrocarbons and for many reactions of chemical synthesis [2]. When an alkali metal dissolves in ammonia and certain amines it dissociates into cations and electrons, as is shown by the electrical conductance and paramagnetism of such solutions. These systems can therefore serve as electron donors for aromatic and unsaturated compounds. Interaction of aromatic compounds with electrons of alkali metals leads to formation of aromatic anions – Ar^- radicals. It is now accepted that reduction of aromatic hydrocarbons in liquid ammonia and certain amines in presence of alkali metals and alcohols is represented by the following mechanism:

$$Ar + e \rightleftarrows Ar^- + ROH \rightleftarrows \cdot ArH + RO^- \xrightarrow{e} ArH^- \rightarrow ArH_2 + RO^-.$$

Benzene is thus reduced to cyclohexane and cyclohexene.

Naphthalene anions were used as initiators in polymerization of styrene, butadiene, and isoprene [3]. It is presumed that the initiation stage in these reactions is electron transfer from the anion to the monomer. Dainton [4] reported the preparation of polystyrene of high molecular weight (mol.wt. $7 \cdot 10^5$) by polymerization of styrene in tetrahydrofuran and in 1, 2-dimethoxyethane in presence of dissolved potassium.

The electron paramagnetic resonance spectra of certain aromatic anions (naphthalene, diphenyl, benzene, toluene, xylenes) dissolved in 1, 2-dimethoxyethane, tetrahydrofuran, and dioxane have been investigated [5, 6, 7]. However, the available literature data on the structure and properties of aromatic anions are inadequate and, as will be shown, in some cases erroneous.

The present communication deals with a study by the EPR method of the structure and properties of certain organic and heterocyclic anions*.

EXPERIMENTAL

The selected solvent was 1, 2-dimethoxyethane, which is the most convenient ether for preparation of both polycyclic and monocyclic aromatic anions. Whereas solvents such as tetrahydrofuran and dioxane can be used with equal success for preparation of naphthalene anions, 1, 2-dimethoxyethane is more convenient for preparation of benzene, toluene, and xylene anions. The anions were prepared in evacuated ampoules with capillary tubes for measurements in the EPR spectrometer. The concentrations of the aromatic hydrocarbons were varied from 1 to 0.05 M.

* A brief communication by V. V. Voevodskii, S. P. Solodovnikov, and V. M. Chibrikin on EPR spectra of alkyl-substituted benzenes, stilbene, and dibenzyl was published in Dokl. AN SSSR 129, 5, 1082 (1959).

The alkali metal used was metallic potassium. Anions of benzene and alkyl-substituted benzenes, which are unstable at room temperature, were prepared at temperatures between − 20 and − 70°. The spectra of such anions were measured at temperatures between 0 and − 70°; cold nitrogen was blown through the resonator for this purpose. The temperature during the experiments was measured and regulated to an accuracy of about 2-4° by means of a thermocouple near the specimen in the resonator. The EPR-2 spectrometer was used for all the measurements.

RESULTS

1. Structure of Aromatic Anions

Studies of the EPR spectra of aromatic anions showed that at concentrations below 10^{-3} M they have hyperfine structure (HFS) due to the interaction of the unpaired electron with the magnetic moments of the protons in the benzene ring [5, 6, 7]. The mechanism of this interaction was considered by McConnell, who showed that hyperfine splitting is due to indirect interaction of an unpaired electron in the π system with the C−H bond.

The simplest aromatic anion is the benzene anion; Fig. 1 shows that its spectrum consists of seven hyperfine structure components. The intensity distribution in the spectrum conforms to a binomial law, 1 : 6 : 15 : 20 : 15 : 6 : 1, which is evidence of the interaction of the unpaired electron with six equivalent protons. The distance betwen the components is 3.75 oe. The splitting a_i and the spin density ρ_i of the unpaired electron at the corresponding carbon atom are connected by the empirical relationship $a_i = \rho_i Q$. As all the cabon atoms in the benzene molecule are equivalent, the spin density of the unpaired electron at one carbon atom is 1/6 = 0.16, which gives Q = 22.5 oe. This value will be used in subsequent calculations of spin densities in other anions.

We also investigated various monoalkyl derivatives of benzene with the following substituents: $-CH(CH_3)_2$; $-C_6H_{11}$; $-C(CH_3)_3$; $-CH_3$; $-C_2H_5$.

Figure 2 shows the spectrum of the negative ion radical of cumene. The spectrum consists of five lines with binomial intensity distribution 1 : 4 : 6: 4 : 1 and with splitting of 4.5 oe; each line is split into a doublet with ~ 1 oe between the components. The presence of five components with binomial intensity distribution is evidence of the interaction of the unpaired electron with four equivalent protons which, in accordance with the structure of the cumene molecule, are the hydrogen atoms in the ortho and meta positions. In accordance with the observed splitting, the density of the unpaired electron at the ortho and meta carbon atoms is 0.2. Splitting into a doublet may be due either to the proton in the para position or to the α proton of the substituent. To clarify this point, we studied the spectrum of tert-isobutylbenzene, which does not contain α protons; no additional splitting into a doublet was observed. This suggests that in the spectra of the negative cumene and cyclohexylbenzene ions (the spectrum of cyclohexylbenzene is analogous to the spectrum of cumene) this splitting is caused by α protons of the substituent.

The EPR spectra of toluene and ethylbenzene anions were also studied. The spectrum of toluene (Fig. 3) consists of five principal lines with binomial intensity distribution and 4 oe splitting. Each line of the quintuplet is additionally split into eight components. This splitting is due to interaction of the unpaired electron with protons of the methyl substituent and with the proton in the para position. The splitting at the protons of the methyl substituent is 1.5 oe, and that due to the proton in the para position is 0.5 oe. It should be noted that no additional splitting at the methyl group protons and the proton in the para position was reported in [7]. The results obtained in the present investigation give a more complete picture of the spin density distribution in the toluene anion. The spectrum of ethylbenzene can be interpreted analogously to the spectrum of toluene.

The presence of five components in the EPR specta of these negative ions of monosubstituted alkyl derivatives of benzene indicates that in all these radicals the carbon atoms in the ortho and meta positions are equivalent. The density of the unpaired electron at the carbon atom linked to the substituent is the same as (or even higher than) the density of the unpaired electron in the ortho and meta positions. The basis for this conclusion is that the sum of the spin densities in the ortho and meta positions is considerably less than unity. At the same time it was shown that there is little or no splitting due to protons in the para position. This is due to the orientation effect of the alkyl substituent, which leads to this distribution of spin density.

The disubstituted benzene derivatives studied were ortho-, meta-, and para-xylene. The spectrum of p-xylene consists of five lines, with binomial intensity distribution and with splitting of 4 oe. The spectrum of the o-xylene anion consists of seven HFS lines with binomial intensity distribution and 3.8 oe splitting. This leads to the conclusion that in the case of o-xylene the HFS is due to six protons of the methyl groups. The spectrum of m-xylene is more complex, indicating that both the protons of the ring and the protons of methyl substituents are involved in the splitting. The authors of [7] consider that the spectra of p- and o-xylene ions consist of five lines, and this, in their

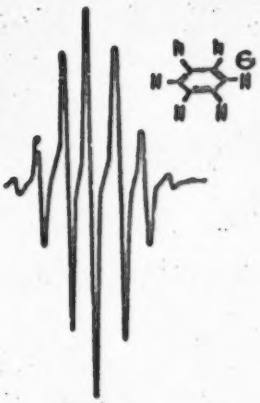

Fig. 1. EPR spectrum of the benzene anion.

Fig. 2. EPR spectrum of the cumene anion.

Fig. 3. EPR spectrum of the toluene anion.

opinion, makes conclusive interpretation of the spectra difficult. Our result explains the gradual change in the spectrum in the sequence from p- to m- and then o-xylene.

The trisubstituted benzene derivative studied was the mesitylene anion; its spectrum consists of seven components with splitting of about 3 oe, which has no simple explanation because this anion contains an odd number of equivalent protons. In subsequent discussion of this result, additional considerations will be put forward.

We attempted to obtain the negative hexamethylbenzene ion, but measurements showed that this ion is not formed in any appreciable amounts under the conditions used.

Dimesitylethane ions are not obtained in appreciable amounts either. These results are evidently due to the increase of the negative charge of the benzene nucleus with increase in the number of substituents, which diminishes the stability of the corresponding anions.

The diphenyl derivatives investigated were dimesitylene and p-ditolyl; the spectrum of the former anion consists of seven components and that of the latter, of 13; the intensity distribution in the spectrum of the ditolyl anion is not binomial (Fig. 4). Analysis of the spectra of these anions is based on the distribution of the unpaired electron density in the diphenyl anion, which, as has been shown [9], corresponds to the following scheme.

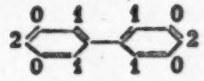

This distribution of spin density leads to multiple splitting, to superposition of the lines, and to breakdown of the binomial law. Therefore the seven lines in the spectrum of the dimesitylene anion can probably be assigned to the six protons of the methyl groups in the para position to the phenyl substituent. No splitting is observed at the protons of the other methyl groups.

The spectrum of p-ditolyl was analyzed on the same principles. Assuming that the splitting at the protons of the methyl groups (4.6 oe) is double the splitting at the protons in the ortho positions (2.3 oe) relative to the phenyl ring, we have 17 lines with the following intensity distribution: 1 : 4 : 12 : 28 : 52 : 84 : 116 : 140 : 150 : 140 : 116 : 84 : 52 : 28 : 12 : 4 : 1. With this distribution of the intensities of the individual components and the final breadth of the lines it is impossible to observe all the components, and evidently two components are missed at each edge. The remaining 13 components would have the following intensity distribution: 1 : 2.3 : 4.35 : 7 : 9.7 : 11.7 : 12.5 : 11.7 : 9.7 : 7 : 4.35 : 2.3 : 1. The intensity distribution found by us from the spectrum of the p-ditolyl anion (1 : 2.3 : 4.67 : 7.65 : 10.3 : 12.3 : 13.6 : 12.3 : 10.3 : 7.65 : 4.67 : 2.3 : 1) is in fairly good agreement with the theoretical.

2. Electron Transfer

One problem associated with the structure of aromatic anions is that of electron transfer along chains of conjugated and saturated bonds from one phenyl ring to another. To clarify this question, we studied the spectra of anions of stilbene, azobenzene, azoxybenzene (anions with chains of conjugated bonds) and diphenylmethane, dibenzyl, $p\text{-}CH_3-C_6H_4-CH_2-\underset{\displaystyle C_6H_5}{CH}-CH_2-C_6H_4-CH_3$ and $C_6H_5-CH_2-CH_2-\underset{\displaystyle CH_2-CH_2-C_6H_5}{CH}-CH_2-C_6H_5$ (anions with chains of saturated bonds).

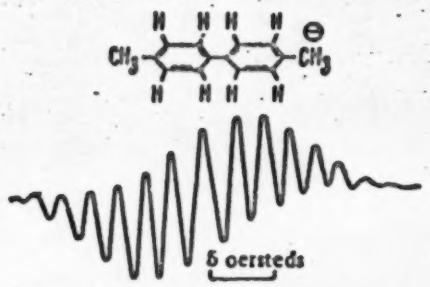

Fig. 4. EPR spectrum of the ditolyl anion.

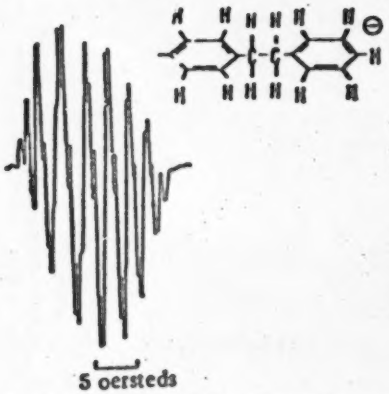

Fig. 5. EPR spectrum of the dibenzyl anion.

Analysis of the spectrum of stilbene indicates the possibility of electron delocalization both along the benzene rings and along chains of conjugated bonds; the spin density is apparently localized mainly at the carbon atoms of the bridge groups.

Analysis of the spectra of azo- and azoxybenzene leads to a similar conclusion concerning total delocalization of the electron in both rings. In the case of anions with chains of saturated bonds, complete breakdown of conjugation between the rings might be expected. Figure 5 (the spectrum of the dibenzyl anion, which is analogous to the spectrum of the diphenylmethane anion) shows that the spectra of the diphenylmethane and dibenzyl anions each have nine principal lines with splitting of 1.9 and 2.5 oe; these can best be explained if their appearance is associated with eight ortho and meta protons. If the electron was localized in one ring only, the spectrum would be analogous to the spectrum of ethylbenzene. This is found to be the case with $p\text{-}CH_3\text{-}C_6H_4\text{-}CH_2\text{-}CH(C_7H_{15})\text{-}CH_2\text{-}C_6H_4\text{-}CH_3$ and $C_6H_5\text{-}(CH_2)_2\text{-}CH(CH_2\text{-}CH_2\text{-}C_6H_5)\text{-}CH_2\text{-}C_6H_5$, the spectra of which have five lines with binomial intensity distribution and with 3.6 oe splitting. It is interesting to note that the splitting in the spectra of alkyl-substituted benzene anions is double the splitting in the spectra of diphenylmethane and dibenzyl anions. The electron exchange frequency between the rings can also be estimated from the magnitude of the splitting in the spectra of diphenylmethane and dipenzyl anions; this was found to be of the order of $10^7 - 10^8$ sec^{-1}.

3. Anions of Heterocyclic Compounds

We attempted to prepare, in 1, 2-dimethoxyethane solution, anions of certain heterocyclic compounds: furan, thiophene, selenophene, pyridine, and quinoline. Of these, only pyridine and quinoline gave paramagnetic anions with spectra having hyperfine structure. Thus, the spectrum of pyridine contains about 50 HFS lines, which is near to the theoretical maximum of 54. It follows that the α, β and γ hydrogen atoms in the pyridine anion are not equivalent, and splitting occurs at the nitrogen nucleus. The spectrum of the quinoline anion contains eight lines with 4.6 oe splitting, each line being split into a triplet with about 1 oe splitting. This additional splitting evidently arises as the result of interaction with the nitrogen atom. The eight lines might possibly be assigned to the seven remaining protons. Details of all the compounds and the spin densities calculated from the splitting values are summarized in Table 1.

4. Stability of Aromatic Anions

All the aromatic anions studied are divided into two groups: those stable at room temperature, and those unstable at room temperature, which must be investigated in the range from 0 to $-70°$. The first group includes benzene and its various alkyl-substituted derivatives, and the second includes polycyclic aromatic anions.

It follows that increase of the electron delocalization region increases the stability of aromatic anions. All this apparently indicates that in the reaction $Ar + K \rightleftharpoons Ar^- + K^+$ the equilibrium is shifted to different extents in the direction of Ar^- formation.

To investigate this question, we determined the effects of temperature on the magnitude of the EPR signal for benzene, toluene, and p-xylene.

The logarithm of the magnitude of the EPR signals of benzene and toluene anions is plotted against the reciprocal temperature in Fig. 6. The heats of reaction of benzene and toluene with K were calculated from the slopes of the lines. From the reaction equation

$$Ar + K \rightleftarrows Ar^- + K^+ \text{ we have } [Ar^-] = \sqrt{k[Ar][K]},$$

TABLE 1. EPR Spectra of Negative Aromatic Anion Radicals

Molecule yielding anion radical	Number of principal lines	Splitting, oe	Number of subsidiary lines*
C_6H_6	7	3,75	
$C_6H_5CH(CH_3)_2$	5	4,5	2
$C_6H_5(C_4H_9)$	5	4,5	2
$C_6H_5C(CH_3)_3$	5	2,8	
$C_6H_5CH_3$	5	4,0	8
$C_6H_5C_6H_5$	5	3,75	8
p $C_6H_4(CH_3)_2$	5	4,0	
o $C_6H_4(CH_3)_2$	7	3,8	
$C_6H_5-CH=CH-C_6H_5$	3	5,65	14
$C_6H_5-CH_2-C_6H_5$	9	1,9	
$C_6H_5-(CH_2)_2-C_6H_5$	9	2,5	6
C_6H_{10}	5	3,6	
p $CH_3-C_6H_4-CH_2-CH(CH_2-C_6H_4-CH_3)_2$	5	3,6	
$C_6H_5-CH_2-CH_2-CH(CH_2-C_6H_5)_2$	7	3,8	
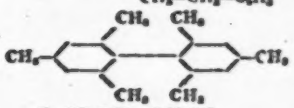			
p $CH_3C_6H_4-C_6H_4CH_3$	13	2,3	
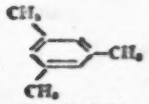	7	3,15	
m-$C_6H_4(CH_3)_2$	13		
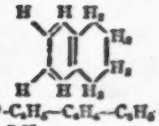	5	2	
p-$C_6H_5-C_6H_4-C_6H_5$	8	2,5	
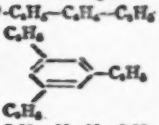	9	2,5	
$C_6H_5-N=N-C_6H_5$	15	2,5	
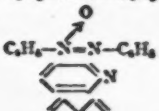	20		
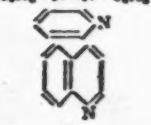	50		
	8	4,6	3
$C_6H_5-\overset{O}{\overset{\|}{C}}-NH_2$	1		
$C_6H_5-\overset{H}{\overset{\|}{N}}-C_6H_5$	1		

*Additional splitting of each of the principal components.

**Splitting at α protons of the substituent.

***Splitting at protons in the para position.

****Splitting at protons in the meta position.

*****Triplet evidently due to interaction of the unpaired electron with the nitrogen nucleus (spin 1).

Additional splitting	Spin density				Notes
	Ortho	Meta	Para	Sum of densities	
					Binomial distribution
1 ••	0,2	0,2	0	0,8	»
1 ••	0,2	0,2	0	0,2	»
	0,12	0,12	0	0,48	Same
1,5 •• 0,5 •••	0,18	0,18	0,02	0,74	»
1,5 •• 0,5 •••	0,16	0,16	0,02	0,66	»
	0,18				»
					»
					»
	0,084	0,084		0,68	»
1	0,11	0,11		0,88	»
	0,16	0,16		0,64	»
	0,16	0,16		0,64	»
					»
					»
4,6 •• 2,3 ••••					Not binomial Binomial. Odd spectrum
					Not binomial. Line superposition
					HFS seen on singlet background, 60 oe in extent
					Even spectrum? Insufficient resolution of spectrum
					Same
1 •••••					
					Singlet with line width of 11 oe between m.n. points on background of wide singlet (70 oe)

where k is the equilibrium constant. Assuming [Ar] and [K] constant, we found $\Delta H = -25.5$ kcal/mole for benzene, and $\Delta H = -15.5$ kcal/mole for toluene. The estimated value for p-xylene was $\Delta H \approx -7$ kcal/mole. The anions of p-xylene are less stable than benzene and toluene anions; the concentration of p-xylene anions is close to the sensitivity limit even at $-40°$. All this makes accurate determination of ΔH for p-xylene difficult. According to Dainton [4], the concentration of dissolved potassium in 1, 2-dimethoxyethane is about $5 \cdot 10^{-4}$ M. This gives $2.5 \cdot 10^{-9}$ and $2.5 \cdot 10^{-8}$ as the order of magnitude for the equilibrium constants of benzene and toluene at temperatures between -40 and $-50°$. Measurements of the effects of temperature on the magnitude of the EPR signals of anions such as naphthalene and stilbene showed that the relationship conforms to the Curie law.

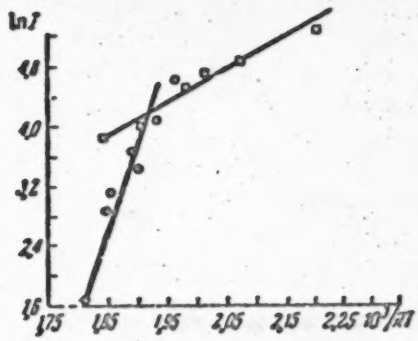

Fig. 6. Logarithm of the magnitude of the EPR signal as a function of reciprocal temperature, for benzene and toluene anions: O) Benzene; □) toluene.

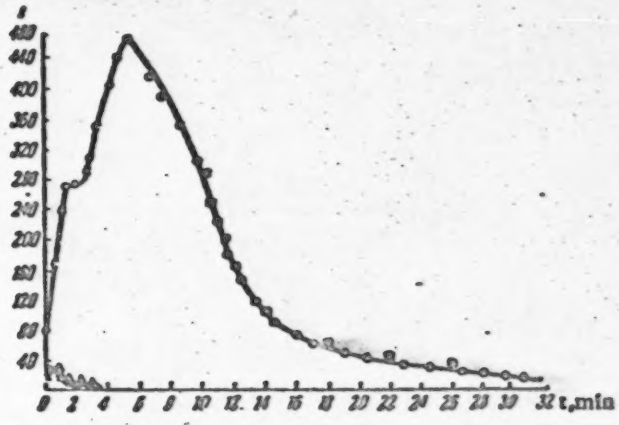

Fig. 7. Variations of the magnitude of the EPR signal with time during unfreezing. Anions: O) Benzene; X) toluene; Δ) p-xylene; □) points calculated from the equation for a second-order equation.

The signals due to various anions were measured under comparable conditions in order to compare the relative stabilities of different aromatic anions. The signal due to the benzene anion, with appropriate corrections for temperature differences, was taken as the basis. The results of these measurements are given in Table 2.

We consider that these results characterize differences in the electron affinities of different aromatic hydrocarbons. An interesting feature is the increase of anion stability when one carbon atom in the benzene ring is replaced by nitrogen, as shown by the magnitude of the EPR signal for pyridine. The result for the dibenzyl anion indicates that the possibility of electron transfer from one phenyl ring to the other at a frequency of $10^7 - 10^8$ sec^{-1} also increases the stability of the ion. This is not found for ions with longer (n = 3, 4, 5) bridges of saturated bonds between the rings.

5. Decomposition Kinetics of Aromatic Anions

An attempt was made to estimate the decomposition rates of benzene, toluene, and p-xylene anions. Ampoules containing the anions were frozen to the temperature of liquid nitrogen and then transferred rapidly to the resonator; the spectrum of the anion was then obtained at 30-second intervals. This was accompanied by temperature measurements during unfreezing of the specimen. Temperature measurements inside the speciments showed that room temperature is reached in 8-10 minutes. Variations of signal magnitude with time are plotted in Fig. 7. During the first few minutes of warming the signal height increases due to the strong narrowing of the line as the temperature rises from the temperature of liquid nitrogen to the melting point and higher. The melting point is quite distinct on the curve for the benzene anion, where the plateau coincides well in time with the melting point on the temperature curve. It is seen in Fig. 7 that toluene and p-xylene anions disappear within 4 minutes, before the temperature has become steady. This makes analysis of the curves difficult. Decomposition of the benzene anion is much slower. At the end of 10 minutes we may assume that further decomposition proceeds at 20°, and the width of the HFS components no longer changes. Analysis of the region of the curve between 10 and 30 min shows that it is represented

TABLE 2. Relative Integral Strengths of EPR Signals for Different Aromatic Anions at 30° and 1 M Concentration of the Aromatic Hydrocarbons

Anion	Signal Strength
Benzene	1
Toluene	1*
Dibenzyl	80
Pyridine	10^3
Naphthalene	10^5
Quinoline	10^6
Stilbene	$3 \cdot 10^6$
p-Terphenyl	$3 \cdot 10^6$

* If the signal strengths of benzene and toluene anions are compared at low temperatures, the signal of the benzene anion is stronger by a factor of 10 than that of toluene. At room temperature they are equal, owing to the ΔH difference.

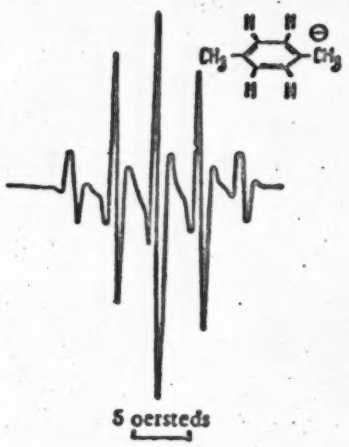

Fig. 8. EPR spectrum of the p-xylene anion.

satisfactorily by the equation for a bimolecular reaction: $I = I_0/(1 + kI_0)$, where I is the magnitude of the signal at time t between 10 and 30 min, I_0 is the magnitude of the signal at t = 10 min (t = 10 min was taken as zero time), and k is the constant for a bimolecular reaction. Points calculated from this equation are marked in Fig. 7 by small squares. We estimated the anion concentration at t = 10 min, i.e., the value of I_0, by comparison with the known signal of diphenylpicrylhydrazyl. The concentration of $[C_8H_8^-]$ at t = 10 min was found to be 10^{-9} M, and hence the constant for the bimolecular reaction $C_8H_8^- + K^+ \rightarrow C_8H_8 + K$ is $k = 0.8 \cdot 10^{-23}$ cc/sec.

6. Hypothesis of the Existence of the ·ArH Radical

It was found in the spectra of cumene, cyclohexylbenzene, and especially p-xylene that in addition to the principal quintuplet there is an EPR signal consisting of 4-6 components, as is seen in Fig. 8, which represents the spectrum of the p-xylene anion. The intensity of this signal is low for cumene and cyclohexylbenzene anions, and somewhat higher for p-xylene anions. We attempted to assign this signal to the ·ArH radical:

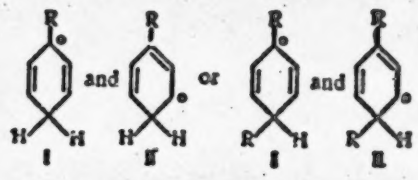

However, a final interpretation of this spectrum is not possible at present. It can only be pointed out that the anomaly observed in the spectrum of mesitylene (odd spectrum) may be associated with this effect. Available literature data [10] on the basicities of aromatic compounds indicate that basicity may vary over a very wide range from compound to compound. It is to be expected that the basicity of an anion is greater than the basicity of the corresponding hydrocarbon.

SUMMARY

1. In monoalkyl benzenes the density of the unpaired electron is considerably less at the carbon atom in the para position that at the other carbon atoms. Additional splitting at the α protons of the substituent and at the protons in the para position was discovered.

2. Distribution of spin density in anions of xylenes was investigated.

3. Spectra of 26 anions of different structures were obtained and analyzed.

4. It is shown that electron transfer may occur not only along bridges of conjugated bonds but also along chains of saturated bonds in diphenylmethane and dibenzyl anions, at a frequency of 10^7-10^8 sec^{-1}.

5. Heterocyclic compounds with nitrogen atoms in the ring yield stable anions.

6. The relative stabilities of anions of various aromatic hydrocarbons were investigated.

7. It is shown that benzene anions decay in accordance with a bimolecular reaction with a rate constant of $0.8 \cdot 10^{-23}$ cc/sec.

LITERATURE CITED

1. M. C. R. Symons, Quart. Rev. 13, 2, 99 (1959).
2. A. J. Birch, H. Smith, Quart. Rev. 12, 17 (1958).
3. M. Szwarc, M. Levy, R. Milkovitch, J. Amer. Chem. Soc. 78, 2656 (1956).
4. F. S. Dainton, D. M. Wiles, A. N. Wright, Summaries of Symposium on Macromolecular Chemistry, Wiesbaden, Federal Germany, October 12-17, 1959 [Russian translation].
5. S. I. Weissman, J. Townsend, D. E. Paul, G. E. Pake, J. Chem. Phys. 21, 2227 (1953).
6. T. R. Tuttle, Jr., R. L. Ward, S. I. Weissman, J. Chem. Phys. 25, 189 (1956).
7. T. R. Tuttle, Jr., S. I. Weissman, J. Amer. Chem. Soc. 80, 20, 5342 (1958).
8. H M. McConnell, D. B. Chensur, J. Chem. Phys. 28, 1, 107 (1958).
9. E. DeBoer, J. Chem. Phys. 25, 190 (1956).
10. H. C. Brown, J. D. Brady, J. Amer. Chem. Soc. 74, 3570 (1952).

EPR SPECTRA OF IRRADIATED DICARBOXYLIC ACIDS

Yu. N. Molin, I. I. Chkheidze, N. Ya. Buben,
and V. V. Voevodskii

Institute of Chemical Physics, Academy of Sciences, USSR
Institute of Chemical Kinetics and Combustion, Siberian Division,
Academy of Sciences, USSR
Translated from Zhurnal Strukturnoi Khimii, Vol. 2, No. 3, pp. 293-300,
May-June, 1961
Original article submitted April 29, 1960

The EPR spectra of dicarboxylic acids of the general formula $(CH_2)_n(COOH)_2$ with n = 1, 2, . . . 8, irradiated by fast electrons (1.6 Mev), were investigated. The EPR spectra were recorded during irradiation at −130° and while the specimens were unfrozen to room temperature. For interpretation of the spectra and elucidation of the nature of the radicals, the EPR spectra of irradiated single crystals of succinic acid and of succinic acid deuterated in the carboxyl group were also investigated. In addition, the radiation yields of the radicals and gaseous products of the radiolysis of succinic acid were determined. Analysis of the spectra shows that starting with n = 2 the form of the EPR spectra does not alter significantly. At −130° the spectrum is a doublet with splitting of $\Delta H \approx 26 - 30$ oe, and at room temperature it consists of two doublets ($\Delta H_1 \approx 40$ oe, $\Delta H_2 \approx 70 - 90$ oe) and a single line, with g = 2.00. Comparison of the EPR spectra and data on gas evolution shows that carboxyl groups are the first to be broken down by radiation.

In the paper by Gordy et al. [1] and in our preceding paper [2] attention was drawn to the unusually low stability of radicals in irradiated oxalic acid. Gordy [1] suggested that irradiation of oxalic acid results in formation of M^+ and M^- ion radicals, and attributed their instability to the possibility of charge migration in the substance owing to the presence of a system of hydrogen bonds. There is another possible explanation, based on the hypothesis that radicals are formed and migration of free valences occurs by transfer of a hydrogen atom [2]. Our preliminary observations showed that the more complex electron paramagnetic resonance (EPR) spectra of dicarboxylic acids in the homologous series beyond oxalic acid contain signals analogous to the signal in the oxalic acid spectrum. We investigated the EPR spectra of dicarboxylic acids in order to obtain data on the nature of the radicals in these acids and on their conversion routes.

The available literature data on the EPR spectra of irradiated carboxylic acids are of fragmentary character. A large number of spectra of irradiated carboxylic and hydroxy acids is described in [1]. However, the conclusions drawn in that paper concerning the structure of the radicals can hardly be regarded as unequivocal. McConnell et al. [3] carried out a detailed analysis of the EPR spectrum of an irradiated single crystal of malonic acid, $CH_2(COOH)_2$ which was "aged" for some time at room temperature. It was shown that the doublet observed under these conditions corresponds to the radical $\dot{C}H(COOH)_2$. Recently a brief communication has appeared, reporting an investigation of EPR spectra of a number of dicarboxylic acids subjected to x-ray irradiation [4]. According to these authors the spectra of all the acids contain lines corresponding to a radical formed as the result of removal of an α-hydrogen atom.

We investigated dicarboxylic acids of the general formula $(CH_2)_n(COOH)_2$, where n = 1, 2, . . . 8. The molecules of all these acids are joined in crystals into infinite chains by hydrogen bonds [5]:

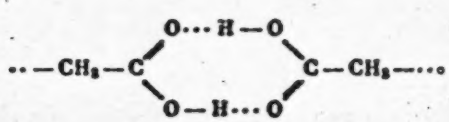

The following procedures were used for interpretation of the EPR spectra.

1. Comparison of the spectra in the series of dicarboxylic acids.
2. Analysis of the spectrum of the deutero-substituted acid.
3. Observation of the spectrum of a single crystal.
4. Observation of changes in the EPR spectrum with rise of temperature.
5. Comparison of the radiation yields of the radicals and the gaseous products of radiolysis.

The specimens were irradiated by electrons of 1.6 Mev energy. The does was calculated from the measured electron flux density.

Measurements of paramagnetic resonance were carried out in the EPR apparatus with an electron beam [6, 7]. The operating frequency of the EPR spectrometer was about 9400 Mc/sec. The spectrum was recorded in the form of the first derivative. The specimens were tablets 5 mm in diameter and about 2 mm thick containing embedded copper – Constantan thermocouples. In some experiments single crystals of succinic acid, several millimeters in size, were also used.

Special cells were used for collecting gaseous products. A weighed sample of acid (0.7 g) was put on the floor of a cell 1.5 cm in diameter. The cell could be cooled in liquid nitrogen. The MKh-1302 mass spectrometer was used for analysis of the gaseous radiolysis products.

Acids with n= 2 to 8 were obtained from the V. V. Korshak Laboratory (Institute of Heteroorganic Compounds, Academy of Sciences, USSR). They were distilled under vacuum and recrystallized repeatedly from aqueous solution. Malonic acid (n = 1) was prepared in the Department of Organic Chemistry, Moscow State University (it was purified by recrystallization from aqueous solution before the experiments).

Figures 1 a, b, 2, and 3 show the EPR spectra of various dicarboxylic acids at – 130° and after unfreezing of the specimens to room temperature. The radiation dose was 10 Mrad in all cases. The specimens were unfrozen in a few minutes. Repeated freezing of the specimen does not alter the form of the spectrum observed at room temperature. It follows that unfreezing results in an irreversible change of the radical structure. The radical concentration fell only slightly during unfreezing to room temperature.

The low-temperature EPR spectrum of malonic acid consists of three lines with good resolution, showing signs of additional structure (Fig. 1 a). The distance between the end lines is about 40 oe. The basic structure of the spectrum may be interpreted either as the superposition of a doublet and a singlet or as the superposition of a doublet on a triplet with intensity ratio 1 : 2 : 1, the outer components of which are superposed on the doublet components. When the temperature is raised to room level the spectrum becomes more complex, but the lines observed at the low temperature remain in the spectrum (Fig. 1 b). When the specimen is heated to 80° a doublet with 22 oe splitting predominates in the spectrum (Fig. 1 c). By the extent of the splitting this doublet corresponds to the spectrum of an irradiated single crystal after aging, which was assigned [3] to the radical $CH(COOH)_2$.

Comparison of the spectra for the series of acids at the same temperature shows that starting with n = 2 that form of the spectra changes little. At low temperatures all the spectra are doublets with splitting between 26 and 30 oe (in the case of succinic acid each component of the doublet is split into two lines). At room temperature every spectrum contains two doublets and a singlet line of g-factor 2.00. The distance between the components of the outer doublet varies in the 78-90 oe range, and between the components of the inner doublet, in the 40-45 oe range. The observed resemblance between the spectra of the acids starting with n = 2 probably means that virtually no radicals are formed by rupture of C – H bonds in the hydrocarbon chain away from the carboxyl group in dicarboxylic acids, as otherwise the spectra would become more complex with increase of n. It particular, formation of such radicals, which would be similar in structure to radicals of the alkyl type, would lead to the appearance of lines beyond the limits of the outermost components of the spectra (ΔH = 80-100 oe). However, no such lines are observed.

Despite this similarity of the spectra, the details of the hyperfine structure undergo certain changes in the acid series. In particular, it is interesting to note that the character of the hyperfine structure exhibits a periodic variation at room temperature. The relative intensity of the central component is higher for the even than for the odd members of the series. Moreover, in the even members of the series all the doublet components are of roughly the same intensity, whereas in the odd members the intensity of the components of the inner doublet is greater than of the outer. This difference between the spectra diminishes with increase of n. Similar regular variations in the character of the hyperfine

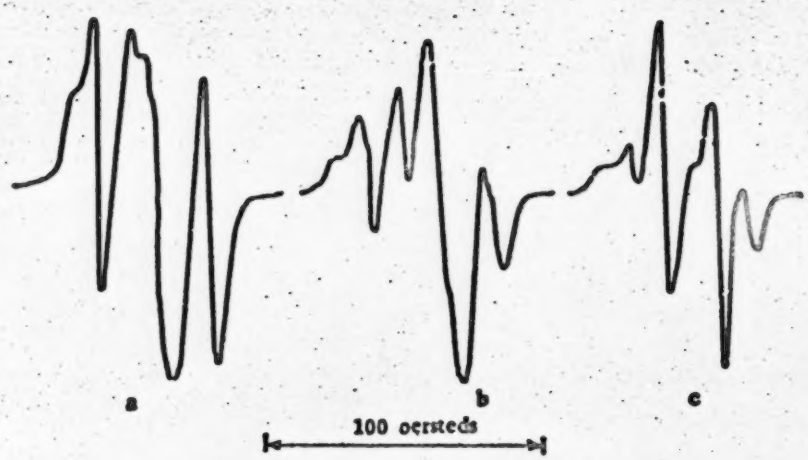

Fig. 1. EPR spectra of irradiated malonic acid: a) at − 130°; b) after unfreezing to room temperature; c) after heating to 80°.

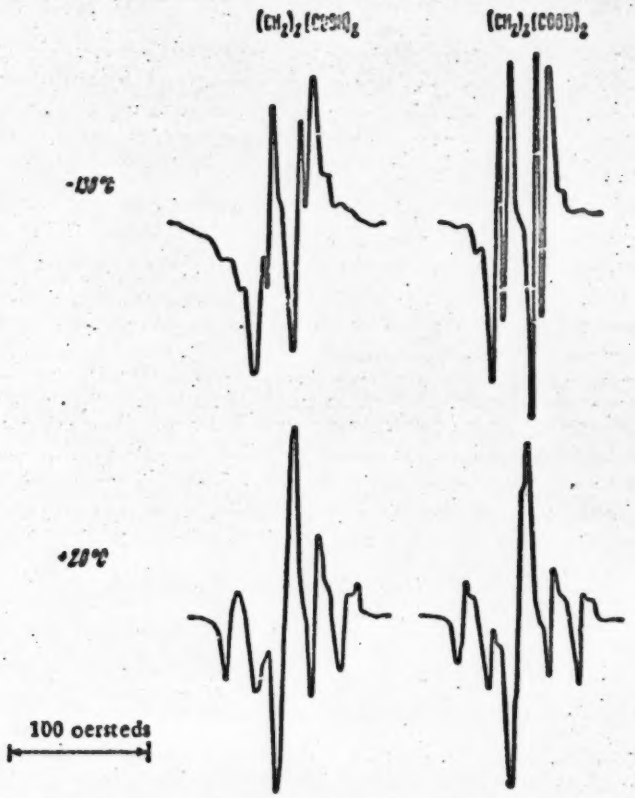

Fig. 2. EPR spectra of irradiated succinic acid at − 130° and after unfreezing to room temperature

structure were observed earlier in the EPR spectra of irradiated frozen alkanes [8]. These variations are analogous to the observed differences in physicochemical characteristics (melting point, solubility, etc. [9]) of odd and even members of these homologous series.

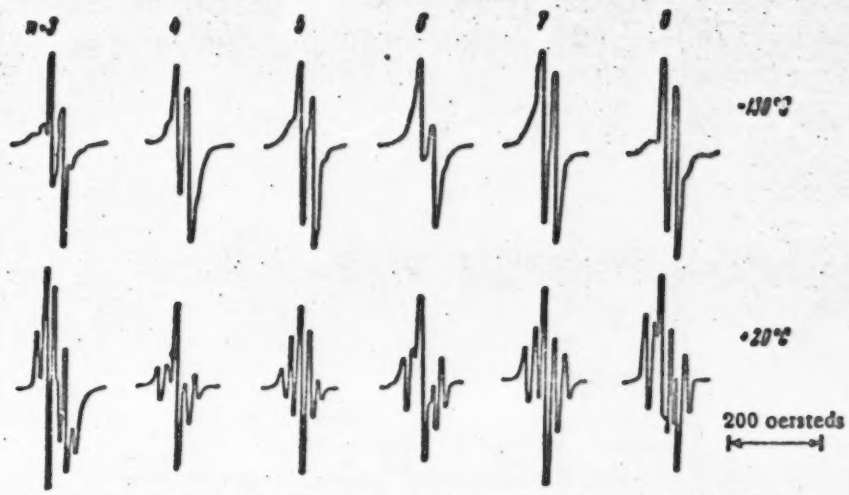

Fig. 3. EPR spectra of irradiated dicarboxylic acids of the type $COOH(CH_2)_n$—COOH (n = 3, 4, . . . 8) at −130° and after unfreezing to room temperature.

The spectra were investigated in greater detail in the case of succinic acid (n = 2). Figure 2 shows the EPR spectra of irradiated succinic acid and irradiated succinic acid deuterated in the carboxyl group. Comparison of the spectra of $(CH_2)_2(COOH)_2$ and $(CH_2)_2(COOD)_2$ shows that the presence of deuterium in the carboxyl group improves resolution of the structure but does not alter the positions of the components in the spectrum. It follows that hydrogen of the carboxyl group is not involved in the observed hyperfine splitting, but merely broadens the hyperfine structure components.

For analysis of the spectrum of succinic acid at room temperature we followed changes in the structure of the spectrum as the specimen was heated to higher temperatures. It was found that as the temperature rises the intensity of the central component diminishes more rapidly than that of the doublets. The doublet components begin to diminish at about 120°, and the intensities of all four lines are weakened to approximately the same extent. This result indicates that all the four lines should probably be assigned to the same radical (I). The single central line is probably due to some other radical (II).

The resolution of the structure of the spectrum of succinic acid at a low temperature is not good enough to make it possible to follow changes in the individual components as the specimen is unfrozen. We therefore used a single crystal, which gave better resolution of the spectrum structure. The form of the EPR spectrum of a single crystal depends significantly on its orientation in the magnetic field. We chose the orientation giving the simplest spectral structure. Comparison of Figs. 2 and 4a shows that the hyperfine structure components in the spectrum of the single crystal and in the spectrum of a polycrystalline specimen are similarly arranged, but the former are narrower.

Figure 4 shows how the spectrum alters when a single crystal is unfrozen from − 130° to room temperature. The temperature of the specimen was not recorded during the unfreezing. Spectra b and c, recorded during the unfreezing, are asymmetric; this is probably caused by a change in the form of the spectrum during the recording (~ 0.5 min). It is seen in Fig. 4 that the intensities of the 1-1 and 3-3 components diminish to approximately the same extent during the unfreezing, while the intensity of the 2-2 components diminishes in accordance with some other law. Therefore it may be suggested that at low temperatures the spectrum is determined mainly by two radicals, one of which (III) gives a doublet with the 2-2 components, and the other (IV), a quadruplet with the 1-1 and 3-3 components. The distances between the components of quadruplet IV are equal (about 20 oe), but the ratio of the component intensities apparently does not conform to the theoretical 1 : 3 : 3 : 1 law for three equivalent protons. Therefore this analysis of the low-temperature spectrum of the single crystal cannot be regarded as final.

Data on the analysis of the EPR spectrum of succinic acid are summarized in Table 1.

For identification of the radicals, we also correlated data on the composition and yields of the gaseous radiolysis products with data on the kinetics of radical accumulation. Curves representing accumulation of radicals in

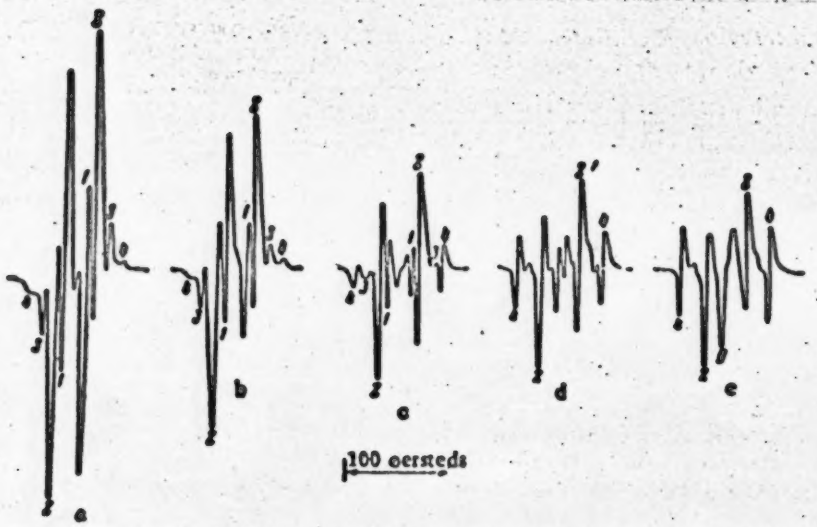

Fig. 4. Changes in the EPR spectrum during unfreezing of an irradiated single crystal of succinic acid: a) at − 130°; b, c, d) during unfreezing; e) at +20°.

TABLE 1

Radical	T°	Structure of spectrum	Splitting*
I	+20	Double doublet	ΔH_{ext} = 81 oe ΔH_{int} = 41 oe
II	+20	Singlet line	
III	−130	Doublet	ΔH = 34 oe
IV	−130	Quadruplet	ΔH = 20 oe**

* Measured for polycrystalline specimens of $(CH_2)_2(COOH)_2$ and $(CH_2)_2(COOD)_2$.
** Between neighboring components.

succinic acid were determined at − 130° and at room temperature. A characteristic feature of the kinetics of radical accumulation is the deviation from a linear law, with "saturation" of the concentration curves at relatively small radiation doses. The limiting concentrations of the radicals were reached at doses of some tens of Mrad, and were a few units $\times 10^{19}$ radicals per gram. Another feature of radical accumulation is the change in the relative intensities of the lines in the EPR spectrum during irradiation, which indicates that different radicals are accumulated in accordance with different kinetic laws. Table 2 shows the radiation yields of radicals in succinic acid, determined in different experiments. The values were calculated from the initial linear regions of the curves. The values of G for low temperatures may be somewhat too low owing to saturation of the EPR signals.

The radiation yields of gaseous radiolysis products in succinic acid are given in Table 3.

When the specimens were irradiated in liquid nitrogen, the measurements were performed after unfreezing to room temperature.

Because of heating by the electron beam, the temperature of the specimen during irradiation could be 10-20° higher than the temperature in absence of irradiation. Two measurements, performed at +20° with different doses, showed that liberation of gaseous products is proportional to the dose. In addition to gaseous products, appreciable amounts of water were formed during radiolysis; the water was deposited in the form of small droplets on the sides of the irradiation cell.

Comparison of the data in Tables 2 and 3 leads to the conclusion that the yields of radicals and CO_2 are of the same order of magnitude, and are much higher than the yields of CO and H_2.

From these results certain preliminary conclusions can be drawn about the mechanism of radiolysis of dicarboxylic acids and the structure of the radicals formed. The predominance of CO_2 (and, apparently, of water) and the almost total absence of hydrogen in the products of radiolysis of succinic acid show that the carboxyl groups of the molecules are the first to undergo decomposition. Since the radical yield is close to the CO_2 yield it is highly probable that CO_2 liberation and radical formation occur in the same step. This process can be represented by a scheme such as the following:

TABLE 2

T°	G, rad/100 ev	T°	G, rad/100 ev
−150	2,6	+20	7,1
−120	3,3	+20	8,0
−110	2,7	+20	5,9

TABLE 3

Temperature of specimen	Dose, Mrad	G, moles/100 ev		
		H_2	CO	CO_2
Room	236	0,05	0,3	4,1
Room	32	0,04	0,4	4,0
Liquid N_2	216	0,02	0,3	2,6

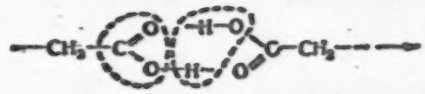

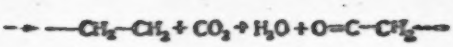

The CO_2 and H_2O molecules are situated between the radicals and prevent their recombination. However, the $\ldots - CH_2 - \dot{C}H_2$ and $O = \dot{C} - CH_2 - \ldots$ radicals formed in accordance with this scheme account for the even character of the spectrum at low temperatures only if it is assumed that one of the β-hydrogens (relative to the free valence) in each of these radicals is not involved in hyperfine splitting of the spectrum. With this assumption the spectrum of the $O = \dot{C} - CH_2 - \ldots$ radical must be a doublet, and that of the $\ldots - CH_2 - CH_2 -$ radical, a quadruplet (provided that the hydrogen atoms involved in the hyperfine splitting are equivalent); this is consistent with the situation observed at low temperatures. The suggested scheme makes it possible to predict, in agreement with experimental data, that the carboxyl hydrogen which passes into the H_2O molecule is not involved in hyperfine splitting.

If we extend this scheme to other dicarboxylic acids, we can predict that the higher members of the series should give similar spectra, because only the α- and β-hydrogens can make substantial contributions to hyperfine splitting. On the other hand, in the case of malonic acid (n = 1) the situation should be altered significantly, owing to formation of the $\dot{C}H_2COOH$ radical in which the unpaired electron can interact only with two α-hydrogens. The spectrum of this radical should be a triplet, and the total splitting at the α-hydrogens should probably be about 40 oe, which is in agreement with experimental data*.

The changes observed in EPR spectra during unfreezing are probably consequences of conversion of the original radicals into more stable ones. As was shown in [3], the stable radical in malonic acid is $\dot{C}H(COOH)_2$. It seems likely that the double doublet I observed in the spectra of the higher acids at room temperature is due to a radical of similar structure, $\ldots - CH_2 - \dot{C}H - C(=O)-O-H$, in which the hydrogen atoms involved in the hyperfine splitting are not equivalent**.

We may add that the high stability of the $\ldots - CH_2 - \dot{C}H - COOH$ radical may be the result of conjugation between the unpaired electron in the p-orbit and the electrons of the double bond.

The singlet line II may be assigned to a radical of the type $\ldots - CH_2 - C(=O)-O$ Such a radical should be almost entirely free of hyperfine interaction, and the possibility of delocalization of the unpaired electron over two oxygen atoms may ensure high stability in the radical.

The views put forward above provide a satisfactory explanation of the main experimental results, with certain assumptions concerning the structure of the radicals. However, the foregoing does not completely exclude other possible radiolysis routes. For example, CO_2 and H_2O may be formed as the result of secondary radical reactions and not in the primary step of chemical radiolysis. On the other hand, it is possible that liberation of CO_2 is not associated with formation of radicals, and that the similarity of the radiation yields is merely a coincidence. Not enough data are available at this time to justify the conclusion that the above views on the mechanism of radiolysis and the

*A discussion of the magnitude of hyperfine splitting at α-and β-hydrogens in organic radicals can be found, for example, in Ingram's book [10].

**After our paper had been submitted for publication, a paper was published [C. Heller, H. M. McConnell, J. Chem. Phys. 32, 1535 (1960)] containing a detailed analysis of the spectrum of a radical of this type in irradiated single crystals of succinic acid.

structure of the radicals formed are conclusively proved.

The authors take this opportunity to thank T. M. Frunze for providing the specimens, A. N. Ponomarev for the mass-spectrometric measurements, and G. K. Vasil'ev for assistance in experiments on radiolysis with collection of the gaseous products.

LITERATURE CITED

1. W. Gordy, W. B. Ard, H. Shields, Proc. Nat. Acad. Sci. 41, 996 (1955).
2. Yu. N. Molin, A. T. Koritskii, N. Ya. Buben, V. V. Voevodskii, Dokl. AN SSSR 124, 127 (1959).
3. T. Cole, C. Heller, H. M.McConnel, Proc. Nat. Acad. Sci. 45, 525 (1959).
4. H. C. Box, H. G. Freund, Bull. Amer. Phys. Soc., ser. II 3.4, 262 (1958).
5. A. I. Kitaigorodskii, Organic Crystal Chemistry [in Russina] (Izd. AN SSSR, Moscow, 1956).
6. Yu. N. Molin, A. T. Koritskii, N. Ya. Buben, V. V. Voevoskiii, Dokl. AN SSSR 123, 882 (1958).
7. Yu. N. Molin, A. T. Koritskii, A. G. Semenov, N. Ya. Buben, V. N. Shamshev, Pribory i tekhnika éksperimenta, 6, 73 (1960).
8. N. Ya. Chernyak, N. N. Bubnov, L. F. Polyak, Yu. D. Tsvetkov, V. V. Voevodskii, Optika i spektroskopiya 6, 564 (1959).
9. A. E. Chichibabin, Fundamental Principles of Organic Chemistry [in Russian] (Goskhimizdat, Moscow, 1954) Vol.1, pp. 164, 447.
10. D. J. E. Ingram, Free Radicals as Studied by Electron Spin Resonance (London, 1958).

All abbreviations of periodicals in the above bibliography are letter-by-letter transliterations of the abbreviations as given in the original Russian journal. *Some or all of this periodical literature may well be available in English translation.* A complete list of the cover-to-cover English translations appears at the back of this issue.

β, δ, AND ζ PHASES IN THE VANADIUM – OXYGEN SYSTEM

P. V. Gel'd, S. I. Alyamovskii, and I. I. Matveenko

Institute of Chemistry, Urals Branch, Academy of Sciences USSR, Sverdlovsk
Translated from Zhurnal Strukturnoi Khimii, Vol. 2, No. 3, pp. 301-307, May-June, 1961
Original article submitted May 13, 1960

Analysis of experimental results and literature data shows that the V – V_2O_3 system contains a solid solution of oxygen in vanadium and α' and δ V_2O_3 phases. The existence of β and ζ phases in the V – O system is not confirmed. It is shown that the δ phase (similar to TiO in structure) has dual defectiveness and a homogeneity region from $VO_{0.88}$ to $VO_{1.33}$. Vanadium trioxide is stable over a narrow concentration range ($VO_{>1.46}$ – $VO_{<1.48}$), within which the changes of lattice constants are very small.

INTRODUCTION

In view of the extension of the uses of vanadium and its alloys and compounds during recent years, interest in the structural characteristics of its oxides has increased considerably. Special attention is devoted to the lower oxides, which play an important part in the production of metallic vanadium and in its high-temperature oxidation. Unfortunately, there is as yet no agreement about their structure.

According to a detailed review [1] of research prior to 1956, the V – O system contains two oxides of variable composition. One of these (the α' phase) is homogenous in the concentration range from $VO_{1.0}$ to $VO_{0.22}$, whereas the second (the δ phase in the terminology of [1]) has a lattice of the sodium chloride type and is stable over a very wide range of concentrations (from $VO_{0.8}$ to $VO_{1.2}$).

Very interesting data are contained in the paper by Gurevich and Ormont [1] on the structure of lower vanadium oxides. First, the authors found that, despite earlier findings, within the homogeneity range $VO_{1\pm x}$ the size of the unit cell does not vary uniformly with composition but undergoes a very abrupt change (by approximately 0.05 kX). They concluded from this that the system V – O contains two lower-oxide phases. One of these, the β phase, is stable in the narrow concentration range $VO_{0.7-x}$ – $VO_{0.7+x}$ (with $x < 0.1$), within which the lattice constant changes from 4.01 to 4.03 kX. The other phase, the δ phase, has a wide homogeneity region, from $VO_{0.8}$ to $VO_{1.2}$. Its lattice constant (lattice of the NaCl type) increases from 4.08 to 4.13 kX with increasing oxygen content. In addition, the existence of yet another lower-oxide phase (the ζ phase) was postulated from the anomalous ratio of the intensities of the x-ray diffraction maxima (indexed on the basis of the NaCl lattice type). According to [1], this phase has a body-centered cubic lattice and is stable between $VO_{1.2}$ and $VO_{1.37}$. It is important to note that they did not succeed in obtaining this compound in the pure state; it always coexisted with a small amount of the δ phase, and the 200, 220, and 222 lines of the latter coincided exactly with the 110, 200, and 211 lines of the ζ phase.

The existence of two lower-oxide phases in the V – O system was recently confirmed by Vol'f, Tolkachev, and Kozhina [2]. Both phases have a lattice of the NaCl type, and the lattice constant depends similarly on concentration in both. The lattice constant of the phase stable between $VO_{0.88}$ and $VO_{1.017}$ varies linearly from 4.016 to 4.063 kX; the second phase is stable between $VO_{1.057}$ and $VO_{1.27}$, and the lattice constant increases from 4.074 to 4.126 kX (at 1600°). Vol'f et al. did not confirm the existence of a body-centered phase and attempted to attribute the lack of agreement with [1] to insufficient purity of the specimens. Analogous views are put forward in papers by Vol'f and Ariva [3] and Morozova [4].

These discrepancies, the considerable differences between data on the constants of the $VO_{1\pm x}$ lattice, and the lack of information on the structural characteristics of these variable-composition phases prompted an additional investigation of their properties. Moreover, data were needed to account for the existence of the wide homogeneity region of vanadium oxycarbides [5] and to determine the precise mechanism of the high-temperature oxidation of vanadium [6].

Starting Materials and Investigation Methods

Vanadium oxides of different compositions were prepared from metallic vandium, the pentoxide (analytical-reagent grade) and the trioxide. The latter was prepared by reduction of vanadium pentoxide in a stream of dry oxygen for 10 hours at a slowly increasing temperature (from 600 to 900°). The composition of the product corresponded to the formula $VO_{2.67}$.

The vanadium* used was made by reduction with carbon; it was plastic and very pure. Its lattice constant was close to 3.020 kX, indicating [7] the presence of 0.04 atomic % of oxygen. The pycnometric density of the original vanadium was 6.09 g/cc. Fine shavings of the metal were hydrogenated (at 800°), powdered thoroughly in an agate mortar, and evacuated for 3 hours at 900°.

The x-ray patterns of vanadium hydride were indexed conclusively in a tetragonal body-centered lattice with a = 3.02 and c = 3.20 kX, which is in adequate agreement with literature data [8].

Vanadium oxide specimens of different compositions were prepared by high-temperature sintering of briquetted mixtures. The starting materials were mixed in the necessary proportions; the mixture was ground thoroughly in an agate mortar and molded into briquets 12 mm in diameter and 12 mm long (under 5000 kg/cm^2 pressure). These rods were fired in a vacuum furnace, first at 1200° and than at 1400° for 60-76 hours. During this operation the specimens were powdered after 40 hours of sintering and then made into briquets again in order to renew the contact surfaces. Samples for x-ray investigations were taken during the firing (at intervals of 15-20 hours). Constant phase composition and unit cell parameters were taken as criteria of equilibrium.

The x-ray phase analysis was carried out with CrK_α and $CuK_{\alpha,\beta}$ radiation in cameras of the RPK (57.3 mm in diameter) and VRS (143.3 mm in diameter) types. The lattice constants were determined from the x-ray patterns taken with chromium radiation in VRS cameras.

The densities of the oxides were determined by the pycnometer method with kerosene or carbon tetrachloride. Before the determinations the specimens were ground, weighed samples in the pycnometers were covered with layers of the liquid under vacuum, and the liquid level was then brought up to the stopper bevel (after air has been admitted to the system). In a number of cases, to ensure better wetting, the system was left for 1-2 days before the final filling. Estimates of the experimental accuracy showed that the error in density determinations did not exceed 0.7%.

Polished sections were examined in ploarized light by means of the MIM-8 microscope.

The microhardness of the phase components was detremined, as usual, with the PMT-3 instrument. Finally, the integral thermo-emf of the specimens (relative to copper) was measured with 100° temperature difference (20-120°) with the apparatus described earlier [9].

Experimental Data and Discussion

Seventeen oxide samples containing from 14.04 to 34.13% oxygen were prepared as described above. The results of x-ray investigations of these samples are given in Table 1.

TABLE 1. Variation of the Lattice Constant of the δ Phase with Composition

Molecular formula	Phase composition	Lattice constant of $VO_{1\pm x}$ phase, kX	Molecular formula	Phase composition	Lattice constant of $VO_{1\pm x}$ phase, kX
$VO_{0.52}$	$VO_{1\pm x}+\alpha'$	4,015±0,002	$VO_{1.30}$	$VO_{1\pm x}+V_2O_3$	4,130±0,001
$VO_{0.63}$	»	4,015±0,002	$VO_{1.32}$	»	4,130±0,001
$VO_{0.75}$	»	4,015±0,002	$VO_{1.34}$	$V_2O_3+V_{1\pm x}$	4,130±0,001
$VO_{0.85}$	$VO_{1\pm x}$	4,016±0,002	$VO_{1.41}$	»	4,129±0,002
$VO_{0.99}$	»	4,047±0,002	$VO_{1.44}$	»	—
$VO_{1.05}$	»	4,064±0,002	$VO_{1.51}$	V_2O_3	—
$VO_{1.11}$	»	4,087±0,002	$VO_{1.65}$	$V_2O_3+V_3O_5$	—
$VO_{1.23}$	»	4,122±0,001			

* Kindly supplied by Yu. A. Polyakov, to whom we offer our thanks.

The specimen of composition $VO_{0.79}$ consisted of a single phase and contained only the tetragonal body-centered α' phase with the constants a = 2.976 and c = 3.387 kX, which is in better agreement with the results reported by Seybolt [10] (a = 2.971; c = 3.381 kX), than with Rostoker's data [11] (a = 2.982; c = 3.330 kX). With increase of oxygen content ($VO_{0.83}$; $VO_{0.93}$; $VO_{0.75}$) two phases appeared in the specimens: in addition to the α' phase, the cubic δ phase was detected (with constant a = 4.015 kX). Repeated vacuum annealing did not alter either the phase composition of the specimens or the lattice constants. In every case the δ phase was present in equilibrium with the α' phase. No signs of the β phase, described in [1], were found. This is possibly because Gurevich and Ormont [1, 5] discovered the oxide $VO_{0.7\pm x}$ in specimens containing carbon in addition to vanadium and oxygen. In other words, the β phase possibly exists in the ternary system V – C – O rather than in the binary system.

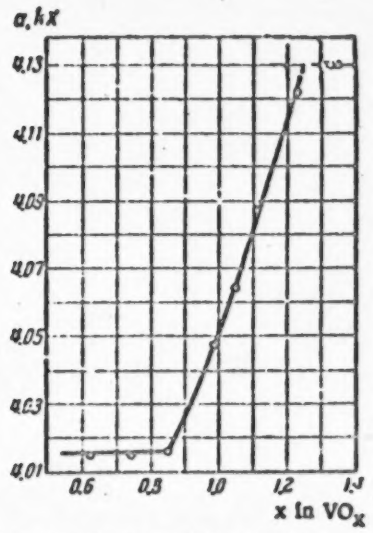

Fig. 1. Variation of the lattice constant of the δ phase with composition.

It was further found, in satisfactory agreement with literature data, that the δ phase ($VO_{1\pm x}$) is stable over a fairly extensive concentration range. The data in Table 1 indicate that the limits of the range are $VO_{>0.75}$ – $VO_{<1.33}$. Graphical refinement of the stability range of the lower vanadium oxide (Fig. 1) confirms that they correspond to the compositions $VO_{0.83}$ – $VO_{1.25}$. These values are in very good agreement with the data in [2] ($0.8 \leqslant x \leqslant 1.27$) and differ somewhat from those in [1] ($0.8 \leqslant x \leqslant 1.2$).

It was of special interest to determine whether the ζ phase, which has, according to [1], a cubic body-centered lattice, can exist, because no oxides of the type MeO_x ($1.2 \leqslant x \leqslant 1.4$) of such structure are known. Further, in view of the geometrical stability limits of structures with different coordination numbers, it can be shown that in this case the lattice should have coordination number 6 (the NaCl type). Finally, as already noted, the x-ray patterns of specimens containing the δ and ζ phases simultaneously were indexed on the basis of the NaCl type of lattice. The data in [1] indicate that some of our specimens ($VO_{1.23}$; $VO_{1.19}$; $VO_{1.22}$; $VO_{1.30}$) might consist of the ζ phase only. This was not found to be the case, although the specimens were annealed for 76 hours to stabilize the system.

At the same time, it is known [12] that equilibrium is reached quite rapidly in the V – O system, especially in specimens with fairly high oxygen concentrations.

Analysis of the x-ray patterns showed that the experimental data can be satisfactorily interpreted with the assumption that only one phase of the NaCl type is present in such specimens. However, it becomes necessary to explain the anomalous relationship between the line intensities, to which Gurevich and Ormont [1] first drew attention. For example, it is found that calculated intensities of different lines (with the assumption that the system is of the single-phase type, and that the δ phase is present) differ sharply from the experimental values in patterns obtained with chromium radiation. For example:

$$(I_{200} : I_{111})_{calc} = 4{,}4 \quad ; \quad (I_{200} : I_{111})_{meas} = 10;$$
$$(I_{222} : I_{311})_{calc} = 2{,}3 \quad ; \quad (I_{222} : I_{311})_{meas} = 7{,}5.$$

As was pointed out earlier, because of this result such specimens were regarded [1] as two-phase systems consisting mainly of a cubic body-centered ζ phase with a small amount of a cubic face-centered δ phase. However, patterns obtained with copper radiation refute this interpretation and leave no doubt that only the δ phase is present. Analysis of these x-ray patterns and calculations show that the measured and calculated relative intensities are similar:

$$(I_{200} : I_{111})_{meas} = 5 \; ; \quad (I_{200} : I_{111})_{calc} = 5{,}2; \quad (I_{222} : I_{311})_{meas} = 1{,}1,$$
$$(I_{222} : I_{311})_{calc} = 1{,}4.$$

Accordingly, the suggestion [2] that the anomalous line intensity ratio reported by Gurevich and Ormont [1] is due to impurities is incorrect. A more correct explanation is that the anomaly is due to the proximity of the K absorption edge of vanadium and $\lambda_{K\alpha}$ of chromium. In the selection of the atomic factor of vanadium in this case it is necessary

to apply the Hönl corrections [13], which are very substantial here. Accordingly, the denominator of the expression $I_{100}/I_{111} = k(f'_V + f'_O)/(f''_V - f''_O)$ becomes considerably less than the numerator. As a result, in the x-ray patterns of specimens rich in oxygen ($VO_{1.2} - VO_{1.3}$), the ratios of individual line intensities becomes anomalous. This effect diminishes considerably with increase of vanadium content and is virtually nonexistent in $VO_{0.9}$. Transition from oxides to oxycarbides leads to a similar result, because the atomic factor of carbon is somewhat less than that of oxygen.

It should be noted that the hypothesis of the formation of a cubic body-centered ζ phase cannot be reconciled with the results of pycnometric determinations either. If this phase was formed, the density of specimens of the composition, say, $VO_{1.25}$ should be 4.7 g/cc. As the density of the trioxide is 4.99 g/cc, specimens in the $VO_{1.29} - VO_{1.34}$ range should have densities < 5 g/cc. In fact the density is > 5 g/cc, which indicates that the system V – O does not contain the ζ phase.

A more systematic correlation of x-ray and pycnometric results is necessary for precise determinatio of the structural characteristic of the δ phase. This is demonstrated, in particular, by the data of Mathewson et al. [14], who found that the experimental density of $VO_{1.00}$ (5.5 g/cc) is approximately 15% less than the x-ray density (6.5 g/cc.). Similar observations are reported elsewhere [2, 4, 12]. Our measurements (Table 2) also confirm that the actual density of the δ phase is considerably less than the calculated over the entire homogeneity range. In agreement with the views put forward by others [2, 12], this suggests that the δ phase has defect structure. In this respect $VO_{1\pm x}$ is very similar to the phases: $TiO_{1\pm x}$, $CrP_{1\pm x}$, $VS_{1\pm x}$, $VSe_{1\pm x}$, in which, as was first shown by Ehrlich [15], both sublattices are of the defect type. With the aid of a similar model of the structure of $VO_{1\pm x}$, it is easy to estimate the number n_V of vanadium atoms and n_O of oxygen atoms in the unit cell, and the hole concentration Δn (in %) from experimental data on the lattice constants and densities. Calculated values of the density ρ found from the formula $\rho = nA_{aV}/NV$ (n is the number of particles, A_{aV} is the average atomic weight, N is the Avogadro number, and V is the volume of the unit cell), given in Table 2, show that the δ phase has high dual defectiveness. On oxygen-rich specimens the number of vacancies in the vanadium sublattice is fairly high (about 21%), whereas the oxygen sublattice is almost devoid of vacancies (1.5-2%). Conversely, in the opposite concentration region ($VO_{0.85}$) the oxygen deficiency reaches 26%, and the vanadium deficiency, about 13%.

TABLE 2. Calculation of the Defectiveness of the δ Phase

Composition	Density of $VO_{1\pm x}$, g/cc		Total number of atoms in unit cell, n	Number of vanadium atoms, n_V	Number of oxygen atoms, n_O	Hole concentration, $\frac{\delta - n}{\delta} \cdot 100$, %
	X-ray*	Pycnometric				
$VO_{0.62}$	6,58	5,81	6,45	3,49	2,96	19,4
$VO_{0.63}$	6,58	5,78	6,43	3,48	2,95	19,6
$VO_{0.75}$	6,58	5,63	6,38	3,45	2,93	20,2
$VO_{0.85}$	6,58	5,76	6,49	3,51	2,98	18,9
$VO_{0.99}$	6,64	5,58	6,69	3,38	3,33	16,4
$VO_{1.05}$	6,33	5,55	6,85	3,34	3,51	14,4
$VO_{1.11}$	5,97	5,40	6,86	3,25	3,61	14,3
$VO_{1.23}$	5,42	5,30	7,10	3,18	3,92	11,3
$VO_{1.30}$	5,32	5,18	7,08	3,14	3,94	11,5
$VO_{1.32}$	5,32	5,16	7,07	3,14	3,93	11,6
$VO_{1.34}$	5,32	5,11	7,01	3,12	3,89	11,2
$VO_{1.41}$	5,32	5,08	7,07	3,14	3,93	11,6

* Densities are calculated with the following assumptions:
1) the stoichiometric VO lattice is free from defects;
2) at $VO_{>1.0}$ defects are present in the cation sublattice;
3) at $VO_{<1.0}$ defects are present in the anion sublattice.

It should be noted that there are no superstructure lines in the x-ray patters of the δ phase for any of the compositions. Therefore the distribution of defects can be regarded as statistical; in this respect $VO_{1\pm x}$ (and also $TiO_{1\pm x}$) differs essentially from such compounds as NbO. The latter, as has been noted earlier [16, 17] has a lattice of the NaCl type, with only three atoms each of niobium and oxygen in the unit cell, with the holes in an ordered arrangement. It is possible that this is precisely the reason why oxygen atoms are not replaced by carbon in the NbO lattice.

whereas in the systems Ti – O – C and V – O – C in presence of lower-oxide phases the oxycarbides have extensive homogeneity regions [5, 18]. Finally, the high defectiveness of the lattice and the disordered arrangement of the holes indicate that the mobility of the particles is relatively high, so that equilibrium in the V – O system is reached fairly rapidly and there is no V – O interlayer in the scale layer on vanadium.

Some additional data on the properties of the δ phase were obtained as the result of microscopic investigations. First, it was found that $VO_{1\pm x}$ forms very brittle crystals, the microhardness of which can be determined only under the minimum loads (50 g; the grains crack if the load is increased). It was further found that the hardness of vanadium monoxide is high and varies irregularly with composition:

Composition of speciment	$VO_{0.93}$	$VO_{0.99}$	$VO_{1.05}$	$VO_{1.11}$	$VO_{1.23}$	$VO_{1.23}$
Microhardness, kg/mm²	1950	1800	2100	1800	1950	1800

Finally, examination of the specimens by polarized light revealed weak but distinctly reproducible optical anisotropy which increases with the oxygen content. Therefore either the cubic lattice of the δ phase is somewhat distorted (for example, with tetragonal or rhombic distortion), or a thin film of higher oxides (which have a lower order of symmetry than cubic) is formed during preparation of the sections. Careful analysis of the x-ray patterns did not confirm distortion of the cubic lattice. The lines were neither split nor diffuse (with the use of RPK and VRS cameras). Graphical extrapolation of the experimental data by the method of Bradley and Jay [19] leads to the same conclusion. In this method the lattice constants calculated from different diffraction maxima are plotted against $\cos^2\theta$. Extrapolation to $\cos^2\theta = 0$ gives the true lattice constant; therefore irregular scattering of the experimental points indicates lattice distortions. Figure 2 shows satisfactory linear relationships between a_θ and $\cos^2\theta$ for samples differing in composition; this indicates the absence of any significant distortions of the cubic structure. It is therefore possible that the optical anisotropy is caused by surface effects which develop during preparation of the sections. It must be noted, however, that it was observed to the same degree both in freshly prepared specimens and in specimens which had been kept for some time. Therefore this effect cannot be explained with certainty and further investigation is needed.

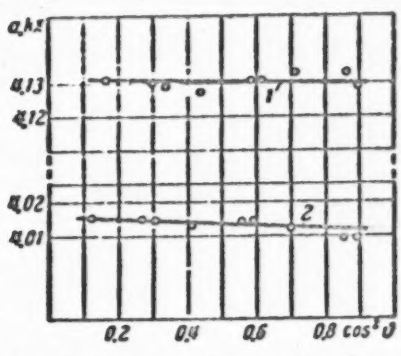

Fig. 2. Variation of a_θ with $\cos^2\theta$: 1) for $VO_{1.25}$; 2) $VO_{0.93}$.

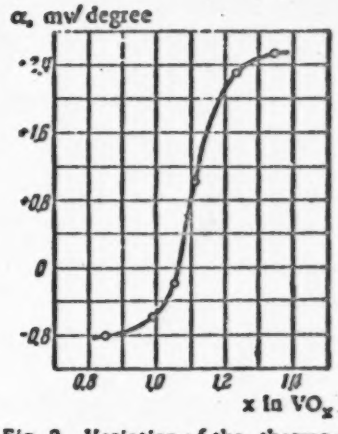

Fig. 3. Variation of the thermo-emf of the δ phase with composition.

The dual defectiveness of the δ phase lattice prompted an interest in the effect of composition on the thermoelectric properties of the specimens. Measurements showed (Fig. 3) that the integral (20-120°) thermo-emf (relative to copper) increases regularly with the oxygen content. The thermo-emf passes through zero near the composition ($VO_{1.05}$) at which, according to [2], the lattice constant changes abruptly. In other words, the sign of the thermo-emf suggests that the nature of the predominant carriers of current alters with the oxide composition. Electronic conduction predominates in specimens rich in vanadium (i.e., in electron donors), whereas hole conduction is predominant in specimens rich in oxygen (acceptor atoms). Thus, in its thermoelectric properties $VO_{1\pm x}$ is analogous to typical ionic semiconductors [20]. It is accordingly of undoubted interest to study other electrical characteristics of vanadium oxides (electrical conductivity, Hall constant), whereby the concentration and mobility of the carriers could be assessed.

Estimation of the stability region of vanadium trioxide is difficult because of the insufficient number of specimens studied. However, as Table 1 shows, x-ray analysis clearly reveals the presence of vanadium monoxide together with

the V_2O_3 phase in the specimen of the composition $VO_{1.44}$. On the other hand, x-ray phase analysis of a specimen with the composition $VO_{1.48}$ shows noticeable reflections of both V_2O_3 and V_2O_5. Accordingly we can say, in agreement with [21], that vanadium trioxide is stable over a relatively narrow composition range ($VO_{>1.44} - VO_{<1.48}$). According to literature data, the lattice constants remain unchanged over the entire stability range V_2O_3. Comparison of the x-ray patterns of specimens in which V_2O_3 coexists either with $VO_{1.2}$ or with V_2O_5 did not reveal any distinct differences between the constants. For greater precision, patterns for both specimens were obtained simultaneously in a camera of the VRS type on the same film. There was a slight shift of the corresponding lines in the large-angle region. As was to be expected, the lattice constants of vanadium trioxide enriched with oxygen were somewhat greater than the constants for specimens containing excess vanadium.

LITERATURE CITED

1. M. A. Gurevich, B. F. Ormont, Zhur. neorgan. khimii 2, 2581 (1957).
2. É. Vol'f, S. S. Tolkachev, I. I. Kozhina, Vestn. Leningr. univ. Ser. fiz. i khim. 10, 2, 87 (1959).
3. É. Vol'f, S. M. Ariya, Zh. obshch. khimii 29, 2470 (1959).
4. É. Vol'f, M. P. Morozova, Zh. obshch. khimii 29 3146 (1959).
5. N. A. Gurevich, B. F. Ormont, Zh. neorgan. khimii 3, 403 (1958).
6. V. I. Arkharov, B. S. Borisov, T. V. Dolgal', Electron-Diffraction Investigation of Texture in Oxide Films at Various Stages of High-Temperature Oxidation of Metals [in Russian]. Paper at the 6th Scientific and Technical Conference on the Application of X Rays to Investigation of Metals. Leningrad, June 23-28, 1958.
7. M. A. Gurevich, B. F. Ormont, Fiz. metallov i metallovedenie 4, 112 (1957).
8. W. Rostocker, Metallurgy of Vanadium [Russian translation] (Izd. inostr. lit. Moscow, 1959) p. 57.
9. V. A. Lipatova, P. V. Gel'd, K. N. Davydov, Tr. Ural'sk. politekhn. inst. 72, 105 (1957).
10. A. U. Seybolt, H. T. Sumsion, J. Metals 5, 292 (1953).
11. W. Rostoker, A. S. Yamamoto, Trans. Amer. Soc. Metals 47, 1002 (1955).
12. N. Schonberg, Acta chem. scand. 8, 221 (1954).
13. R. W. James, Optical Principles of the Diffraction of X Rays [Russian translation] (Izd. inostr. lit., Moscow 1950) pp. 129, 552.
14. C. H. Mathewson, F. Spire, C. H. Samans, Trans. Amer. Soc. Steel Treating 20, 357 (1932).
15. P. Ehrlich, Z. Elektrochem. 45, 362 (1939).
16. G. Brauer, Z. anorgan. allgem. Chem. 248, 1 (1941).
17. S. I. Alyamovskii, G. P. Shveikin, P. V. Gel'd, Zh. neorgan. khimii 3, 2437 (1958).
18. V. S. Kutsev, B. F. Ormont, Zh. fiz. khimii 29, 597 (1955); 31, 1866 (1957).
19. A. J. Bradley, A. H. Jay, Proc. Phys. Soc. 44 563 (1932).
20. A. F. Ioffe, Izv. AN SSSR, Ser. fiz. 15, 477 (1951); S. V. Airapetyants, B. A. Efimova, Zh. tekhn. fiziki 28, 1768 (1958).
21. G. Anderson. Acta chem. scand. 8, 1599 (1954).

All abbreviations of periodicals in the above bibliography are letter-by-letter transliterations of the abbreviations as given in the original Russian journal. *Some or all of this periodical literature may well be available in English translation.* A complete list of the cover-to-cover English translations appears at the back of this issue.

COVALENT ATOMIC RADII IN MULTIPLE BONDING

G. B. Bokii and L. O. Atovmyan

Institute of Inorganic Chemistry, Siberian Division, Academy of Sciences USSR, Novosibirsk
N. S. Kurnakov Institute of General and Inorganic Chemistry, Academy of Sciences, USSR

Translated from Zhurnal Strukturnoi Khimii, Vol. 2, No. 3, pp. 308-311, May-June, 1961
Original article submitted August 31, 1961

Covalent multiple-bond radii of metallic atoms (based on x-ray structural data) have been tabulated. The relationship between valence and coordination number in multiple bond formation is examined. It is shown that bond ionicity has more influence on interatomic distances in multiple bonding than with single bonds.

Multiple Bonds

Cases of multiple bond formation between nonmetal atoms are well known in chemistry. The tendency to form such bonds is especially pronounced in nonmetallic elements of the second period and diminishes in the subsequent periods. In 1940 Pauling suggested that although multiple bond formation is mainly characteristic of nonmetals, atoms of transition metals can form not only single but also multiple covalent bonds by utilizing the electrons and orbitals of the penultimate shell [1]. However, lack of experimental data made verification of this hypothesis impossible.

In 1954 Jaffe [2] considered the symmetry and direction of the d orbitals and the possibility of overlapping, and calculated the overlapping integrals for the corresponding molecular orbitals. He showed that whereas conclusions concerning the formation of d π bonds with nd orbitals taken into account are not definite, there is no doubt about the significant role of π bonds due to (n − 1)d orbitals. However, only interatomic distances can provide direct proof of the existence of multiple bonding.

Covalent Radii (Å) with Single and Multiple Bonds

								B 0,83 0,66₄	C 0,77 0,65₄ 0,60₄	N 0,7 0,62 0,54₄	O 0,66 0,60₄ 0,52₄	F 0,64	Single Double Triple
								Al 1,26	Si 1,17 1,04 0,98₄	P 1,10 0,96	S 1,04 0,83₄	Cl 0,99 0,76	Single Double Triple
V ^{5}1,13(5)* ^{4}0,96(4)	Cr ^{6}1,17(6) ^{4}0,93(4)	Mn ^{7}1,12(4) ^{4}0,96(4)	Fe ^{6}1,19(5) ^{4}1,95(5)	Co	Ni	Cu	Zn	Ga	Ge 1,22 1,17 1,12₄	As 1,21 1,15	Se 1,17 1,01	Br 1,14	Single Double Triple
Nb	Mo ^{6}1,29(6) ^{4}1,22(4)	Tc	Ru ^{6}1,36(6) ^{4}1,17(6)	Rh	Pd	Ag	Cd	In	Sn 1,40 1,355 1,314	Sb 1,40	Te 1,37	I 1,33 1,19	Single Double Triple
Ta	W ^{6}1,25(6) ^{4}1,21(4)	Re ^{6}1,24(6) ^{4}1,08(4)	Os ^{6}1,42(6) ^{4}1,25(6) ^{4}1,05(6)	Ir	Pt	Au	Hg	Tl	Pb 1,45 1,43 1,368	Bi 1,46	Po	At	Single Double Triple
	U ^{6}1,42(7) 0,976(2)												

*The superscript figure to the left of the value for the radius represents the formal valence, and the figure in parentheses to the right is the coordination number of the metal in the compound for which the radius was calculated. The double-bond radii for Si, Ge, Sn, and Pb were calculated theoretically [35].

In presence of a multiple bond between two atoms the corresponding interatomic distances are considerably smaller than in ordinary covalent bonding. On the basis of structure investigations, tables of multiple-bond atomic radii were compiled for nonmetals, analogous to tables of covalent radii with single bonds [1, 3]. These tables can now be supplemented by radii in multiple bonding (multiple-bond radii) of many transition metals. These values are given in the table, in which two regions are distinguished. Multiple-bond radii for nonmetals and semimetals have been recalculated from experimental data, because the existing tables (see, for example, [4]) are appreciably out of date. All the multiple bond radii for metals are calculated for the first time; the starting data for these calculations were derived mainly from the results of x-ray investigations of the corresponding oxygen compounds. The values given in the table were obtained by subtraction of the oxygen multiple-bond radius (0.60$_5$ A) from experimental values of the Me = O interatomic distances. Data were used from the following publications: V [5], Cr [5, 6], Mo [7, 8], W [8, 9], U [10, 11], Mn [12, 13], Re [13, 14], Fe [15], Ru [16], Os [16, 17] B [18], C [19, 20], Si [21], Ge [22], Sn [23], Pb [24], N [25, 26], P [27], As [28], O [29, 30], S [31], Se [32], Cl, [12], I [33].

Multiple bond formation in the light elements is especially characteristic with linear, triangular, or tetrahedral coordination (NO^+, N_2, CO, CO_2, SO_3, PO_4^{3-}, SO_4^{2-}, ClO_4^-), as has been repeatedly pointed out by various writers [1, 34, 36]. If we consider the metals of groups V, VI, and VII, we notice the far-reaching analogy to the nonmetals of the same groups. These metals also form characteristic tetrahedral complexes with very shortened bonds (CrO_4^{2-}, MoO_4^{2-}, WO_4^{2-}, MnO_4^-, ReO_4^-, VO_4^-, etc.). Linear groupings in octahedral complexes of heavy metals (OsO_2, RuO_2, UO_2) [16] are analogs of linear groups of light elements with multiple bonds. However, in this case formation of compounds with linear local groups is probably difficult here owing to the large number of free electrons in heavy-metal atoms. The number of metal compounds with multiple bonds which have been investigated increases from day to day, and these compounds attract the attention of both experimental and theoretical workers.

Multiple Bonding and Valence

A survey of the structure of chemical compounds of metals with univalent nonmetals shows that as each metal is consecutively replaced by the next in the same period there is a tendency for the bond character to change from ionic to covalent [34, 37]. Whereas in the case of ionic bonding the coordination number of the metal is determined by the ratio of the radii, in covalent bonding it is determined by the corresponding hybridization. As the valence of a metal increases, its radius decreases, and in consequence its coordination number diminishes. However, this decrease has a limit determined by the formation of directed covalent bonds. Further increase of valence leads to accumulation of the bond electrons in the coordination polyhedron characteristic of the metal, i.e., to formation of metal – ligand multiple bonds. It follows that formation of multiple bonds should be most characteristic for compounds of metals which exhibit high valences.

Since the formation of multiple bonds influences physicochemical properties, it is convenient to subdivide complex compounds into two large groups: ordinary complex compounds, and complex compounds with multiple bonds [38]. In general, the relationship between valence and coordination number conforms to a simple rule. The formal valence of a complex-forming metal is less than the coordination number in ordinary complex compounds. On the other hand, in compounds with multiple bonds the formal valence of the central atom is either equal to or greater than its coordination number. We considered from this point of view complex compounds which have been structurally investigated and found to contain double bonds. Most of them conform to this rule. Complex uranyl compounds do not. It is known from numerous structural investigations that the U–O bonds in the UO_2 group are multiple bonds. In uranyl compounds the number of ligands surrounding the uranyl group varies from compound to compound; this indicates that the bonds are ionic in character. Therefore, if we refer to the coordination number with known covalent bonding, it must be taken as two for uranyl compounds, which then conform to the above rule.

Effect of Ionicity on Multiple Bonding

It is usually stressed in relation to compounds with covalent bonds that there is a continuous transition from homopolar to heteropolar bonding. A bond of the intermediate type may be represented either as a heteropolar bond with polarization (distortion of the anion electron shells in the field of the positive ion) taken into account, or as a homopolar bond with a correction for bond ionicity. In crystal chemistry the bond character is usually correlated with changes of interatomic distance. However, the sums of the covalent radii often coincide (within the limits of experimental error) with the sums of the ionic radii. Therefore, it is in general impossible to determine by the methods of structure analysis the degree of deviation from one or the other limiting bond type. The situation is quite different with compounds containing multiple bonds, where the limiting covalent (multiple-bond) radius is considerably less than the ionic radius. In such cases the interatomic distances are much more sensitive to increases due to a defi-

nite proportion of ionic character (ionicity) in the bond than is the case with ordinary compounds. Therefore, if the usual covalent radii are not completely additive as we pass from one compound to another, the deviations from additivity with multiple-bond radii must be even greater. An especially striking example of this is provided by the lack of agreement between the U–O interatomic distance of the uranyl group in different compounds. The following values (in A) have been reported for different ligands surrounding the UO_2 group: NO_3 1.68 [40], CO_3 1.67 [39], CH_3COO 1.70 [40], Cl 1.73 [41], AsO_4 1.89 [42], OH 1.89 [43], F 1.91 [44], C 1.91 [11].

Here polymers as well as island (complex) compounds are considered, because very few island structures have been investigated.

There is no doubt that the U – O bond in the UO_2 group is not purely covalent either. According to Pauling [1], the ionic character of a multiple bond is double that of a single bond. This means that electrons involved in multiple bonds are more mobile than those in single bonds. Therefore the ionicity of the U – O bond in the UO_2 group must depend to a greater extent on the presence of other compounds containing single bonds only. In other words, the effective electrongativity of uranium varies from compound to compound.

Changes of the U – O distance in the uranyl group can also be interpreted in the light of the covalent bond theory, as was done by Dyatkina et al. [45]. In their view, the unshared pairs of electrons from oxygen are involved in additional bonding with uranium in its free orbitals leading to a decrease of the U – O distance. Analogous additional bonds can, of course, also be formed with other central atoms.

As yet we cannot take into account the effects of additional bonding, bond ionicity, and a number of other factors on interatomic distances. Therefore the values of the multiple-bond "radii" given in this paper probably do not refer to purely double bonds. In many instances the multiple bond may be complicated by these additional effects. Neverthless we hope that the multiple-bond metal radii, even in this form, may facilitate the use of these data in theoretical chemistry. Of course, the table given in this paper may be improved in the future.

LITERATURE CITED

1. L. Pauling. Nature of the Chemical Bond [Russian translation] (Goskhimizdat, Moscow, 1947).
2. H. Jaffe. Usp. Khimii 26, 9, 1060 (1957).
3. A. I. Kitaigorodskii. X-ray Structure Analysis [in Russian] (Gostekhizdat, Moscow-Leningrad, 1950).
4. G. B. Bokii. Introduction to Crystal Chemistry [in Russian] (Izd. MGU, 1954).
5. K. J. Palmer. J. Amer. Chem. Soc. 60, 2360 (1938).
6. F. Hanič. Chem. Zvesti 10, 2,8 (1956).
7. J. Donohue, W. Shand. J. Amer. Chem. Soc. 69, 222 (1947).
8. Tables of Interatomic Distances and Configurations in Molecules and Ions (London, 1958).
9. J. A. A. Ketelaar, G. W. van Oosterhaut. Rec. Trav. Chim. 62, 197 (1943).
10. J. H. Dieke, A. B. F. Duncan. Spectroscopic Properties of Uranium Compounds (New York, 1949).
11. W. H. Zachariasen. Acta crystallogr. 1, 281 (1948).
12. S. Ramasechan, F. A. Sc. K. Venkatesan, N. V. Mani. Proc. Ind. Acad. Sci. 46, 2, 95 (1957).
13. R. Javan, A. Engelbrecht. Phys. Rev. 96, 649 (1954).
14. I. Beintema. Z. Kristallogr. 97, 300 (1937).
15. G. Johausen, W. Lipscomb. J. Chem. Phys. 27, 1417 (1957).
16. G. B. Bokii, L. O. Atovmyan, T. S. Khodashova. Dokl. AN SSSR 128, 1, 78 (1959).
17. J. L. Hoard, J. D. Grenko. Z. Kristallogr. 87, 100 (1934).
18. A. E. Duglas, G. Herzberg. Canad. J. Research. 18A, 179 (1940).
19. J. G. Fox, G. Herzberg. Phys. Rev. 52, 638 (1937).
20. R. T. Lagemon. A. H. Nielsen, F. P. Diken. Phys. Rev. 72, 284 (1947).
21. L. H. Woods. Phys. Rev. 63, 426 (1943).
22. R. F. Barow, I. W. Ievons. Proc. Phys. Soc. 51, 989 (1939).
23. P. H. Mahanti, A. K. Sen Gupta. Z. Phys. 109, 39 (1938).
24. E. C. Vago, R. F. Barow. Proc. Phys. Soc. 59, 449 (1947).
25. H. A. Stuart. Die Struktur des freien Moleküls (Springer Verlag, Berlin, 1952).
26. B. Stoicheff. Canad. J. Phys. 82, 630 (1954).
27. T. Ito, K. H. Mori. Acta crystallogr. 4, 412 (1951).

28. K. H. Mori, T. Ito. Acta crystallogr. 3, 290 (1950).
29. S. C. Miller, C. H. Townes. Phys. Rev. 90, 537 (1953).
30. C. Jousseran, L. Grillet, M. Duffioux. Compt. rend. 205, 39 (1937).
31. F. Mazzi. Acta crystallogr. 8, 137 (1955).
32. M. Bailey, A. F. Wells. J. Chem. Soc. 968 (1951).
33. L. A. Hazlewood. Z. Kristallogr. 98, 439 (1938).
34. Ya. K. Syrkin, M. E. Dyatkina. The Chemical Bond and the Structure of Molecules [in Russian] (Goskhimizdat, Moscow-Leningrad, 1946).
35. J. L. Kovanau. J. Chem. Phys. 12, 467 (1947).
36. F. Hanič. Chem. Zvesti. 10, 5, 268 (1956).
37. S. S. Batsanov. Structural Refractometry [in Russian] (Izd. MGU, Moscow, 1959).
38. G. B. Bokii. Zh. strukt. khim. 1, 1, 72 (1960).
39. T. Comer, P. E. Harper. Acta crystallogr. 8, 847 (1955).
40. W. H. Zachariasen. Acta crystallogr. 12, 526 (1959).
41. L. H. Jones. Spectrochim. Acta 6, 409 (1959).
42. F. Hanič. Czech. J. Phys. B10, 169 (1960).
43. G. Bergstrom, G. Lundgren. Acta Chem. scand. 10, 673 (1956).
44. W. H. Zachariasen. Acta crystallogr. 1, 277 (1948).
45. M. E. Dyatkina, V. P. Markov, I. V. Tsapkina, Yu. N. Mikhailov, Zh. neorgan. khimii 6, 3, 575 (1961).

All abbreviations of periodicals in the above bibliography are letter-by-letter transliterations of the abbreviations as given in the original Russian journal. *Some or all of this periodical literature may well be available in English translation.* A complete list of the cover-to-cover English translations appears at the back of this issue.

STERIC HINDRANCES AND CONFORMATION OF MOLECULES

COMMUNICATION 5. CRYSTAL STRUCTURE OF HEXACHLOROBENZENE

I. N. Strel'tsova and Yu. T. Struchkov

Institute of Heteroorganic Compounds, Academy of Sciences, USSR
Translated from Zhurnal Strukturnoi Khimii, Vol. 2, No. 3, pp. 312-328, May-June, 1961
Original article submitted October 24, 1960

Factors determining the conformation of hexahalobenzene molecules in both vapor and crystal form are considered. The crystal structue of hexachlorobenzene was refined, and it was found that the molecule in crystal form is planar to an accuracy of ± 0.02 A. A new method is proposed for estimation of equilibrium intermolecular distances in crystals, based on curves representing the interaction energy of atoms without valence bonding and minimalization of the calculated lattice energy. The equilibrium distances were found to depend distinctly on the direction relative to the molecular plane. The lattice energies of the real hexachlorobenzene structure and of a hypothetical structure with nonplanar molecules were calculated. Values of the force constant for removal of the C – Cl bond from the plane of the benzene ring, with which the hexachlorobenzene molecule must be definitely planar in crystal and vapor form, were calculated.

This paper represents a continuation of our series of structural investigations of the conformation of "overcrowded" substituted benzenes with considerable steric hindrances, in particular, hexasubstituted benzene derivatives. It was shown in the previous communication [1] that molecules of tetrabromo-m-xylene and tetrabromo-o-xylene are planar in crystals, despite considerable steric hindrances between the substituents. It was therefore desirable to refine the crystal structure of hexachlorobenzene, as the literature information on the conformation of this molecule is contradictory.

INTRODUCTION

If the bond lengths were C – C = 1.40 and C – Cl = 1.71 A, the intermolecular Cl . . . Cl distance in the planar symmetrical model of the hexachlorobenzene molecule would be 3.11 A, or considerably shorter than the equilibrium distance Cl . . . Cl ≥ 3.6 A, corresponding to van der Waals interaction. As in other symmetrical hexasubstituted benzenes, these steric hindrances can be diminished only if the substituents are taken out of the ring plane alternately upward and downward. This would make their arrangement similar to the arrangement of the carbon atoms in the chair conformation of the cyclohexane nucleus (Fig. 1). In leaving the plane the substituents can in principle take carbon atoms of the nucleus with them, so that the benzene nucleus itself ceases to be planar and assumes the chair conformation. Evidently the displacements z_C of the carbon atom from the mean plane of the molecule must be less than the displacement z_X of the substituents, so that the CCC valence angle may be less than, but close to, 120°.

Thus, in an overcrowded molecule of a hexasubstituted benzene, loss of planarity is advantageous for decreasing steric hindrances, but distortion of the normal valence angles is disadvantageous; this may be expressed as "a compromise between steric hindrance and deformation of valence angles." For the real conformation, the corresponding (conformational) part of the potential energy of the molecule must be at a minimum:

$$W(R, \omega) = V(R) + U(\omega) \rightarrow \text{minimum}$$

or

$$W(z) \rightarrow \text{minimum},$$

since R and ω may be expressed in terms of z. Here V(R) is the energy of interaction between atoms without valence bonding (energy of "spatial interaction"), which depends on the distance R between them, and U(ω) is the deforma-

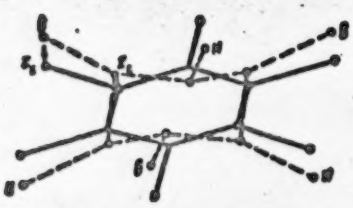

Fig. 1. Nonplanar model of the hexachlorobenzene molecule.

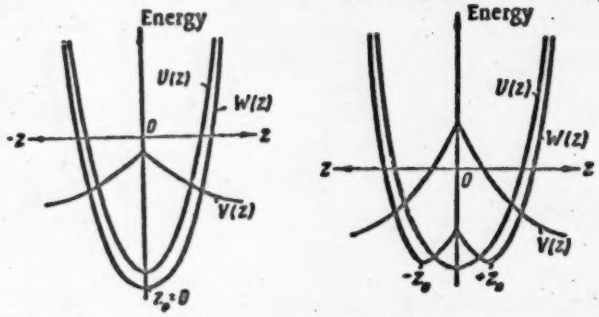

Fig. 2. Relationship between the spatial interaction energy V (z) and valence angle distortion U (z) (W is the conformational part of the energy of the molecule): left – coplanarity retained; right – coplanarity lost.

tion energy of the valence angle ω. In accordance with the form of these functions, a given molecule may undergo a definite loss of coplanarity, or may retain it. This is illustrated by the schematic graphs in Fig. 2, which show that if distortion of the valence angles requires a large amount of energy the molecule remains planar.

Experimental data on the conformation of the hexachlorobenzene molecule are contradictory*. According to an x-ray investigation [2], its molecule is planar in crystals; however, this investigation contains crude errors which will be discussed below. An earlier electron-diffraction study of C_6Cl_6 in vapor form, carried out by Bastiansen and Hassel [4], indicates that the molecule is nonplanar: $z_{Cl} = 0.36$, $z_{Cl} = 0$ Å, so that the C – Cl bonds diverge from the plane of the benzene nucleus by an angle $\alpha \approx 12°$. This value was evidently determined inaccurately, because according to the same authors [4], the deviation from planarity in the hexabromobenzene molecule is of the same magnitude. In a later private communication (cited in [5]) Bastiansen and Hassel rejected their earlier result and stated that according to more precise electron-diffraction determinations the C_6Cl_6 molecule in the vapor state is planar.

All the infrared spectroscopic data on crystalline C_6Cl_6 and its solutions in the 2-15 μ region may be interpreted on the basis of a planar hexagonal molecular model [6]. On the other hand, the spectrum of C_6Cl_6 crystals in the near ultraviolet region [7] appears to indicate a nonplanar molecule with $6\bar{2}m$ symmetry, although the authors themselves note that there is some uncertainty in the interpretation of the spectrum. Duchesne and Monfils [8], who investigated pure quadrupole spectra of a number of chlorobenzenes, consider that the anomalous increase of the quadrupole bond constant eqQ in presence of neigboring (ortho) chlorine atoms in the benzene ring must be due to a decrease of the degree of double bonding in structures of the $C = Cl^+$ type. They attribute this decrease to the nonparallel character of the π orbitals which is the consequence of loss of planarity in the molecule as the result of steric hindrance. With this assumption they find from the change of eqQ that the C – Cl bonds diverge from the plane of the benzene nucleus in C_6Cl_6 by 25°. However, as Bray et al. [9] point out, the interpretation given by Duchesne and Monfils for the quadrupole spectra of polyhalobenzenes is by no means conclusive, because eqQ depends not only on the degree of double bonding but on such bond characteristics as ionicity, hybridization, and bond orientation in the molecule and the crystal. These effects cannot be separated in experiments with polycrystalline specimens. Moreover, the π orbital of the chlorine atom overlaps more effectively with the σ function of the carbon atom than with the $2p\pi$ function. However, the first type of overlapping increases on loss of coplanarity, whereas the latter diminishes. In other words, according to Bray the degree of double bonding should increase when C – Cl bonds diverge from the plane of the nucleus, and this refutes the reasoning of Duchesne and Monfils. Bray et al. consider that the increase of resonance frequency is caused by an inductive effect which diminishes the ionicity of C – Cl bonds in presence of ortho substituents. The question of the conformation of hexahalobenzene molecules

* Data on other hexahalobenzenes are very meager. The conformation of the hexabromobenzene molecule, with even greater steric hindrance (Br . . .Br = 3.28 instead of the equilibrium distance ≥ 3.90 Å), in crystals should be similar to the conformation of the hexachlorobenzene molecule, since crystals of C_6Cl_6 and C_6Br_6 are isomorphous [3]. Hexabromobenzene has also been investigated by electron diffraction in vapor form [4]. Schmidt (private communication, cited without any details in [5]) states that despite the considerable strain C_6Br_6 and C_6I_6 molecules in crystals are planar. In the case of hexaiodobenzene this result requires verification, because theoretical calculations (see below) indicate that the molecule should be nonplanar.

can be solved by means of quadrupole resonance only after investigation of single crystals by the Zeeman splitting method, whereby the asymmetry factor and the direction of the C – X bonds can be determined.

Without going into the causes of the contradiction between the results obtained for hexachlorobenzene by different methods, we must emphasize that analysis and correlation of experimental results often reveals real differences of conformation in different states of aggregation (for example, in vapor, liquid, and crystals). These differences in the molecular conformation, which are usually small, are not surprising, because the crystal field which determines the tendency to close packing in a crystal, and which is caused by interaction of atoms in neighboring molecules without valence bonding, is quite capable of producing small changes of conformation, since the lattice energy of a molecular crystal is close to the conformational part of the energy of the molecule. This fact has been pointed out previously [1, 10]. The classic example is the diphenyl molecule: it is planar in crystals [11], while in the vapor state one benzene ring is turned through 45° relative to the other about the central C – C bond [12]. Ali and Coulson [13] also showed that intermolecular forces in a crystal are sufficient to cause small deformation with loss of planarity in molecules of certain polycyclic hydrocarbons. Such loss of planarity was in fact observed in the crystal structures of anthracene [14] and α-phenazine [15]. Thus, in the anthracene crystal deviations of carbon atoms from the median plane of the molecule reach 0.012 A (which is considerably greater than the experimental error); this effect is satisfactorily explained by intermolecular interaction. It is quite obvious that the opposite effect is possible in principle; a nonplanar molecule may become planar on entering a crystal, under the influence of the crystal field [16]. These comments show that a thorough analysis of the influence of the crystal field, which is not always possible as yet, is needed in order to draw conclusions concerning the conformation of a "free" molecule (in vapor) from data for a "crystalline" molecule, and vice versa. An example of such analysis for hexachlorobenzene is given below. Incidentally, it should be noted that data on conformation in crystals are more conclusive than the results obtained by studies of conformation in the vapor and liquid states.

The results of theoretical calculations of the conformation of hexachlorobenzene (and hexabromobenzene) molecules, which are reviewed in [5], are also highly contradictory. Hill [17] used the theory of viscosity and the kinetic theory to derive the following expression for the energy of interaction (in ergs) between a pair of atoms X. . .X at a distance R apart:

$$V(R) = -2{,}25\varepsilon\,(R_0/R)^6 + 8{,}28\cdot 10^5\,\varepsilon \exp(-R/0{,}0736\,R_0), \qquad (1)$$

where the constants R_0 (equilibrium distances) and ϵ have the following values:

X	Cl	Br	I
R_0(A)	3,7	3,9	4,3
$\varepsilon\cdot 10^{13}$, ergs	21,8	30,6	89,2

Substituting these values for the energy of Cl . . .Cl interaction in kcal/mole, for example, we have

$$V(R) = -0{,}706\,(R_0/R)^6 + 2{,}598\cdot 10^5 \exp(-13{,}59\,R/R_0).$$

Coulson and Stocker [5] used Eq. (1) and the expression put forward in [18] for the energy of loss of coplanarity $U(z) = kz^2/2$; found that the molecules of C_6Cl_6 and C_6Br_6 should be planar, and the C_6I_6 molecule nonplanar, with $z_C = 0.05$, $z_I = 0.403$ A and $\alpha = 9°$. Coulson points out that this result depends little on the value of the constant $\underline{k}$; the effects of ϵ and R_0, which are now known very accurately, are much greater. We consider that this conclusion is unjustified, because the general conclusions concerning the conformation of a molecule are insensitive to the choice of the van der Waals interaction curve [19], and the force constants $\underline{k}$ which determine the energy required to remove the C – X bonds from the plane of the nucleus are known only very roughly. It is very significant that the polar nature of the C – Cl bonds has virtually no effect on interaction of atoms not bonded by valence forces and has no appreciable influence either on conformation of the molecule [5] or on the molecular packing in the crystal [19].

Coulson [5] used yet another approach in estimating interaction between atoms not linked by valence bonds, based on the concept of the so-called pseudovalent forces. This method was first used by Eyring [20] in relation to hindered rotation in ethane: H. . .H interaction is considered as the result of action of exchange forces between randomly oriented spins of the hydrogen atoms, and the energy curves are based on spectroscopic data for the H_2 molecule. (Later a similar method was used by Adrian [21] in an examination of the loss of planarity in sterically hindered systems of the diphenyl type.) In our view, this quantum-mechanical approach, which yields certain approximate estimates in the case of hindered rotation, is inapplicable to rigid systems, because the directed character of the bonding orbitals is not taken into account. By this variant of the Coulson calculation method (the unreliability

of which, especially in relation to C_6I_6, is pointed out by Coulson himself) the molecules of all hexahalobenzenes should be planar.

Coulson [5] made an interesting attempt to estimate the Cl . . .Cl potential from a consideration of molecular interaction in CCl_4. For liquid CCl_4 the empirical law for this interaction is represented by the expression [22]: $U(r) = K[(\sigma/r)^{12} - (\sigma/r)^6]$, where K and σ are constants and r is the distance between the centers of the molecules. The quantity U (r) is regarded as the statistical mean value of the potential of Cl . . .Cl interaction over all the mutual orientations of the free molecules,

$$U(r) = \frac{1}{8\pi^2}\iint V(R)\,d\omega_1\,d\omega_2,$$

where ω_1 and ω_2 are solid angles describing the orientation of the molecules. The best value for V (R), found by trial and error, is of the form

$$V(R) = D_1/R^2 + D_2/R^4 + D_3/R^5 + D_4/R^6, \qquad (2)$$

where D_1, D_2, D_3, and D_4 are empirical constants. Coulson claims that in this instance this expression for the potential was more appropriate than the more usual formulas, such as (1) or $A/R^6 + B/R^{12}$. He considers that this is because in this method polar effects are taken into account to a certain extent (which is why lower powers of 1/R than $1/R^6$ appear). Use of the force equation (2) leads to a nonplanar model of the C_6Cl_6 molecule: $z_C = 0.050$, $z_{Cl} = 0.332$ A and $\alpha = 9°$. Although the idea is interesting, this method is too unreliable, because the values of the constants D_1. . . .D_4 are highly sensitive to the choice of the points (values of r) used for fitting V (R) to U (R). There are other ill-founded assumptions (C. . .Cl and C. . .C interactions are neglected, and mutual orientation of the molecules in the condensed phase is "fitted" so that projections of one enter depressions in the other). Coulson himself admits that Eq. (2) gives values 2-3 times too high for the spatial strain energy; for example, the internal rotation barrier in hexachloroethane is found to be 35 kcal/mole instead of the experimental value of 12 ± 2 kcal/mole [23]. Results of calculations with Eq. (2) also contradict experimental data for 1,2,4,5-tetrabromobenzene [24]. It seems that at the present time the Hill curve [Eq. (1)] must be regarded as the most satisfactory potential curve for interaction of halogen atoms.

This survey of experimental and theoretical data reveals much contradiction in the available information on the conformation of hexahalobenzene molecules. The results for hexachlorobenzene are given below. Later we intend to study the conformation of hexaiodobenzene.

EXPERIMENTAL

The crystal structure of hexachlorobenzene has been determined by Tulinsky and White [2] from the x0z projection. Thus, only the x and z coordinates were determined experimentally, while the y coordinates were calculated on the assumption that C – C = 1.39 ± 0.02 A and C – Cl = 1.70 ± 0.02 A, and it was further assumed from the form of the x0z projection that the molecule is planar. The value $R_{h0l} = 0.17$ shows that x and z in [2] were determined with adequate accuracy. On the other hand, the y coordinates given in [2] are obviously incorrect as they give inadmissibly large variations for the bonds: $C_1 - C_2 = 1.47$; $C_2 - C_3 = 1.36$; $C_3 - C_1 = 1.47$; $C_1 - Cl_1 = 1.58$; $C_2 - Cl_2 = 1.70$; $C_3 - Cl_3 = 1.71$ A. In a letter to us, Tulinsky [25] admitted that an error had been made in calculation of y*. However, even if the calculation had been correct, the conclusion that the molecule is planar, deduced from the x0z projection only, cannot be reliable. Since the angle between the plane of the molecule and the x0z plane is not large (22°; see below), small deviations from planarity would have little effect on x and z but would strongly influence y. For example, if chlorine atoms are taken out of the plane of the benzene nucleus to a distance of 0.36 A along the normal (electron-diffraction data [4]), the change of y_{Cl} would be ~ 0.36 A, while changes of x_{Cl} and z_{Cl} would not exceed 0.04 A. Therefore deviations of 0.1-0.2 A from planarity cannot be detected at all from the x0z projection. Therefore to solve the problem of the conformation of the hexachlorobenzene molecule in crystals it is necessary to determine the y coordinates objectively (experimentally), and this was the purpose of the experimental section of our work.

* The paper [2] contains a further error: values of 2z instead of z are given.

Hexachlorobenzene crystals obtained from solution in benzene are thin colorless needles, with the b axis lengthwise along the needle; the simple forms are {100}, {101}, and {001} pinacoids. Our values for the unit cell constants agreed with those given in [2]:

$a = 8.08 \pm 0.02$ Å $\beta = 117.0° \pm 0.2°$
$b = 3.87 \pm 0.01$ $V = 464$ Å^3
$c = 10.65 \pm 0.03$ $N = 2$

Space group $P2_1/c$; the molecules occupy special positions at the centers of symmetry.

The y coordinates were calculated from the values of x and z in [2] on the assumption that the molecule is planar and that C – C = 1.40 A, C – Cl = 1.70 A. These starting coordinates are given in Table 1. Certain values of y given in [2] are included for comparison. The y coordinates were then refined by the method of least squares from reflection of the h1l type, as was done in our determination of the structure of tetrabromo-m-xylene [1]. The experimental data were obtained from the h1l trace obtained by photographing the reciprocal lattice with molybdenum radiation and containing 204 reflections of measurable intensity. Only the Lorentz and the polarization factors were taken into account when structue factors were calculated from the intensities (estimated visually from blackening). The constant of the isotropic temperature factor $B = 3.9$ Å^2 was determined by comparison of F_{meas} and F_{calc} by the method of least squares. The reliability factor R_{h1l} was 27.4% before and 21.2% after refinement of y.

TABLE 1. Atomic Coordinates

Atom	x from [2]	z from [2]	y			Final		
			from [2]	our calcn.	MLS*	x	y	z
Cl_1	0,403	0,066	0,153	0,274	0,244	0,408	0,245	0,066
Cl_2	0,278	0,204	—0,153	—0,023	—0,031	0,279	—0,033	0,204
Cl_3	—0,123	0,141	—0,275	—0,248	—0,280	—0,123	—0,278	0,138
C_1	0,189	0,031	0,072	0,123	0,118	0,183	0,111	0,030
C_2	0,123	0,095	—0,072	—0,010	—0,015	0,126	—0,015	0,092
C_3	—0,058	0,064	—0,128	—0,112	—0,118	—0,058	—0,125	0,062

*After refinement by the method of least squares.

The corrected values of y (Table 1) and the original x and z were then used to find the equation for the median plane passing through the center of symmetry and as close as possible to all the chlorine atoms in the molecule. The distances of the chlorine atoms from it were found to be: Cl_1 – 0.013, Cl_2 + 0.014, Cl_3 – 0.013 A. It follows that the molecule is planar to an accuracy of ± 0.02 A, and a second refinement of y by the method of least squares was therefore not performed. We consider that no further refinement is possible, either from the x0z projection or by the method of least squares from h1l with the aid of the isotropic temperature factor. Some correction of the coordinates can be achieved if an ideal model of the molecule, which was taken to be a planar model with C – C = 1.40 and C – Cl = 1.71 A, is fitted to the experimentally determined positions of the atoms. The fitting was performed by rotation of the model about three axes. The best agreement with experimental data was determined by the method of least squares. The ideal coordinates so found (Table 1) were taken as the final values and were used subsequently for calculation of the intermolecular distances. The validity of this correction is confirmed by the change in the reliability factors: R_{h0l}† decreased by 1.8%, and R_{h0l}† by 2.6%.

Description of the Structure and Molecular Packing

The hexachlorobenzene molecule in crystals is planar (to an accuracy of 0.01 A) with 6/mmm symmetry. The bond lengths are: C – C = 1.40 ± 0.02, C – Cl = 1.71 ± 0.02 A. In the rectangular system of x* yz coordinates (0x* axis normal to the 0y and 0z crystallographic axes) the equation for the plane of the molecule is: – 0.2634x + 0.9256 y + 0.2727z = 0. The molecular plane is inclined to the x0z plane at an angle of 22.2°; the distance between planes of molecules linked by b translation is 3.58 A. The molecular packing in projections on the ac and ab faces is shown in Figs. 3 and 4. Certain shortest intermolecular distances are also shown, together with the numbering of the molecules (I in 000, II in 100, III in $10\frac{1}{2}$, IV in $00\frac{1}{2}$, V in 010).

†As in original – Publisher.

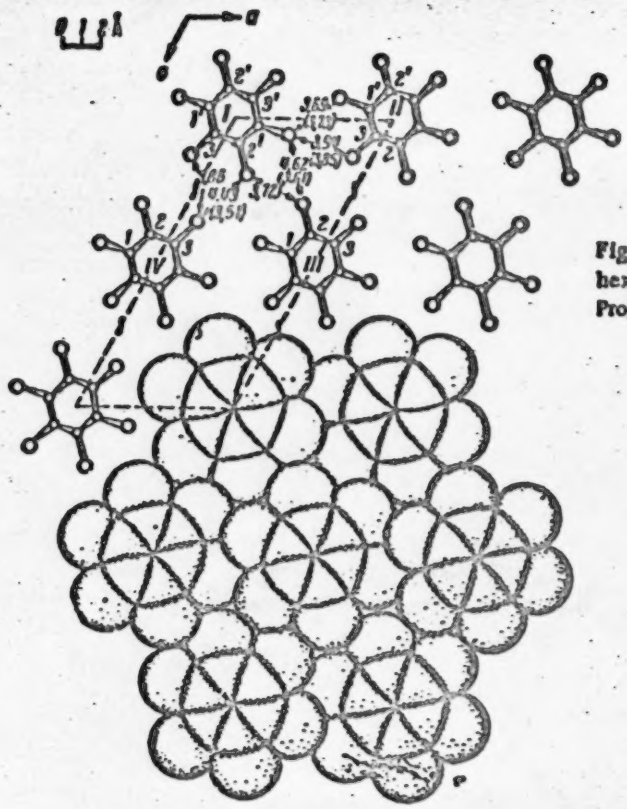

Fig. 3. Structure of hexachlorobenzene. Projection on ac.

Analysis of Intermolecular Distances

All intermolecular distances less than 5 A are given in Table 2, which also gives the number of distances and the values of the distances for a hypothetical structure with nonplanar molecules (see below).

In this work we used for the first time a new method for finding the equilibrium distances, i.e., intermolecular "radii," from the intermolecular distances in the crystals. In the past, intermolecular radii were usually determined from the shortest intermolecular distances in the crystal (method I). However, because of the complex form of the molecules, they cannot be packed in the crystal so that all the intermolecular distances correspond to the equilibrium values. The real arrangement of the molecules corresponds to the minimum energy of interaction between them, and in this arrangement some distances (relatively few) are below the equilibrium values, while the others are above. Therefore method II, used by us in [26], was more correct: the equilibrium distance was taken to be the arithmetic mean of the real distances in the crystal, from the minimum value to the value differing by 0.2 A from it. However, even this method should give low values of the equilibrium distances. A correct result can only be obtained from the curves for the interaction energy against the distances between the atoms (method III). A certain likely value of R_0^1 is taken as the equilibrium value; the curve is used to find the energies corresponding to real distances in the structure; and the lattice energy is found by summation of these energies for all the distances. A different value of R_0^1 is then taken and the lattice energy again found. The value of R_0 at which the lattice energy is minimal is taken as the true equilibrium distance. Each of these methods has its own model curve for the molecular interaction energy; Fig. 5 shows that the curves for methods I and II are very crude forms of the real curve (method III).

Curves of the form

$$U(R) = -A/(R/R_0)^6 + Be^{-\alpha(R/R_0)},$$

where R is the distance in the crystal, R_0 is the equilibrium distance, and A, B, and α are constants, were used as the curves for molecular interaction energy.

The Hill curve [17]: $U = -0.706(R/R_0)^{-6} + 2.597 \cdot 10^5 \exp[-13.59(R/R_0)]$ was used for Cl . . . Cl interactions, and the Kitaigorodskii curve [27]: $U(C \ldots C) = -0.147(R/R_0)^{-6} + 0.301 \cdot 10^5 \exp[-13.00(R/R_0)]$ for C . . . Cl interactions. Since the literature contains no data on a curve for C . . . Cl interaction, we used, as is the general practice

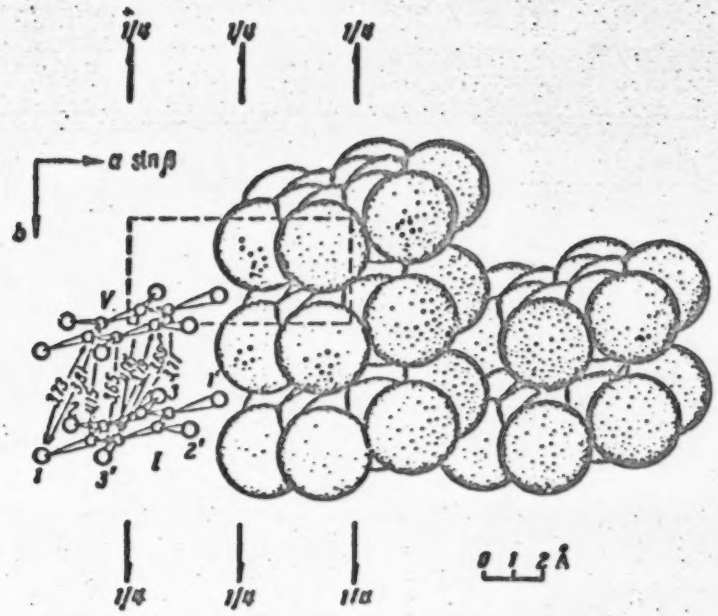

Fig. 4. Structure of hexachlorobenzene. Projection on ab.

[28], a curve in which the constants A, B, and α are the geometric means of the corresponding parameters for C. . .C and Cl. . .Cl interactions: $U(C...Cl) = -0.322(R/R_0)^{-6} + 0.884 \cdot 10^5 \exp[-13.29(R/R_0)]$. In all cases the energy is expressed in kcal/mole, i.e., for a number of the corresponding distances equal to the Avogadro number. Therefore the sum of U must be divided by 2 in calculations of lattice energies.

Using these potential curves and varying the equilibrium distances R'_0, we obtain the following relationships for fractions of the "lattice energy" $\varphi = \Sigma U/2$ for interactions of different types:

Cl . . . Cl interaction

R'_0, Å	3,4	3,6	3,8	4,0
φ, kcal/mole	−7,9	−9,1	−9,6	−8,1

minimum $\varphi_{min} = -9.8$ kcal/mole at $R_0 = 3.72 \pm 0.02$ Å.

Cl. . .C interaction

R'_0	3,6	3,8	4,0	4,2
φ	−3,8	−4,5	−4,6	−4,4

minimum $\varphi_{min} = -4.7$ kcal/mole at $R_0 = 3.94 \pm 0.02$ Å.

C. . .C interaction

R'_0	3,6	3,8	4,0
φ	−1,7	−2,0	−1,9

minimum $\varphi_{min} = -2.0$ kcal/mole at $R_0 = 3.88 \pm 0.02$ Å.

Only interactions at distances not greater than 5 Å, given in Table 2, were taken into account in calculations of φ. Interaction at greater distances corresponds to only weak attraction (less than 0.001 kcal/mole) and, as approximate estimates [27] show, constitutes not more than 10% of the lattice energy. Thus, our "effective lattice energies" are too low in absolute values by that amount, but the tendency in the variation of φ with variations of the accepted equilibrium distances and with variations of the intermolecular distances due to changes in the molecular conformation (see below) is correctly represented. In this instance the effective lattice energy is $\varphi = -9.8 - 4.7 - 2.0 = -16.5$ kcal/mole.

Therefore our claculation method, based on variation of the equilibrium distances, give the following structure parameters:

Equilibrium distances Cl. . .Cl = 3.78 ± 0.02Å
Cl. . .C = 3.94 ± 0.02Å
C. . .C = 3.88 ± 0.02Å
Effective lattice energy = 16.5 kcal/mole.

Incidentally, this method gives equilibrium values appreciably greater (by 0.2-0.3 Å) than the sums of the generally accepted intermolecular radii. Calculations of conformation [19] also indicate that the equilibrium distances are greater than the shortest intermolecular distances in a crystal. The latter are not direct functions of the structure of the electron shells of the atoms but depend in a complex manner on the packing; i.e., it might be expected that they would be more or less random in character. However, the fact that the shortest intermolecular distances in different structures are relatively constant, remarkable at first sight, is a direct consequence of the steepness of the repulsion branch of the interaction curve.

TABLE 2. Intermolecular Distances (in Å)

Atoms	Experiment		Nonplanar model		Atoms	Experiment		Nonplanar model	
	d	d'**	d	d'		d	d'	d	d'
	Contacting molecules I. . .II				$Cl_1...C_3'$	4.91(4)	>5(4)	4.63(4)	>5(4)
					$Cl_1...Cl_3$	4.46(4)	>5(4)	4.16(4)	>5(4)
$Cl'...Cl'$	3.94(4)	3.85(4)	3.96(4)	3.89(4)	$Cl_1...C_3'$	4.32(4)	>5(4)	4.02(4)	>5(4)
$Cl_1...Cl_1'$	3.69(2)	3.73(2)	4.29(2)	3.70(2)	$Cl_2...C_1$	>5(4)	4.24(4)	>5(4)	3.92(4)
					$Cl_2...C_2$	4.29(4)	4.17(4)	4.58(4)	3.85(4)
					$Cl_2...C_3$	4.41(4)	>5(4)	4.09(4)	4.09(4)
	Contacting molecules I. . .III				$Cl_2...C_3'$	>5(4)	>5(4)	>5(4)	4.83(4)
$Cl_2...Cl_2$	3.61(4)	4.62(4)	3.55(4)	>5(4)	$Cl_2...C_2$	>5(4)	4.40(4)	>5(4)	4.05(4)
$Cl_2...Cl_2$	3.72(2)	3.72(2)	3.69(2)	3.69(2)	$Cl_2...C_1'$	>5(4)	4.15(4)	4.96(4)	4.65(4)
					$Cl_2...C_2$	>5(4)	3.79(4)	>5(4)	4.12(4)
	Contacting molecules I. . .IV				$Cl_2...C_2'$	>5(4)	4.71(4)	>5(4)	4.93(4)
$Cl_2...Cl_3$	3.51(4)	4.43(4)	3.79(4)	4.06(4)	$Cl_2...C_3$	4.74(4)	3.65(4)	4.65(4)	4.00(4)
$Cl_2...Cl_3$	3.86(2)	3.86(2)	3.85(2)	3.85(2)	$Cl_2...C_3'$	>5(4)	3.76(4)	>5(4)	>5(4)
					$C_1...C_3$	3.87(2)	3.87(2)	3.87(2)	3.87(2)
	Contacting molecules I. . .V				$C_1...C_3'$	4.03(2)	>5(2)	4.03(2)	>5(2)
					$C_2...C_2$	3.63(4)	4.55(4)	3.63(4)	4.55(4)
$Cl_1...Cl_1$	3.87(2)	3.87(2)	3.87(2)	3.87(2)	$C_2...C_2'$	4.24(4)	4.87(4)	4.24(4)	4.87(4)
$Cl_2...Cl_2$	3.87(2)	3.87(2)	3.87(2)	3.87(2)	$C_2...C_3$	3.71(4)	<5(4)	3.71(4)	>5(4)
$Cl_2...Cl_2$	3.87(2)	3.87(2)	3.87(2)	3.87(2)	$C_2...C_3'$	4.17(4)	4.06(4)	4.17(4)	4.06(4)
$Cl_2...Cl'$	>5(4)	4.87(4)	>5(4)	4.56(4)	$C_3...C_3$	3.87(2)	3.87(2)	3.87(2)	3.87(2)
$Cl_2...Cl_2'$	4.16(4)	>5(4)	4.72(4)	>5(4)	$C_3...C_3'$	4.87(2)	4.68(2)	4.87(2)	4.68(2)
$Cl_2...Cl_2$	4.01(4)	>5(4)	3.61(4)	>5(4)	$C_3...C_3$	3.69(4)	4.50(4)	3.69(4)	4.50(4)
$Cl_2...C_2$	3.73(4)	4.69(4)	3.38(4)	4.06(4)	$C_3...C_3'$	>5(4)	4.06(4)	>5(4)	4.06(4)
$Cl_2...Cl$	4.06(4)	>5(4)	4.69(4)	>5(4)	$C_3...C_3'$	3.87(2)	3.87(2)	3.87(2)	3.87(2)
$Cl_2...C_2$	3.81(4)	>5(4)	3.46(4)	>5(4)	$C_3...C'$	>5(2)	4.08(2)	>5(2)	4.08(2)

* Intermolecular distances essentially associated with the short b translation, i.e., between molecule I and molecules taken out of positions II, III, IV, and V by b translation.

** Numbers of the corresponding distances for atoms in the same molecule are given in parentheses.

The literature contains references [29] to the dependence of the intermolecular radius, i.e., the equilibrium distance, on the orientation of the corresponding interatomic vector with respect to the chemical bonds formed by the interacting atoms. It was found, in particular, that the iodine atom is shorter by 0.4-0.6 Å in the direction of the chemical bond than in perpendicular directions [30]. Table 2 shows that similar "anisotropy" of atomic shape in the

presence of molecular interaction occurs in our structure. For consideration of this effect, it is convenient to subdivide the interactions detailed in Table 2 into three groups:

a) Interactions of I – II – I – III, I – IV molecules; the corresponding interatomic vectors form angles of 0-20° with the plane of the molecule, i.e., they lie roughly in that plane.

b) Interactions of I – II', I – III', I – IV' (molecules II', III', IV' are taken out of positions II, III, IV by b translation; these are the distances d' in table 2); the interatomic vectors are at angles of 30-50° to the plane of the molecule.

c) Interactions of I-V molecules; the interatomic vectors are close to the normal to the plane of the molecule (angles of 70-90°).

Table 2 shows that the equilibrium distances increases from a to b and from b to c. Figure 6 shows the corresponding graphs for the interaction energy U against the accepted equilibrium distance R_0'; the minima of these curves determine the true equilibrium distances and the increments of the effective lattice energy. The final results are:

Interaction	Equilibrium distance, A	ΣU/2, kcal/mole
Cl. . .Cl, type a	3.64	−3.25
Cl. . .Cl, type b	3.80	−2.90
Cl. . .Cl, type c	3.94	−4.10
Cl. . .C, type c	3.94	−4.70
C . . .C, type c	3.98	−2.00

Hence the effective lattice energy is $\varphi = -17$ kcal/mole, or less by 0.5 kcal/mole than the value calculated without the anisotropy of atomic shape taken into account. These equilibrium distances show that the intermolecular radius of the chlorine atom depends appreciably on the direction, being 1.82 A in the plane of the molecule and 1.97 A in the normal to that plane. This is a real difference, because the values of the intermolecular radius of the carbon atom in the normal to the molecular plane, calculated from C. . .Cl and C. . .C equilibrium distances, are in good agreement: 1.97 and 1.94, mean $1.95_5 - 0.01_5$ A. At the same time, if this anisotropy is disregarded, additivity of the intermolecular radii is worse: the values of the carbon radius are 2.08 and 1.94 A.

This dependence of the atomic size on direction is general: in isostructural crystals of tetrabromo-o-xylene [1], tetrabromo-m-xylene [2], 1,2-dichlorotetramethylbenzene [2], hexachlorobenzene and hexabromobenzene [3], and also in the similar structure of hexamethylbenzene [2], the intermolecular radius in the molecular plane is less by 0.15 – 0.20 A than in the normal to that plane.

This method for determination of equilibrium distances obviously requires verification. It must be demonstrated that: 1) these distances are constant in numerous structures of the same type; 2) the dependence of these distances on direction is of the same character in molecules of similar chemical structure; 3) the calculated effective lattice energy is close to the experimental value. Verifications 1 and 2 merely require analysis of distances in many structures which have already been interpreted, but verification 3 is difficult because data on lattice energies of organic crystals are meager. In particular, such verification must justify the assumption in our calculations of the equilibrium distances, that in a real structure attraction and replusion equilibrium becomes established in interactions of all types, i.e., C. . .C, C. . .Cl and Cl. . .Cl. In view of the nondirectional nature of van der Waals interaction this assumption appears to be quite reasonable; evidently it would be invalid only in presence of strong specific interaction between the molecules (hydrogen bonds; interaction between strong dipoles).

Steric Strain in the Molecule

In order to explain the difference between the conformations of the hexachlorobenzene molecule in crystals and in vapor, we considered the following hypothetical structure. The real unit cell of the hexachlorobenzene crystal contains nonplanar molecules the chlorine molecules of which are alternately above and below the planes of the benzene nuclei at a distance of 0.36 A ([4], see above). The arrangement of the carbon atoms in this hypothetical structure is the same as in the real structure, because the benzene ring remains planar even in the nonplanar electron-

diffraction model. The intermolecular distances for this hypothetical structure are given in the column headed "Nonplanar model" in Table 2. Calculation of the effective lattice energy for this hypothetical structure gives $\varphi = -13.9$ kcal/mole, which is greater by 3.1 kcal/mole than the value for the real structure*.

This difference indicates that packing of planar molecules is more advantageous from the energy aspect. The packing coefficients for the hypothetical and real structure are, of course, equal; their value is 0.82 with the equilibrium distances used.

We consider that the expressions given above for the energy of molecular interaction are also suitable for calculations of steric strains in the molecule, because in both cases interaction of atoms not linked by valence bonds (in different molecules or in the same molecule) is considered. Most investigators adhere to this view (see, for example, [19, 27]) although some [24] add the qualifying statement that "as yet there are not sufficient data for deciding whether functions determined from studies of intermolecular interactions are applicable to interamolecular interactions. It is possible that the potential curve varies with the angle formed by the interatomic vector and the covalent bond." We consider that the nature of the interactions (i.e., the potential curve) for nonbonded atoms of these elements is universal, and that the dependence of the interaction energy on the orientation of the vector between the interacting atoms in relation to their covalent bonds is accounted for by the change of the equilibrium distance with direction (see above).

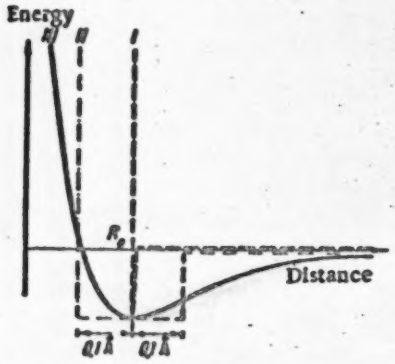

Fig. 5. Molecular interaction energy curves for different methods of determining the equilibrium distances.

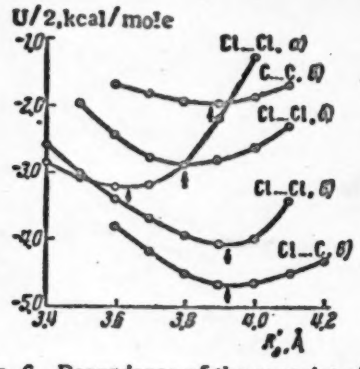

Fig. 6. Dependence of the energies of different interactions on the equilibrium distance adopted. Arrows indicate minima.

In calculations of the energy of steric strains in the hexachlorobenzene molecule we consider interactions of neighboring chlorine atoms only, because the other distances between the nonbonded atoms in the molecule are close to or greater than the equilibrium values. Moreover, the shortest Cl. . .Cl distances are precisely the most sensitive to loss of planarity. The main uncertainty in the calculation lies in the choice of the equilibrium distance, because the available data on the dependence of intermolecular radii on direction are very limited. For example, it is not known whether the solid of rotation (the rotation axis is the covalent bond) is the van der Waals "sphere" of the univalent atom in the polyatomic molecule. In the structure of hexachlorobenzene the interatomic vectors of interactions a form angles of 0-60° with C – Cl bonds, while the vectors of interactions c form angles of 70-90°. The angle between the Cl. . .Cl intramolecular vector and the C – Cl bond is 60°. Therefore we may assume that the equilibrium distance for intramolecular Cl. . .Cl interaction is between 3.64 and 3.94 A. We performed the calculations for both equilibrium distances, for the planar and nonplanar ($\alpha = 12°$) models; the results were:

Steric stress energy in the hexachlorobenzene molecule (kcal/mole)

	Planar	Nonplanar
$R_0 = 3.64$ A	+ 2.6	+1.6
$R_0 = 3.94$ A	+ 16.9	+12.4

*The equilibrium distances found for the real structure were used in calculation of the lattice energy of the hypothetical structure.

The calculated energy depends sharply (by a tenth-power) on the equilibrium distance. Despite this, we can draw certain conclusions concerning the force constant k for removal of C–Cl bonds from the plane. For this we must compare the conformation packing fractions of the energy for the planar and nonplanar conformations. The condition for planarity of a molecule in a crystal is:

$$\Phi_{planar} = \varphi_{planar} + V_{planar} + U_{planar} < \Phi_{nonpl} = \varphi_{nonpl} + V_{nonpl} + U_{nonpl},$$

where φ is the effective lattice energy, V is the steric strain energy, U is the energy of removal of C – Cl bonds from the plane, $U_{planar} = 0$. For $R_0 = 3.64$ A we have

$$-17.0 + 2.6 < -13.9 + 1.6 + U_{nonpl}, \text{ i.e., } U_{nonpl} > -2.1,$$

and for $R_0 = 3.94$ A

$$-17.0 + 16.9 < -13.9 + 12.4 + U_{nonpl}, \text{ i.e., } U_{nonpl} > 1.4.$$

Since U is known to be positive, the equilibrium distance for intramolecular interaction is close to $R_0 = 3.84 - 3.94$ A. The force constant is estimated from the condition

$$U = k\alpha^2/2 > 1.4/6 \text{ kcal/mole}$$

and hence $k > 0.073 \cdot 10^{-11}$ erg/rad^2.

The planarity condition for a free molecule (in vapor) is

$$V_{planar} < V_{nonpl} + U_{nonpl},$$

i.e., for $R_0 = 3.64$ A

$$2.8 < 1.6 + U_{nonpl}, \text{ i.e., } U_{nonpl} > 1.0,$$

and for $R_0 = 3.94$ A

$$16.9 < 12.4 + U_{nonpl}, \text{ i.e., } U_{nonpl} > 4.5.$$

Taking the upper value, we have $k > 0.234 \cdot 10^{-11}$ erg/rad^2.

Unfortunately, there are no reliable values for the force constants of removal of peripheral bonds from the plane of the benzene nucleus. According to Coulson's estimate [5], for the C – Cl bond $k = 0.372 \cdot 10^{-11}$ erg/rad^2. It follows that the hexachlorobenzene molecule must be planar in the vapor state as well as in crystals. This conclusion probably also applies to hexabromobenzene and hexaiodobenzene. The reason is that the increase of intermolecular radius from Cl to Br and from Br to I is approximately equal to the increase in the C – X bond length, so that the steric strain energy is approximately the same for all three hexahalobenzenes. Nonplanarity may occur in presence of even greater steric hindrance, for example in hexamethyl-, hexaethyl-, and poly-tert-butylbenzenes in free and uncoordinated rotation of the substituents about the C – C bonds, i.e., in the high-temperature modifications (if such exist) of their crystals, or in free molecules. In such cases, groups such as CH_3 must be represented by spheres of radius ~2.4 A and the distance $CH_3 \ldots CH_3 = 2.94$ A is shortened to $1.9/4.8 = 0.4$ of the equilibrium, i.e., it is considerably greater than in hexachlorobenzene ($0.7/3.9 = 0.18$ of the equilibrium). At room temperature the rotation of the CH_3 groups is probably coordinated, i.e., a hydrogen atom of one CH_3 group is always in the space between two hydrogens of another, and the steric hindrance is much less. At 110°K a phase transition occurs [31]; this is attributed [32] to a halt in the rotation of the CH_3 groups, engaged like gear wheels; the molecule in this configuration must also be planar.

In di-, tri-, tetra-, and apparently even pentasubstituted benzenes steric hindrance is partially removed by deformation of the valence angles in the plane with retention of planarity. Thus, in the 1,2,4,5-tetrabromobenzene crystal the Br . . . Br distance increases by 0.08 A (above the 3.30 A in the ideal model) by an increase of the CCBr angle in the plane by 1.5° [24]. The same increase results if the C – Br bonds are taken out of the plane of the

nucleus through 14°. If the elastic constants for both deformations were magnitudes of the same order (which seems probable [5]) the quantity of energy required for loss of planarity would be roughly 100 times as much as for deformation in the plane. Therefore retention of planarity (of course, with the exception of hexasubstituted derivatives) may be explained on purely geometrical grounds rather than by the greater rigidity of the molecule in removal of the bonds from the plane. It is only if the steric hindrance is considerably greater (for example, in peri-disubstituted naphthalenes [33] that separation of the substituents in the plane may prove insufficient for removal of "excess" steric strains, and planarity would then be lost. Moreover, if the divergence of the C – X bonds in the plane of the nucleus is considerable (10° or more), appreciable X . . .H repulsion arises, which also favors loss of planarity.

SUMMARY

1. The factors determining the conformation of hexahalobenzene molecules in the vapor state and in crystals are considered. A survey of the literature reveals the contradictory nature of experimental data and theoretical calculations.

2. The crystal structure of hexachlorobenzene has been refined. To an accuracy of ± 0.02 A the molecule is planar in crystals; C – C = 1.40 ± 0.02; C – Cl = 1.71 ± 0.02 A.

3. A new method is proposed for estimation of equilibrium intermolecular distances in crystals, based on the use of curves for the energy of interaction of atoms not linked by valences and on minimalization of the effective lattice energy.

4. The equilibrium distances are found to depend distinctly on the direction relative to the plane of the molecule. The equilibrium Cl. . .Cl distance is 3.64 A in the molecular plane and 3.94 in the normal to it.

5. The effective lattice energies have been calculated for the real hexachlorobenzene structure (– 17.0 kcal/mole) and for a hypothetical structure with nonplanar molecules (– 13.9 kcal/mole).

6. The values of the force constant for removal of the C – Cl bond from the plane of the benzene nucleus, with which the hexachlorobenzene molecule must be planar in crystals and in vapor, were estimated.

7. The results suggest that molecules of all hexahalobenzenes must be planar not only in crystals but also in the vapor state.

LITERATURE CITED.

1. I.N. Strel'tsova and Yu.T. Struchkov, Izv. AN SSSR, Otd. khim.n., 2, 250 (1961).
2. A. Tulinsky and J.G. White, Acta crystallogr. 11, 7 (1958).
3. W.G. Plummer, Phil. Mag. 50, 1213 (1925); G. Gafner and F.H. Gerbstein, Acta crystallogr. 13, 9, 702 (1960).
4. O. Bastiansen and O. Hassel, Acta chem. scand. 1, 489 (1947).
5. C.A. Coulson and D. Stocker, Mol. Phys. 2, 4, 397 (1959).
6. R. Kopelman and O. Schnepp, J. Chem. Phys. 30, 597 (1959).
7. O. Schnepp and R. Kopelman, J. Chem. Phys. 30, 868 (1959).
8. J. Duchesne and A. Monfils, J. Chem. Phys. 22, 562 (1954).
9. P.J. Bray, R.G. Barnes and R. Bersohn, J. Chem. Phys. 25, 813 (1956); P.A. Casabella, P.J. Bray, S.L. Segel and R.G. Barnes, J. Chem. Phys. 25, 1280 (1956).
10. J.D. Dunitz and V. Prelog, Angew. Chem. 72, 23, 896 (1960).
11. Dhar Jagattaram, Indian J. Phys. 7, 43 (1932).
12. O. Bastiansen, Acta chem. scand. 3, 408 (1949).
13. M.A. Ali and C.A. Coulson, J. Chem. Soc., 1558 (1959).
14. D.W.J. Cruickshank, Acta crystallogr. 9, 915 (1956).
15. F.L. Hirshfeld and G.M.J. Schmidt, J. Chem. Phys. 26, 923 (1957).
16. E. Harnik, F.H. Herbstein, G.M.J. Schmidt and F.L. Hirshfeld, J. Chem. Soc., 3288 (1954).
17. T.L. Hill, J. Chem. Phys. 16, 399 (1948).
18. C.A. Coulson and S. Senet, J. Chem. Soc., 1813 (1955).
19. A.I. Kitaigorodskii, Dokl. AN SSSR 137, 116 (1961).
20. H. Eyring, J. Amer. Chem. Soc. 54, 3191 (1932).
21. F.J. Adrian, J. Chem. Phys. 28, 608 (1958).

22. J.O. Hirschfelder, C.F. Curtiss and R.B. Bird, Molecular Theory of Gases and Liquids (Wiley, 1954) p. 114.
23. N.W. Luft, J. Phys. Chem. 59, 92 (1955).
24. G. Gafner and F.H. Herbstein, Acta crystallogr. 13, 706 (1960).
25. A. Tulinsky, Letter to Yu.T. Struchkov, November 30, 1959.
26. Yu. T. Struchkov and T. L. Khotsyanova, Izv. AN SSSR, Otd. khim. n., 5, 829 (1960); 8, 1377 (1960); Lyan Dunchai and Yu. T. Struchkov, Izv. AN SSSR, Otd. khim. n., 12, 2099 (1959).
27. A.I. Kitaigorodskii and K.V. Mirskaya, Kristallografiya (in the press) (1961).
28. E. Mason and W. Rice, J. Chem. Phys. 22, 522 (1954).
29. L. Pauling, Nature of the Chemical Bond [Russian translation] (Goskhimizdat, Moscow-Leningrad, 1947) p. 187; M.J. Robertson, Organic Crystals and Molecules (Oxford, 1956) p. 216; J. Dostrovsky, E.D. Hughes and C.K. Ingold, J. Chem. Soc., 172 (1946).
30. T.L. Khotsyanova, A.I. Kitaigorodskii and Yu.T. Struchkov, Zh. fiz. khimii 27, 9, 1341 (1953); A.I. Kitaigorodskii, T.L. Khotsyanova and Yu.T. Struchkov, Zh. fiz. khimii 27, 6, 781 (1953).
31. H.C. Wolf, Z. Naturforsch. A13, 336 (1958).
32. O. Schnepp, J. Chem. Phys. 29, 56 (1958).
33. A.I. Kitaigorodskii, Yu.T. Struchkov, G.L. Avoyan and M.A. Davydova, Dokl. AN SSSR 136, 607 (1961); M.A. Davydova and Yu.T. Struchkov, Zh. strukt. khimii 2, 1, 69 (1961).

All abbreviations of periodicals in the above bibliography are letter-by-letter transliterations of the abbreviations as given in the original Russian journal. *Some or all of this periodical literature may well be available in English translation.* A complete list of the cover-to-cover English translations appears at the back of this issue.

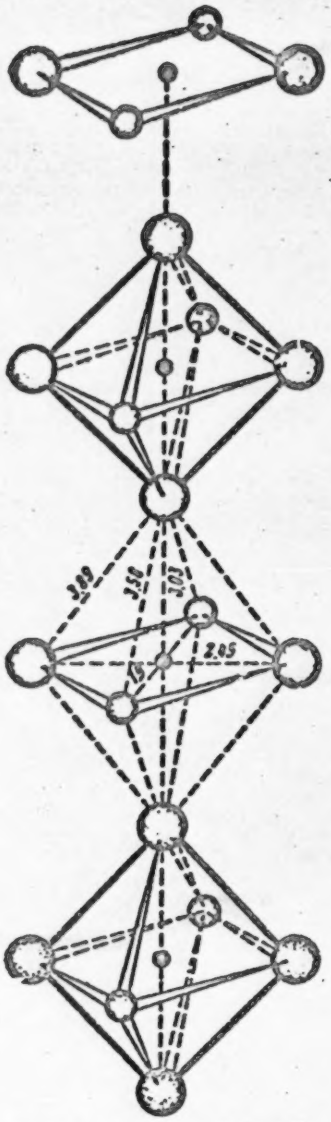

Fig. 1. Structure motif in $[Pt^{II}(NH_3)_2 \cdot Br_2] \cdot [Pt^{IV}(NH_3)_2Br_4]$

radii are 4.05 and 3.0A). It follows that in every case the mutual arrangement of the atoms can be interpreted in the light of the usual concepts concerning the packing of charged or neutral complexes, without additional covalent interaction.*

Description of MA_4X_2 complexes on the basis of $dsp^3 + p_z d_{z^2}$ hybridization implies the participation of electrons of the outer d orbital in the bonds. This also occurs in paramagnetic compounds of nickel with undistorted octahedral complexes [$NiPy_4X_2$, $Ni(NH_3)_4X_2$, etc.]. It is natural to describe the latter (within the framework of the valence pair theory) on the basis of sp^3d^2 hybridization. However, in all Ni^{II} compounds of this type which have been studied structurally the Ni–X distances are considerably less than in the above-named structures: in $NiPy_4Cl_2$ Ni – Cl = 2.39 and Ni–N_{Py} = 2.09 A [7]; in $NiPy_4Br_2$ Ni – Br = 2.62 and Ni – N_{Py} = 2.1 A [8]; in $Ni(NH_3)_4(NCS)_2$ Ni – NCS = 2.07 and Ni – NH_3 = 2.15 A [9]. It is even more significant that in all cases the distances between the contacting ligands are 0.3–0.35 A less than the sums of the corresponding intermolecular or ionic radii. This means that the share of forces of a covalent character in M–ligand bonds is quite substantial here, although the electrons of the inner d shell of the Ni atom are not formally used in bonds. Thus, comparison of structure data on high-spin Ni^{II} compounds with regular octahedral coordination and on low-spin Ni^{II}, Pd^{II}, and Pt^{II} compounds with distorted octahedral coordination leads to the conclusion that the electron formula dsp^3d is unsuitable for the latter.

The coordination of Ni^{II} in purely electrostatic interaction with all ligands is considered theoretically in [10]. The author showed that under certain conditions the singlet (diamagnetic) $^1A_{1g}$ state may be the most advantageous not only with square but also with distorted octahedral coordination. It is therefore likely that further development of a theory which takes into account covalent interaction with some ligands and electrostatic with others would make it possible to establish in what cases external ions (or ligands in neighboring complexes) would show a tendency to approach a metal atom in square dsp^2 coordination. Experimental data on the crystal structures of $[Pt(NH_3)_4]Cl_2 \cdot H_2O$, $[Pd(NH_3)_4]Cl_2 \cdot H_2O$ [11], $Pt(NH_3)_2Cl_2$ [12], $Pt(NH_3)_4 \cdot PtCl_4$ [13], trans-$Pt(NH_3)_2(SCN)_2$ [14], cis-$Pt(NH_3)_2(SCN)_2$ [15], $Ni[P(C_2H_5)_3]_2Br_2$ [16], etc. and of a number of internal-complex compounds show that in general this tendency is rather rare.

* The data in [2] are unfortunately insufficient for a similar calculation in respect of $[Pt(NH_3)_4(NCCH_3)_2] \cdot H_2O$. It may be noted, however, that the Pt — $\overset{C}{\underset{N}{\|}}$ distance in this compound (~3.0 A) is considerably greater than the Pt — $\overset{C}{\underset{C}{\|}}$ distance in $K[Pt(C_2H_4)Br_3] \cdot H_2O$ (~2.2 A) [6].

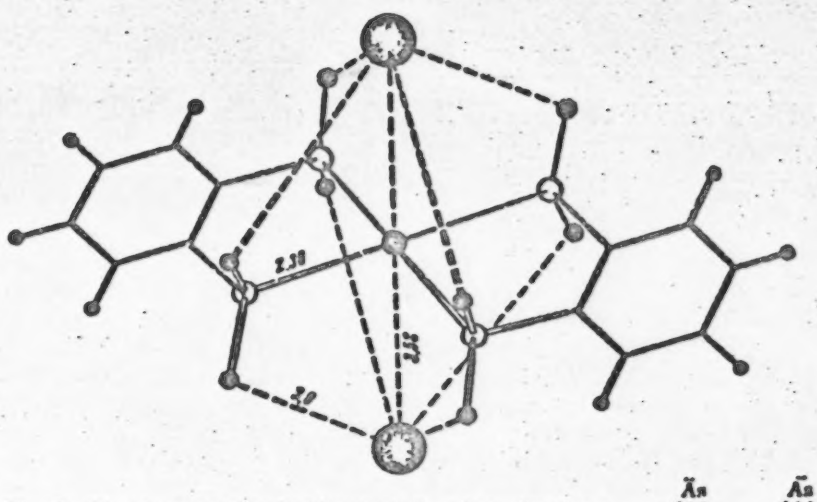

Fig. 2. Structure motif in Pt(diarsine)$_2$I$_2$, where diarsine =

LITERATURE CITED

1. C.M. Harris, R.S. Nyholm and N.C. Stephenson, Nature 177, 1127 (1956).
2. C.M. Harris and N.C. Stephenson, Chemistry and Industry 14, 426 (1957).
3. D. Hall and P.P. Williams, Acta crystallogr. 11, 624 (1958).
4. J.N. Dempsey and N. C. Baenziger, J. Amer. Chem. Soc. 77, 4984 (1955).
5. J.R. Holdne and N.C. Baenziger, J. Amer. Chem. Soc. 77, 4987 (1955).
6. G.B. Bokii and T.A. Kukina, Kristallografiya 3, 400 (1957).
7. M.A. Porai-Koshits and A.S. Antsyshkina, Dokl. AN SSSR 92, 333 (1953).
8. A.S. Antsyshkina and M.A. Porai-Koshits, Kristallografiya 3, 676 (1958).
9. É.K. Yukhno and M.A. Porai-Koshits, Kristallografiya 2, 239 (1957).
10. G. Maki, J. Chem. Phys. 28, 651 (1958).
11. R.N. Dickinson, Z. Kristallogr. 88, 281 (1934).
12. M.A. Porai-Koshits, Tr. Inst. kristallografii 9, 229 (1954).
13. M. Atoji, J.W. Richardson and R.E. Rundle, J. Amer. Chem. Soc. 79, 3017 (1957).
14. Ya.Ya. Bleidelis and G.B. Bokii, Kristallografiya 2, 281 (1957).
15. Ya.Ya. Bleidelis, Izv. AN Latv. SSR 1, (114), 121 (1957).
16. V. Scatturin and A. Turco, J. Inorg. Nuclear Chem. 8, 447 (1958).

All abbreviations of periodicals in the above bibliography are letter-by-letter transliterations of the abbreviations as given in the original Russian journal. *Some or all of this periodical literature may well be available in English translation.* A complete list of the cover-to-cover English translations appears at the back of this issue.

INFRARED ABSORPTION SPECTRA OF RING SILICATES. III*

I.I. Plyusnina

M.V. Lomonosov Moscow State University
Translated from Zhurnal Strukturnoi Khimii, Vol. 2, No. 3, pp. 330-336, May-June, 1961
Original article submitted June 20, 1960

The paper contains the results of an investigation of infrared absorption spectra of silicates with an oxygen–silicon ring motif, and of certain other silicates.

I. In some theoretical investigations atomic groups are considered separately for calculation of the vibrational frequencies of such groups. This is possible with molecular compounds because the interatomic forces within the molecule are considerably greater than the intermolecular forces; the infrared spectra of such compounds have sharp absorption bands. Radicals of the simplest oxy acids, such as $[CO_3]^{2-}$, $[SO_4]^{2-}$, $[PO_4]^{3-}$, $[NO_3]^{-}$, are groups of atoms in which the bonds are much stronger than and often qualitatively different from the bonds between these groups and other ions. Because of these structural characteristics of complex ions the corresponding salts, such as $NaNO_3$, $CuSO_4$ and $CaCO_3$, like molecular compounds, give selective absorption bands in the infrared spectra, corresponding to the vibrational frequencies of the NO_3, SO_4, and CO_3 groups. In the case of silicates, x-ray structural analysis has demonstrated the existence of tetrahedral SiO_4 groups in their crystals, analogous in structure to the tetrahedral radicals in sulfates and phosphates. In comparison with SO_4 and PO_4, the SiO_4 tetrahedron has [1, 2]: 1) the largest size; 2) the greatest charge; 3) the least stable internal bonds (Table 1).

The silicate structure type is intermediate in the chemical sense and is the key to an understanding of the properties of silicates. Whereas the tetrahedrons in phosphates and sulfates are typical complex ions, with internal bonds almost entirely of a homopolar character, which may be regarded as single entities, the silicate tetrahedron occupies an intermediate position between such complex ions and similar tetrahedral groups in certain oxides, such as MgO_4 in spinels, which do not in principle differ in any respect from the other structural elements of the "coordination lattice" [1].

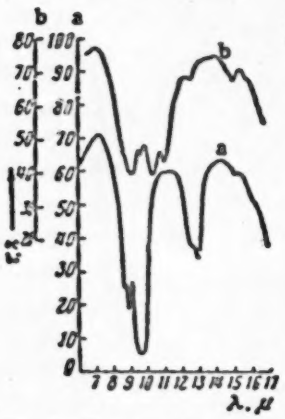

Fig. 1. Transmission spectra of apophyllite (a) and axinite (b).

However, the silicon–oxygen bond differs substantially from the simple ionic bond between a metal and oxygen, and this justifies the view that silicon–oxygen tetrahedrons are elementary building units the packing of which, together with metal ions, gives rise to the general silicate structure [3]. The Si–O bond is transitional between a purely ionic and a covalent bond; this is demonstrated, for example, by x-ray data [4].

It is therefore evident that, contrarily to the opinion of certain investigators [5, 6], the term "SiO_4 tetrahedron" does not imply "merely a geometrical picture of the spatial environment of four oxygen atoms around one silicon atom." The SiO_4 group, despite the transitional nature of its properties, is a complex ion the oxygen atoms of which, in general, are bonded more firmly to Si than to the metal. The primary experimental proof of this is the invariable presence of selective absorption bands, similar to the bands in the spectra of molecular compounds, in the infrared spectra of silicates. The silicate absorption bands at 8-12 and 20 μ are characteristic of the SiO_4 group; one confirmation of this is that replacement of one metal ion by another has little influence on the form of the spectrum (grenade form), and that the spectrum of quartz also has bands at 8-12 and 20 μ.

Among the causes of the complex character of the infrared spectra of silicates is the fact that combination of silicon–oxygen tetrahedrons into radicals in the form

*For communications I and II, see [13] and [14].

TABLE 1. Comparative Characteristics of Tetrahedral Anions in the Crystal Structures of Sulfates, Phosphates, and Silicates [1, 2]

Central X atom	X–O distance, A	Average length of O–O edge, A	Charge of complex		Charge of X	Bond force per atom of O
			total	per O atom		
S	1.49	2.45	–2	–0.5	+6	1.5
P	1.54	2.49	–3	–0.75	+5	1.25
Si	1.5–1.7•	2.53	–4	–1	+4	1.0

• Mean 1.6 A.

of rings, chains, etc. leads to partial distortion of the SiO_4 tetrahedrons with a consequent lowering of their symmetry. It follows from x-ray data that interatomic Si–O and O–O distances in a given tetrahedron in a silicate structure differ appreciably. For example, in the structure of the ring silicate cataplelte the distances are: O_{II}–O_{II} = 2.55, O_I –O_I = 3.03, Si–O_{II} = 1.52 and Si–O_I = 1.70 A [7].

This hypothesis apparently has a direct connection with the changed views on the role of silicon–oxygen radicals in silicate structures. It has now become evident that the high stability of silicon–oxygen radicals does not make them rigid; on the contrary, they are very adaptable to requirements of morphological character and crystal habit imposed by the other elements in the structure [8], so that they can undergo considerable distortion.

Thus, in the interpretation of the spectra of ring silicates we can probably apply the conclusion of Duval and Lecomte that the fundamental vibrations of the XY_4 group are split as the result of a lowering of its symmetry [9]. Similar conclusions have now been reached with regard to a number of organosilicon compounds [10–12].

II. Our earlier investigations [13, 14] were concerned with the transmission and reflection spectra of ring silicates. Earlier meager data published by other workers on the transmission spectra of ring silicates were concerned mainly with the 2–15 μ region, and the results for different minerals were not correlated. In addition, confusion was introduced into the interpretation of the spectra because minerals such as rhodonite, wollastonite, and pectolite were assumed to be of the ring type.

Our investigations showed that the infrared absorption spectra of ring silicates of various compositions have, in addition to the bands at 8–12 and 17–20 μ which are common for all silicates, an intense band in the 12–13.5 μ region, which we regard as characteristic for ring silicates. The infrared transmission and reflection spectra of ring silicates were found to depend directly on the manner in which the silicon–oxygen tetrahedrons are joined in rings. The position of the first and especially of the second fundamental band in the spectrum is characteristic of silicates with three-membered and six-membered rings, and of twinned rings of both types. This permits spectroscopic identification of silicates with silicon–oxygen ring radicals.

The following conclusions could be drawn from our experimental data: a) The spectra of silicates the structures of which contain $[Si_3O_9]$, $[Si_6O_{18}]$, $[Si_6O_{15}]$ and $[Si_{12}O_{30}]$ rings are characteristic for each type of ring, i.e., are determined by the ring type. Thus, in the case of silicates with three-membered rings $[Si_3O_9]$ the first fundamental band

TABLE 2. Comparison of the Spectra of Certain Silicates

Mineral	Origin	λ of absorption bands, μ
Wollastonite, $Ca[SiO_3]$	Tadzhik SSR	9,05 9,46 9,77 10,34 10,86 11,12
Pectolite, $Ca_2Na[Si_3O_8](OH)_2$	Front mountain range, NW Caucasus	9,58 10,02 10,27 10,77 11,05
Xonotlite, $Ca_6[Si_6O_{17}](OH)_2$	Same	8,35 9,35 9,90 10,27 10,77 11,38 11,66
Axinite, $Ca_2(Mn,Fe)(Al_2B)[Si_4O_{12}](OH)$	Polyakov mine, Zlatoust region, Ural	9,07 9,37 9,57 9,91 10,12 10,69 11,23 11,31 12,5 12,8
Apophyllite, $KCa_4[Si_4O_{10}]_2F \cdot 8H_2O$	Akhaltsek, Georgian SSR	8,70 9,04 9,76 12,30 13,16

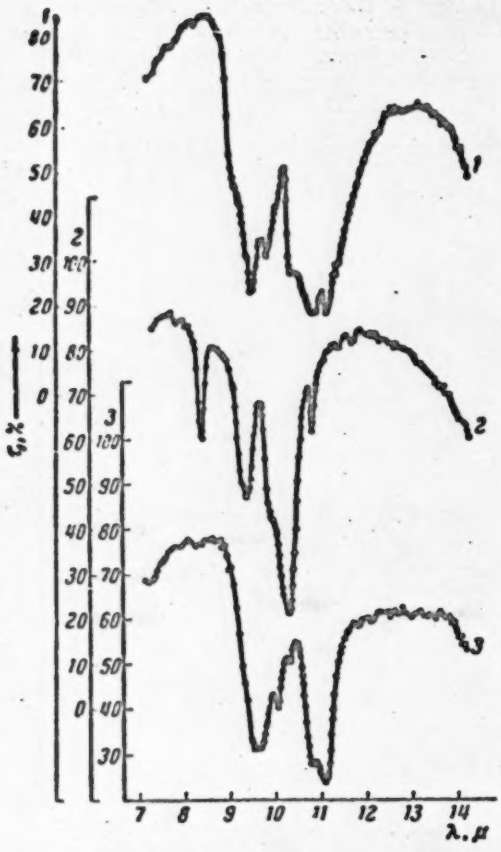

Fig. 2. Transmission spectra of minerals of the wollastonite group: 1) Wollastonite; 2) xonotlite; 3) pectolite.

is in a region of longer wave lengths than the same band in the spectra of silicates with six-membered rings [Si_6O_{18}] (8-10.5 μ, with the exception of dioptase). In silicates with three-membered rings this band is narrower and simpler in structure. In the general case this band is a doublet, more pronounced for silicates with three-membered rings and "complicated" for silicates with six-membered rings.

The first fundamental band of milarite and tourmaline is in the 8.5-9.5 and 7.5-10 μ region respectively; i.e., bands for minerals with twinned six-membered rings are shifted even further into the short-wave region. This displacement of the first fundamental band of silicates with six-membered or twinned rings into the short-wave region cannot be attributed to the influence of the atomic weight of the cations (since the displacements are roughly equal for different groups of cations); this influence can exist, if at all, only within a given group of minerals with the same ring type. The shift of the first fundamental band toward shorter wave lengths in silicates with twinned rings is also demonstrated clearly for the pair catapleite–elpidite, which are similar in chemical composition but have different rings (three-membered and twinned three-membered):

$$Na_2Zr[Si_3O_9] \cdot 2H_2O \text{ and } Na_2Zr[Si_6O_{15}] \cdot 3H_2O.$$

In the spectrum of catapleite the first fundamental band is in the 9.73-10.44 μ region, and in the spectrum of elpidite it is in the 8.88-9.66 μ region, and the structure of the latter band is more complex.

b) The spectra of ring silicates invariably had strong absorption bands in the 12-13.5 μ region. This second fundamental band is at shorter wave lengths (12.4-13.0 μ) for silicates with six-membered rings than for silicates with three-membered rings (13-13.5 μ).

The influence of differences in the structure is especially pronounced in the spectra of catapleite and elpidite: the second fundamental band for catapleite is at 13.40 μ, and for elpidite at 12.73 μ, which is a shift of 0.7 μ. With regard to twinned six-membered rings, the following may be noted: in the spectra of milarite and tourmaline the band characteristic of the ring is at 12.59 and 12.72 μ respectively, i.e., at shorter wave lengths than in the spectra of silicates with three-membered rings.

Analogous results were obtained for organic compounds. The influence of ring size in organic compounds on the pulsation frequencies of the rings was investigated by Barrow and Searles [15] by means of infrared spectra, and by Kohlrausch and Reitz [16] by means of Raman spectra. The results show that the frequency of the strong infrared band decreases and that of the strong Raman band increases with decrease of ring size.

Comparison of the reflection spectra of crystalline plates of the same minerals showed that the intensity of the second fundamental ("ring") band depends on the orientation of the crystal section. The intensity is greatest with crystal plates containing the silicon–oxygen rings in their planes. Dioptase is an exception; the reverse is true in this case. The greater intensity of the second fundamental band in the spectrum of a dioptase plate cut parallel to the optical axis can probably be correlated with the specific character of the silicon–oxygen rings in this mineral, which are nonplanar, have $\bar{3}$ symmetry, and do not have a horizontal plane of symmetry. Moreover, in contrast to other silicates with six-membered rings, dioptase is optically positive.

The strong band in the 12-13.5 μ region is specific for silicates with a ring structure of the silicon–oxygen radical. Admittedly, the spectra of certain silicates without ring structure may contain weak bands in the 12-13.5 μ region, due to other structural characteristics. It is possible, for example, that the absorption bands observed in this

wave-length region in the spectra of certain micas and framework silicates are due to the fact that silicon–oxygen rings form sheets in micas and three-dimensional frameworks in framework silicates. An example is apophyllite, $KCa_4[Si_8O_{20}]F \cdot 8H_2O$. This is a layer silicate [17], the layers of which consist of four-membered silicon–oxygen rings. The layers are puckered, so that individual rings can be easily identified — each ring lies above or below four rings linked to it. The rings in apophyllite are less "rigidly" linked than the rings in other layer silicates, and dynamically they are closer to the rings of ring rather than of layer silicates. Accordingly, the spectrum of apophyllite contains a strong band at 13.16 μ (Fig. 1a, Table 2). This band is also characteristic of the silica modifications (quartz, 12.65 μ; α-cristobalite, 12.60 μ; α-tridymite, 12.70 μ) which are also known to have six-membered rings in their structures. The rings in the quartz structure are differently oriented relatively to the optical axis, and possibly because of this the intensity of the band depends little on the orientation of the section [18]. Of course, it is somewhat formal to identify silicon–oxygen rings in the structures of these minerals.

At the same time, we are inclined to agree with Matossi, who notes in his theoretical paper [19] that the presence of a 12.5–13.5 μ band in the spectra of ring silicates does not mean that every band in this region in the spectrum of any silicate is characteristic of rings. Cases are apparently possible when rings cannot be identified in the silicate structure, but absorption bands are found in this region owing to other causes. We therefore admit that bands may appear in the 12–13.5 μ region in the spectra of certain silicates without ring structure, but spectra of ring silicates must invariably contain strong bands in this region.

III. It should also be noted here that the infrared reflection and transmission spectra of two-component glasses investigated by various workers [20, 21] also contain a band in the 12–13.5 μ region. The position of the maximum of this band differs with glasses of different compositions, and is characterized by the following wave lengths: 13.35, 13.1, 12.9, 12.6 μ [20] and 13.5, 13.25, 13.0, 12.65–12.7 μ [21]. Maxima of the absorption bands for ring silicates are also found at these wave lengths. Therefore the presence of bands at 13.5, 13.35, and 13.25 μ in the spectra of glasses may be partially correlated with the presence of SiO_4 tetrahedrons joined in three-membered rings $[Si_3O_9]$, and the presence of 12.5–13 μ bands, with the presence of rings consisting of six tetrahedrons. The strength of the 12.5–13.5 μ bands for glasses decreases with increasing contents of metal oxides; this may indicate destruction of the rings.

IV. The band in the 12.5–13.5 μ region in the spectra of aluminosilicates and Al silicates probably should not be attributed to the presence of Al in fourfold coordination [22], since in silicates in which Al simulates Si and is in fourfold coordination their properties are so similar that independent bands due to AlO_4 tetrahedrons are hardly to be expected. We consider that replacement of Si by Al in aluminosilicates may cause some displacement of the bands, or merely a broadening of the first fundamental band. Moreover, the examples given in the literature [22] of a correlation between the presence of AlO_4 tetrahedrons and the presence of 720–730 cm^{-1} bands cannot be regarded as satisfactory, because framework silicates were considered, so that silicon–oxygen rings could be distinguished in their structure.

V. In the preceding communication [13] we unfortunately did not give the transmission spectra of minerals of the wollastonite group, for which the wave lengths of the absorption bands were published. It is evident that the transmission spectra (Fig. 2, Table 2) of minerals of the wollastonite group which belong to chain silicates do not contain the band for the ring structure.

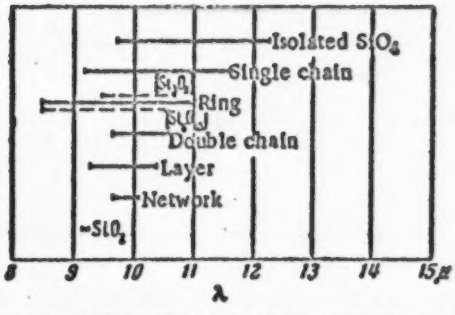

Fig. 3. Effect of silicate structure on the wave length of the intense absorption bands.

The spectra of wollastonite and pectolite are similar, which is consistent with the similarity of their structures, based on silicon–oxygen chains. The structure of xonotlite consists of columns of Ca octahedrons interlayered with twin chains or bands of SiO_4 tetrahedrons, and accordingly the absorption bands of xonotlite in the 8–11 μ region are at shorter wave lengths than those of wollastonite and pectolite (Fig. 3).

As an example of the possible use of spectra for identification of silicates, let us consider the transmission spectrum of axinite (Fig. 1b, Table 2). According to Ito [23], the axinite structure contains four-membered $[Si_4O_{12}]$ rings. The axinite spectrum, which we investigated in the 7–15 μ region, contains no bands in the 12–13.5 μ region. Comparison with spectra of ring silicates suggests that the existence of isolated $[Si_4O_{12}]$ rings in axinite is doubtful.

Launer [24] used the data of various authors for compiling a summary table of the spectral ranges of strong infrared absorption bands of silicates with different silicon–oxygen radicals. We added our data on ring silicates (Fig. 3)

for the 8-12 μ region to this table. Evidently ring silicates also have a definite absorption band in the 8-12 μ region. The first fundamental band for ring silicates is at longer wave lengths than the first band for framework silicates and at shorter wave lengths than that for island silicates; i.e., it is in an intermediate position in the wave length scale for silicates with different silicon–oxygen radicals.

LITERATURE CITED

1. V.S. Sobolev, Introduction to Silicate Mineralogy [in Russian] (Izd. L'vovsk. gos. univ., 1949).
2. Tables of interatomic distances and configuration in molecules and ions. Ed. L.E. Sutton (London, 1958).
3. W.L. Bragg, "Structure of Silicates" [Russian translation] in collection: Fundamental Ideas of Geochemistry, No. 3 (ONTI, Leningrad, 1937).
4. E. Schiebold, "Structure of Silicates" [Russian translation] in collection: Fundamental Ideas of Geochemistry, No. 3 (ONTI, Leningrad, 1937).
5. V.A. Kolesova, Dissertation: Raman Scattering and the Structure of Glassy Bodies [in Russian] (Inst. Silicate Chemistry, Academy of Sciences USSR, Leningrad, 1953).
6. V.A. Kolesova, Zh. éksperim. i teor. fiziki 26, 1, 124 (1954).
7. B.K. Brunowski, Die Struktur des Katapleits, Acta physicochimica URSS 5, 6 (1936).
8. N.V. Belov, Mineralog. sb. L'vovsk. geol. obshch. 9, 3 (1955).
9. Cl. Duval and L. Lecomte, Compt. rend. 239, 249 (1954).
10. A.N. Lazarev, Fiz. sb. L'vovsk. univ., No. 3 (8). Proceedings of the 10th Conference on Spectroscopy [in Russian] (195?) Vol. II, p. 440.
11. A.N. Lazarev, Optika i spektroskopiya 4, 6, 805 (1958).
12. A.N. Lazarev and M.G. Voronkov, Proceedings of Tech. Conference [in Russian] (1958) Vol. 3, p.52.
13. G.B. Bokii and I.I. Plyusnina, Nauch. dokl. vyssh. shkoly, geol.-geogr. n. 3, 116 (1958).
14. I.I. Plyusnina and G.B. Bokii, Kristallografiya 3, 6, 752 (1958).
15. G.M. Barrow and S. Searles, J. Amer. Chem. Soc. 75, 1175 (1953).
16. K.W.F. Kohlrausch and A.W. Reitz, Z. physik. Chem. B45, 249 (1949).
17. Strukturbericht. Bd. 2, S. 145 (Leipzig, 1936).
18. N.A. Sevchenko and V.A. Florinskaya, Optika i spektroskopiya 4, 2, 261 (1958).
19. F. Matossi, J. Chem. Phys. 17, 679 (1949).
20. L. Houziaux, Silicates industr. 21, 12, 491 (1956).
21. V.A. Florinskaya, Zh. Strukt. khimii 2, 2, 183 (1961).
22. V.A. Kolesova, Optika i spektroskopiya 6, 1, 38 (1959).
23. T. Ito and J. Takeuchi, Acta crystallogr. 5, 202 (1952).
24. Ph. Launer, Amer. Mineralogist 37, 9-10, 764 (1952).

All abbreviations of periodicals in the above bibliography are letter-by-letter transliterations of the abbreviations as given in the original Russian journal. *Some or all of this periodical literature may well be available in English translation.* A complete list of the cover-to-cover English translations appears at the back of this issue.

METHODS FOR X-RAY STRUCTURAL ANALYSIS OF BIOLOGICAL MATERIALS

L.L. Razumova

Institute of Biological Physics, Academy of Sciences, USSR
Translated from Zhurnal Strukturnoi Khimii, Vol. 2, No. 3, pp. 337-345, May-June, 1960
Original article submitted October 7, 1960

The paper discusses modern concepts of structure and structural changes under various influences, in relation to a large group of proteins and tissues – materials which give x-ray patterns of the α type in the native state – and methods for interpretation of the x-ray patterns of these materials. Certain logically necessary experiments were carried to confirm and justify some of the conclusions.

There are at the present time two main trends in the application of x-ray structural analysis to interpretation of the structure and structural changes of biological materials. One of these, extremely laborious, now being followed by Kendrew-Perutz school, is concerned with detailed investigations of the structure of proteins which can be obtained in the form of single crystals. A great achievement here was the interpretation of the structure of myoglobin to a degree of resolution such that not only the spatial configuration of the polypeptide chain but also the nature of chain spiralization and the form of the side groups could be deduced.

However, far from every protein can be obtained in the form of single crystals. Moreover, in biological research the most interesting conversions are those involving proteins and their complexes in tissues of the organism, where proteins are present in the noncrystalline state. Such materials can be and are being investigated by x-ray structural analysis, but in a different form. In this second trend much simpler methods of x-ray diffraction analysis of polycrystalline and amorphous substances are used. These methods cannot give a detailed picture of the configuration of atoms or individual atomic groups in protein molecules, but they can reveal certain general characteristics of structure and of the structural changes taking place in biological materials during various processes. The main obstacle in the use of these methods is the nature of the resultant x-ray patterns – they are very poor in reflections. Published results indicate that this leads to ambiguities and inconsistencies in the interpretation of such patterns. The interpretation must therefore be based on certain preliminary concepts of the structure, derived either from special experiments with the air of x-ray diffraction or from data obtained by other physicochemical methods. It is always necessary in such cases to assess the compatibility of any given concept with the results which follow directly from the characteristics of a particular x-ray pattern.

The present paper is concerned with an elucidation of existing possibilities of x-ray structural analysis in relation to a large group of noncrystalline proteins, namely fibrous proteins of the keratin and myosin type.

One of the aims is the selection of a rational procedure for interpretation of the x-ray patterns of fibrous proteins in the region including intra- and intermolecular dimensions. (Methods for interpreting low-angle scattering patterns corresponding to macromolecular periods are not considered here.)

In order to illustrate that valuable information can be obtained by the simple and generally accessible methods of x-ray structural analysis with the aid of the concepts detailed below relating to the interpretation of the x-ray patterns of proteins, we consider structural changes in proteins in the process of α-β transformation, which has been studied for a long time.

First, we draw attention to certain information, which does not allow of ambiguous interpretation, obtained earlier in x-ray diffraction studies of proteins. The first point to be noted is Astbury's classification [1] of fibrous proteins into two classes in accordance with their x-ray diffraction characteristics. The collagen class includes proteins contained in tendons, bones, fish scales, etc. The other and very extensive class includes many of the most important proteins of animal tissues, which was described by Astbury as the class of keratin, myosin, epidermin, and fibrinogen proteins, or the KMEF class for short. This class is being continuously supplemented by new members, such as flagella

proteins [2] and proteins extracted from nerve tissue [3]. Globular proteins (for example, egg albumin) can give x-ray patterns of the same type as proteins of KMEF class. However, here we shall refer to the structure of proteins included in the KMEF class.

Further, it is known that the x-ray patterns obtained with the primary beam perpendicular to the axis of axially orientated dry specimens* of proteins of the KMEF class refer, in accordance with the state of the protein, to one of the types shown in Fig. 1, designated as α, ∥ β, (parallel to β) and ×β (transverse to β) patterns. The α pattern is characteristic of native proteins, and ∥ β and ×β patterns are characteristic of the same proteins after special treatment. For example, in order to obtain the ∥ β pattern the protein specimen is strongly stretched in the moist state [4]. Some proteins of the KMEF groups have so far been converted from the α state only into the ∥ β state, others only into the ×β state, while certain proteins, in accordance with the treatment conditions, have been converted into either the ∥ β or the ×β form. Conversion of proteins from the α into the β form is known as the α-β transformation and has been the subject of many investigations, because not only the structural and mechanical characteristics but even some of the in vivo functions of proteins [5] have been correlated with their tendency to undergo this transition.

Thus, the information provided with certainty up to now by x-ray investigations consists of the division of fibrous proteins into two classes in accordance with their x-ray diffraction characteristics, and the existence of different patterns for proteins of the KMEF class, dependent on their state. All other x-ray information should probably be regarded with caution in view of the contradictory statements in the published papers.

It must be emphasized that in structure analysis from x-ray patterns which are not rich in reflections all possible sources of x-ray information must be fully utilized; not only the position but also the form and intensity of the reflections must be taken into consideration; some additional information may be analysis of the background intensity of the pattern. This approach to intepretation of x-ray patterns has not yet been finally adopted, although the reflections observed in all the patterns in Fig. 1 can be divided even by their appearance into two types: diffuse isotropic rings and more distinct anisotropic lines or arcs. It follows from the theory of x-ray scattering that these two systems of reflections characterize at least two structural phases** of the substance, differing in order and orientation.

Up to now the main attention in discussion of x-ray patterns has been devoted to the anisotropic, "quasicrystalline" reflections [6, 7], which were used as criteria for evaluation of various structural models. The very strong diffuse rings present in the diffraction patterns of all three types (α, ∥ β, ×β), which characterize the less ordered part of the substance, were not taken into account in analysis of x-ray patterns. Admittedly, certain authors [4, 8] have for a long time postulated the coexistence of regions of higher and lower structural order in proteins, but they did not correlate them with the reflections on the x-ray patterns. Recent physicochemical investigations by Doty [9] have justified the view that in solution some of the protein chains are present in a "randomly coiled" state; there is now a tendency to apply this view to dry proteins [10]. It is therefore all the more timely to correlate this structural phase with definite elements in the x-ray patterns of proteins. It is natural to assume that the x-ray characteristics of this phase, the "less ordered" part of the substance, in the x-ray patterns given by dry proteins are the diffuse isotropic rings.

The anisotropic "quasicrystalline" reflections in the patterns (Fig. 1) call for the following comments. When dry proteins in either the α or the β form are wetted, the anisotropic reflections in the patterns behave differently: the sharp reflections (narrow in the radial direction) are retained while the diffuse anisotropic spots or arcs spread and disappear. This indicates that the structure characterized by the anisotropic reflections is stabilized by bonds differing in strength. The weak bonds which are destroyed on hydration of the protein, leading to the disappearance of the diffuse equatorial spots on the pattern, we describe as "packing" bonds, as the appearance of the corresponding reflections as the result of dehydration may be correlated with lateral packing of the polypeptide chains (see below). The sharp reflections disappear only by treatment with reagents which break down hydrogen bonds (for example, see the work of Rudall [11] on the return of epidermin from the ×β into the α state by the action of saturated urea solutions). This confirms the connection between the sharp reflections in the x-ray patterns and the structural elements in which the periodicity is fairly uniform owing to hydrogen bonding of definite types of polypeptide chain segments.

* Orientation of proteins is effected only in moist specimens. Loss of water during drying deprives the protein chains of mobility, i.e., in a certain sense "fixes" their position.

** In this paper the term "structural phase" or simply "phase" is used to denote the combination of structural elements (polypeptide chains or regions of these chains) for which the x-ray patterns indicate the same structural characteristics; structural elements of the same type, constituting a "phase", may evidently be separated in space (in particular, by alternation of structural elements belonging to different "phases").

Thus, all the reflections in the α and β patterns can be classified, either by their form or by their behavior when the proteins are wetted, into groups which depend on the structural elements from which they originate.

Since the background of the x-ray patterns of proteins is fairly clear and uniform, we consider that in the first approximation it may be ignored in interpretation of large-angle x-ray patterns, apart from certain special cases when it undergoes significant changes.

We start with a discussion of the information obtained from the characteristic anisotropic reflections in the x-ray patterns of orientated α and β forms. The characteristic reflections of the α patterns of dry orientated proteins are considered to be the 5.1 A meridional reflection and the 9.8 A equatorial reflection. The former indicates the presence of protein chains in the form of α spirals [6]. Its meridional position indicates orientation of the spiral axes approximately along the axis of the specimen. The other anisotropic reflection, the equatorial 9.8 A reflection, is correlated either with lateral packing of α spirals [6] or with packing of the stretched protein chains in layers in the direction of their side chains [12]. The disappearance of the 9.8 A equatorial reflection when the protein is wetted is evidence in favor of its packing character; the interdependence of the 5.1 and 9.8 A reflections in the α pattern is supported by Bendit's data [13] for keratin; he found that the intensities of both these reflections diminished simultaneously when the specimens had been subjected to considerable stretching. If it could be proved that the 9.8 A reflection corresponds to packing of α spirals this would mean that the spirals are in "bundles" and not distributed singly within the protein. However, without additional investigations it is impossible to decide conclusively whether the 9.8 A reflection corresponds only to the α spiral phase or whether it is associated with packing of any orientated chains (possibly even chains of unlike configuration) in contact in the direction of their side chains.

In addition to the diffuse rings, the ∥ β pattern has three principal reflections, which are regarded as characteristic for it: 4.6 and 9.8 A equatorial reflections and a weaker meridional reflection of about 3.5 A. These reflections have been explained with the aid of a model in which the chains are packed in layers [12] stretched with retention of the valence angles of the polypeptide chains with a repeat of 4.6 A in the layer (in the direction of the principal chains) and 9.8 A between the layers (in the direction of the side chains), and a pleated sheet model [6]. The second model is based on the concept of polypeptide chains extended with definite kinks along the axis of the specimen (not only are the valence angles retained, but the chains conform to the principle of best packing and are linked by hydrogen bonds), forming pleated sheets; the distances between the chains in the sheet are again 4.6 A, and the sheets are 9.8 A apart. In both models the 3.5 A meridional reflection corresponds to a projection of the length of the amino acid residue onto the fiber axis. The "packing" model is now regarded as obsolete, and the pleated sheet model is generally accepted for interpretation of ∥ β x-ray patterns. We consider, as the result of an examination of various ∥ β patterns, that each model has its applicability region, dependent on the method of preparation of the ∥ β form. The following applicability criterion may be applied. If the pleated layer model is valid, then only the 9.8 A equatorial reflection should disappear when the protein is wetted, while the 4.6 A equatorial reflection should persist, because the principal chains in the pleated sheet model are linked by hydrogen bonds, which are not destroyed by water at room temperature. In the model which does not postulate hydrogen bonding between the chains both equatorial reflections should disappear in presence of water. Astbury succeeded in returning specimens stretched to the ∥ β state into the α state by simple relaxation in water [1]. Since this transformation is possible, it is evident that the ∥ β form was not stabilized by hydrogen bonds in this case and the "packing" model is applicable. If the ∥ β form is obtained by the action of harsher agents, hydrogen bonds may be formed between the polypeptide chains and the pleated sheet model is then valid. It is to be expected that the x-ray patterns for these two cases would also differ in the form of the 4.65 A equatorial reflection. In fact, if the ∥ β form is made by stretching of moist specimens, i.e., in the case of the "reversible" β state [1], the 4.65 A reflection is in the form of a spot which is fairly wide in the radial direction (Fig. 1b). On the other hand, if the ∥ β form of keratin is obtained by the combined action of extension, compression, and temperature [12], when the pleated sheet model is valid, the 4.65 A equatorial reflection is in the form of a long narrow arc.

In the x-ray pattern of the ×β form the 9.8 and 3.5 A reflections are equatorial, and the 4.6 A reflection is meridional. Astbury and Rudall [10, 11] consider that this pattern also represents the existence of sheets 9.8 A apart and approximately parallel to the axis of the specimen; however, in the sheets the polypeptide chains are perpendicular to the specimen axis.

In addition to the ∥ β and ×β patterns, there is yet another variety of pattern, the so-called "disorientated" β pattern (Fig. 1d). Patterns of this type are given by proteins subjected to certain denaturation treatments (e.g., boiling in water, treatment with alcohol or concentrated acetic acid, etc.). In these β patterns a sharp 4.65 A ring appears on the background of the diffuse 4.6 A ring. Denaturation of this type is regarded as unification of the distances between nonorientated protein chains, as "growing together" of the protein chains by means of hydrogen bonding [1, 14].

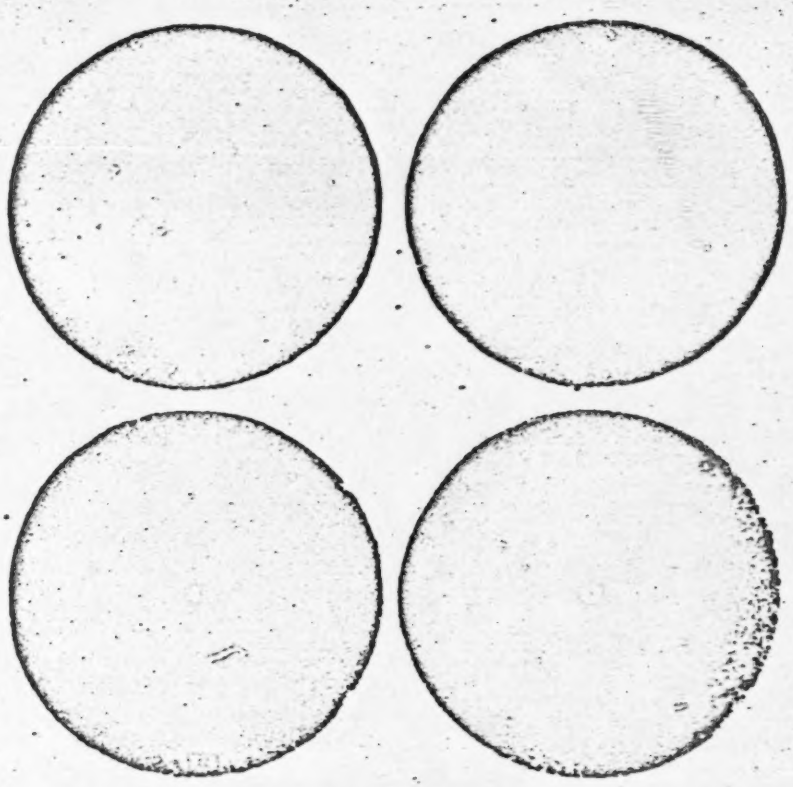

Fig. 1. Typical x-ray patterns of dry orientated samples of protein, KMEF class: a) α form; b) ‖β form; c) ×β form; d) disorientated β form. The arrows indicate the characteristic reflection of the pattern.

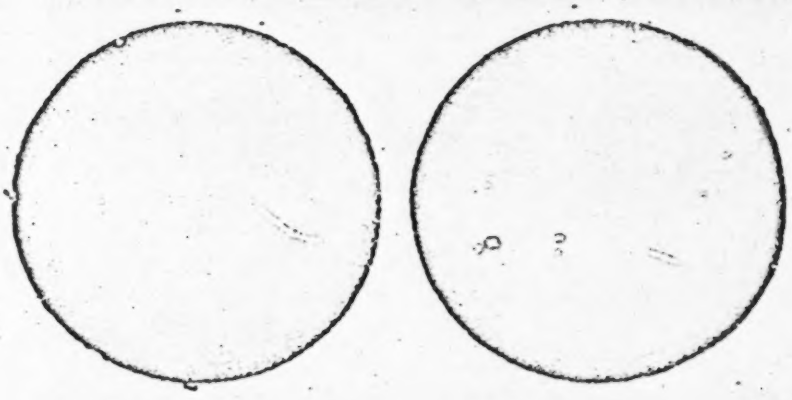

Fig. 2. X-ray patterns of orientated samples of protein in the β state: a) wetted sample of disorientated β form (the 3.7 Å reflex is characteristic of water); b) sample with transition from α to β form not carried out. The arrows indicate the characteristic reflection of the pattern.

As already noted, diffuse isotropic rings are inevitably present in the α and β patterns of orientated proteins. These rings correspond to "liquid" (short range) order in the protein substance [15]. They have the same periods on all x-ray patterns of dry proteins – about 4.6 and 9.8 A. Whereas in models postulating the existence of sheets in proteins these are periods in the sheet in the direction of the principal chains (4.6 A) and between the sheets in the direction of the side chains (9.8 A), in the case of molecular packing these values must correspond to the effective diameters of the polypeptide chain in these two directions. The isotropic character of the diffuse rings shows that these chains do not have any predominant direction even in orientated specimens. The isotropic character of this part of the protein chains in a dry orientated specimen may either be due to the fact that they cannot be orientated in the moist specimen (which is possible if the bonds within the "globule" of chains are stronger than the bonds with neighboring chains undergoing orientation), or to loss of orientation by this part of the chains in the course of drying.

We must note once again that the diffuse rings, which we associate with the "liquid" type of chain packing in dry proteins, are not found in the x-ray patterns of moist proteins. Evidently in the undried state, which is closest to the physiological state for most proteins (apart from keratin), the protein chains which give rise to the diffuse rings in the patterns of dry proteins are separated by water and, like solutions of other macromolecules, do not give reflections in the large-angle region. When the protein is dried, these chains come into mutual contact while retaining their van der Waals diameter, and are packed in the most advantageous manner.

The intensity ratio of the 4.6 and 9.8 A rings depends on the nature of the protein and the preliminary treatment [16]. However, in the cases examined by us up to now the intensity of the diffuse isotropic 4.6 A ring on orientated α patterns is appreciably greater than that of the 9.8 A ring. The explanation may be that in the course of drying the conditions are more favorable for molecular packing of nonorientated protein chains in the direction of the principal chains than of the side chains. The considerable intensity of the diffuse isotropic rings in comparison with the reflections due to the α and β phases indicates a considerable content of a "disordered" phase in proteins.

Let us now apply the information deduced from the α and β x-ray diffraction patterns to analysis of the structural transformation of proteins from the α into the β form. It is held in the literature that the α-β transformation consists in straightening of chains which are in the α state. Recently Skertchly [17] suggested that the α-β transformation in proteins proceeds through an intermediate phase. If proteins contain a disordered phase, it is possible that it also must be influenced in some manner by the α-β transformation. However, before drawing conclusions about the mechanism of the α-β transformation, we must note that fo... varieties of the β state are distinguished from x-ray characteristics. It is probable that the mechanism of the α-β transformation is not the same in every case. Let us consider the α-β transformation in the case of a disorientated β phase. As already stated, a disorientated β pattern is given by orientated specimens subjected to certain denaturation treatments; it is interpreted as the consequence of the fact that the distances between the polypeptide chains become more uniform as the result of hydrogen bonding than they are in molecular packing. Whereas the 4.6 A diffuse ring disappears when the specimen is wetted, the sharp 4.65 A ring persists (Fig. 2a); this confirms the relative stability of the bonds which form between the chains during denaturation. If the denaturation has not gone too far, the x-ray pattern contains reflections of the orientated α phase together with a sharp ring of the disorientated β phase (Fig. 2b). The isotropic character of the sharp 4.65 A ring is due to the isotropic distribution of the newly formed hydrogen bonds in the orientated specimen and supports the view that cross linking of the chains by hydrogen bonds occurs in the isotropic, "disordered" part of the specimen, at least during the first stages; as the denaturation becomes more extensive the α phase anisotropic reflections become weaker and disappear; it is possible that their disappearance is associated with the appearance of internal stresses (tensile forces) in the specimen, leading to lengthening, weakening, and ultimate rupture of the hydrogen bonds in the α spirals and to uncoiling of the spirals.

It is interesting to note that complete disappearance of the diffuse isotropic rings cannot be achieved even on extensive denaturation of the protein. The impression arises that hydrogen bonding between the chains is limited to a certain proportion of the chains, possibly because of a certain relative "rigidity" of the structural formations in the isotropic phase.

Thus, the first stage in the transition from the α phase to the disorientated β phase, i.e., in denaturation, is probably cross linking of some of the polypeptide chains in the isotropic phase of the protein, followed by "deterioration" of the α phase.

As already noted, two different possibilities must be considered in the α-β transformation in the case of the β form: the appearance of a "packing" structure, containing extended chains orientated in the direction of the axis of the specimen and linked by weak packing bonds, and the formation of a structure containing orientated extended chains with definite kinks and cross-linked by hydrogen bonds.

In the transformation from the α state to the reversible "packing" ∥β state, chains susceptible to the process undergo orientation. Here the "classic" model of the α-β transformation (uncoiling of the orientated α spirals owing to weakening and rupture of hydrogen bonds during stretching) may also be valid. In the transition to the reversible ∥β form a disorientated phase may also be seen to persist after disappearance of the α phase (Fig. 1b).

The transition from the α to the ∥β state, represented by the pleated sheet model, evidently involves two processes: stretching and orientation of the protein chains, as in the transition to the packing ∥β form, and cross linking of these chains by hydrogen bonds, as in denaturation (in the transition to the disorientated β form). Whereas in the case of the orientated α form denaturation occurs in the isotropic part of the protein, in the transition to a pleated sheet structure cross linking of the chains occurs in this part with the chains already orientated somewhat by the additional stretching. It should be noted that the greater length of the 4.65 A equatorial arc in this case, in comparison with that observed on the x-ray patterns of the packing ∥β form, indicates that as the chains become cross linked their orientation along the specimen axis deteriorates. Here, as in the disorientated β phase and the packing ∥β phase, the isotropic diffuse rings persist; evidently a certain proportion of the protein substance does not undergo either orientation or denaturation.

In ×β patterns, in contrast to ∥β patterns, the 4.65 A reflection is meridional. This indicates that the chains are transverse to the specimen axis; the sharpness of the reflection (as in the x-ray patterns of the disorientated β form) suggests cross linking of the chains by hydrogen bonds. The strongest ×β patterns were obtained from stretched specimens previously subjected to thermal denaturation (for example, myosin and egg albumin heated in an aqueous medium above 60°), when x-ray patterns of the disorientated β form might be expected to appear. Sometimes subsequent drying of the specimen under isometric conditions may play the role of stretching.

To account for the fact that the orientating effect of stretching leads to a transverse and not a parallel arrangement of the polypeptide chains as indicated in the ×β patterns, we must assume that by the start of orientation, i.e., the start of drying, the protein contains formations of the rod or band type [10, 11] in which the polypeptide chains are at right angles to their length. Stretching then leads to partial orientation of these formations. The sharp 4.65 A reflection in ×β patterns shows considerable azimuthal diffusion; this indicates that orientation of these formations is difficult. Since the same protein, such as myosin, can be converted by special procedures not only into the ×β but also to the ∥β form, it is probable that the original protein did not contain band or rod formations, which arose during conversion of the specimen into the ×β form. In the case of myosin the protein may have undergone thermal denaturation, leading to cross linking of the polypeptide chains in the "nonregular" part of the moist protein. The small width of the 4.65 A denaturation reflections indicates that lateral cross linking involves a relatively large number of polypeptide chains. Stretching of a denatured protein converts it either into the ×β state (myosin), where the chains are at right angles to the specimen axis, or into the ∥β state (edestin), represented by the pleated sheet model, in accordance with the ratio between the lengths of the cross-linked chains and the lateral extent of the cross linking.

There are reports of the ×β patterns from specimens subjected to milder treatments (bacterial flagellae [2], orientated actamyosin films during syneresis [5]). However, in such cases the characteristic 4.65 A arc is of low intensity, while the treatment methods do not exclude the possibility of some denaturation. It should be noted that the connection between the ×β pattern and the denaturation effect is not contradictory to the possibility of a transverse arrangement of the polypeptide chains relative to the fiber axis in certain native fibers (silk from the outside of the cocoon of the Chrysopa insect [18]).

Proteins can in certain instances be obtained in the ×β form from specimens giving the ∥β form if they are subjected to denaturation before orientated drying. It follows that the ×β form is produced by orientation of a previously denatured protein. During denaturation in absence of strong orientating influences the cross-linked chains are distributed with equal probability over the entire protein volume; this leads to the isotropic character of the sharp 4.65 A reflection on the x-ray pattern of the disorientated β form.

The packing ∥β form is produced as the result of stretching of protein chains in substantial orientation. If denaturing influences are superposed on this distinct orientation, the formation of a pleated sheet structure "hardened" by hydrogen bonds is possible. Some proteins form a pleated sheet structure as the result of stretching after denaturation. The significant difference between the packed ∥β state and the other β forms is the character of the bonding between the polypeptide chains in the β phase: it is due to molecular packing in the packing ∥β form, and to hydrogen bonds in the other cases.

Thus, two quite different processes are implied when we speak of the α-β transformation: stretching, orientation, and molecular packing in the transition to the packing ∥β form, and denaturation of a definite type, consisting

of cross linking of the polypeptide chains in the "hardened" β, disorientated β, and $x\beta$ forms. The β phase appears (the chains become cross linked) in the "disordered" phase of the protein (at least, at the start of denaturation). However, we did not observe total disappearance of the diffuse isotropic rings in the x-ray pattern after orientation and denaturation, and no such observations are reported in the literature. The stability of a certain proportion of the "disordered" phase to orientation and denaturation is a characteristic property of it; this may be due to the fact that the structure of a protein is determined not only be packing and hydrogen bonds but also by valence bonds in the side groups of neighboring polypeptide chains [19].

Some of the views on protein structure discussed here had been put forward earlier, as indicated by the literature citations in the text. However, the authors cited either did not develop these views further or even used structural models incompatible with such views in the discussion of their results. We therefore considered it necessary to present a general picture of the molecular structure of fibrous proteins of the KMEF class and of some of their most important transformations in the light of the information which follows directly from analysis of x-ray patterns based on the theory of x-ray scattering in liquids and amorphous solids [15], using the experience gained in work with other complex natural high polymers [20].

In conclusion, we may note that x-ray diffraction studies based on combined analysis of different elements in the x-ray patterns of biological materials existing in different states may provide new information when certain other structural transformations are considered; for example, different types of protein denaturation, in studies of the role of water in protein structure, in studies of muscle contraction processes, and in investigations of other important biological materials, including nucleic acids of nerve tissue.

LITERATURE CITED

1. W.T. Astbury, Proc. Roy. Soc. B134, 303 (1947).
2. W.T. Astbury and C. Weibull, Nature 163, 280 (1949).
3. F.O. Smith, J. Cellular and Compar. Physiol 49, Suppl. 1, 165 (1957).
4. W.T. Astbury and S. Dickinson, Proc. Roy. Soc. B129, 307 (1940).
5. F.G.E. Pautard, Nature 182, 788 (1958).
6. L. Pauling and R.B. Corey, Fortschr. d. chem. org. Naturstoffe (1954) (Russian translation in the collection: Modern Problems of Biochemistry, Izd. inostr. lit., Moscow, 1957, p. 38).
7. N.A. Andreeva and V.I. Iveronova, Biofizika 2, 281 (1957).
8. H. Zahn, Z. Naturforsch. 2b, 104 (1947).
9. J.T. Jung and P. Doty, J. Amer. Chem. Soc. 79, 761 (1957).
10. W.T. Astbury, Disc. Faraday Soc. 25, 80 (1958).
11. K.M. Rudall, Adv. Prot. Chem. 7, 255 (1952).
12. W.T. Astbury and W.A. Sisson, Proc. Roy. Soc. A150, 533 (1935).
13. E.G. Benditt, Nature, 179, 535 (1957).
14. W.T. Astbury and R. Lomax, J. Soc. Chem. Ind. 53, 979 (1934).
15. V.I. Danilov, Scattering of X-rays in Liquids [in Russian] (Moscow-Leningrad, ONTI, 1935).
16. D.P. Riley and V.W. Arndt, Proc. Roy. Soc. B141, 93 (1953).
17. A.B.B. Skertchly, Nature 181, 639 (1958).
18. K.D. Parker and K.M. Rudall, Nature 179, 905 (1957).
19. V.A. Belitser, Uspekhi sovremennoi biologii 50, 3 (1960).
20. V.I. Kasatochkin and L.L. Razumova, Izv. AN SSSR, Ser. fiz. 20, 751 (1956).

All abbreviations of periodicals in the above bibliography are letter-by-letter transliterations of the abbreviations as given in the original Russian journal. *Some or all of this periodical literature may well be available in English translation.* A complete list of the cover-to-cover English translations appears at the back of this issue.

VAN DER WAALS INTERACTION OF HYDROCARBON MOLECULES

N.P. Borisova and M.V. Vol'kenshtein

Institute of High Polymers, Academy of Sciences, USSR, Leningrad
Translated from Zhurnal Strukturnoi Khimii, Vol. 2, No. 3, pp. 346-349,
May-June, 1961
Original article submitted July 4, 1960

Van der Waals interaction between two methane molecules in different relative positions has been calculated. Agreement with experimental data can be obtained if the Hill potential is used for the interaction of hydrogen atoms; carbon-carbon and carbon-hydrogen interaction must also be taken into account in accordance with the mutual orientation of the molecules. The contribution of steric interaction to the internal rotation barrier for ethane is negligibly small.

The conformation properties of molecules are especially important in relation to the behavior of polymers. Macromolecules are rotationally isomeric cooperative systems, and their physical characteristics are determined by the range of possible rotational isomers and by variations of this range under the action of various influences on the macromolecule [1]. However, until now there has been no reliable method for calculating the energy difference between rotational isomers – the principal quantity responsible for conformational properties of a molecule. The purpose of the present paper is a consideration of interaction between hydrogen atoms not linked by valence bonds in hydrocarbons.

In calculation of the steric interaction of hydrogen atoms in ethane, Eyring [2] used the potential for two H_2 molecules, calculated from valence schemes. Assuming that the interaction energy of two H atoms is $^1/_6$ of the energy of interaction of two H_2 molecules, Eyring obtained the van der Waals potential shown in Fig. 1 (curve 1). The same figure shows the corresponding experimental curve 2 based on the potential of H_2–H_2 interaction found from the second virial coefficient [3]. The curves diverge considerably for small distances; this is probably due to the inapplicability under these conditions of the Lannard-Jones potential on which the experimental curve is based [4].

According to Eyring, the contribution of H–H interaction to the internal rotation barrier for ethane is 0.3 kcal/mole. This contribution becomes considerably greater if the experimental curve is used instead of the theoretical. Mason and Kreevoy [5] used the H ... H potential calculated by Hirschfelder and Linnett [6]. This is the interaction potential of two H atoms in the triplet state. In [5] the potential is equated to one half of the "triplet" potential in calculation of the steric effects:

$$U_{H-H} = \frac{1}{2}\varphi(r, \text{Å}) = \frac{1}{2}[37 \cdot 10^3 \exp(-3{,}07\, r) - 90\, r^{-6}]. \quad (1)$$

Curve 3 (Fig. 1), based on Eq. (1), corresponds to stronger repulsion than the experimental curve. Curve 3 corresponds to attraction at $r > 3.7$ A. It should be noted that the distance between nearest nonbonded H atoms in hydrocarbons may be considerably less (about 2 A). We consider that potential (1) is unsatisfactory, as it is not permissible to assume just the triplet state of two H atoms. It is more reasonable to take into account the singlet state also [7]:

$$U_{H-H} = \frac{1}{4}U_{^1\Sigma} + \frac{3}{4}U_{^3\Sigma}; \quad (2)$$

here $U_{^1\Sigma}$ and $U_{^3\Sigma}$ are the energies of the singlet and triplet states, taken from [6]. The analytical form of Eq. (2) is

$$U(r, \text{Å}) = 12 \cdot 10^3 \exp(-2{,}65\, r) - \frac{16}{r^6} \quad (3)$$

Figure 1 shows that curve 4, based on Eq. (3), is close to the experimental curve. Several writers [4, 8] have doubted the applicability of the potential for free H atoms to calculations of steric H–H interaction in hydrocarbons. However, the opposite point of view is put forward in [5, 9]; the authors of these papers consider that it is quite permissible to use the "triplet" potential.

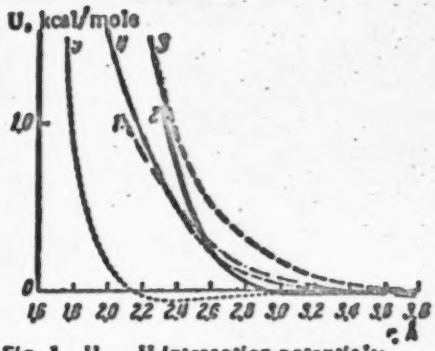

Fig. 1. H ... H interaction potentials: 1) According to Eyring; 2) experimental curve; 3) by Eq. (1); 4) by Eq. (3); 5) according to Hill.

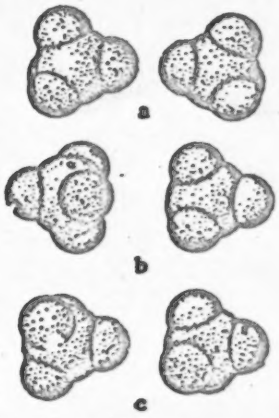

Fig. 2. Different mutual positions of methane molecules.

Let us consider the steric interaction of two methane molecules, so that a reasonable potential for H ... H interaction may be chosen. In the extreme position a (Fig. 2) repulsion should be considerably greater than in the other extreme position b. The experimental curve for $CH_4...CH_4$ interaction [10] is averaged over all mutual orientations of the molecules, and should therefore lie between the curves for positions a and b. For the calculation we must know the C...H and C...C potentials in addition to the H...H potential. The C...H potential was determined by A.I. Kitaigorodskii (Fig. 3):

$$U_{C-C}(r, \text{Å}) = 37 \cdot 10^3 e^{-2.6r} - \frac{330}{r^6}. \qquad (4)$$

For H...H interaction we take potential (3), and the C...H potential (Fig. 4)

$$U_{C-H}(r, \text{Å}) = 68 \cdot 10^3 e^{-2.8r} - \frac{230}{r^6} \qquad (5)$$

is found from (3) and (4) with the aid of the so-called combination rule [11].

Figure 5 shows our calculated curves for positions a and b, and the experimental curve. It is evident that the calculations are not in agreement with experiment. It cannot be assumed that the interaction between H atoms linked by valence bonds to C atoms is the same as for H atoms in H_2 molecules. According to x-ray diffraction studies of paraffins [12], the average van der Waals radius of hydrogen bonded to a C atom is 1.2 A, whereas Fig. 1 indicates that this radius is approximately 1.5 A. The region $2.2 < r < 3.0$ A is a repulsion region for free H atoms, and an attraction region for hydrogen atoms in C–H.

Hill [4] proposed the following potential for interaction of H atoms in C–H bonds:

$$U_{H-H}(r, \text{Å}) = 350 \cdot 10^3 e^{-3.2r} - 18r^{-6} \qquad (6)$$

This formula is based on the Lennard-Jones potential with parameters found from crystallographic and thermodynamic data. The potential (6) indicates attraction in the $2.2 < r < 3.0$ A region (Fig. 1). It seems likely that the difference in the behavior of free H atoms and H atoms bonded to C is determined mainly by the influence of the C atoms. This influence consists in deformation of the electron shell of the H atom, which decreases exchange repulsion of the hydrogens. The agreement of the curve based on Eq. (3) with the experimental curve for $H_2...H_2$ interaction and with the Eyring curve shows that the H–H valence bond does not have this influence. Another reason why the sphere of action is less for bound than for free hydrogens is the attraction between H and the C atom with which it is not linked by a valence bond [8]. However, this effect, which appears only at $r > 3.0$ A, cannot have an appreciable influence on the interaction energy. Calculation of the $CH_4...CH_4$ interaction based on the Hill potential (6) and the potential for C–H found from (4) and (6) (Fig. 4),

$$U_{C...H}(r, \text{Å}) = 30 \cdot 10^3 \exp(-4.6r) - 80r^{-6} \qquad (7)$$

gives agreement with experimental data.

Fig. 3. C...C interaction potential.

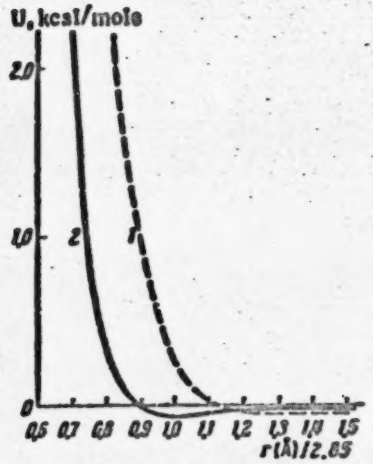

Fig. 4. C...H interaction potentials: 1) By Eq. (5); 2) by Eq. (7).

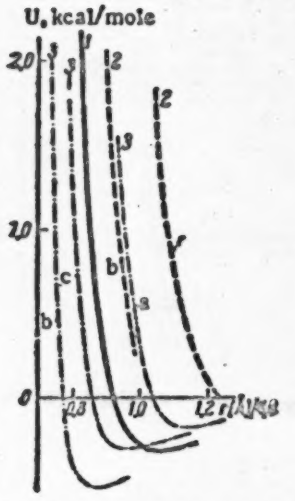

Fig. 5. Interaction potentials of two methane molecules in different positions (indicated by letters as in Fig. 2): 1) Experimental curve; 2) by Eqs. (4), (3), and (5); 3) by Eqs. (4), (6), and (7).

Figure 5 shows that the curves for the extreme positions a and b do in fact lie on either side of the average experimental curve. The curve for position c (Fig. 2), calculated by the same method, is between the experimental curve and curve b. The steric interaction of CH_4 molecules depends considerably on their mutual orientation; the assumption that CH_4 molecules are approximately spherical is very rough and is valid only for large distances. Analysis of the calculated results shows that in position a strong repulsion is due to interaction of the nearest H atoms, in position c, to interaction of C with the nearest H, and in position b, to H...H and C...C interactions. The remaining interactions correspond to attraction at the distances under consideration, but they do not make any substantial contribution to the final curve. From this we may conclude that, despite what is stated in [5], there is no significant shielding of C atoms by hydrogens. It is therefore necessary to take into account C...H and C...C as well as H...H interactions. This evidently applies also to interaction of methyl groups in hydrocarbons. We used the above results to calculate the H...H interaction in the ethane molecule, $H_3C–CH_3$. It corresponds to attraction with energy –0.2 kcal/mole, virtually independent of the angle of rotation of the CH_3 group about the C–C bond. Therefore the contribution of this interaction to the internal rotation barrier in ethane is negligibly small. Howlett [9] (and a number of others; see [1]) attributes the internal rotation barrier in ethane to rupulsion of H atoms. Howlett introduces a correction for the angular dependence of the "triplet" potential (1) on the orientation of the C–H bonds. This essentially takes into account the effect of bond orientation, considered by Pauling [13] and by G. and F. Harris [14]. This effect is unrelated to the steric repulsion of hydrogen atoms; we consider that Howlett's method is artificial.

The calculations described above can be used for analysis of internal rotation in hydrocarbons.

We thank T.M. Birshtein and O.B. Ptitsyn for valuable discussions.

LITERATURE CITED

1. M.V. Vol'kenshtein, Configuration Statistics of Polymer Chains [in Russian] (Izd. AN SSSR, Moscow, 1959).

2. H. Eyring, J. Amer. Chem. Soc. 54, 3191 (1932).
3. J. Lennard-Jones, Physica 4, 941 (1937).
4. T. Hill, J. Chem. Phys. 16, 399, 938 (1948).
5. E. Mason and M. Kreevoy, J. Amer. Chem. Soc. 77, 5808 (1955); 79, 4851 (1957).
6. J. Hirschfelder and J. Linnett, J. Chem. Phys. 18, 130 (1950).
7. C.A. Coulson and D. Stocker, Mol. Phys. 2, 397 (1959).
8. H. Stuart, Die Struktur des freien Moleküls (Springer Verlag, Berlin, 1952).
9. K. Howlett, J. Chem. Soc., 4353 (1957).
10. I. Amdur and E. Mason, J. Chem. Phys. 22, 843 (1954).
11. E. Mason and W. Rice, J. Chem. Phys. 22, 522 (1954); I. Amdur, E. Mason and A. Harkness, J. Chem. Phys. 22, 1071 (1954); E. Mason, J. Chem. Phys. 23, 49 (1955).
12. A. Müller, Proc. Roy. Soc. A154, 624 (1936); 178, 227 (1941).
13. L. Pauling, Proc. Nat. Acad. Sci. USA 44, 211 (1958).
14. G. Harris and F. Harris, J. Chem. Phys. 31, 1450 (1959).

INTERNAL ASYMMETRY IN COMPLEX COMPOUNDS

I. CALCULATION METHOD AND PRINCIPAL FORMULAS IN THE APPROXIMATION OF THE CRYSTAL FIELD THEORY

I. B. Bersuker

Institute of Chemistry, Moldavian Branch, Academy of Sciences USSR
Translated from Zhurnal Strukturnoi Khimii, Vol. 2, No. 3, pp. 350-360, May-June, 1961
Original article submitted February 27, 1960

The paper contains the results of an investigation of the internal asymmetry arising in the first coordination sphere of six-coordinated complex compounds as the result of the asymmetry of the ψ electron cloud of the incomplete d shell of the central atom (the explanation of this asymmetry is based on the Jahn – Teller theorem). The equilibrium configuration of similar ligands in the general case of an ionic complex is a distorted octahedron (with one diagonal either longer or shorter than the other two); it remains a regular octahedron only if the central ion has the electron configurations d^3, d^5, d^8, or d^{10}. Formulas for the degree of distortion of the octahedron, with the approximation in question, were obtained for all cases, together with formulas for the additional splitting of terms arising owing to the internal asymmetry.

INTRODUCTION

It is known that the principal physicochemical properties of complex compounds are closely related to the symmetry of the spatial arrangement of the ligands around the central atom in the first coordination sphere. Such properties include light absorption in the visible region (color), the infrared, microwave, and Raman spectra, optical activity, isomerism, reactivity, etc. Therefore a definite idea of the symmetry of the complex is needed in investigations of these properties.

In studies of complex compounds it is usually assumed that the spatial configuration of the ligands around the central ion in the first coordination sphere, in absence of external perturbations, corresponds to the maximum symmetry for the given coordination number. For example, if the coordination number is six and the ligands are all the same the complex is taken to be octahedral; with coordination number four it is tetrahedral or square, etc. There would be no objections to these assumptions if the field of the central atom was spherically symmetrical, or at least had a fairly high degree of symmetry. However, owing to the presence of incomplete d (or f) shells the central atom (complex former) does not in general give rise to a sufficiently symmetrical field around itself in interacting with the ligands, so that although the ligands are all the same they may occupy asymmetric positions in relation to this central atom. Therefore in the general case complexes cannot have maximum symmetry.

Deviations from maximum symmetry in complex compounds in the crystalline state may arise also by the influence of the external or the succeeding coordination sphere. In distinction from these distortions of symmetry, we shall describe as internal the asymmetry due to the asymmetry of the ψ electron cloud of the central atom. In free molecules or ions in solution asymmetry can evidently be only of the internal type.

In the literature, internal asymmetry is usually termed the Jahn – Teller effect, named for the authors of the theorem [1] which gives a rigorous quantum-mechanical interpretation of the effect. Hoever, we prefer the term "internal asymmetry," because the Jahn – Teller effect is not restricted to deviations from maximum symmetry [8, 9]. Several theoretical investigations of various aspects of internal asymmetry have been reported [2-6]. Nearly all these investigations are based on the assumption that a six-coordinated complex is a regular octahedron, and involve a search for the amplitude of asymmetric normal vibrations of the octahedron which minimize the energy of the complex as a function of the corresponding normal coordinates. This approach to the problem may give rise to certain objections of principle. A real complex in the equilibrium state is not, in the general case, a regular octahedron and

therefore need not have the normal vibrations of a regular octahedron, so that its energy is not a function of the corresponding normal coordinates. For example, if a real complex is tetragonal, its normal vibrations no longer include triple degenerate vibrations of the $T_1(g, u)$ $T_2(g, u)$ type which, in the case of a regular octahedron, may lead to trigonal distortion.

In other words, the above-mentioned investigations are concerned with the changes a complex would undergo if it was octahedral, and not with the actual symmetry of the complex. In addition, most of the papers cited do not give quantitative characteristics of the internal asymmetry. The first quantitative investigation, that of Van Vleck [2], deals with particular cases in which, as we shall show, asymmetry happens to be less significant than in other cases. The calculation method and the very rough final evaluation of the effect give rise to certain objections. In a recent paper [6] asymmetry was expressed quantitatively as a function of an indefinite parameter.

This paper contains some of the results obtained in an investigation of internal asymmetry in complex compounds of the transition metals; this study is largely free of the above-mentioned defects. The first communication is confined to an approximation of the crystal field theory, ligands being considered as point ions or dipoles, and the central atom being taken as an atom of a transition metal with electron configuration d^n ($n = 1, 2, \ldots, 10$) outside of the completed shells. We also restrict ourselves to cases in which the maximum spin of the central atom is not diminished in the complex (high-spin or ionic complexes), and where the coordination number is six. For such cases we derive a general theory, i.e., a calculation method and fundamental formulas (interaction of electron motion with vibrations is not considered).

In subsequent communications we shall give the results obtained by application of the theory to studies of the physicochemical properties of complexes, results of more general calculations by the molecular-orbital method, and applications of the theory to complexes with fourfold coordination.

Our results can evidently be used for studying not only complex compounds but other similar systems.

Qualitative Results by the Methods of the Group Theory

Internal asymmetry can be characterized qualitatively by the methods of the group theory with the aid of the Jahn – Teller theorem [1].

By this theory, a nonlinear multiatomic configuration can be stable only if its principal electronic term is nondegenerate. If the principal electronic term is degenerate in a particular symmetrical configuration, that configuration cannot be stable. It follows that the real spatial configurations of complexes must be sought for symmetry at which the principal electronic term is not degenerate.

If we know the electron configuration of the central ion and therefore the L degeneration of its electronic term, we can use the methods of the group theory [7] to find the symmetry of the "crystal" ligand field leading to splitting of the electronic term such that the principal electronic term is not degenerate. We disregard spin degeneration as insignificant in the cases under consideration [10].

The table shows the results obtained by this method for different electron configurations of central complex-forming ions. Only the maximum symmetry for coordination numbers six and four is given from all the possible cases.

The table shows that for coordination number six, with d^3, d^8, d^5 and d^{10} electron configurations, the complexes are strictly octahedral without internal asymmetry (it will be remembered that here and subsequently only cases of high spin are considered). Internal asymmetry is obligatory for all other electron configurations.

It is easy to see that these qualitative results are insufficient by themselves for determining the real arrangement of the ligands around the central ion (even with the assumption that the maximum possible symmetry, with the Jahn – Teller theorem taken into account, is achieved), as a given type of symmetry indicated in the table for a particular complex may be achieved in different ways. The true equilibrium positions of the ligands can be found by quantitative calculation.

Calculation Method

It is known that in the adiabatic approximation the equilibrium interatomic distances in molecules are found from the condition of minimum total interaction energy in the system, averaged for electron motion. Consider a complex with the central ion having electron configuration [A] d^n, (where [A] is the configuration of spherically symmetrical closed shells) with N similar ligands; let us find its energy E as a function of the distance $\vec{R}_i$ from the central

ion to the ligands. For this, we write the Hamiltonian of the system in the form

$$H = H_0 + H(d^n), \tag{1}$$

where H_0 is the Hamiltonian of the whole system without the external d electrons of the central ion, and $H(d^n)$ is the Hamiltonian of interaction of the d electrons with each other, with the shell, and with the ligands.

Maximum Possible Symmetry of Complexes with Consideration of the Jahn–Teller Effect

Electron configuration of central ion	Symmetry of complex	
	Coordination number 6	Coordination number 4
d^1, d^6	Tetragonal D_{4h}	Tetragonal D_{4h}
d^2, d^7	Tetragonal D_{4h}	Cubic – tetrahedral T_d
d^3, d^8	Cubic – octahedral O_h	Tetragonal D_{4h}
d^4, d^9	Tetragonal D_{4h}	Tetragonal D_{4h}
d^5, d^{10}	Cubic – octahedral O_h	Cubic – tetrahedral T_d

Suppose that, as usual, the variables for the external and internal electrons of the central atom can be separated. Then in the adiabatic approximation we can represent the energy of the complex as a function of the distances to the ligands [Hamiltonian (1) averaged for electron motion] in the form of a sum of two parts:

$$E(\vec{R}_1, \ldots, \vec{R}_N) = W(\vec{R}_1, \ldots, \vec{R}_N) + \varepsilon^{(n)}(\vec{R}_1, \ldots, \vec{R}_N), \tag{2}$$

where $W(\vec{R}_1, \ldots, \vec{R}_N)$ is the energy of interaction of the ligands with each other and with the shell, and $\varepsilon^{(n)}(\vec{R}_1, \ldots, \vec{R}_N)$ is the energy of interaction of the ligands with the external d electrons.

The equilibrium positions $\vec{R}_{0i}(R_{0i}, \theta_{0i}, \varphi_{0i})$ of the ligands are found from the conditions for the extremal of E for all $\vec{R}_i$:

$$\left(\frac{\partial E}{\partial \vec{R}_i}\right)_{\vec{R}_i = \vec{R}_{0i}} = \left(\frac{\partial W}{\partial \vec{R}_i}\right)_{\vec{R}_i = \vec{R}_{0i}} + \left(\frac{\partial \varepsilon}{\partial \vec{R}_i}\right)_{\vec{R}_i = \vec{R}_{0i}} = 0, \quad i = 1, 2, \ldots N \tag{3}$$

with the appropriate supplementary condition for the second derivatives. It should be noted that in Eqs. (3) only the term $\varepsilon^{(n)}$ can give rise to internal asymmetry, since $W(\vec{R}_1, \ldots, \vec{R}_N)$ is the interaction energy of the shell the field of which is spherically symmetrical, with equal ligands. Therefore under the influence of interaction W alone the complex would have maximum symmetry with the equilibrium positions of the ligands at the points $\vec{R}_{0i}(R_{0i}, \theta_{0i}, \varphi_{0i})$, which satisfy the equations

$$\left(\frac{\partial W}{\partial \vec{R}_i}\right)_{\vec{R}_i = \vec{R}_{0i}} = 0, \quad i = 1, 2, \ldots N, \tag{4}$$

with supplementary conditions for the second derivatives.

Accordingly, Eqs. (3) can be interpreted as follows. Interaction of the ligands with the shell creates conditions for a distribution with maximum symmetry at the points $\vec{R}^{\,\circ}_{0i}$ for the ligands. Under the influence of additional electronic repulsion by the d electrons the ligands deviate from the positions $\vec{R}^{\,\circ}_{0i}$, and this gives rise to the returning force of attraction by the shell, given by the first term in (3). The equilibrium positions $\vec{R}_{0i}$ are therefore the positions of the ligands in which the d electron repulsion forces are balanced by the returning attraction force of the shell. Since different ligands undergo different repulsion by d electrons because of the asymmetric character of the ψ cloud of the latter, the deviations of their actual positions $\vec{R}_{0i}$ from the positions of maximum symmetry $\vec{R}^{\,\circ}_{0i}$ are also unequal. This gives rise to internal asymmetry.

Thus, for quantitative estimation of internal asymmetry we must first find the relationships for the symmetrical part $W(\vec{R}_1, \ldots, \vec{R}_N)$ of the interaction of the central ion with the ligands, and for the unsymmetrical part $\varepsilon^{(n)}(\vec{R}_1, \ldots, \vec{R}_N)$ of this interaction. Quantum-mechanical calculation of the part W involves considerable mathematical difficulties. However, it can be represented by parameters which can be calculated approximately or measured independently. Taking (1) into account, we have:

$$W = \frac{1}{2}\sum_{i,j} k'_{ij}(R_i - R'_{oi})(R_j - R'_{oj}) +$$

$$+ \frac{1}{2}\sum'_{i,j,pq} k'_{ijpq}(\vec{R}_i - \vec{R}'_{oi})_p (\vec{R}_j - \vec{R}_{oj})_q + \text{const}, \quad p, q = R, \theta, \varphi. \tag{5}$$

Here k'_{ij} are the force constants for the interaction of the shell with the ligands, corresponding to changes of distances R_i only, and k'_{ijpq} are the remaining force constants. The first sum in (5) represents the terms with $p = q = R$, lacking in the second sum.

The unsymmetrical part of the energy of interaction of the central ion with the ligands, $\epsilon^{(n)}(\vec{R}_1, \ldots, \vec{R}_N)$, can be calculated in our approximation for all possible configurations $d^n (n = 1, 2, \ldots, 10)$ of the central ion. It can be shown that for this it is sufficient to determine $\epsilon^{(n)}$ for only two configurations: $n = 1$ and $n = 2$.

We rewrite the Hamiltonian (1) in the form

$$H = H_0 + H(d^n) + H(d^{10-n}) - H(d^{10-n}) = H_0 + H(d^{10}) - H(d^{10-n}).$$

But $H(d^{10})$ is the Hamiltonian of the closed d shell, which is also spherically symmetrical. Therefore

$$H = H_0 + H(d^n) = H'_0 - H(d^{10-n}), \tag{6}$$

where $H'_0 = H_0 + H(d^{10})$ is the Hamiltonian of the interaction of the spherically symmetrical body of complete shells (including the d^{10}) shells with the ligands. With the aid of (6), we can replace Eq. (2) by

$$E(\vec{R}_1, \ldots, \vec{R}_N) = W'(\vec{R}_1, \ldots, \vec{R}_N) - \epsilon^{10-n}(\vec{R}_1, \ldots, \vec{R}_N). \tag{7}$$

Here W' differs from W by the addition of the energy of interaction of the d^{10} shell with the ligands. Thus, we can already reduce the number of d electron configurations in calculation of $\epsilon^{(n)}$ from ten to five. We now take into account that in cases of high spin, such as we are considering, all the electrons occupy nonequivalent distances if possible. Hence, analogously to Eq. (7), we have:

$$E = (\vec{R}_1, \ldots, \vec{R}_N) = W'(\vec{R}_1, \ldots, \vec{R}_N) - \epsilon^{(5-n)}(\vec{R}_1, \ldots, \vec{R}_N). \tag{8}$$

Thus, for the d^3 configuration we can take the asymmetric part of the interaction $-\epsilon^{(5-3)} = -\epsilon^{(2)}$ and further

for	d^1	– interaction –	$\epsilon^{(1)}$
"	d^2	"	$\epsilon^{(2)}$
"	d^3	"	$\epsilon^{(3)}$
"	d^4	"	$\epsilon^{(2)}$
"	d^5	"	$-\epsilon^{(2)}$
"	d^6	"	$-\epsilon^{(1)}$
"	d^{10}	"	$\epsilon^{(0)}$

Calculation of the Asymmetric Part of the Energy of Interaction with the Ligands

Let us calculate the energies of interaction of one and two d electrons with the ligands ($\epsilon^{(1)}$ and $\epsilon^{(2)}$), which express the asymmetric part of the energy of interaction with the ligands ϵ^n. In accordance with our approximation of the crystal field theory we consider that the energy of interaction of d electrons with the ligands is a small perturbation in comparison with intraatomic interactions in the central ion:

$$V = \sum_{i=1}^{N} \frac{q_i}{|\vec{r} - \vec{R}_i|}, \tag{9}$$

where q_i is the effective charge of the i-th ion. For configuration d^1 the fivefold degenerate D state may be approximately represented by five hydrogen-like d functions with effective nuclear charge:

$$\psi_m(r, \theta, \varphi) = f(r) \cdot Y_2^m(\theta, \varphi), \quad m = 2, 1, 0, -1, -2. \tag{10}$$

Here $f(r)$ is the corresponding radial part of the hydrogen-like d function, including the energy parameter α_1 and $Y_2^m(\theta, \varphi)$ is the spherical function.

Expanding V into a series by spherical functions and using the addition theorem for spherical functions, we can obtain the following expressions for the matrix elements of the perturbation (9):

$$V_{mm'} = \sum_{i=1}^{N} q_i \{A_{mm'} F_4(R_i) Y_4^{m-m'}(\theta_i, \varphi_i) + \\ + B_{mm'} F_2(R_i) Y_2^{m-m'}(\theta_i, \varphi_i) + D_{mm'} F_0(R_i) Y_0^{m-m'}(\theta_i, \varphi_i)\}, \tag{11}$$

where

$$F_n(R) = \frac{1}{R^{n+1}} \int_0^R r^n f^2(r) r^2 dr + R^n \int_R^\infty \frac{1}{r^{n+1}} f^2(r) r^2 dr,$$

$$A_{mm'} = (-1)^{m'} \frac{5}{27} \sqrt{4\pi} C^{224}_{-m'm} C^{224}_{00}, \quad B_{mm'} = (-1)^{m'} \sqrt{\frac{4\pi}{5}} C^{222}_{-m'm} C^{222}_{00}. \tag{12}$$

$$D_{mm'} = (-1)^{m'} 5 \sqrt{4\pi} C^{220}_{-m'm} C^{220}_{00},$$

and $C^{abc}_{\alpha\beta}$ are the Clebsh – Gordan coefficients [11].

To calculate $\epsilon^{(1)}$ we derive, in accordance with the perturbation theory, a secular equation which in this case is an algebraical equation of the fifth order:

$$|V_{mm'} - \delta_{mm'} \varepsilon^{(1)}| = 0, \quad m, m' = 2, 1, 0, -1, -2. \tag{13}$$

It is hardly possible to solve this equation in the general form. We shall use the qualitative results obtained by the methods of the group theory. It is seen in the table that for configurations d^1, d^4, d^6, d^9, for which $\epsilon^{(1)}$ is asymmetric part of the energy of interaction with the ligands, the symmetry of a complex with N = 6 cannot be higher than tetragonal. Henceforth we shall take this symmetry as the starting basis. For this symmetry many of the matrix elements in (13) are zero, and it is easy to obtain the following expressions for the five roots of the secular equation (the symmetry types of the corresponding electron levels are given in parentheses):

$$\begin{gathered} \varepsilon_1^{(1)}(B_{1g}) = \frac{1}{2}(V_{00} + V_{22} + V_{2-2} + \sqrt{(V_{00} - V_{22} - V_{2-2})^2 + 8V_{20}^2}) \\ \varepsilon_2^{(1)}(A_{1g}) = \frac{1}{2}(V_{00} + V_{22} + V_{2-2} - \sqrt{(V_{00} - V_{22} - V_{2-2})^2 + 8V_{20}^2}) \\ \varepsilon_3^{(1)}(B_{2g}) = V_{22} - V_{2-2} \\ \varepsilon_{4,5}^{(1)}(E_g) = V_{11}. \end{gathered} \tag{14}$$

Thus, the fivefold degenerate electronic term D is split into four levels, one of which (E_g) remains doubly degenerate, in the tetragonal ligand field.

For configuration d^2 the principal term of the free ion ^3F is sevenfold degenerate. In this case the seven wave functions by which this state can be represented are made up in the form of linear combinations of paired antisymmetric products of the $\underline{d}$ functions (10). The corresponding matrix elements of the perturbation (9) entering the seventh-order secular equation are expressed linearly through the matrix elements (11). Taking the tetragonal symmetry as the basis in this case too, we can obtain:

$$\begin{gathered} \varepsilon_1^{(2)}(B_{1g}) = \frac{8}{5} V_{11} + \frac{2}{5} V'_{22} \\ \varepsilon_2^{(2)}(B_{2g}) = V_{00} + V_{22} - V_{2-2} \\ \varepsilon_3^{(2)}(A_{1g}) = V_{00} + V'_{22} + V_{2-2} \\ \varepsilon_{4,5}^{(2)}(E_g) = V_{11} + \frac{4}{5} V_{22} + \frac{1}{5} V_{00} + \sqrt{\frac{1}{25}(V_{22} - V_{00})^2 + \frac{3}{5} V_{2-2}^2} \\ \varepsilon_{6,7}^{(2)}(E_g) = V_{11} + \frac{4}{5} V_{22} + \frac{1}{5} V_{00} - \sqrt{\frac{1}{25}(V_{22} - V_{00})^2 + \frac{3}{5} V_{2-2}^2}. \end{gathered}$$

The sevenfold degenerate term ^5F is split into five, of which two levels remain double degenerate, in the tetragonal ligand field.

Quantitative Characterization of Internal Asymmetry

We can obtain an approximate quantitative characterization of internal asymmetry, in accordance with the calculation method adopted, from the system of equations (3) with substitution of expressions derived from Eqs. (5), (14), and (15) for W and $\epsilon^{(n)}$.

Let us consider six-coordinated complexes with similar ligands. Under the influence of only the symmetrical part W of the interaction such complexes must be strictly octahedral with the ligands situated at the points $\bar{R}_{0i}$ (R_{0i}°, θ_{0i}°, φ_{0i}°) (the numbering corresponds to the ligand positions 1–4, 2–5, and 3–6 at the ends of the "diagonals" of the octahedron):

$$\begin{gathered} R_{0i}^{\circ} = R_0^{\circ},\ i = 1, 2, \ldots, 6, \\ \theta_{01}^{\circ} = 0,\quad \theta_{03}^{\circ} = \theta_{05}^{\circ} = \theta_{06}^{\circ} = \pi/2,\quad \theta_{04}^{\circ} = \pi \\ \varphi_{02} = 0,\quad \varphi_{03} = \pi/2,\quad \varphi_{05} = \pi,\quad \varphi_{06} = 3\pi/2. \end{gathered} \tag{16}$$

These points satisfy Eqs. (4). The points $\vec{R}_{0i}$ (R_{0i}, θ_{0i}, φ_{0i}) of the true equilibrium positions of the ligands should satisfy Eqs. (3). In all cases the corresponding conditions must also be satisfied for the second derivatives. To simplify the mathematical problem we shall assume that the complexes under consideration exist in the stable state and that the distances R_{0i} do not exceed reasonable limits. It is easy to see that these assumptions do not restrict the general nature of our results. A more significant assumption, used below, is that in the original tetragonal symmetry (the highest possible, according to a qualitative investigation by the methods of the group theory) interaction between different levels can be neglected. With these assumptions the following results can be obtained.

Configurations d^1 and d^9. In this case $\epsilon^{(n)} = \epsilon^{(1)}$. It is easy to show that of the four values of (14) for $\epsilon^{(1)}$ the minimum is either $\epsilon_3^{(1)}$ (E_2g) or $\epsilon_{4,5}^{(1)}$ (E_g), in accordance with the ratio between the coordinates of the ligands. Let us test each for the minimum. With random deviation of the ligands from the tetragonal arrangement the doubly degenerate $\epsilon_{4,5}^{(2)}$ (E_g) level is split into two: $\epsilon_4^{(1)} = V_{11} + V_{1-1}$ and $\epsilon_5^{(1)} = V_{11} - V_{1-1}$. Substitution of each of the three values $\epsilon_3^{(1)}$, $\epsilon_4^{(1)}$ and $\epsilon_5^{(1)}$ into (3), with $V_{mm'}$ in accordance with (11) taken into account, gives 18 equations for the 18 coordinates of the six ligands. These equations, first yield the following result (in all three cases):

$$\begin{gathered} \theta_{01} = 0,\quad \theta_{02} = \theta_{03} = \theta_{05} = \theta_{06} = \pi/2,\quad \theta_{04} = \pi \\ \varphi_{02} = 0,\quad \varphi_{03} = \pi/2,\quad \varphi_{05} = \pi,\quad \varphi_{06} = 3\pi/2. \end{gathered} \tag{17}$$

Thus, the six ligands in the equilibrium position remain on three mutually perpendicular axes around the central atom. This was to be expected in view of the symmetry of the repelling ψ cloud of the d electrons.

For determination of the six equilibrium distances R_{0i} there remain six equations

$$\sum_{j=1}^{6} k_{ij}^{\circ}(R_{0j} - R_0^{\circ}) + \left(\frac{\partial \epsilon^{(1)}}{\partial R_i}\right)_{R_i = R_{0i}} = 0,\quad i = 1, 2, \ldots, 6. \tag{18}$$

Taking the derivatives $\partial \epsilon_3^{(1)}/\partial R_i$ and substituting into this system we have

$$R_{01} = R_{04},\ R_{02} = R_{03} = R_{05} = R_{06},\ R_{01} < R_{02}. \tag{19}$$

i.e., the equilibrium positions of the ligands correspond to an octahedron in which the 1 – 4 diagonal is shorter than the 2 – 5 and 3 – 6 diagonals (a shortened octahedron). Here $\epsilon_4^{(1)}$ and $\epsilon_5^{(1)}$ form a doubly degenerate term $\epsilon_{4,5}^{(1)}$, lying above $\epsilon_3^{(1)}$. The splitting $\Delta E = \epsilon_{4,5}^{(1)} - \epsilon_3^{(1)}$ is:

$$\Delta E = \frac{2q}{21}\left([9F_2(R_{01}) - 5F_4(R_{01})] - [9F_2(R_{02}) - 5F_4(R_{02})]\right) \tag{20}$$

If we start from the $\epsilon_4^{(1)}$ level and solve the system (18) for it, we have:

$$R_{01} = R_{04} = R_{03} = R_{06},\ R_{05} = R_{08},\ R_{02} > R_{05},$$

which is also a shortened octahedron, but in contrast to the preceding case, the 2 – 5 diagonal is the shortened one. Here the levels $\epsilon_3^{(1)}$ and $\epsilon_3^{(2)}$ form the doubly degenerate term $\epsilon_{3,3}^{(1)}$ with splitting $\Delta E = \epsilon_{3,b}^{(1)} - \epsilon_3^{(1)}$ equal to that given by (20). Similarly, for the $\epsilon_3^{(1)}$ level we obtain an octahedron with a shortened 3–6 diagonal.

Thus, in the case of d^1 and d^9 electron configurations the equilibrium positions of six similar ligands correspond to a distorted octahedron in which any one diagonal may be shorter than the other two.

We now introduce a quantitative measure for asymmetry, $\xi = 2(R_{03} - R_{01})$, equal to the difference between the lengths of two unequal diagonals. In finding ξ we confine ourselves to cases when it is fairly small in comparison with the length of the diagonal, so that $\epsilon_3^{(1)}$ can be expanded into a power series of ξ, and take only terms as far as the second power of ξ. It may be noted further that the true force constants of the complex k_{ij} can be easily expressed in terms of the constants k'_{ij} with the aid of Eq. (2):

$$k_{ij} = \left(\frac{\partial^2 E}{\partial R_i \partial R_j}\right)_{R_{0i}} = k'_{ij} + \left(\frac{\partial \epsilon^{(n)}}{\partial R_i \partial R_j}\right)_{R_{0i}} \tag{21}$$

Expanding $\epsilon_3^{(1)}$ as powers of ξ, eliminating the unknown parameter R_0^* from the two Eqs. (18), and taking (21) into account, we have

$$\xi = -\frac{2q}{21 K_1'}[9F_2'(R_{02}) - 5F_4'(R_{02})]. \tag{22}$$

Here $K_1 = k_{11} - 2k_{12} + k_{16}$, where k_{11}, k_{12} and k_{16} are the force constants for a ligand on the short diagonal. They differ from the corresponding constants for a ligand on the long diagonal, but the difference is small: the difference $K_1 - K_2$ is smaller by a factor of 10 than the difference $R_{02} - R_{01}$. The values $F'_n(R)$ represent derivatives of the expression $F_n(R)$, given by Eq. (12).

If the ligands can be regarded as point dipoles, we can perform the calculations first for a system of negative point charges, and then for a system of positive point charges at distances ΔR from the negative ones; then, if ΔR is small, we have

$$\xi = \frac{2\mu}{21 K_1}[9F_2''(R_{02}) - 5F_4''(R_{02})]. \tag{23}$$

where μ is the dipole moment of the ligand. In our approximation the additional splitting of levels ΔE due to internal asymmetry is represented by the equation

$$\Delta E = \frac{1}{2} K_1 \xi^2. \tag{24}$$

Configurations d^9 and d^3. Here $\epsilon^{(n)} = -\epsilon^{(1)}$. The negative sign of $\epsilon^{(1)}$ reverses the sequence of the splitting levels in the tetragonal field, so that in this case the lowest levels are $-\epsilon_1^{(1)}$ and $-\epsilon_2^{(1)}$. These levels are tested for minimum essentially in the same way as before, with a small additional complication in the calculation; it is found that in the equilibrium position the ligands lie on three mutually perpendicular axes with angular coordinates corresponding to (17). From the equations for the equilibrium distances we have:

$$\begin{gathered} R_{01} = R_{04},\quad R_{02} = R_{05} = R_{03} = R_{06}, \\ R_{01} > R_{02} \quad \text{or} \quad R_{01} < R_{02}. \end{gathered} \tag{25}$$

Here, if $R_{01} > R_{02}$, then the minimum level is $-\epsilon_1^{(1)}$, and at $R_{02} > R_{01}$ the minimum energy corresponds to $-\epsilon_2^{(1)}$. Thus, in this case we have an equilibrium configuration with the ligands at the vertices of an octahedron with one diagonal either shorter or longer than the other two (a shortened and an elongated octahedron respectively). Here, as in the previous instance, it is quite immaterial which of the diagonals differs from the other two.

We again introduce a quantitative measure of asymmetry in the form of the difference between the lengths of two diagonals, $\xi = 2|R_{01} - R_{02}|$. Then, by the method described just previously, we easily find

$$\xi = -\frac{q}{14K_1}[12F_3'(R_{02}) + 5F_6'(R_{02})] \tag{26}$$

for ligands which are ions of effective charge q, and

$$\xi = \frac{\mu}{14K_1}[12F_3'(R_{02}) + 5F_6'(R_{02})] \tag{27}$$

for ligands which are point dipoles of moment μ. Accordingly, for the additional splitting of levels $\Delta E = |\epsilon_8^{(2)} - \epsilon_1^{(2)}|$ due to internal asymmetry we have

$$\Delta E = \frac{2}{3}K_1\xi^2. \tag{28}$$

Configurations d^3 and d^7. In this case $\epsilon^{(n)} = \epsilon^{(2)}$. The electronic term in the free central ion is sevenfold degenerate. In a cubic field this term is split into three: T_{1g} (triply degenerate), T_{2g} (triply degenerate), and A_{2g} (nondegenerate). The lowest of these, T_{1g}, undergoes further splitting in a tetragonal field into E_g (doubly degenerate) and B_{1g} (nondegenerate). They correspond, according to Eqs. (15), to energies $\epsilon_1^{(2)}$ (B_{1g}) and $\epsilon_{6,7}^{(2)}$ (E_g), which must be tested for minimum.

In random deviation of the ligands from the positions of tetragonal symmetry the level $\epsilon_{6,7}^{(2)}$ (E_g) is split into two with the energies

$$\epsilon_6^{(2)} = V_{11} + \frac{4}{5}V_{22} + \frac{1}{5}V_{00} + \frac{1}{5}V_{1-1} - \frac{\sqrt{6}}{5}V_{20} -$$

$$-\frac{1}{5}\left[(V_{22} - V_{00} - V_{1-1} + \sqrt{6}V_{20})^2 + 15\left(V_{2-2} + V_{1-1} - \sqrt{\frac{2}{3}}V_{20}\right)^2\right]^{\frac{1}{2}},$$

$$\epsilon_7^{(2)} = V_{11} + \frac{4}{5}V_{22} + \frac{1}{5}V_{00} - \frac{1}{5}V_{1-1} + \frac{\sqrt{6}}{5}V_{20} -$$

$$-\frac{1}{5}\left[(V_{22} - V_{00} - V_{1-1} - \sqrt{6}V_{20})^2 + 15\left(-V_{2-2} + V_{1-1} - \sqrt{\frac{2}{3}}V_{20}\right)^2\right]^{\frac{1}{2}}$$

Any one of the three levels $\epsilon_1^{(2)}$, $\epsilon_6^{(2)}$ and $\epsilon_7^{(2)}$ may be the minimum, dependent on the ratio of the ligand coordinates. If we assume that $\epsilon_1^{(2)}$ is the minimum, substitution of the expression for it into Eq. (3) gives the following equilibrium coordinates for the ligands:

$$\theta_{01} = \theta_{01}^0, \quad \varphi_{01} = \varphi_{01}^0,$$
$$R_{01} = R_{04}, \quad R_{02} = R_{05} = R_{03} = R_{06}, \quad R_{01} > R_{02}, \tag{30}$$

i.e., the equilibrium configuration of the ligands corresponds to positions at the vertices of an octahedron with the 1 – 4 diagonal longer than the 2 – 5 and 3 – 6 diagonals (elongated octahedron).

If we assume that $\epsilon_6^{(2)}$ or $\epsilon_7^{(2)}$ are minimal, we obtain an analogous result, with the difference that with minimal $\epsilon_6^{(2)}$ the 2 – 5 diagonal is the longer, and with minimal $\epsilon_7^{(2)}$ it is the 3 – 6 diagonal. If $\epsilon_1^{(2)}$ is minimal, $\epsilon_6^{(2)} = \epsilon_7^{(2)}$ form a double degenerate term E_g, and if $\epsilon_6^{(2)}$ is minimal, this term is formed by $\epsilon_1^{(2)} = \epsilon_7^{(2)}$, and finally, with minimal $\epsilon_7^{(2)}$ the doubly degenerate term is formed by the coinciding levels $\epsilon_1^{(2)}$ and $\epsilon_6^{(2)}$.

For $\xi = 2(R_{01} - R_{02})$, as previously, we find

$$\xi = -\frac{q}{70 R_0^7}\left[24 F_2^*(R_{01}) - 25 F_4^*(R_{01})\right] \tag{31}$$

for ligands of charge q, and

$$\xi = \frac{\mu}{70 R_0^7}\left[24 F_2^*(R_{01}) - 25 F_4^*(R_{01})\right] \tag{32}$$

for point-dipole ligands of moment μ.

The additional splitting $\Delta E = \epsilon_{\delta_1}^{(2)} - \epsilon_{\delta_2}^{(2)}$ of the term T_{1g} due to internal asymmetry may be found from the formula

$$\Delta E = \frac{1}{2} K_1 \xi^2. \tag{33}$$

Configurations d^3 and d^8. For these cases $\epsilon^{(n)} = -\epsilon^{(2)}$ and the term $-\epsilon_2^{(2)}$ (A_{2g}) is the lowest in a tetragonal field. Substitution of the expression for this term from (15) into Eq. (3) gives a regular octahedron for the equilibrium configuration of the ligands. Thus, in this case there is no internal asymmetry.

Configurations d^5 and d^{10}. In this case $\epsilon^{(n)} = \epsilon^{(3)} = 0$; the asymmetric part of the interaction with the ligands is absent and the complexes are again highly symmetrical without internal asymmetry.

SUMMARY

The equilibrium spatial configuration of ligands around a central ion in six-coordinated high-spin (ionic) complexes with electron configurations d^n ($n = 1, 2, \ldots, 10$) in the approximation of the crystal field theory has been determined theoretically. Formulas have been derived for all cases whereby it is possible to determine the deviations of the ligand positions from a regular octahedron (internal asymmetry), and formulas for additional splitting of electronic terms due to internal asymmetry. The results of applications of the theory to investigations of the physicochemical properties of complexes will be given in future communications.

I am deeply grateful to Professor A. V. Ablov for discussions and valuable comments.

LITERATURE CITED

1. H. A. Jahn and E. Teller. Proc. Roy. Soc. A161, 220 (1937).
2. J. H. Van Vleck. J. Chem. Phys. 7, 72 (1939).
3. U. Öpik and M. H. L. Pryce. Proc. Roy. Soc. A238, 425 (1957).
4. H. C. Longuet-Higgins, U. Öpik, M. H. L. Pryce and R. A. Sack. Proc. Roy. Soc. A244, 1 (1958).
5. W. L. Clinton and B. Rice. J. Chem. Phys. 30, 542 (1959).
6. A. D. Liehr and C. J. Ballhausen. Ann. Phys. (USA) 3, 304 (1958).
7. H. Bethe. Ann. Phys. 3, 133 (1929).
8. W. Moffitt and A. D. Liehr. Phys. Rev. 106, 1195 (1357).
9. W. Moffitt and W. Thorson. Phys. Rev. 108, 1251 (1957).
10. H. A. Jahn. Proc. Roy. Soc. A164, 117 (1938).
11. A. Simon. ORNL – 1718 (1954). (Russian translation in the book: Deformation of Atomic Nuclei. Izd. inostr. lit., Moscow, 1958).

COVALENT REFRACTIONS OF METALS

S. S. Batsanov

Institute of Inorganic Chemistry, Siberian Division, Academy of Sciences, USSR
Translated from Zhurnal Strukturnoi Khimii, Vol. 2, No. 3, pp. 361-366, May-June, 1961
Original article submitted March 25, 1960

Values of the refractions of metals calculated from their atomic volumes and from the molecular refractions of organometallic compounds were compared and found to be close. However, if "volume" refractions of metals are used in calculations, they must be recalculated for the coordination numbers which are typical for most of their chemical compounds. Metal refractions can also be calculated from covalent radii of the metals because of the proportionality of atomic volumes and refractions. The average deviation between the results of the two calculation methods is 15%, so that it is possible to compile a system of average values for the refractions of metal atoms. These calculation methods, like calculations based on the additivity principle for molecular compounds, characterize atoms in covalent or similar bonds. These refraction increments can therefore be termed the covalent refractions of metals, in distinction from the atomic refractions found by quantum-mechanical calculations for free atoms.

The various refractometric methods of structural chemistry are based on comparisons of experimental results with theoretically calculated molecular refractions. Therefore refinement of the calculation methods at once extends the range of applications of structural refractometry.

In the field of molecular refraction, the problem of metal refraction has been studied least, and the purpose of the present paper is to fill this gap.

1. Direct measurements of the refractions of metals in the gaseous state are known only for elements of the 2b subgroup (Table 1), although even these data are not sufficiently reliable, because the influence of anomalous dispersion is not excluded in such measurements and, moreover, temperature corrections for conversion to standard conditions are needed. The refractions of metallic atoms can also be found from the molecular refractions of organometallic compounds, on the additivity principle. The relevant data are also meager; they are all presented in Table 1. The average values are given, and the standard deviation is as a rule ± 0.5 cm^3. Finally, quantum-mechanical calculations of the electronic polarizabilities of atoms generally give values for isolated atoms and are therefore unsuitable for chemical refractometry.

In 1956 we proposed a method for determination of the atomic refractions of metals from their specific gravities [1, 2]. On certain crystallochemical grounds and in view of the extremely high refractive indices of metals we assumed that $R_{met} = A/d$.

Certain of our values for atomic refraction are given in Table 1 for comparison.

The agreement between the refractometric constants determined experimentally and derived by the "volume" method is quite satisfactory. However, a possible objection to our method for determining the refractions of metal atoms is that our constants are valid only for the purely metallic state and that their applicability in calculations of molecular refractions requires special verification.

In general, the zone theory of metals indicates that there is great similarity between metallic and covalent bonds; the main difference apparently lies in the different coordination numbers of metallic and covalent structures.

This is confirmed by Pauling [16, 17], who showed that with a correction for coordination number the metallic radii of elements can be converted to their covalent radii, which coincide with those calculated from the corresponding molecular compounds.

TABLE 1. Refractions of Metals

Metal	R_{D}	R^{∞}_{incr}	Lit.	R^{∞}_{gas}	Lit.	Metal	R_{D}	R^{∞}_{incr}	Lit.
Be	4,8	3,0	[3]			Ga	11,6	8,0	[10]
Mg	13,8	5,0	[3, 4]			In	15,3	11,5	[10]
Zn	8,0	8,9	[5]	12,1	[15]	Tl	16,9	14,0	[10]
Cd	12,7	12,2	[6]	17,5	[15]	Ti	10,7	14,1*	[11]
Hg	13,8	11,8	[7]	13,0	[15]	Sn	16,0	13,7	[12]
Cu	7,0$_3$	8,0	[8]			Pb	17,9	17,0	[12]
Ni	6,5$_8$	8,0	[8]			Sb	18,1	17,7	[13]
Al	9,9	7,5	[9]			U	12,5	11,8*	[14]

*For b = D.

TABLE 2. Coordination Numbers in Metallic Structures and Compounds

Period	Group 2a	3a	4a	5a	6a	7a	8a			1b	2b	3b	4b	5b
II	Be 12 4													
III	Mg 12 6											Al 12 4,6		
IV	Ca 12 8	Sc 12 6	Ti 12 4,6	V 8 6	Cr 12 6	Mn 12 6	Fe 8 6	Co 12 6	Ni 12 6	Cu 12 4	Zn 6 4	Ga 7 8		
V	Sr 12 8	Y 12 9	Zr 12 6	Nb 8 6	Mo 8 6	Tc 12 6	Ru 12 6	Rh 12 6	Pd 12 6	Ag 12 6	Cd 6 6	In 12 6	Sn 4 4	Sb 3 6
VI	Ba 8 8	La 12 9	Hf 12 8	Ta 8 6	W 8 6	Re 12 6	Os 12 6	Ir 12 6	Pt 12 6	Au 12 6	Hg 6 4	Tl 12 6	Pt 12 4,8	Bi 3 6
Lanthanides	Ce 12 8	Pr 12 8	Nd 12 8	Pm — —	Sm 12 8	Eu 8 8	Gd 12 8	Tb 12 8	Dy 12 8	Ho 12 8	Er 12 8	Tu 12 8	Yb 12 8	Lu 12 8
Actinides	Th 12 8	Pa 10 8	U 12 8	Np 12 8	Pu — 8	Am — 8								

Further, Gordy and Thomas [18] found that the energy characteristics (electronegativities) of atoms calculated from the work functions for the free metals are also in good agreement with the electronegativities of the respective elements calculated from thermochemical data for molecular compounds.

Finally, Agafonov [19] in 1959 established a direct relationship between electronegativities (X) and refractions (R) of atoms, in the form $X = a - bn \log R/c$, where a, b, and c are constants and n is the number of valence electrons. It was found that our values for the refraction of metal atoms lie on the same straight line as the atomic refractions of nonmetals. Since the latter were determined by direct experiment, there is no doubt about the validity of "metallic" refractions.

It follows from all the foregoing that metal refractions determined by the additivity rule or by the volume method (see Table 1) characterize the corresponding atoms in covalent or similar bonds. It is therefore convenient to call them covalent refractions, by analogy with, say, covalent radii, and to restrict the concept of "atomic refraction" to the constant for the free atom.

2. Since the difference between atomic and covalent radii is determined entirely by the difference between the coordination numbers (CN), it is reasonable to apply the corresponding corrections also to the atomic refractions of all metals with the exception of the elements of subgroup Ia, and also of Ba, Cd, Eu and Sn, which have the same coordination numbers in the majority of their compounds as in metallic structures.

Table 2 shows values of CN characteristic of the pure metals (top lines) and most chemical compounds (bottom lines). In the case of gold and platinum compounds the latter values differ from the experimental CN = 4. However, in such cases the coordination polyhedron is a square, which is equivalent to an octahedron in the crystallochemical sense (see [20]), and therefore CN = 6 is taken for Au and Pt in Table 2.

The atomic volumes of metals were recalculated for different CN as follows. Subtraction of the actual volume of the atom for CN corresponding to a metallic structure from the atomic volume of the metal gives the volume V_0 of the voids free from atoms. It is also known [21] that in crystalline structures V_0 decreases with increasing CN:

CN	12	10	8	6	4
V_0	26%	30%	32%	48%	66%

Using these values, we can easily calculate the change of free volume with change of CN. Addition of the actual atomic volume to V_0 for the new coordination number gives the total atomic volume (refraction) of the metal for the CN characteristic of most of its chemical compounds.

TABLE 3. Refractions of Metals, Equal to Their Atomic Volumes

Metal	R	Metal	R	Metal	R	Metal	R
Cu	8,1	Pr	21,1	U	12,7	Mo	10,5
Ag	11,4	Nd	21,0	Np	11,8	W	10,6
Au	11,4	Sm	22,1	Al	11,4(4) 11,2(6)	Mn	8,15
Be	5,4	Gd	20,1	Ga	12,5	Tc	9,4
Mg	15,55	Tb	19,5	In	17,2	Re	10,0
Ca	25,9	Dy	19,3	Tl	19,6	Fe	7,9
Sr	33,6	Ho	19,2	Ti	12,6(4) 12,2(6)	Co	7,5
Zn	8,6	Er	18,5	Zr	15,7	Ni	7,5
Hg	13,45	Tm	18,4	Hf	15,0	Ru	9,1
		Yb	25,1	Pb	20,35(4) 20,05(6)	Rh	9,3
Sc	17,0						
Y	20,8	Lu	18,2	V	9,1	Pd	10,0
La	22,7	Th	20,1	Nb	12,2	Os	9,55
Ce	21,0	Pa	14,7	Ta	12,1	Ir	9,7
				Cr	8,3	Pt	10,2

Table 3 contains the final results of our calculations; values of R at CN = 4 and 6 are given for Al, Tl, and Pb.

Apart from the elements mentioned earlier, Sb and Bi are also omitted from this table; these have lower CN in the metallic state than in chemical compounds, so that no corrections are required for these metals either.

3. There are other possible approaches to the determination of covalent refractions of metals from their geometrical characteristics.

In 1956 Atoji [22] found that the ratio of the refraction to the cube of the covalent radius is constant for the halogens. He used this relationship for finding the electronic polarizability of the mercury atom from its covalent radius. He also noted that this relationship between R and r^3 holds for other elements. Table 4 illustrates the $R - r^3$ relationship for some of the most reliably studied elements of groups IV – VII of the periodic system. The covalent

refractions are taken from the paper [2] cited above, and the radii are taken from the last reference given in our paper [23] (see also [24]).

Table 4 shows that the values of the coefficient k for elements of the second period are grouped around 4.8, while the average value of k for the other elements is 6.0. We used these coefficients and the covalent radii [23] for calculating the refractions of all metals.

TABLE 4. Relationship Between Refraction and Covalent Radius

Element	R_∞	r^3_{cov}	$k=R/r^3$	Element	R_∞	r^3_{cov}	$k=R/r^3$
F	1,6	0,3732	4,29	N	2,20	0,4052	5,43
Cl	5,71	1,000	5,71	P	8,6	1,331	6,46
Br	8,09	1,482	5,46	As	10,3	1,816	5,67
I	14,08	2,353	5,98	Sb	18,1	2,803	6,46
O	1,99	0,4052	4,91	C	2,08	0,4565	4,56
S	7,6	1,125	6,75	Si	9,06	1,602	5,65
Se	10,8	1,602	6,74	Ge	11,08	1,816	6,10
Te	14,4	2,571	5,66	Sn	16,08	2,744	5,86
				Pb	17,9	3,375	5,30

TABLE 5. Refractions of Metals R, Equal to kr^3

Metal	R	Metal	R	Metal	R	Metal	R
Li	11,0	Hg	18,3	Lu	22,3	Ta	13,8
Na	23,7	Sc	17,9	Ac	34,4	Bi	19,8
K	49,4			Th	23,4	Cr	10,1
Pb	59,6	Y	25,0	Pa	17,5	Mo	13,8
Cs	75,9	La	28,4	U	21,5(4+)	W	13,2
Fr	80,3	Ce	25,5		14,8(6+)		
Cu	11,7	Pr	25,5	Np	11,4	Mn	10,1
Ag	17,2	Nd	25,5	Pu	20,2	Tc	10,4
Au	17,5	Pm	28,0	Am	19,8	Re	11,7
		Sm	26,5	Al	12,0	Fe	10,4
Be	4,2	Eu	36,2	Ga	11,7	Co	9,85
Mg	15,8	Gd	24,6	In	18,7	Ni	9,6
Ca	31,6	Tb	24,1	Tl	20,2	Ru	12,0
Sr	41,8	Dy	23,7	Ti	13,8	Rh	12,3
Ba	45,9	Ho	23,2	Zr	18,3	Pd	13,2
Ra	53,2	Er	22,8	Hf	17,9	Os	12,3
Zn	12,3	Tu	22,3	V	10,6	Ir	12,6
Cd	17,5	Yb	29,5	Nb	13,8	Pt	13,2

The discrepancies between the data in Tables 3 and 5 are due, on the one hand, to the approximate character of the equation $R/r^3 = k$ and to errors in determination of certain covalent radii, and on the other, to partial ionization of metals in their structures; if this is ignored, low values are obtained for the atomic volumes of elements at low CN.

However, in view of the fact that the average variation in our determinations of refraction is only 15% (this is only a fraction of, or even an order of magnitude below, the standard deviations in parallel calculations of electronic polarizabilities of metals by different quantum-mechanical methods [25, 26]), we consider that it is permissible to represent the refractions of metal atoms as the arithmetic averages of the values found by different methods. In certain instances (W, Fe, etc.) we had to modify the calculation somewhat in order to retain the consecutive variations of atomic refractions of the elements in the periodic table.

The final system of the covalent refractions of metals is given in Table 6. Comparison of these values with the refraction increments obtained from data on organometallic compounds (Table 1) shows that the latter values are somewhat lower than our constants. This lowering does not make the system inferior to the original one, because it

is due to the polar character of the Me – C bonds in the corresponding organic compounds and the consequent lowering of the atomic refractions of the metals.

TABLE 6. Covalent Refractions of Metals

Period	Group														
	1a	2a	3a	4a	5a	6a	7a	8a			1b	2b	3b	4b	5b
II	Li 11,8	Be 4,8													
III	Na 23,2	Mg 15,7											Al 11,6		
IV	K 46,4	Ca 28,7	Sc 17,5	Ti 13,1	V 9,8	Cr 9,2	Mn 9,1	Fe 9,0	Co 8,6	Ni 8,5	Cu 9,9	Zn 10,5	Ga 12,1		
V	Rb 56,4	Sr 37,7	Y 22,9	Zr 17,0	Nb 13,0	Mo 12,1	Tc 9,9	Ru 10,5	Rh 10,8	Pd 11,6	Ag 14,3	Cd 15,1	In 17,9	Sn 18,0	Sb 18,1
VI	Cs 70,9	Ba 41,6	La 25,5	Hf 16,5	Ta 13,0	W 12,0	Re 10,3	Os 10,9	Ir 11,1	Pt 11,7	Au 14,5	Hg 15,9	Tl 19,9	Pb 20,2	Bi 21,0
VII	Fr 89	Ra 53	Ac 34												

Lanthanides	Ce 23,2	Pr 23,3	Nd 23,2	Sm 24,3	Eu 32,6	Gd 22,3	Tb 21,8	Dy 21,5	Ho 21,2	Er 20,6	Tm 20,3	Yb 27,3	Lu 20,2
Actinides	Th 21,7	Pa 16,1	U 13,7(6+) 21(4+)	Np 11,6	Pu 20	Am 20							

It is proposed to use this system of covalent refractions for refinement of a new method of calculating molecular refractions of chemical compounds [2]. However, at this time these values cannot yet compete in accuracy with the refraction increments calculated from data for organometallic compounds.

LITERATURE CITED

1. S. S. Batsanov. Zh. fiz. khimii 30, 2640 (1956).
2. S. S. Batsanov. Zh. neorgan. khimii 2, 1220 (1957).
3. W. Strohmeier and K. Hümpfner. Z. Elektrochem. 60, 1111 (1956).
4. W. Strohmeier. Z. Elektrochem. 60, 58 (1956).
5. E. Krause and W. Fromm. Ber. 59, 931 (1926).
6. E. Krause. Ber. 50, 1813 (1917).
7. E. Krause. Ber. 59, 935 (1926).
8. J. Macgueen and J. Smith. J. Chem. Soc., 1821 (1956).
9. H. Gutowsky. J. Amer. Chem. Soc. 68, 2204 (1946).
10. W. Strohmeier and K. Hümpfner. Z. Elektrochem. 61, 1010 (1957).
11. A. Deluzarche. Compt. rend. 239, 1489 (1954).
12. W. Jones, D. Evans, T. Gulwell and D. Griffits. J. Chem. Soc., 35 (1935).
13. E. Krause and A. Grosse. Die Chemie der metallorganische Verbindungen (Leipzig, 1937).
14. T. Taylor, E. Smith, J. Torgesen, H. Mathesen and J. Taylor. Chem. Abstrs. 18, 16630 (1959).
15. C. Cuthbertson and E. Metcalfe. Phil. Trans. A207, 142 (1908).
16. L. Pauling. J. Amer. Chem. Soc. 69, 542 (1947).
17. L. Pauling. Nature of the Chemical Bond [Russian translation] (Gosl' Izdat, Moscow, 1947).
18. W. Gordy and W. Thomas. J. Chem. Phys. 24, 439 (1956).
19. I. L. Agafonov. Zh. neorgan. khimii 4, 1270 (1959).

20. G. B. Bokii. Introduction to Crystal Chemistry [in Russian] (Izd. MGU, Moscow, 1954).
21. G. S. Zhdanov. Vestn. Mosk. univ 4, 61 (1957).
22. M. Atoji. J. Chem. Phys. 25, 174 (1956).
23. S. S. Batsanov and V. I. Durakov. Zh. strukt. khimii 1, 353 (1960).
24. S. S. Batsanov. Structural Refractometry [in Russian] (Izd. MGU, Moscow, 1959).
25. J. Fischer-Hjalmars and M. Sundbom. Acta Chem. scand. 11, 1068 (1957).
26. M. Sundbom. Arkiv Physik 13, 539 (1958).

All abbreviations of periodicals in the above bibliography are letter-by-letter transliterations of the abbreviations as given in the original Russian journal. *Some or all of this periodical literature may well be available in English translation.* A complete list of the cover-to-cover English translations appears at the back of this issue.

BRIEF COMMUNICATIONS

CHEMICAL SHIFTS OF NUCLEAR MAGNETIC RESONANCE SIGNALS OF FLUORINE IN AQUEOUS SOLUTIONS CONTAINING F^-, HF_2^-, AND NH_4^+ IONS

Wang I-ch'iu

Physical Scientific Research Institute of the A. A. Zhdanov Leningrad State University

Translated from Zhurnal Prikladnoi Khimii, Vol. 2, No. 3, pp. 367-368, May-June, 1961
Original article submitted January 12, 1961

It was shown in [1-3] that the position of the magnetic resonance of fluorine in aqueous HF and KHF_2 solutions depends on concentration; in the case of dilute solutions this is due to changes in the proportions of different fluorine-containing components (F^-, HF, HF_2^-) with concentration. It is also known [4-7] that in aqueous KF and NaF solutions the chemical shifts depend on concentration and also on the presence of other electrolytes in solution. These effects, which are usually considerably at not very low concentrations, can only be attributed to interaction of fluoride ions with other ions, because dissociation is complete. For a full elucidation of magnetic shielding of F^{19} in such systems it is desirable to extend such investigations to other objects and, in particular, to make comparisons with the same effect in the corresponding crystals.

We accordingly studied the chemical shifts of the resonance of fluorine in the systems $NH_4F - H_2O$ (I), $KF - NH_4Cl - H_2O$ (II), $NH_4HF_2 - H_2O$ (III) and $KHF_2 - NH_4Cl - H_2O$ (IV) and in polycrystalline NH_4F at room temperature. The first system was investigated in [7], but the quantitative results were not published; we must point out that the authors of that paper drew an erroneous conclusion concerning the magnitude of the chemical shift of the HF_2^- ion (see [3]).

The method for measuring the chemical shifts of δ was described earlier [1-3]. All the investigations were carried out at field level $H \approx 4670$ gauss. The reference standard was Freon 11 ($CFCl_3$), but the measured values of $\delta = (H - H_c)/H_c$ were converted to a scale relative to elemental fluorine (δ_{CFCl_3} relative to F_2 is $41.84 \cdot 10^{-6}$). The experimental error of δ in solutions was approximately $1.5 \cdot 10^{-6}$. Solutions of acid salts which react with glass were investigated in polystyrene ampoules.•

The results are plotted in the figure (the abscissa represents the molar concentration of ammonium ions, and the ordinate gives values of $\delta \cdot 10^6$). Curve I shows that magnetic shielding of fluorine decreases with increase of ammonium fluoride concentration, and at concentrations > 3M the relationship is linear (the slope is $= -1.13 \cdot 10^{-6}$/M). The total range of the variation is considerable ($\sim 1.8 \cdot 10^{-5}$). Investigation of the ternary system $KF - NH_4Cl - H_2O$ (curve II) shows that addition of ammonium chloride also diminishes magnetic shielding of the F^{19} nucleus. According to our data for the $KF - KCl - H_2O$ system, and according to [7], the influence of Cl^- on the resonance of F^- consists in a slight decrease of δ_{F^-}. This decrease did not exceed $2 \cdot 10^{-6}$ at the highest concentration used in this investigation. Thus, in both systems the decrease is primarily to interaction with NH_4^+ ions. This is confirmed further by the fact that curves I and II intersect at concentration $C \approx 4M$, which is the point at which not only the NH_4^+ but also the F^- concentrations are equal. The divergence of the curves on each side of the intersection point is evidently attributable to the ratio of the amounts of NH_4^+ and F^- ions (this ratio is constant in system I and varies in system II).

For the solid NH_4F phase δ_{F^-} was found to be $(5.0 \pm 0.2) \cdot 10^{-6}$. Extrapolation of curve I to $C = 35.5$ M, which corresponds to the concentration of the solid salts, gives $\delta = 5.045 \cdot 10^{-4}$. This agreement, and the results of comparison of δ_{F^-} for ionic crystals [8] with literature data on the effects of concentration on this value in the systems $KF - H_2O$, $NaF - H_2O$ [6] and $KF - H_2O - X$ [7] (X = NaCl, RbCl, CsCl, etc.), shows that with increase of concentration the values of δ_{F^-} for solutions tend to the corresponding values for the solid salts, although in general extrapolation does not give exact agreement.••

•It was found that specimens in glass ampoules give lower values of δ_{F^-}, with a different dependence on concentration. This effect is almost negligible for neutral salts (see figure).

•• The existence of such a relationship was postulated in [7] from indirect considerations.

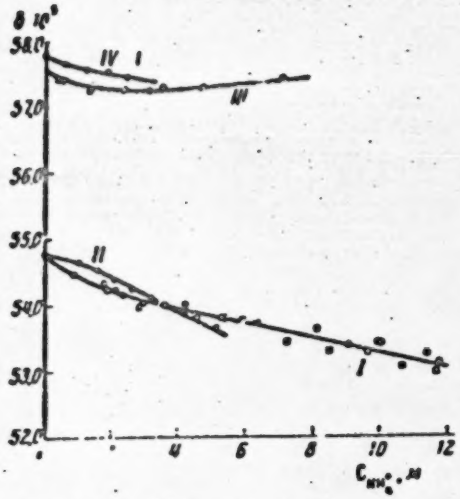

Chemical shifts of resonance in the systems $NH_4F - H_2O$ (I), $KF - NH_4Cl - H_2O$ (II), $NH_4HF_2 - H_2O$ (III) and $KHF_2 - NH_4Cl - H_2O$ (IV). For system I: ○) measurements for solutions in glass ampoules; □) measurements in polystyrene ampoules. For II, $C_{KF} = 4.1$ M; for IV, $C_{KHF_2} = 1.3$ M.

This result shows that magnetic shielding of the nucleus in concentrated solutions and in solids* is effected by a similar mechanism, and therefore the respective structures must be interrelated to a considerable extent. Moreover, it is likely that for electrolyte solutions of not very low concentrations (C > 4M, and even lower in some cases) the dependence of chemical shifts on concentration is due primarily to transient association of ions.

The results of measurements in acid solutions are shown in the same figure (curves III and IV). The influence of NH_4^+ ions is much less in these cases than in systems I and II. If curve III and the curve for the system $KHF_2 - H_2O$ (see [3]) are extrapolated to zero concentration, it is found that δ for both systems lies within the limits of experimental error. An attempt to explain the course of the curves at low concentrations based on the assumption that ammonium ions influence only F^- (and not HF_2^- or HF) gave only qualitative agreement with the experimental data; it follows that there is probably some interaction with HF_2^- ions and HF molecules. A fuller interpretation is difficult at this stage, as experimental data on acid salts are meager and unfortunately there are no data at all on shielding of acid salts in the solid phase.

It must be pointed out that considerable broadening of the lines was observed at NH_4HF_2 concentrations of about 5 M. A similar effect was observed in the ternary system IV at NH_4^+ concentration of about 3 M. The cause of this is not clear as yet. This effect may possibly be due to a decrease of the fluorine exchange rate between different states in this concentration range.

The author offers his sincere thanks to F. I. Skripov for guidance in the work.

LITERATURE CITED

1. N. M. Borodin and F. I. Skripov. Izv. vyssh. uch. zav., Radiofizika 1, 3, 37 (1958).
2. É. Z. Utyanskaya, A. U. Stepanyants, M. I. Vinnik and N. M. Cherkov. Dokl. AN SSSR 124, 5, 105 (1959).
3. Van I-tsyu and F. I. Skripov. Dokl. AN SSSR 136, 1, 58 (1961).
4. J. N. Shoolery and B. J. Alder. J. Chem. Phys. 23, 805 (1955).
5. A. Carrington and T. Hines. J. Chem. Phys. 28, 727 (1958).
6. R. E. Connick and R. E. Poulson. J. Phys. Chem. 62, 1002 (1958).
7. A. Carrington, F. Dravnics and M. C. R. Symons. Mol. Phys. 3, 174 (1960).
8. Van I-tsyu. Dokl. AN SSSR 136, 2, 317 (1961).
9. J. Kondo and J. Yamasita. J. phys. Chem. Solids 10, 245 (1959).

All abbreviations of periodicals in the above bibliography are letter-by-letter transliterations of the abbreviations as given in the original Russian journal. *Some or all of this periodical literature may well be available in English translation.* A complete list of the cover-to-cover English translations appears at the back of this issue.

---

* The latter have been studied to some extent; for example, see [9].

PARAMAGNETIC RESONANCE IN SOLUTIONS OF COMPLEX COPPER SALTS

DETERMINATION OF THE CHARACTERISTIC PARAMETERS OF BROWNIAN ROTATION OF COMPLEXES

A. I. Rivkind

Physicotechnical Institute of the Kazan' Branch of the Academy of Sciences, USSR

Translated from Zhurnal Strukturnoi Khimii, Vol. 2, No. 3, pp. 369-370, May-June, 1961
Original article submitted October 7, 1960

It is known [1] that in the EPR spectra of liquid solutions of bivalent copper complex salts, measured in the 3-centimeter radio wave band, the width of the hyperfine components varies and increases sharply with increase of the nuclear magnetic quantum number m_I. According to [2], this anomaly is a relaxation effect: Brownian rotation of magnetically isotropic complex particles ("microcrystallites") relatively to the external magnetic field H_0 induces relaxational transitions the probability of which depends on m_I. We recently investigated the asymmetric hyperfine structure spectra of copper complexes in solution, with variations of the solvent viscosity, sizes of the complex particles, and frequency of the oscillating magnetic field [3, 4]. It was found that in reality the asymmetry of the spectra is caused by purely structural broadening of the hyperfine components and not by relaxation. The ratio between the characteristic frequency $\nu_C = 1/2\pi\tau_C$ of the Brownian rotation of the complexes and the Larmor frequency ν_0 plays the determining role. In the case of "slow" rotation ($\nu_C < \nu_0$) anisotropy of the g factor and of the nuclear hyperfine

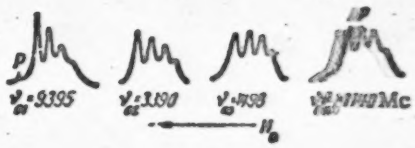

interaction constant are not leveled out completely during the period of Larmor precession of the electron spin and lead to the appearance of an unresolved structure of the hyperfine components. One consequence of this is that the characteristic parameters of thermal rotational motion of paramagnetic particles can be determined directly from the form of the hyperfine structure [obtained at two adjacent Larmor frequencies (ν_{0i}, ν_{0j})]. The only necessary condition is that the spectrum remains asymmetric at the higher of these frequencies while at the lower the components must be equal in intensity and width. The required value of ν_C must then lie between ν_{0i} and ν_{0j}.

An attempt was made in the present investigation to make use of this possibility by measurement of spectra over a sufficiently wide range of frequencies ν_0. The object of the investigation was an approximately 0.05 M solution of cupric cupfenonate complexes in dioxane, which gives easily detected EPR curves. The complexes have the chemical structure

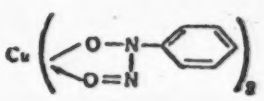

The solution was prepared from the solid complex salt of the same composition. The figure shows oscillograms of the spectra obtained at room temperature at frequencies of ν_{01} = 9395, ν_{02} = 3390, ν_{03} = 1498 and ν_{04} = 1140 Mc. The narrow lines (p) in the two outside oscillograms are signals given by the free α, α-diphenyl-β-picrylhydrazyl radical

used for calibration of the constant magnetic field H_0. The direction of increase of the field strength H_0 is indicated by the horizontal arrow. The positions of the hyperfine structure peaks measured at frequency ν_{63} correspond to the following values of the effective g factors

m_I	$-^5/_2$	$-^3/_2$	$+^1/_2$	$+^3/_2$
g	2.035	2.101	2.168	~2.19

The hyperfine structure constant a_0 is ~ 70 oe.

The spectral asymmetry decreases with decreasing frequency of the oscillating magnetic field, so that at frequency ν_{63} only slight differences in the widths and intensities of the $m_I = -^3/_2, -^1/_2, +^1/_2$ hyperfine lines can be detected, and at frequency ν_{64} even these differences disappear (see figure).* Evidently the characteristic frequency of Brownian rotation of copper cupferronate complexes in dioxane lies in the $\nu_{63} - \nu_{64}$ range, which corresponds to the characteristic time $\tau_C = 1/2\pi\nu_0 \approx (1.1 - 1.4) \cdot 10^{-10}$ sec. The value found for τ_C must be regarded as a quantity found by direct measurement. Direct information on interaction in the second coordination (solvation) sphere of complexes can be obtained from measurements by this method of the values of τ_C for the same complex particles but in different solvents (variation of other conditions, such as temperature, is also of interest).

We must point out in conclusion that the variations of the form of the spectra with frequency as shown in the figure are in no way represented by the theory in [2], and are essentially contradictory to that theory.[3] However, in one communication [5] the relaxational mechanism of this theory is confirmed on the basis of measurements of asymmetric hyperfine structure spectra given by a solution containing VO^{2+} ions at two different frequencies of the oscillating magnetic field. The probable reason for the discrepancy is that the measurements with VO^{2+} ions were carried out only in the 3-centimeter and millimeter bands, i.e., when $\nu_0 > \nu_C$, whereas measurements at frequencies $\nu_0 < \nu_C$ are also needed to give the full picture.

LITERATURE CITED

1. B. R. McGarvey. J. Phys. Chem. 60, 71 (1956).
2. H. M. McConnell. J. Chem. Phys. 25, 709 (1956).
3. A. I. Rivkind. Zh. fiz. khimii 35 (1961) (in the press).
4. A. I. Rivkind. In collection: Paramagnetic Resonance [in Russian] (Izd. Kazanskogo Univ., 1960) p. 50.
5. R. N. Rogers. Bull. Amer. Phys. Soc. 5, 253 (1960).

All abbreviations of periodicals in the above bibliography are letter-by-letter transliterations of the abbreviations as given in the original Russian journal. *Some or all of this periodical literature may well be available in English translation.* A complete list of the cover-to-cover English translations appears at the back of this issue.

---

*The hyperfine component $m_I = +^5/_2$ (on the extreme right of the oscillograms) was not considered, as its diffuse character at frequencies ν_{63} and ν_{64} is caused not by structural broadening but by the influence of the conditions of the intermediate (weak) fields, which at these frequencies begin to appear for the spectral components lying in the directions of lower values of the field strength H_0 [3].

NUCLEAR QUADRUPOLE RESONANCE IN CERTAIN BROMINE AND IODINE COMPOUNDS

G. K. Semin

Institute of Heteroorganic Compounds, Academy of Sciences, USSR
Translated from Zhurnal Strukturnoi Khimii, Vol. 2, No. 3, pp. 370-373, May-June, 1961
Original article submitted August 15, 1960

Data on the nuclear quadrupole resonance (NQR) spectra of certain bromine and iodine compounds are given; for some of these the NQR frequencies were determined for the first time, while for others the NQR spectra were either determined more precisely or frequencies were determined at temperatures not previously investigated. The experiments were performed with a NQR radiospectrometer [10] which is a superregenerative frequency-modulated single-cycle generator – detector on a two-wire line. The measurements were carried out at the temperature of liquid nitrogen and at room temperature; the search ranges were 140-210 and 230-320 Mc. The frequency was measured by means of a heterodyne wavemeter of the VVT-D type. The results are given in the Table.

NQR was observed for the first time in 2,6-Br_2^{79}-4-NO_2-$C_6H_2NH_2$, p-$O_2Br_2^{79}C_6$, p-$(CH_2Br^{79})_2C_6H_4$ and FC_6Br_5. It is interesting to note that in bromanil (p-$O_2C_6Br_4^{79}$) the number of spectral lines remained unchanged in the transition from the temperature of liquid nitrogen to room temperature; this indicates that, in contrast to chloranil [14], this compound does not undergo a phase transition in this temperature range. In 2,6-Br_2^{79}-4-NO_2-$C_6H_2NH_2$ the NQR frequency, as was to be expected, is between the frequencies for the corresponding nitro- and aminobromobenzenes. Comparison of the NQR frequencies of p-$(CH_2Br)_2C_6H_4$ and p-$(CH_2Br)C_6H_4(CH_3)$ [5] revealed a decrease of 1% in the ionic character of the C – Br bond. The intensity of the NQR signal of p-$(CH_2Br)_2C_6H_4$ drops sharply with rise of temperature, and the frequency at room temperature is lower by 5.67 Mc. In general, the resonance frequency of halogenated benzenes [11, 12] depends very sharply on temperature; this is probably due to the start of rotation of the end groups.

The spectrum of FC_6Br_5[21] contains about five lines. This makes investigation of NQR with the superregenerative spectrometer difficult, and weakness of the signal complicates the measurements further; the spectrum of this compound is being determined more precisely.

TABLE 1. NQR of Certain Iodine-Containing Substances

Substance	T°, K	NQR frequency, Mc*	Signal/noise ratio	Literature and notes
HIO_3	297	202.370±0.003	10 – 12	[2]
IC_6H_5	77	274.465±0.003	8	A resonance wave meter was used for measurements at 83°K in [3]. No measurements were performed at 77°K.
	77	274.978±0.003	8	
p-IC_6H_4	297	276.637±0.003	2 – 3	[2, 3, 7]
	77	280.081±0.004	10	
p-$IC_6H_4NH_2$	297	261.524±0.004	1	[2]. A resonance wave meter was used for measurements at 83° K in [3]. No measurements were performed at 77° K.
	77	264.280±0.003	15	

* $\pm 1/2 \rightarrow \pm 3/2$ transition.

The NQR frequency of $I^{127}C_6H_5$ (Table 1) was measured precisely for the first time (at 77° K); the two lines arose owing to the nonequivalent crystallographic positions of the iodine atoms. Earlier measurements at 83° K were performed with a resonance wave meter [3], which gives an error of several Mc. Table 1 also contains the NQR frequency of p-$I^{127}C_6H_4NH_2$ at 77° K, also measured for the first time.

Substances in which NQR signals could not be detected are given in Table 3. The absence of NQR in o-$(CH_3)_2C_6Br_4$ and m-$(CH_3)_2C_6Br_4$ is due to the fact that the orientation of the molecules in the crystals is random, as was demonstrated by x-ray diffraction in [13].

TABLE 2. NQR of Certain Bromine-Containing Substances

Substance	T°, K	NQR frequency, Mc		Signal/noise ratio		Literature and notes
		Br^{81}	Br^{79}	Br^{81}	Br^{79}	
$NaBrO_3$	290 77	149,525 151,784	178,869 —	10 10	10	[4,8]
$p\text{-}Br_2C_6H_4$	299 77	— —	267,949±0,003 271,125±0,002	— —	5—7 25—30	[4,5,8] [4]
$p\text{-}BrC_6H_4OH$	299,5 77 77	— — —	264,815±0,005 268,378±0,003 269,830±0,003	— — —	3 10—12 10—12	[2,3,5,8] Resonance wavemeter used in [3] and [8]
$p\text{-}BrC_6H_4NH_2$	299 77	— —	262,134±0,004 265,525±0,003	— —	1,5 3	[2,3,5,8] Resonance wavemeter used in [3] and [8]
$p\text{-}(CH_2Br)_2C_6H_4$*	291 77	— —	252,027±0,001 257,697±0,003	— —	1,5 10—12	Measured for the first time
$2,6\text{-}Br_2\text{-}4\text{-}NO_2\text{-}C_6H_2NH_2$	286 77	— —	278,821±0,005 282,458±0,003	— —	2 10	Measured for the first time
$p\text{-}O_2C_6Br_6$	296 77		294,153±0,004 295,081±0,006 298,309±0,003 298,974±0,002		3—6 3—6 10 10	Measured for the first time
FBr_5C_6**	77		305,61 305,99 307,20 309,30 309,72		1,2 1,5 » » »	Measured for the first time
CBr_4	77	Series of lines between 264 and 269 Mc		10—15		[3,6]

* Specimen provided by Yu. T. Struchkov.

** Preliminary data. Specimen provided by G. G. Yakobson.

TABLE 3. Substances in which NQR Signals Could Not Be Detected

Substance	Frequency range searched	T, °K
o-$(CH_3)_2HgC_6$	230—307	300
	230—300	77
m-$(CH_3)_2HgC_6$	230—307	300
	230—300	77

I thank A. I. Kitaigorodskii and Yu. T. Struchkov for constant interest in the work.

LITERATURE CITED

1. P. Casabella and P. Bray. J. Chem. Phys. 26, 1280 (1956).
2. G. Ludwig. J. Chem. Phys. 25, 159 (1956).
3. J. Hatton and B. Rollin. Trans. Faraday Soc. 50, 358 (1954).
4. A. Schawlow. J. Chem. Phys. 22, 1211 (1954).
5. P. Bray. J. Chem. Phys. 22, 2023 (1954).
6. R. Barnes. J. Chem. Phys. 22, 1944 (1954).
7. P. Bray, R. Barnes and R. Benson. J. Chem. Phys. 25, 813 (1956).
8. D. Alderdice, R. Brown and T. Iredale. J. Chem. Phys. 30, 344 (1959).
9. K. Shimomura. J. Phys. Soc. Japan 14, 235 (1959).
10. G. K. Semin. Proceedings of Conference on Paramagnetic Resonance [in Russian] (Kazan', 1959).
11. H. C. Meal. J. Amer. Chem. Soc. 74, 6121 (1952).
12. R. Livingston. J. Phys. Chem. 57, 496 (1953).
13. I. N. Stel'tsova and Yu. T. Struchkov. Izv. AN SSSR, Otd. Khim. n., 2, 250 (1961).
14. É. I. Fedin. Zh. strukt. khimii 2, 1, 215 (1961).

REVIEWS

CLASSIFICATION OF INORGANIC CYCLIC COMPOUNDS

I. Haiduc

Babes-Bolyai University, Cluj, Rumanian People's Republic
Translated from Zhurnal Strukturnoi Khimii, Vol. 2, No. 3, pp. 374-382, May-June, 1961
Original article submitted October 3, 1960

Inorganic cyclic compounds are very numerous and constitute a peculiar section of inorganic chemistry. The proposed classification includes all known inorganic cycles and makes it possible to predict the existence of new compounds of this type.

It has become clear in recent years that many other elements in addition to carbon can form rings. Many compounds containing rings without carbon, i.e., inorganic cyclic compounds, have been studied; however, it was only recently pointed out that these compounds constitute a peculiar section of inorganic chemistry [1] which may, in the near future, become just as important as the chemistry of complex compounds. The purpose of this paper is to draw the attention of inorganic chemists to cyclic compounds.

Admittedly, several reviews of inorganic polymers have been published [2-10], but both cyclic (low-molecular) and high-molecular compounds were considered together. A distinction between these two groups of compounds was drawn for the first time by us in [11], where we showed that inorganic polymers may have cyclic structure (with a low degree of polymerization, such as trimers and tetramers), or a high-polymer structure. Of course, these two groups are closely related: monocyclic compounds are the lowest members of polymer series, the highest members of which are chain polymers [11] (Table 1).

TABLE 1. Low and High Polymers

Cyclic lowest polymers	$(RBS)_3$	$(R_2SiO)_n$ $n = 3, 4, 5, 6\ldots$	$(MePO_2)_3$ $(MePO_2)_4$	$(Cl_2PN)_3$ $(Cl_2PN)_4$	S_8 S_8
Corresponding high polymers	$(RBS)_x$	$(R_2SiO)_x$	$(MePO_2)_x$	$(Cl_2PN)_x$	S_x

In our opinion, the most rational criterion for classification of inorganic cyclic compounds is the structure of the cyclic skeleton. This gives rise to the first subdivision:

1) Monocyclic compounds with only one inorganic ring in the structure.

2) Polycyclic compounds with two or more cycles joined in various ways in the structure.

1. Monocyclic Compounds

Monocyclic compounds can be divideded into three groups:
a) homocyclic compounds;
b) heterocyclic compounds with alternation (or pseudoheterocyclic compounds);
c) true heterocyclic compounds.

a) Homocyclic compounds have rings consisting of atoms of the same element. In this group, rings consisting of silicon, germanium, nitrogen, phosphorus, arsenic, sulfur, and selenium are known at the present time.

Silicon rings can be either saturated, as in $[(CH_3)_2Si]_6$ [12], or unsaturated, as in Si_4Cl_4, Si_6H_6, $Si_6(CH_3)_6$ [13];

R = CH_3

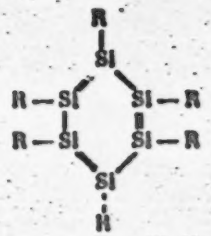

R = Cl, H, CH_3

Four-membered rings formed by silicon and germanium have also been described: in $[(C_6H_5)_2Si]_4$ [14] and $[(C_6H_5)_2Ge]_4$ [15]:

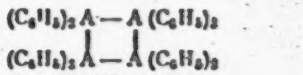

A = Si [14], Ge [15].

Of the elements of the fifth group, nitrogen, phosphorus, and arsenic form the following homocyclic compounds:

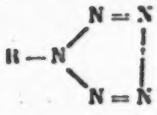

[16]

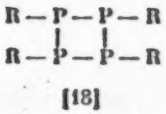

[18]

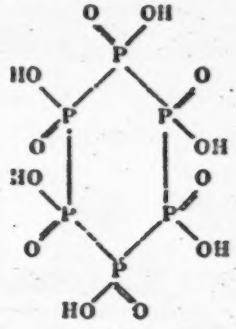

[17]

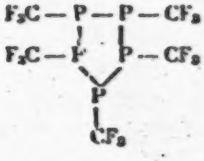

[18]

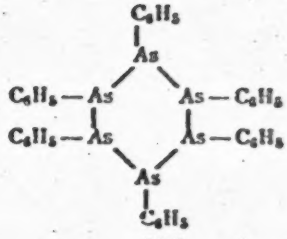

[19]

[20]

Elemental sulfur and selenium form cyclic molecules

[21]

[22]

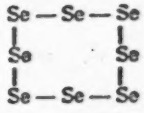

[23]

b) Heterocyclic compounds with alternation have rings in which atoms of two elements, A and B, alternate:

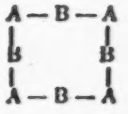

In view of the special role of such alternation in the formation of inorganic rings, we found it useful to segregate these compounds in a separate group. Assuming that the ring is formed by three- or fourfold repetition of the same group AB, we proposed the term [1, 11] "pseudoheterocyclic compounds."

Boron forms six-membered rings in borazole [24-27], boroxole [24, 28], borosulfole [29, 30], and a four-membered ring in $B_2S_2(SH)_2$ [29]:

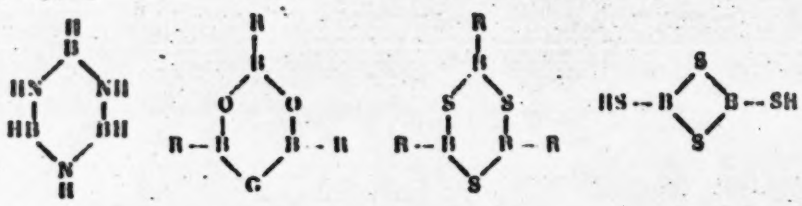

Silicon forms a large number of six-, eight-, and multimembered rings, which are known in cyclosiloxanes [31, 32], cyclosilazanes [33-34], and cyclosilthianes [35].

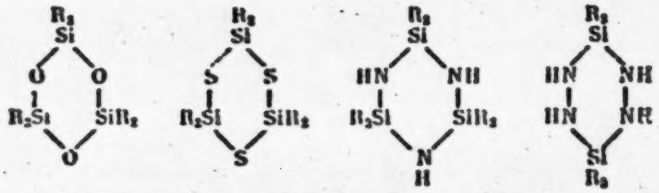

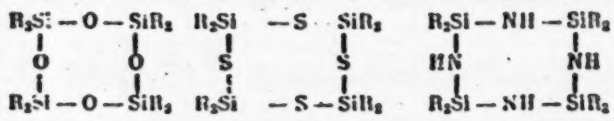

Cyclic compounds of germanium have also been prepared: $(R_2GeO)_3$, $(R_2GeO)_4$ [36] and probably $(R_2GeNH)_3$.

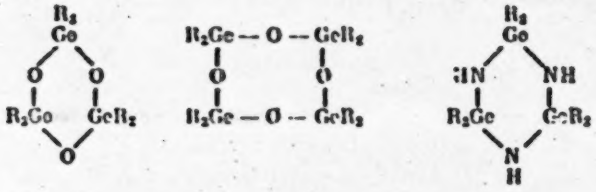

Cyclic compounds of phosphorus have been studied for a long time. The following have been reported in the literature: phosphorus – oxygen rings in metaphosphoric acids $(HPO_3)_n$ [37, 38], phosphorus – nitrogen rings in phosphonitrile compounds $(R_2PN)_n$ [38-42], and in metaphosphinic acids $(HOPONH)_n$ [43]; phosphorus – sulfur rings have also been reported in the compound $(C_6H_5PSO)_3$ [44]:

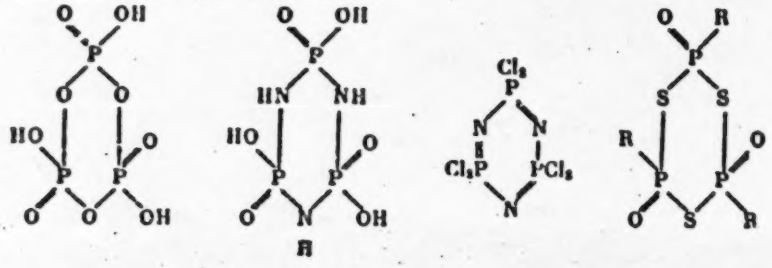

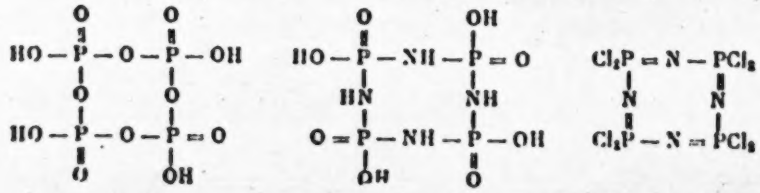

Monocyclic arsenic compounds have not been described in the literature. We consider that the compounds R – AsO [45], R – AsS [46, 46] and R – AsNH [47], the molecular weights of which correspond to trimers and tetramers, are cyclic:

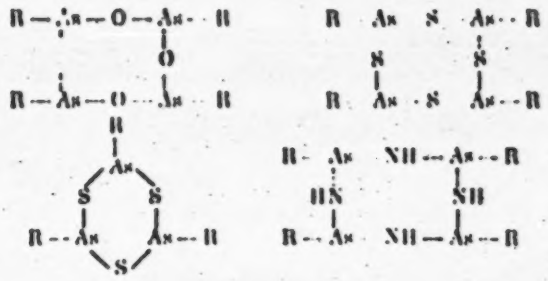

The S – N pair forms a great variety of cyclic compounds [48-51]

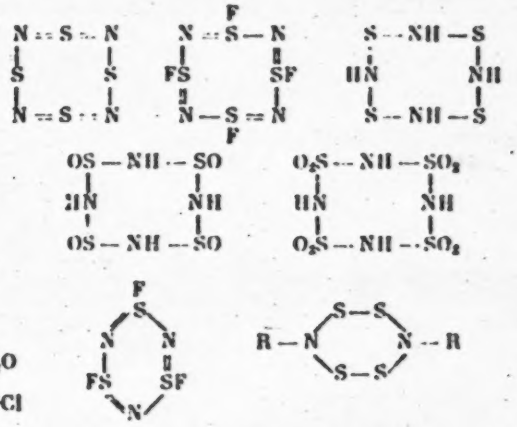

The "ice" form of sulfur trioxide consists of cyclic molecules [52]

Mass spectrum investigations of MoO_3 and WO_3 vapors revealed cyclic molecules: Mo_3O_9, Mo_4O_{12}, Mo_5O_{15} and W_3O_9, W_4O_{12}, W_5O_{15} [53]:

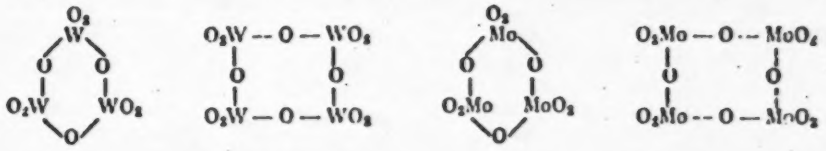

All these cycles have been included in a systematic table (Table 2), which indicates that new inorganic rings may be expected: Ge_4N_4, Ge_3S_3, Ge_4S_4, P_4S_4, As_3O_3, As_3S_3, Sb_3O_3, Sb_4O_4, Sb_3N_3, Sb_4N_4, Sb_3S_3, Sb_4S_4, etc. [54].

Oxygen in rings can be partially replaced by the NH group or S, or vice versa. Such rings were obtained by Sokolov [55] in the compounds:

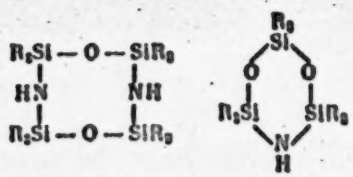

This greatly increases the possibility of obtaining new inorganic rings.

c) True heterocyclic compounds have been studied very little as yet. Mainly compounds containing sulfur have been reported [48, 50]

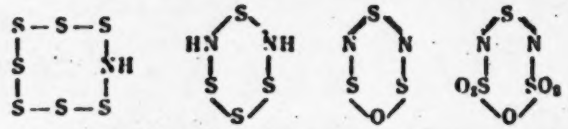

TABLE 2 Systematic Table of the Most Important Rings Known in Monocyclic Compounds*

	Alternating element	Principal element							
		B	C	Si	Ge	P	As	Sb	S
Homocyclic	—	—	C_3	—	—	—	—	—	—
		—	C_5	Si_4	Ge_4	P_4	—	—	—
		—	C_6	—	—	P_5	As_5	—	—
		—	C_8	Si_6	—	P_6	As_6	—	S_6
		—	C_9	—	—	—	—	—	S_8
Pseudoheterocyclic	O	B_2O_3	C_3O_3	Si_2O_3	Ge_2O_3	P_2O_3	—	—	S_2O_3
		—	C_4O_4	Si_4O_4	Ge_4O_4	P_4O_4	As_4O_4	—	—
		—	—	Si_5O_5	—	P_4O_5?	—	—	—
		—	—	Si_6O_6	—	P_6O_6?	—	—	—
	N	B_3N_3	C_3N_3	Si_3N_3	Ge_3N_3	P_3N_3	—	—	S_3N_3
		—	—	Si_4N_4	—	P_4N_4	As_4N_4	—	S_4N_4
	S	B_2S_2	—	Si_2S_2	—	—	—	—	—
		B_2S_3	C_6S_2	Si_3S_3	—	P_2S_3	As_2S_2	—	S_6
		—	C_6S_4	Si_4S_4	—	—	As_4S_4	—	S_8

* Only the ring composition is given, without substituents.

2. Polycyclic Compounds

Polycyclic compounds are very diverse, because of the various possibilities of ring combination. Polycyclic compounds are classified in accordance with the number of atoms common to the linked rings.

a) Compounds with linked rings without a common atom, joined by bridges:

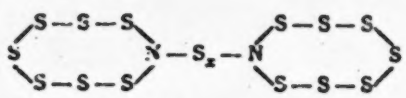

$x = 1, 2$ [56]

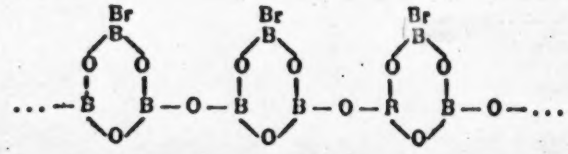

[57]

b) Spiro compounds in which the rings have one common atom:

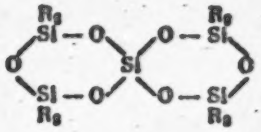

[58]

[59]

c) Compounds with fused (condensed) rings, having at least two atoms in common. Condensed cyclic structures can be low-molecular or high-molecular.

Low-molecular compounds containing 2, 3, or several condensed (fused) rings, for example:

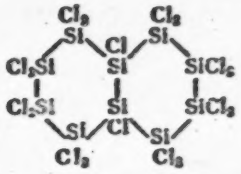

[60]

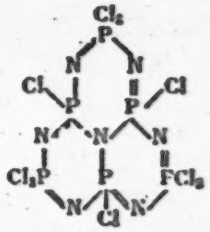

[61]

This group also includes inorganic compounds of the urotropin structure (P_4O_6 [62], P_4O_{10} [62], As_4O_6 [63], Sb_4O_6 [63], $P_4C_6S_4$), and compounds with an incomplete urotropin structure P_6S_3 [64] and P_4S_7 [65]:

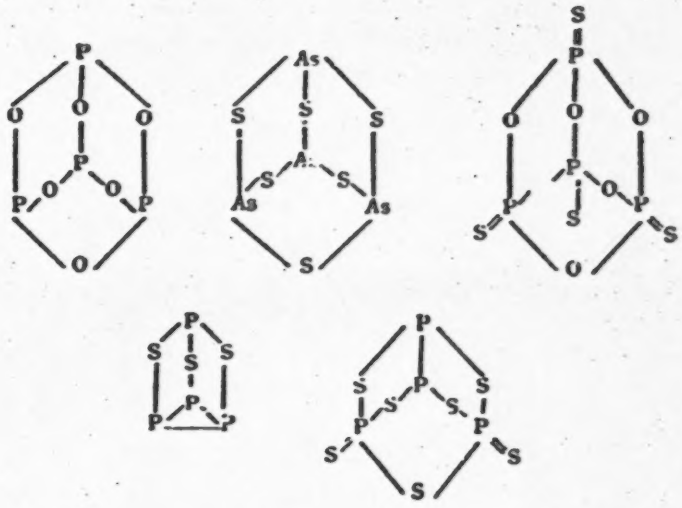

Heteropoly acids are also compounds with condensed cyclic structure [66].

High-molecular polycyclic compounds may have one-dimensional, two-dimensional, or three-dimensional structures. In one-dimensional structures the rings are linked in one direction only, forming bands of indefinite length:

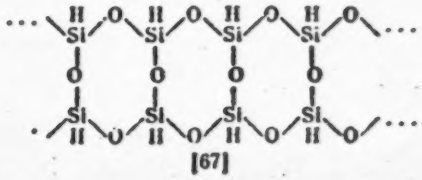

[67]

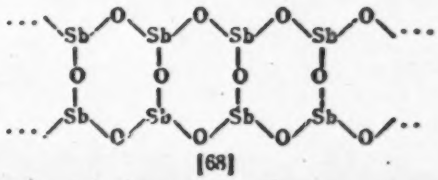

[68]

In two-dimensional polycyclic compounds the structure grows in a plane to form a sheet. Many silicates have this type of structure [69]. This group also includes boron nitride BN and siloxene [70], $Si_6O_3H_6$:

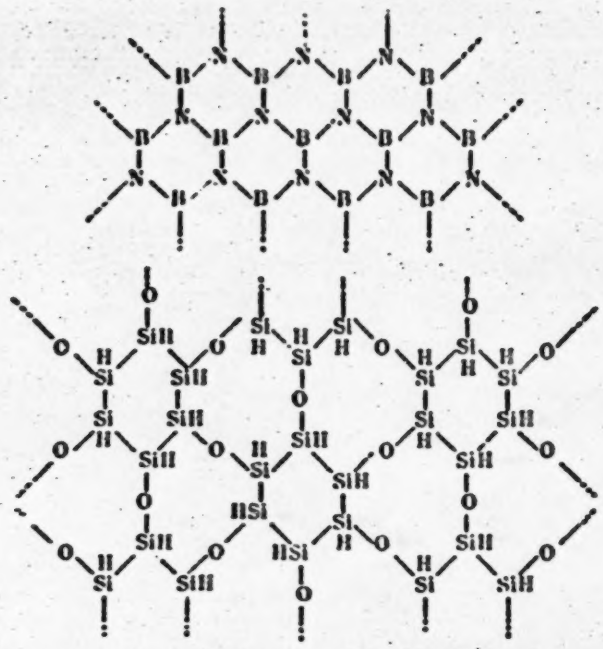

Three-dimensional polycyclic compounds are represented by silica $(SiO_2)_n$ and many silicates of the framework type.

It follows from our proposed classification that inorganic cyclic compounds constitute a peculiar section of inorganic chemistry. It also follows from the classification that numerous new inorganic cycles are obtainable. Systematic investigations in this direction would be very interesting by their scientific significance and in relation to the practical uses of inorganic cyclic compounds and their organic derivatives.

SUMMARY

1. Inorganic cyclic compounds constitute a peculiar section of inorganic chemistry.

2. Inorganic cyclic compounds can be classified by the following groups:

Monocyclic compounds, which are further subdivided into a) homocyclic, b) heterocyclic with alternation (pseudoheterocyclic), and c) true heterocyclic compounds.

Polycyclic compounds, which include a) compounds with linked rings, b) spiro compounds, and c) compounds with fused (condensed) rings (low- and high-molecular).

3. The preparation of new inorganic cycles is possible.

LITERATURE CITED

1. I. Haiduc. Introduction to the Chemistry of Inorganic Cycles [in Rumanian]. Ed. RPR. (Bucureşti, 1960).
2. V. V. Korshak and K. K. Mozgova. Usp. khimii 28, 783 (1959).
3. A. A. Berlin and V. P. Parini, Usp. khimii 18, 546 (1949).
4. A. A. Berlin and V. P. Parini, Khim. nauka i prom. 1, 44 (1956).
5. A. Michel. Bull. Soc. Chim. France 1956, 1103.
6. K. A. Andrianov. Usp. khimii 27, 1757 (1958).
7. H. J. Emeléus. Proc. Chem. Soc. 1959, 202.
8. K. A. Andrianov. Khimiya i tekhnol. polimerov 4, 26 (1960).

9. D. B. Sowerby and L. F. Audrieth. J. Chem. Educ. 37, 2, 86 (1960).
10. A. B. Burg. J. Chem. Educ. 37, 482 (1960).
11. I. Haiduc. Rev. Chimie (Bucuresti) 7, 721 (1956).
12. C. A. Burchard. J. Amer. Chem. Soc. 71, 963 (1949).
13. G. Urry. Angew. Chem. 70, 379 (1958).
14. F. S. Kipping. J. Chem. Soc. 119, 647, 830 (1921).
15. C. A. Kraus and C. L. Brown. J. Amer. Chem. Soc. 52, 4031 (1930).
16. J. Ugi, H. Perlinger and L. Behringer. Chem. Ber. 91, 2324 (1958).
17. B. Blaser and K. H. Worms. Z. anorgan. allgem. Chem. 300, 225 (1959).
18. W. Mahler and A. B. Burg. J. Amer. Chem. Soc. 79, 6161 (1958).
19. M. Ya. Kraft, T. M. Borodina, I. N. Strel'tsova, Yu. T. Struchkov. Dokl. AN SSSR 131, 1074 (1960).
20. J. H. Burns and J. Waser. J. Amer. Chem. Soc. 79, 859 (1957).
21. J. Donohue, A. Caron and E. Goldish. Nature 182, 518 (1958).
22. S. C. Abrahams. Acta crystallogr. 8, 661 (1955).
23. J. Marsh, L. Pauling and McCoullough. Acta crystallogr. 8, 323 (1955).
24. B. M. Mikhailov. Usp. khimii 28, 1450 (1959).
25. B. M. Mikhailov. Usp. khimii 29, 972 (1960).
26. J. C. Sheldon and B. C. Smith. Quart. Revs. 14, 200 (1960).
27. E. M. Smolin and L. Rapoport. S-Triazines and Derivatives. Interscl. Publ. (New York, 1959).
28. M. F. Lappert. Chem. Rev. 56, 959 (1956).
29. E. Wiberg and W. Sturm. Angew. Chem. 67, 483 (1955).
30. Z. V. Zvonkova. Kristallografiya 3, 564 (1958).
31. K. A. Andrianov. Organosilicon Compounds [in Russian]. Goskhimizdat, Moscow, 1955.
32. E. G. Rochow. Introduction to the Chemistry of the Silicones. 2nd Ed., J. Wiley, New York, 1951.
33. M. Yokoi and K. Yamasaki. J. Amer. Chem. Soc. 75, 4139 (1953).
34. U. Wannagat and H. Niederprüm. Angew. Chem. 70, 745 (1958).
35. M. Yokoi, T. Nomura and K. Yamasaki. J. Amer. Chem. Soc. 77, 4484 (1955).
36. W. Metlesics and H. Zeiss. J. Amer. Chem. Soc. 82, 3324 (1960).
37. E. Thilo. Naturwiss. 46, 367 (1959).
38. J. R. Van Wazer. Phosphorus and its Compounds. Vol. 1, Interscl. Publ., New York, 1958.
39. N. L. Paddock and H. T. Searle. In vol. Advances in Inorganic Chemistry and Radiochemistry. Vol. 1, Academic Press, New York, 1959.
40. N. L. Paddock. Endeavour 19, 134 (1960).
41. L. F. Audrieth. Record. Chem. Progress 20, 56 (1959).
42. I. A. Gribova and U Ban-yuan'. Usp. khimii 30, 3 (1961).
43. O. T. Quimby, A. Narath and F. H. Lohman. J. Amer. Chem. Soc. 82, 1099 (1960).
44. L. Anschutz and H. Wirth. Naturwiss 43, 16 (1956).
45. F. F. Blicke and D. Smith. J. Amer. Chem. Soc. 51, 3479 (1929).
46. A. E. Kretov and A. Ya. Berlin. Khim. zh., ser. obshch. khimii 1, 411 (1931).
47. V. Ipatjew, G. Razuwajew and V. Stromski. Ber. 62, 598 (1929).
48. M. Goehring. Ergebnisse und Probleme der Schwefel – Stickotoffverbindungen. Akademie Verlag, Berlin, 1957.
49. N. S. Voznesenskii. Usp. khimii 24, 440 (1955).
50. H. Garcia-Fernandez. Bull. Soc. Chim. France, 1958, 265.
51. L. F. Audrieth. J. Chem. Educ. 34, 545 (1957).
52. R. Westrik and C. MacGillavry. Rec. Trav. Chim. Pays-Bas 60, 794 (1941).
53. J. Berkowitz, M. G. Inghram and W. A. Chupka. J. Chem. Physics 26, 842; 27, 85 (1957).
54. I. Khaiduk (I. Haiduc). Zh. obshch. khimii 30, 1395 (1960).
55. N. N. Sokolov. Methods of Synthesis of Polyorganosiloxanes [in Russian]. Gos. Energoizdat, Moscow, 1958.
56. M. Becke-Goehring, H. Jenne and V. Rekalic. Chem. Ber. 92, 855 (1959).
57. J. Goubeau. Angew. Chem. 67, 234 (1955).
58. W. L. Roth and D. Harker. Acta crystallogr. 1, 34 (1948).
59. W. Bussem, H. Fischer and E. Grunner. Naturwiss. 23, 740 (1935).
60. R. Schwarz. Angew. Chem. 67, 117 (1955).
61. H. I. Krause. Z. Electrochem. 59, 1044 (1955).
62. G. C. Hampson and A. J. Stosik. J. Amer. Chem. Soc. 60, 1814 (1938).

BIBLIOGRAPHY

INFORMATION LIST OF PAPERS ON RADIOSPECTROSCOPY AND ITS APPLICATIONS IN CHEMISTRY. PART 2*

Translated from Zhurnal Strukturnoi Khimii, Vol. 2, No. 3, pp. 383-385, May-June, 1961

I. General Problems

1. V. S. Grechishkin. Instrument for observation of nuclear quadrupole resonance with the use of Zeeman modulation (LGU, NIFI); Vestn. Leningr. Univ. 22, 19 (1959).
2. V. S. Grechishkin. Influence of instrumental factors on the reproducibility of line form in nuclear quarupole resonance (LGU, NIFI); Vestn. Leningr. Univ. 10, 14 (1959).
3. V. V. Moskalev. Determination of the second moment of the absorption line from the derivative of the dispersion line (LGU, NIFI); Collected Reports of the Kazan' Conference on Magnetic Radiospectroscopy [in Russian], Kazan', 1960.
4. V. V. Frolov. Spectrometer for nuclear magnetic resonance in intermediate fields (LGU, NIFI); Vestn. Leningr. Univ. 10, 49 (1960).
5. N. M. Aleksandrov and V. V. Moskalev. Correction to the second moment of the nuclear magnetic resonance line with the use of a phase detector (LGU, NIFI); Vestn. Leningr. Univ. 10, 55 (1960).
6. V. V. Anufriev, M. P. Votinov, Yu. N. Tolparov, V. L. Maksimov, A. I. Savin, and A. V. Stafeev. Experience in the use of radiospectrometers for studying processes in dielectrics (Lengr. ped. inst.); Tr. Leningr. Elektrotekhn. inst., 1960.
7. V. M. Ryzhkov, O. O. Bronzov, and A. P. Stepanov. Nuclear magnetometer (Ural'sk. politekhn. inst.); Pribory i tekhnika éksperimenta 5, 41 (1960).
8. G. V. Skrotskii and A. A. Kokin. Possible role of coherent effects in magnetic resonance (Ural'sk. politekhn. inst.); Izv. vyssh. uch. zav., Radiofizika 3, 4, 650 (1960).
9. A. A. Kokin and G. V. Skrotskii. Constancy of the magnetomechanical ratio (Ural'sk. politekhn. inst.); Geofizicheskii pribor, 6 (1960).
10. A. A. Kokin, V. M. Ryzhkov, and G. V. Skrotskii. Possible use of the Overhauser effect for intensification of the free precession signal (Ural'sk. politekhn. inst.); Geofizicheskii pribor 6 (1960).
11. V. M. Ryzhkov and A. P. Stepanov. Errors of a geomagnetomer based on the free nuclear precession effect (Ural'sk. politekhn. inst.); Geofizicheskii pribor 6 (1960).

II. Electron Paramagnetic Resonance

12. V. V. Antuf'ev, M. P. Votinov, E. V. Kuvshinskii, and A. G. Savin. Study of the aging of titanium-containing ceramics by means of electron paramagnetic resonance (Leningr. ped. inst.); Fizika tverdogo tela 3, 286 (1961).
13. E. M. Lapinskaya, M. A. Khenokh, M. P. Votinov, V. F. Evdokimov, and V. V. Antuf'ev. Action of radiation from Co^{60} on hippuric acid in the solid state (Leningr. ped. inst.); Proceedings of 2nd All-Union Conference on Radiation Chemistry [in Russian] (Moscow, 1961).
14. M. P. Votinov, M. A. Khenokh, E. A. Kuzicheva, V. F. Evdokimov, and V. V. Antuf'ev. EPR spectra of γ-irradiated solid carbohydrates (Leningr. ped. inst.); Proceedings of the 2nd All-Union Conference on Radiation Chemistry [in Russian] (Moscow, 1961).
15. B. I. Liogon'kii, L. S. Lyubchenko, A. A. Berlin, L. A. Blyumenfel'd, and V. P. Parini. Electron paramagnetic resonance spectra of linear aromatic polymers (IKhF); Vysokomolek. soed. 2, 1494 (1960).
16. Yu. N. Molin, I. I. Chkheidze, N. Ya. Buben, and V. V. Voevodskii. EPR spectra of irradiated dicarboxylic acids (IKhF); Zh. strukt. khimii 2, 3, 293 (1961).

* The first part of this list was published in Zhurnal strukturnoi khimii 1, 2, 270 (1960). This, the second part of the list, contains publications reported to the Commission on Radiospectoscopy at the beginning of 1961.

17. V. N. Panfilov, Yu. D. Tsvetkov, and V. V. Voevodskii. Detection of hydrogen atom in a rarefied hydrogen flame by the EPR method (IKhF); Kinetika i kataliz 1, 333 (1960).
18. Yu. I. Pechetskaya and V. B. Kazanskii. Study of the thermal decomposition of chromic anhydride on alumina by the EPR method (IKhF); Zh. Fiz. khimii 34, 11, 3617 (1960).
19. L. A. Blyumenfel'd and V. A. Benderskii. Magnetic anddielectric properties of highly ordered macromolecular structures (IKhF); Dokl. AN SSSR 133, 1451 (1960).
20. F. P. Chernyakovskii, A. E. Kalmanson, and L. A. Blyumenfel'd. Electron paramagnetic resonance in triphenylmethane dyes (IKhF); Optika i spektroskopiya 9, 786 (1960).
21. Shén Péi-gen', L. A. Blyumenfel'd, and A. E. Kalmanson. Influence of denaturation and formation of complexes with proteins on the magnetic properties of nucleic acids (IKhF); Biofizika 5, 645 (1960).
22. V. L. Tal'roze and L. A. Blyumenfel'd. Relationship between the electrical conductivity of organic substances with conjugated bonds and EPR spectra (IKhF); Dokl. AN SSSR 135, 1450 (1960).
23. I. V. Aleksandrov. Hyperfine structure of the spectrum (IKhF); Optika i spektoskopiya, submitted June 27, 1960.
24. A. L. Buchachenko, Ya. S. Lebedev, and M. B. Neiman. Investigation of antioxidant radicals by the EPR method. 1. Phenoxy radicals (IKhF); Zh. strukt. khimii, submitted November 14, 1960.
25. Yu. D. Tsvetkov, Ya. S. Lebedev, and V. V. Voevodskii. Study of the physicochemical properties of irradiated polytetrafluoroethylene (IKhF); Proceedings of the 13th All-Union Conference on Spectroscopy [in Russian] (Izd. AN SSSR, Moscow, 1961).
26. Ya. S. Lebedev, Yu. D. Tsvetkov, and V. V. Voevodskii. Origin of the compensation effect in reactions of radical recombination in irradiated Teflon (IKhF); Kinetika i kataliz 1, 496 (1960).
27. Yu. D. Tsvetkov, Ya. S. Lebedev, and V. V. Voevodskii. Investigation of free radical reactions in irradiated Teflon. III. Reaction of recombination of fluoroalkyl and peroxide radicals (IKhF); Vysokomolek. soed. 3, No. 6 (1961).
28. V. B. Kazanskii, G. B. Pariiskii, V. V. Voevodskii, and A. I. Bunshtein. Study by the EPR method of the properties of hydrogen atoms adsorbed on silica gel surface (IKhF); Proceedings of the 13th All-Union Conference on Spectroscopy [in Russian] (Izd. AN SSSR, Moscow, 1961).
29. V. B. Kazanskii, G. B. Pariiskii, and V. V. Voevodskii. Study by the EPR method of the properties of hydrogen atoms adsorbed on silica gel surface (IKhF); Kinetika i kataliz 1, 539 (1960).
30. Yu. D. Tsvetkov, Ya. S. Lebedev, and V. V. Voevodskii. Study of radical recombination in irradiated Teflon (IKhF); Proceedings of Conference on Radiation Chemistry [in Russian] (Moscow, 1961).
31. V. V. Voevodskii. Mechanism of the radiolysis of water (IKhF); Kinetika i kataliz, submitted October 14, 1960.
32. N. Ya. Buben, A. T. Koritskii, and V. I. Shamshev. Effect of additions on low-temperature radiolysis of polyethylene (IKhF); Proceedings of the 2nd Conference on Radiation Chemistry [in Russian] (Moscow, 1961).
33. V. B. Kazanskii, G. B. Pariiskii, and V. V. Voevodskii. EPR study of the properties of hydrogen atoms and defects formed during irradiation of silica gel (IKhF); Proceedings of the 2nd Conference on Radiation Chemistry [in Russian] (Moscow, 1961).
34. Yu. I. Molin, I. I. Chkheidze, N. Ya. Buben, and V. V. Voevodskii. EPR study of energy transfer to aromatic groups in radiolysis of certain organic compounds (IKhF); Kinetika i kataliz 2, 192 (1961).
35. O. P. Samoilova and L. A. Blyumenfel'd. Changes in the magnetic properties of a yeast culture during growth and cell division (IKhF); Biofizika 6, 15 (1961).
36. Yu. I. Molin. Role of the reaction of hydrogen atoms in radiolysis (IKhF); Kinetika i kataliz, submitted October 31, 1960.
37. Yu. I. Molin and V. K. Ermolaev. Causes of changes of proton relaxation time in aqueous solutions during radiolysis (IKhF); Kinetika i kataliz 2, No. 3 (1961).
38. A. L. Bubachenko, M. B. Neiman, and Ya. S. Lebedev. Investigation of radical reactions of antioxidants in the liquid phase by the EPR method (IKhF); Tr. po khimii i khim. tekhnologii 1, 37 (1961).
39. A. N. Nesmeyanov, V. V. Korshak, V. V. Voevodskii, N. S. Kochetkova, S. L. Sosin, R. B. Materikova, T. N. Bolotnikova, V. M. Chibrikin, and N. M. Bazhin. Synthesis and certain opticomagnetic properties of ferrocene polymers (IKhF); Dokl. AN SSSR 137, 1370 (1961).
40. I. V. Aleksandrov and G. M. Zhidomirov. Calculation of the time of spin lattice relaxation for radicals in molecular crystals (IKhF); Zh. éksperim. i teor fiziki, submitted December 8, 1960.
41. I. V. Aleksandrov and G. M. Zhidomirov. Theory of spin lattice relaxation in radicals in liquids (IKhF); Zh. éksperim. i teor. fiziki, submitted December 8, 1960.
42. G. A. Kapralova and A. E. Shilov. Radical formation in reactions of molecular fluorine with hydsocarbons at the temperature of liquid nitrogen (IKhF); Kinetika i kataliz 2, No. 3 (1961).

43. Shén pĕi-gen*, L. A. Blyumenfel'd, A. É. Kalmanson, and A. G. Pasynskii. EPR spectra of biological materials. IV (IKhF); Biofizika, submitted January 5, 1961.
44. A. I. Burshtein. Interaction of white light with matter (IKhF); Zh. éksperim. i teor. fiziki, submitted January 10, 1961.
45. A. I. Burshtein. External relaxation (IKhF); Zh. éksperim. i teor. fiziki, submitted January 10, 1961.
46. V. V. Azatyan, V. I. Panfilov, and A. B. Nalbandyan. Detection of hydrogen atoms in a carbon monoxide and oxygen flame with added molecular hydrogen, by the EPR method (IKhF); Kinetika i kataliz 2, 295 (1961).
47. G. M. Zhidomirov, Yu. D. Tsvetkov, and Ya. S. Lebedev. Study of internal movements in polyisobutylene by the EPR method (IKhF); Zh. strukt. khimii, submitted January 26, 1961.
48. Z. S. Egorova, Yu. M. Malinskii, V. L. Karpov, A. É. Kalmanson, and L. A. Blyumenfel'd. Chemical changes in polyvinyl chloride under the influence of ionizing radiations (IKhF); Vysokomol. soed. 2, 891 (1960).
49. I. S. Zyryanov, T. G. Izyumova, and G. V. Skrotskii. Influence of electron resonance on optical properties of paramagnetic and ferromagnetic substances (Ural'sk. politekhn. inst.); Izv. vyssh. uch. zav., Fizika, 3, 32 (1960); Izd. Tomsk. univ.
50. Yu. A. Izyumov and G. V. Skrotskii. Form of the electron paramagnetic resonance line in ferromagnetic substances (Ural'sk. politekhn. inst.); Fizika tverdogo tela 2, 1766 (1960).
51. A. A. Kokin. Magnetic resonance in systems having electronic and nuclear paramagnetism simultaneously (Ural'sk. politekhn. inst.); Izv. vyssh. uch. zav., Fizika, 4, 198 (1960).
52. A. K. Chirkov and A. A. Kokin. Form of the electron resonance lines in systems of particles with an anisotropic g factor (Ural'sk. politekhn. inst.); Zh. éksperim. i teor. fiziki 39, 1381 (1960).

III. Nuclear Magnetic Resonance

53. I. M. Aleksandrov and F. I. Skripov. Nuclear magnetic resonance in polycrystalline carbon monofluoride (LGU, NIFI); Vestn. Leningr. univ. 22, 59 (1959).
54. I. M. Aleksandrov. Nuclear magnetic resonance in polycrystalline diaspore and carbon monofluoride (LGU, NIFI); Vestn. Leningr. univ. 22, 24 (1959).
55. V. S. Grechishkin. A new application of nuclear resonance (LGU, NIFI); Priroda, 8, 85 (1959).
56. F. I. Skripov. Some aspects of the theory of a nuclear resonance generator with a moving specimen (LGU, NIFI); Collection, p. 126.
57. A. V. Mel'nikov, A. A. Morozov, and F. I. Skripov. Further investigations with a high resolving force, carried out in the earth's magnetic field (LGU, NIFI); Collection, p. 146.
58. I. M. Aleksandrov and F. I. Skripov. Determination of the structure parameters of certain crystals by the nuclear magnetic resonance method (LGU, NIFI); Collection, p. 176.
59. P. M. Borodin and F. I. Skripov. Relationships in the chemical shifts of nuclear magnetic resonance of fluorine in its aliphatic compounds (LGU, NIFI); Collection, p. 190.
60. Van I-tsyu and F. I. Skripov. Effect of concentration on the magnetic shielding of F^{19} nuclei in the systems $KHF_2 - H_2O$ or $KHF_2 - KF - H_2O$ (LGU, NIFI); Dokl. ANSSSR 136, 58 (1961).
61. Van I-tsyu. Chemical shifts of the nuclear magnetic resonance signals of fluorine in ionic crystals (LGU, NIFI); Dokl. AN SSSR 136, 317 (1961).
62. I. V. Aleksandrov. Influence of tunnel transitions on the form of the NMR line in crystals (IKhF); Dokl. AN SSSR 133, 1057 (1961).
63. L. M. Yagupol'skii, V. F. Bystrov, and É. Z. Utyanskaya. Investigation of chemical shifts of the magnetic resonance of F^{19} in fluorobenzenes with fluorine-containing substituents (IKhF); Dokl. AN SSSR 135, 377 (1960).
64. É. Z. Utyanskya. Proton magnetic resonance spectrum of pentaethanodiferrocene (IKhF); Zh. fiz. khimii, submitted November 2, 1960.

IV. Nuclear Quadrupole Resonance

65. V. S. Grechishkin and F. I. Skripov. Application of nuclear quadrupole resonance to determination of lattice vibration frequencies in a series of chlorates (LGU, NIFI); Dokl. AN SSSR 126, 1229 (1959).
66. V. S. Grechishkin. Observation of line form in purely quadrupole resonance (LGU, NIFI); Pribory i tekhika éksperimenta 2, 31 (1959).

*For abbreviations, see the first part of the list [Zh. strukt. khimii 1, 2, 270 (1960)].

67. V. S. Grechishkin. Width of the quadrupole resonance line of chlorine in barium, sodium, and potassium chlorates (LGU, NIFI); Zh. éksperim. i teor fiziki 36, 636 (1959).
68. V. S. Grechishkin. Nuclear quadrupole resonance (LGU, NIFI); Uspekhi fiz. nauk 69, 189 (1959).
69. V. S. Grechishkin and F. I. Skripov. Application of nuclear quadrupole resonance to investigations of electric field gradient in a number of crystals (LGU, NIFI); Collection, p. 160.

V. Ferromagnetic Resonance

70. G. V. Skrotskii and T. G. Izyumova. Kerr magnetooptical effect in a ferromagnetic material in a radiofrequency field (Ural'sk. politekhn. inst); Fizika tverdogo tela 2, 1732 (1960).
71. G. V. Skrotskii and L. V. Kurbatov. Influence of long-range fluctuations on the relationship between temperature and the width of the ferromagnetic resonance absorption line (Ural'sk. politekhn. inst.); Fizika metallov metallovedenie 10, No. 3 (1960).
72. G. V. Skrotskii and T. G. Izyumova. Theory of the Faraday optical effect in ferromagnetic single crystals of garnet in a multifrequency field. (Ural'sk. politekhn. inst.); Fizika tverdogo tela 2, 10 (1960).

All abbreviations of periodicals in the above bibliography are letter-by-letter transliterations of the abbreviations as given in the original Russian journal. *Some or all of this periodical literature may well be available in English translation.* A complete list of the cover-to-cover English translations appears at the back of this issue.

INTERNATIONAL UNION OF CRYSTALLOGRAPHY

COMMISSION ON CRYSTAL STRUCTURE DATA

LIST OF 1956 PUBLICATIONS CONTAINING NEW DATA ON CRYSTAL STRUCTURES

Translated from Zhurnal Strukturnoi Khimii, Vol. 2, No. 3, pp. 386-392, May-June, 1961

C. ORGANIC COMPOUNDS

1. Abrahams S. C., Grenville-Wells H. J., Cr. str. of diphenyl sulfoxide. Technical Report 105. Laboratory for Insulation Research. Mass. Inst. of Technology, May 1956.
2. Abrahams S. C., Robertson J. M., Cr. str. of p-nitroaniline. Acta Cryst. 9, 986.
3. Abrahams S. C., Silverton J. V., Crystallogr. study of diphenyl sulphoxide – diphenyl sulphone syst. Acta Cryst 9, 281.
4. Abrahams S. C., Speakman J. C., Crystallogr. study of trimethylsulphonylmethane. J. Chem. Soc., 2562.
5. Abrahamsson S., On cr. str. of 9DL-methyloctadecanoic acid. Acta Cryst. 9, 663.
6. Alderman P. R. H., Owston P. G., Square pyramidal configuration in five-coord. nitrosyl complex. Nature 178, 1071.
7. Alexander L. E., Pitman D. T., Cr. str. of dialuric acid monohydrate. Acta Cryst. 9, 501.
8. Almenningen A., Bastiansen O., Accuracy of e. diffrn. method for detn. of str. pars. in gaseoud state. Supplement to Research 9, 9, S35.
9. Almenningen A., Bastiansen O., Munthe-Kass T., Str. pars. of dimethyldiacetylene. Acta Chem. Scand. 10, 261.
10. Amórós J. L., Canut M. L., Estudios acerca de la dinámica reticular en cristales moleculares. III. Relaciones entre dilatación térmica, vibraciones atómicas y radiación difusa en al ácido Oxálico dihidratado. IV. Crecimiento de los cristales de ácido Adípico. Publ. dept. crist. mineral., Barcelona 2, 155, 223.
11. Andresen E. K., Lindqvist I., Cr. str. of hexathiaadamantane, $(CH)_4S_6$. Arkiv. Kemi 9, 169.
12. Astbury W. T., Pautard F. G. E., Extraneous X-ray diffrn. pats. from algal flagella. Nature 178, 372.
13. Bacon G. E., Curry N. A., Study of α-resorcinol by n. diffrn. Proc. Roy. Soc., Ser. A 235, 552.
14. Bader A. R., Gutowsky H. S., Heeschen J. P., Proton magn. resonance a. str. of diketene – acetone adduct. J. Org. Chem. 21, 821.
15. Bader A. R., Gutowsky H. S., Williams G. A., Yankwich P. E., Proton magn. resonance spectrum a. str. of diketene. J. Am. Chem. Soc. 78, 2385.
16. Bak B., Christensen D., Hansen L., Rastrup-Andersen J., Microwave detn. of str. of pyrrole. J. Chem. Phys. 24, 720.
17. Bak B., Christensen D., Rastrup-Andersen J., Tannenbaum E., Microwave spectra of thiophene, 2- a. 3-monodeutero-, 3,3'-dideutero-, a. tetradeuterothiophene. Str. of thiophene mol. J. Chem. Phys. 25, 892.
18. Baker R. F., Fine str. of tobacco mosaic virus. Nature 178, 636.
19. Barbezat Mme. S., Jacquot Mme. A., Salmon J., Contribution des r. X a l'etude des constituants cristallisés des végétaux. Bull. Soc. franç. minéral. et crist. 79, L.
20. Barrer R. M., Intracr. free volumes in some host lats. Nature 178, 1410.
21. Bartunek R., Über d. wechselden Gehalt d. Natronlaugen an NaOH-Hydraten u. d. Ausbild. verschiedenartiger Röntgendiagramme v. Natronzellulosen. Kolloid. Z. 146, 35.
22. Bear R. S., Selby C. C., Str. of paramyosin fibrils according to X-ray diffrn. J. Biophys. Biochem. Cytol 2, 55.
23. Bekoe D. A., Hulme R., Cr. str. of p-chlorbenzene iododichloride. Nature 177, 1230.
24. Bernal J. D., Symmetry of azulene crs. Nature 177, 40.
25. Bertinotti F., Giacomello G., Liquori A. M., Str. of heterocyclic compds. containing N. I. Cr. a. mol. str. of s-tetrazine. Acta Cryst. 9, 510.
26. Bertinotti F., Liquori A. M., Pirisi R., Struttura di molecole eterocicliche azotate. Struttura cristallina dell α'-α'-dipiridile. Gazz. chim. ital. 86, 893. (Ital.).
27. Bireswarbanerjee, Priyadaranjanray. Complex compds. of bi-positive Ag with pyridine carboxylic acids. I. Argentic nicotinate a. isonicotinate. J. Indian Chem. Soc. 33, 503.

28. Blakeslee A. E., Hoard J. L., Str. of Ag-perfluorobutyrate. J. Am. Chem. Soc. 78, 3029.
29. Bluhm, M. M., Kendrew J. C., Cr. forms a. mol. weight of α-chymotrypsinogen. X-ray study. Biochim. Biophys. Acta 20, 562.
30. Borgen O., Preliminary X-ray investn. of naphthazarine. Acta Chem. Scand. 10, 887.
31. Brandt, J. L., Livingston R. L., E. diffm.investn. of mol. str. of 1,1 -trifluoroethane. J. Am. Chem. Soc. 78, 3573.
32. Brown, R. N., N-chloro-succinimide. Acta Cryst. 9, 193.
33. Bryden J. H., Cr. str. of 2-methyl-5-aminotetrazole. Acta Cryst. 9, 874.
34. Bryden J. H., Burkhardt L. A., Hughes E. W., Donohue J., Cr. str. of nitroguanidine. Acta Cryst. 9, 573.
35. Bryden J. H., McCullough J. D., Cr. str. of p-chlorobenzeneseleninic acid. Acta Cryst. 9, 528.
36. Buerger M. J., Barney E., Hahn T., Cr. str. of diglicine hydrobromide. Z. Krist. 108, 130.
37. Bullen G. J., Trinuci. mols. in cr. str. of bisacetylacetonenickel (II). Nature 177, 537.
38. Burkhardt L. A., X-ray diffm. pats. of some guanidine derivatives. Anal. Chem. 28, 323.
39. Burki H., Nowacki W. D., Kr.-str. v. linksdrehendem (=α) 7-Bromocholesterylbromid, -chlorid u. -methyläther (isotype Reihe). Z. Krist. 108, 206.
40. Burns D. M., Iball J., Bond lengths in chrysene. Acta Cryst. 9, 314.
41. Cant E. M., Note on cyclo-(hexaglycyl). Acta Cryst. 9, 681.
42. Carlisle C. H., Shrinkage of ribonuclease. Acta Cryst. 9, 974.
43. Carlisle C. H. Ehrenberg M., Preliminary X-ray investn. of prestimerin. Acta Cryst. 9, 323.
44. Caspar D. L. D., Str. of tobacco mosaic virus. Radial density distribn. in tobacco mosaic virus particle. Nature 177, 928.
45. Caspar D. L. D., Str. of busy stunt virus. Nature 177, 475.
46. Chaudhuri B., Hargreaves A., Cr. a. mol. str. of bishydroxydurylmethane. Acta. Cryst. 9, 793.
47. Clar E., Kelly W., Robertson J. M., Rossmann M. G., Circumanthracene a. dinaphtho (7' : 1'-1 : 13) (1" : 7"-6: 8)-peropyrene. J. Chem. Soc., 3878.
48. Cochran W., Comparison of calculated a. measured e. distribns. in benzene ring. Acta Cryst. 9, 924.
49. Cohen C., Hanson J., X-ray diffm. study of F-actin. Biochizi. Biop ;. Acta 21, 177.
50. Cotbridge D. E. C., Cox E. G., Five-covalent terpyridyl complexes of bivalent mets. I. Stereochem. of Zn, Cd, a. Cu compds. J. Chem. Soc., 594.
51. Corsmit A. F., Schuyff A., Feil D., On cr. str. of L-cystine hydrochloride. Proc. Konikl. Ned. Akad. Wetenschap. Ser. B, 59, 479.
52. Crick F. H. C., Ox haemoglobin; preliminary X-ray studies. Acta Cryst. 9, 908.
53. Crick F. H. C., Watson J. D., Str. of small viruses. Nature 177, 473.
54. Crowfoot-Hodgkin D., X-ray anal. of str. of vitamin B_{12}. Anal. Chem. 28, 270.
55. Cruickshank D. W. J., Detailed refnt. of cr. a. mol. str. of anthracene. Acta Cryst. 9, 915.
56. Cruickshank D. W. J., Variation of vibration amplitudes with temp. in some mol. crs. Acta Cryst. 9, 1005.
57. Cruickshank D. W. J., Entropy of cr. naphthalene. Acta Cryst. 9, 1010.
58. Culpin M. F., Kemp K. W., Orientation of str. of 6.6 nylon fibres. Proc. Phys. Soc. Lond. 69B, 1301.
59. Davies D. R., Pasternak R. A., Refnt. of cr. str. of succinamide. Acta Cryst. 9, 334.
60. Dean C., Lindstrand E., Polymorphism of para-dichlorobenzene. J. Chem. Phys. 24, 1114.
61. Dégellh R., Pickworth J., U. c. dims. a.sp.grs. of some simple peptides. Acta Cryst. 9, 828.
62. Delbouile L., Str. of hexafluorobenzene mol. J. Chem. Phys. 25, 182.
63. Dodgen H. W., Ragle J. L., Obsn. of hindered rotation in solid 1,2-dichloroethane by nucl. quadrupole resonance. J. Chem. Phys. 25, 376.
64. Dolmetsch H., Elemente d. Feinstr. natürlicher Zellulosefasern in hochverdünnten Lösg. Kolloid. Z. 145, 141.
65. Donohue J., Lavine L. R., Rollett J. S., Cr. str. of histidine hydrochloride monohydrate. Acta Cryst. 9, 655.
66. Donohue J., Trueblood K. H., Cr. str. of p-nitroaniline. Acta Cryst. 9, 960.
67. Dunitz J. D., Orgel L. E., Rich A., Cr. str. of ferrocene. Acta Cryst. 9, 373.
68. Dunitz J. D., Rollett J. S., Cr. str. of dibenzyl phosphoric acid. Acta Cryst. 9, 327.
69. Eeles W. T., Str. of 4,5-dimethyl phthalic thio-anhydride. Acta Cryst. 9, 365.
70. Ehrlich H. W., Beevers C. A., Cr. str. of 2 : 13-benzfluoranthene. Acta Cryst. 9, 602.
71. Eia G., Hassel O., Str. of addition compd. containing two Br mols. a. one mol. of hexamethylene tetramine. Acta Chem. Scand. 10, 139.
72. Eichborn E. L., On str. of 4-nitropyridine-N-oxide. Acta Cryst. 9, 787.
73. Feitknecht W., Zur Kenntnis d. Metallhydroxyd-Einschlussverbb. I. Über Zn-Hydroxydflavianate. II. Über d. Bau d. Zn-Hydroxydflavianate. III. Über einige Hydroxydflavianate zweiwert. Metalle. IV. Über weitere aromat. Hydroxydsalze d. Zn. Helv. Chim. Acta 39, 564; 576; 584; 589.

74. Font-Altaba M., Estrutura cristalina del derivado manganoso de la O-Bencensulfonimida. II. Publ. dept. cryst. mineral., Barcelona 2, 163.
75. Foss O., Sp. grs. a. mol. symmetries of two thiocyanates. Acta Chem. Scand. 10, 136.
76. Foss O., X-ray crystallogr. data on certain five-membered cyclic disulphides. Acta Chem. Scand. 10, 871.
77. Foss O., X-ray crystallogr. data on Na a. K thiosulphonates. Acta Chem. Scand. 10, 868.
78. Foss O., Tjomsland O., Solvates of Ba-pentathionates with acetone a. tetrahydrofuran. Acta Chem. Scand. 10, 424.
79. Foss O., Tjomsland O., Str. of thiuret hydroiodide. Acta Chem. Scand. 10, 869.
80. Foss O., Tjomsland O., Solvates of Ba-pentathionates with ethanol. Acta Chem. Scand. 10, 421.
81. Franklin R. E., X-ray diffrn. studies of cucumber virus 4 a. three strains of tobacco mosaic virus. Biochim. Biophys. Acta 19, 203.
82. Franklin R. E., Location of ribonucleic acid in tobacco mosaic virus particle. Nature 177, 928.
83. Franklin R. E., King A., Nature of helical groove on tobacco mosaic virus particle. X-ray diffrn. studies. Biochim. Biophys. Acta 19, 403.
84. Fredga A., Olsson K., Hexathia-adamantane. Arkiv Kemi. 9, 163.
85. Frey H. M., Deuteration of azulene a. str. of azulinium ion. J. Chem. Phys. 25, 600.
86. Friedlander P. H., Robertson J. M., Cr. str. of dimethylketen dimer. J. Chem. Soc. 8, 3083.
87. Friedlander P. H., Sayre D., Cr. str. of 1 : 2-benzanthracene. Nature 179, 999.
88. Frossard L., Etude du trioxalatochromiate de Na et de Mg. Schweiz. mineral. petrog. Mitt. 36, 1.
89. Furberg S., Hordvik A., Taugbøl K., X-ray crystallogr. data on some nucleic acid components. Acta Chem. Scand. 10, 135.
90. Giacomello G., Liquori A. M., Ripamonti A., Isosterism a. mol. Fourier transforms cr. str. detn. of 2,4-dihydroxybenzoic acid as related to that of 2-hydroxy-4-aminobenzoic acid. Nature 177, 944.
91. Gilbert R. E., Lonsdale K., Anisotropic temp. vibrations in crs. I. Direct measrts. of Debye fs. for urea. Acta Cryst. 9, 697.
92. Gilmour A., Jobling A., Nelson S. M., Al tri-soaps. J. Chem. Soc., 1972.
93. Go Y., Noguchi J., Asai M., Hayakawa T., (Glycyl-L-alanyl)-polymer resembling cr. part of silk fibroin. Confirmation of Meyer-Mark model. J. Polym. Sci. 21, 147.
94. Goldish E., Hedberg K., Schomaker V., Mol. str. of cyclobutene, C_4H_6. J. Amer. Chem. Soc. 78, 2714.
95. Gould E. S., Post B., Cr. str. of trans-ethanediseleninic anhydride. J. Amer. Chem. Soc. 78, 5161.
96. Grant D. F., Rogers D., Str. of hydroxydihydroeremophilone. Chem. and Ind. (London) 15, 278.
97. Green D. W., North A. C. T., Aschaffenburg R., Crystallogr. of β-lactoglobulines of cows' milk. Biochim. Biophys. Acta 21, 583.
98. Greene-Kelly R., Montmorillonite complexes with saturated ring compds. J. Phys. Chem. 60, 808.
99. Grenville-Wells H. J., Anisotropic temp. vibrations in crs. II. Effect of changes in at. scatrg. fs. a. temp. pars. on accuracy of detn. of str. of urea. Acta Cryst. 9, 709.
100. Gribova E. A., Zhdanov G. S., Gol'der G. A., X-ray str. investn. of indigo and thioindigo. Kristallografiya 1, 53.
101. Grunwald E., Lowenstein A., Meiboom S., Study of protolysis of methylammonium ion in water by proton magn. esonance. J. Chem. Phys. 25, 382.
102. Gupta M. P., Cr. strs. of K a. Rb hydrogen fumarates. Acta Cryst. 9, 263.
103. Gupta M. P., Barnes W. H., U. c., sp. gr. a. indexed X-ray diffrn. powd. data for K hydrogen malonate, $KHC_3H_2O_4$. Canad. J. Chem. 34, 563.
104. Hall, D., Lewellyn F. J., Cr. str. of formamidoxime. Acta Cryst. 9, 108.
105. Halla F., Ruston W. R., Tassel R. van., Zur Kristallographie d. Lävoglukosans. Acta Cryst. 9, 768.
106. Hamor T. A., Robertson J. M., Cr. a. mol. str. of pteridine. J. Chem. Soc., 3586.
107. Harris, C. M., Nyholm R. S., Stephenson, N. C., Some new stereochem. arrgts. of divalent Pd. a. Pt. Nature 177, 1127.
108. Hassel O., Hvoslef J., Str. of addition cmpd. containing two mols. of iodine monochloride a. one mol. of 1,4-dioxan. Acta Chem. Scand. 10, 138.
109. Hassel O., Rømming C., [Trans] naphthodioxan characterized by its Hg chloride compd. Acta Chem. Scand. 10, 136.
110. Hassel O., Rømming C., Str. of 1 : 1-compd. pyridine-I-monochloride. Acta Chem. Scand. 10, 696 (Corrections — Ibid., 1957, 11, 195).
111. Hedberg K., Mol. str. of trisilylamine $(SiH_3)_3N$. J. Am. Chem. Soc. 77, 6491.

112. Hermans P. H., Weidinger A., E. quantitativer Vergleich d. Weitwinkel-Röntgenstreuung d. Celluloseanteiles in gequollenen u. trockenen Reyonfasern. Makromol. Chem. 17, 18, 75.
113. Hexter R. M., Relative magnitude of cr. fields; cr. str. of methyl iodide. J. Chem. Phys. 25, 1288.
114. Hine R., Rogers D., Cr. a. mol. str. of (+)-S-methyl-L-cysteine S-oxide; standard of absolute configuration for asymmetric S. Chem. and Ind. (London), 1428.
115. Hirshfeld F. L., Schmidt G. M. J., Three examples of accurate cr.-str. anal. by low-temp. X-ray photography. Acta Cryst. 9, 233.
116. Hodgkin D. S., Kamper J., Mackay M., Pickworth J., Trueblood K. N., White J. G., Str. of vitamin B_{12}. Nature 178, 64.
117. Holden, J. R. Baenziger N. C., Partial str. of bis-benzonitrile Pd chloride. Acta Cryst. 9, 194.
118. Hoogsteen K., U. c. dims. a. sp. gr. of 6-mercaptopurine monohydrate. Nature 178, 379.
119. Hoppe W., Str.-analyse starrer Atom-gruppen (Moleküle) durch Unters. d. diffusen Röntgenstreung an elast. Wärmewellen in Kristallen. D. diffuse Streuung d. Anthrachinonmoleküls. Z. Krist. 107, 433.
120. Horton W. S., Uranyl cupferrates. J. Am. Chem. Soc. 78, 897.
121. Housty J., Polymorphisme du paradichlorobenzene et str. de sa forme tricl. J. phys. radium 17, 12, S49.
122. Housty J., Clastre J., Str. de la forme tricl. du paradichlorobenzene. Compt. rend. 242, 267; Cahiers phys. 74, 28.
123. Iball J., Young D. W., Str. of 3 : 4-benzpyrene. Nature 177, 985.
124. Immergut, E. A. Ranby, B. G., Heterogeneous acid hydrolysis of nature cellulose fibers. Ind. Eng. Chem. 48, 1183.
125. Iton T., Mol. str. of methylamine. J. Phys. Soc. Japan 11, 264.
126. Jensen L. H., Cr. str. of n-dodecanoic acid hydrazide. J. Am. Chem. Soc. 78, 3993.
127. Jones R. E., Cr. str. of acetic acid. Univ. of California Radiation Lab., 3641.
128. Jones F. T., Black D. R., White L. M., D-Fructose2,4-dinitrophenylhydrazone dioxane solvate. Anal. Chem. 28, 268.
129. Joos P., Laue-Klasse u. Raumgruppe v. Thymol, $C_{10}H_{14}O$. Z. Krist. 107, 238.
130. Jost K. H., Röntgenstr.-analyse d. Chamazulens. Naturwiss 43, 224.
131. Kabalkina S. S., Cr. str. of copper dipyridine dichloride. Dokl. AN SSSR 110, 1013.
132. Kargin, V. A., Koretskaya T. A., E. micr. and e. diffn. investn. of spherulite forms. and crystallites in cr. polymers. Dokl. AN SSSR 110, 1015.
133. Katayama M., Cr. str. of unstable form of chloroacetamide. Acta Cryst. 9, 986.
134. Kay M. I., Katz, L., Cr. data for two new coordn. compds. Acta Cryst. 9, 822.
135. Kendrew J. C., Parrish R. G., Cr. str. of myoglobin. III. Sperm-whale myoglobin. Proc. Roy. Soc., Ser. A 238, 305.
136. Kendrew J. C., Pauling P. J., Cr. str. of myoglobin. II. Finback whale myoglobin. Proc. Roy. Soc., Ser. A 237, 255.
137. Khotsyanova T. L., Cr. str. of diphenyliodonium chloride and iodide. Dokl. AN SSSR 110, 71. Kristallografiya. 1, 524.
138. Khotsyanova T. L., Struchkov Yu. T., Cr. str. of tetraphenylphosphonium iodide and confign. of tetraaryl ions and mols. Kristallografiya 1, 669.
139. Khubchandani P. G., U. c. a. sp. gr. of Al- a. Co-acetylacetonate. Curr. Sci. 25, 285
140. Kilkson R., Hutchinson F., Radial str. of cucumber virus no. 4. Bull. Am. Phys. Soc. 1, 200.
141. Kimura M., Kimura K., Shibata S., On bond length a. mean square amplitude of C-O bond in methyl alcohol. J. Chem. Phys. 24, 622.
142. King M. V., Magdoff B. S., Adelman M. B., Harker D., Cr. forms of bovine pancreatic ribonuclease: techniques of prepn., u. cs., a. sp. grs. Acta Cryst 9, 460.
143. Koide T., Oda T., Nitta J., Phys. props. a. cr. str. of 1,1,1,2-tetrachloro-2-methylpropane. Bull. Chem. Soc. Japan 29, 738.
144. Kondo S., X-ray study on thiacyclohexane. Bull. Chem. Soc. Japan 29, 999.
145. Kratky O., Best. d. Gestalt v. korpuskularen u. fadenförmigen Makromolekülen nach d. Röntgen-Kleinwinkelmethode. Z. Electrochem. 60, 245.
146. Kratky O., Zur molekularen Morphologie d. Seidenfibroin. Mh. Chem. 87, 269.
147. Kratky O., Röntgen-Kleinwinkelunters. d. nativen Seidengels. IV. Z. Naturf. 11, 10.
148. Kratky O., Porod G., Zur Kleinwinkelstreuung d. Cellulose. Z. Electrochem. 60, 188.

149. Kratky O., Schauenstein E., Lipoide im Seidenfibroin. Fette, Seifen, Anstrichmittel 58, 229.
150. Kratky O., Sembach H. D., Verknäuelungsgrad v. gelöstem Cellulosenitrat nach d. Röntgen-Kleinwinkelmethode. Makromol. Chem. 17, 18, 469.
151. Krause B., Renninger M., Kr.-git.-modelle infolge v. elektr. bei Kristallisation. Acta Cryst. 9, 74.
152. Kre I., Jr., Hinch R., Jr. Crystallogr. data. 102. m-Aminophenol (3-aminophenol). Anal. Chem. 28, 137.
153. Krimm S., Schot R., Str. of feather keratin. J. Chem. Phys. 24, 922.
154. Krishna Murti G. S. R., Cr. str. of anthracene at different temps. Indian J. Phys. 30, 537.
155. Krishna Murti G. S. R., Sen S. N., On cr. str. of para-dichloro-benzene at different temps. Indian J. Phys. 30, 242.
156. Krogh-Andersen E., Lindquist I., Cr. str. of hexathiaadamanthane, $(CH)_6S_3$. Arkiv Kemi. 9, 169.
157. Labaw L. W., Wyckoff R. W. G., E. micr. of protein crs. Proc. Konikl. Ned. Akad. Wetenschap., Ser. B 59, 171.
158. Ladell J., McDonald T. R. R., Schmidt G. M. J., Cr. str. of α-trans-cinnamic acid. Acta Cryst. 9, 195.
159. Lang A. R., X-ray study of α-keratin. I. General diffrn. theory for convoluted chain strs. a. approximate theory for coiled coils. II. Diffractometer measrts. of complete diffrn. pat. of Canadium porcupine quill. Acta Cryst. 9, 436; 446.
160. Lin Chun Chia, Kilb R. W., Microwave spectrum a. internal barrier of acetaldehyde. J. Chem. Phys. 24, 631.
161. Liquori A. M., Ripamonti, A., Un metodo per determinare la posizione della molecole nei cristalli organici direttamenti dalle intensità dei riflessi di diffrazione. Ric. sci. 26, 1442 (Ital.).
162. Livingston R. L., Lyon D. H., E. diffrn. investn. of mol. str. of dichlorodifluoromethane. J. Chem. Phys. 24, 1283.
163. Livingston R. L., Vaughan G., E. diffrn. investn. of mol. str. of trifluoroethanol. J. Am. Chem. Soc. 78, 2711.
164. Livingston R. L., Vaughan G., Mol. str. of perfluorotrimethylamine by e. diffrn. J. Am. Chem. Soc. 78, 4866.
165. Lonsdale K., Grenville-Wells H. J., Anisotropic temp. fs. in cub. crs. Nature 177, 986.
166. Loretan M., Note sur la phase hex. de l'isomère δ de l'hexachlorocyclohexane. Schweiz. mineral. petrog. Mitt. 36, 26.
167. Lovell F. M., Crystallogr. data for certain alkaloids. V. Some Delphinium alkaloids. Acta Cryst. 9, 85.
168. Low B. W., Approach to X-ray cr. str. study of proteins. Anal. Chem. 28, 1057.
169. Low B. W., Richards F. M., Berger J. E., Some studies of protein crs. in variety of different media. J. Am. Chem. Soc. 78, 1107.
170. Lynton H., Cox, E. G., Cr. a. mol. str. of thianthren, J. Chem. Soc. 12, 4886.
171. Magdoff B. S., Crick F. H. C., Luzzati V., Three-dim. Patterson function of ribonuclease. II. Acta Cryst. 9, 156.
172. Mason R., Cr. a. mol. str. of succinimide $C_4H_5O_2N$. Acta Cryst. 9, 405.
173. Matthews R. E. F., Home R. W., Green E. M., E. micr. obsn. of periodicities in surface str. of tobacco mosaic virus. Nature 178, 635.
174. Mazzi F., Jona F., Pepinsky R., X-ray study of nonferroelectr. phases of Rochelle salt. Bull. Am. Phys. Soc. 1, 131.
175. Meal H. C., Zeeman quadrupole spectra of p-chloroaniline a. p-chlorobenzylchloride. J. Chem. Phys. 24, 1011.
176. Meggy A. B., Sikirski J., Dimorphism of polyglycine. Nature 177, 326.
177. Menter J. W., Direct study by e. micr. of cr. lats. a. their imperfections. Proc. Roy. Soc., Ser. A 236, 119.
178. Merritt L. L., Jr., Guare C., Lessor A. E. Jr., Cr. str. of Ni salicylaldoxime. Acta Cryst. 9, 253.
179. Merritt L. L., Jr., Schröder E., Crystallogr. data for salicylaldoxime $C_7H_7O_2N$. Acta Cryst. 9, 194.
180. Merritt L. L., Jr., Schröder E. D., Cr. str. of 2,2'-bipyridine. Acta Cryst. 9, 801.
181. Mezharaup G. P., Ievin'sh A. F., Tetraphenyl borates of ammonium, K, Rb, and Cs. Uch. zap. Latv. univ. 9, 49.
182. Mitchell J., Jr., Ryland A. L., Identfn. of org. compds. by micr. a. X-ray diffractometry. Mikrochim. Acta 1-3, 422.
183. Mitra G. B., Basak M. G., X-ray diffrn. study of α-yohimbine. Proc. Indian Sci. Congr. 43, 39.
184. Mokhov N. V., Kirsh N. V., X-ray diffrn. investn. of syst. phenol – water. Zh. fiz. khim. 30, 1319.
185. Moore E. B., Jr., Lipscomb W. N., Cr. a. mol. str. of $Cl_2BC_2H_4BCl_2$. Acta Cryst. 9, 668.
186. Morino Y., Miyagawa I., Chiba T., Shimozawa T., Pure quadrupole spectra of isomers of benzene hexachloride. J. Chem. Phys. 25, 185.
187. Nakatsu K., Saito Y., Kuroya H., Studies on crs. of met. tris-ethylenediamine complexes. I. Cr. str. of DL-tris-ethylenediamine-cobalt (III)-chloride trihydrate, $[Coen_3]Cl_3 \cdot 3H_2O$. Bull. Chem. Soc. Japan 29, 428.
188. Nardelli M., Cavalca L., Braibanti A., Complessi bicoordinati di met. bivalenti con la tiourea. Gazz. chim. ital. 86, 1037 (Ital.).
189. Natta G., Corradini P., Über d. Kr.-str. d. 1,4-cis-Polybutadiens u. d. 1,4-cis-Polyisoprens. Angew. Chem. 68, 615.

190. Natta G., Corradini P., Asta G. Dall', Struttura della catena del polipropilenossido cristallino. Atti accad. nazion. Lince., Rend., Classe sci. fis. mat. e nat. 20, 408 (Ital.).
191. Neumann G., Lundgren G., Aurivillius B., On cr. strs. of Zr- a. Hf-"cupferrates." Acta Chem. Scand. 10, 1670.
192. Nicolaides N., Laves F., Niggli A., Convenient method of locating substituents on hydrocarbon chain of mols. adducting with urea. J. Am. Chem. Soc. 78, 6415.
193. Novoselova A. V., Semenenko K. N., Be oxymonochloroacetate. Zh. neorg. khim. 1, 887.
194. Novoselova A. V., Semenenko K. N., Krasovskaya N. N., Simanov Yu. P., Be oxyacetate. Commun. 2. Some props. of compds. of Be oxyacetate with pyridine. Vestn. Mosk. univ. 3, 87.
195. Novoselova A. V., Simanov Yu. P., Semenenko K. N., Krasovskaya N. N., Compds. of Be oxyacetate with pyridine and dioxane. Zh. neorg. khim. 1, 696.
196. Nowacki W., Bürki H., Bonsma G. F., Jaggi H., Direkte röntgenograph. Konstitutionbest. v. 7α-Bromcholesterylbromid, -chlorid u.-methyläther, v. Erythralin u. Kr.-str.-best. d. Phthalsäure. Chimia (Switz.). 10, 254.
197. Oda T., Koide T., On cr. str. of 2,3-dichloro-2,3-dimethylbutane. Bull. Chem. Soc. Japan 29, 208.
198. Okaya Y., Shimada A., Nitta I., Disord. str. in cr. cyclohexanoxime. Bull. Chem. Soc. Japan 29, 210.
199. Ollom J. F., Sinisgalli A. A., Rexroad H. N., Gunton R. C., Microwave spectrum a. mol. str. of $(CH_3)_2SiBr_2$. J. Chem. Phys. 24, 487.
200. Oyum P., Foss O., Cr. str. of Te dibenzenethiosulphonate. Acta Chem. Scand. 10, 279.
201. Paretzkin B., Cr. data on cinchonine, $C_{19}H_{22}N_2O$. Acta Cryst. 9, 201.
202. Pasternak R. A., Cr. str. of glycl-L-tryptophan dihydrate. Acta Cryst. 9, 341.
203. Peerdeman A. F., Absolute configuration of natural strychnine. Acta Cryst. 9, 824.
204. Penfold B. R., Simpson W. S., Cr. str. of chloroacetamide. Acta Cryst. 9, 831.
205. Pepinsky R., Okaya Y., Detn. of cr. strs. by means of anomalously scattered X-rays. Proc. Nat. Acad. Sci. U. S. A. 42, 286.
206. Perutz M. F., Isomorphous replacement a. phase detn. in noncentrosymmetric sp. grs. Acta Cryst. 9, 867.
207. Petersen D. R., X-ray investn. of str. of Feist's acid. Chem. and Ind. (London), 904.
208. Petitpas T., Mering J., Str. mol. de la cellulose. II. Compt. rend. 243, 47.
209. Pfeiffer R. R., X-ray diffrn. powd. data for some 1,3,4-oxadiazoles. Anal. Chem. 28, 206.
210. Phillips D. C., Crystallogr. of acridine. II. Str. of acridine III. Acta Cryst. 9, 237.
211. Pinnock P. R., Taylor C. A., Lipson H., Redetn. of str. of triphenylene. Acta Cryst. 9, 173.
212. Point J.-J., Homes G. A., Fibre N du polyéthylène. Compt. rend. 242, 2557.
213. Pollock J. McC, Ubbelohde A. R., Woodward I., H bonds in crs X. Isotope effect a. therm. expan. of non-cooperative H bonds in furoic acid. Proc. Roy. Soc., Ser. A 235, 149.
214. Prins J. A., Prins W., Polymorphism of alkyl sulphate soaps. Nature 177, 535.
215. Prosen R. J., Trueblood K. N., Cr. str. of Ag perchlorate-dioxane complex, $AgClO_4 \cdot 3C_4H_8O_2$. Acta Cryst. 9, 741.
216. Przbylska M., Marion L., Cr. str. of des-(oxymethylene)-lycoctonine hydroiodide monohydrate. Canad. J. Chem. 34, 185.
217. Ramachandran G. N., Str. of collagen. Nature 177, 710.
218. Ray L., U. c. dims. a. sp. gr. of rauwolscane. Acta Cryst. 9, 199.
219. Ray L., Str. of rauwolscane by X-ray a. opt. method. Indian J. Pharm. 18, 199.
220. Reed R., Wood M. J., Keech M. K., Helical nature of collagen fibril. Nature 177, 697.
221. Rexroad H. N., Howgate D. W., Gunton R. C., Ollom J. F., Microwave spectrum a. mol. str. of $(CH_3)_2SiI_2$. J. Chem. Phys. 24, 625.
222. Richards J. P. G., Cr. str. of anisic acid (p-methoxybenzoic acid). Research (London) 9, S44.
223. Robertson J. M., Shearer M. M., Str. of azulene. Nature 177, 885.
224. Robertson J. M., White J. G., Cr. str. of monocl. modifn. of 1 : 2-5 : 6-dibenzenthracene. Quant. X-ray investn. J. Chem. Soc., 925.
225. Rogers D., Thomas D. V., Etude crist. du la friedeline. Bull. Soc. chim. France 2, 361.
226. Romain P., Str. de la Br-4-antipyrine et de la I-4-antipyrine — projection sur le plan normal à l'axe ternaire. Bull. Soc. pharm. Bordeaux 95, 75.
227. Romain P., Contribution à l'étude crist. de la 1-phényl-3-methyl-5-pyrazolone (antipyrine déméthylée), l'iode-4-antipyrine la bromo-4-antipyrine. Bull. soc. franç. minéral. et. crist. 79, 345.
228. Romers C., E.-diffn., Investn. into vapours of cyclohexanone a. 2-methylcyclohexanone. Second communication on mol. strs. of ketones. Rec. trav. chim. Pays-Bas 75, 956.
229. Romers C., Creutzberg J. E. G., E.-diffrn. investn. of mol. str. of acetone, 2-butanone a. 3-pentanone. Rec. Trav. chim. Pays-Bas 75, 331.

230. Roof R. B., Jr., Cr. str. of ferric acetylacetonate. Acta Cryst. 9, 781.
231. Rose H. A., Cry..allogr. data. 103, Isovanillin (3-hydroxy-4-methoxybenzaldehyde). Anal. Chem. 28, 267.
232. Rose H. A., Camp A. van. Aricine. Anal. Chem. 28, 1054.
233. Rose H. A., Camp A. van. 2-amino-2-methyl-1,3-propanediol. Anal. Chem. 28, 1700.
234. Rose H. A., Camp A. van. Crystallogr. prop. of 9-aminoacridine hemihydrate. Acta Cryst. 9, 824.
235. Rose H. A., Camp A. van. Note on crystallogr. of l-isomethadone hydrochloride hydrate. J. Am. Pharm. Assoc., Sci. Ed. 45, 653.
236. Rowe I., Post B., Str. of thianthrene. Acta Cryst. 9, 827.
237. Ryhage R., Stenhagen E., Sydow E. von., Information about str. of phthiocerol from mass spectral a. X-ray crystallogr. data. Acta Chem. Scand. 10, 158.
238. Sakurada I., Sur. fines des hauts polymères aux r. X. J. Chem. Soc. Japan, Ind. Chem. Sect 59, 741 (Jap).
239. Sasada Y., Nitta I., Cr. a. mol. st Na-tropolonate. Acta Cryst. 9, 205.
240. Sasisekharan V., Application of Differ ce-Patterson method. Proc. Indian Acad. Sci. A43, 224.
241. Scatturin V., Zanneti , Struttura cristallina del 2. metil-4 Clorometil-5 paranitrofenil ossazolo. I. Gruppo spaziale e constanti reticolari. Ric. sci. 26, 623 (Ital.)
242. Schaffer W., Crystallogr. study of arsonium bromide, $(C_{21}H_{19}As_2)Br$. Acta Cryst. 9, 401.
243. Schwab G. M., Grabmaier J., Simmler W., Über d. str. d. sym. Tetra-(t)-butyl-hexoxasilamantans $[(CH_3)_3CSi]_4O_8$. Z. phys. Chem. 6, 376.
244. Shearer H. M. M., Vand V., Cr. str. of monocl. form of n-hexatriacontane. Acta Cryst. 9, 379.
245. Shugam E. A., Nature of the Cu – O chem. bond in the mol. of Cu acetylacetonate. Tr. Vses. n.-i. inst. khim. reaktivov 21, 108.
246. Shugam E. A., Shkol'nikova L. M., Invest. of cr. str. of Al and Cr acetylacetonates. Kristallografiya 1, 478.
247. Slichter W. P., On morphology of highly cr. polyethylenes. J. Polym. Sci. 21, 141.
248. Sörum H., Barstad J., Dale J. Cr. modifns. of bigeranyl tetrahydrochloride. Acta Chem. Scand. 10, 1663.
249. Sprenkels A. J. J., Cr. str. of Li-ammonium-tartrate-monohydrate. Koniki. Ned. Akad. Wetenschap., Proc., Ser. B 59, 221.
250. Srinivasan R., U. c. a. sp. gr. of some amino acids. Acta Cryst. 9, 1039.
251. Stackelberg M. von, D. str. d. Einschlussverbb. d. Wassers (Gashydrate) u.d. Phenols Rec. trav. chim. Pays-Bas 75, 902.
252. Staritzky E., Cromer D. T., Uranyl oxalate trihydrate, $UO_2C_2O_4 \cdot 3H_2O$. Anal. Chem. 28, 1353.
253. Steinrauf L. K., Jensen L. H., U.c. pars. a. sp. grs. for L-cystine, L-cystine hydrochloride a. L-cystine hydrobromide. Acta Cryst. 9, 539.
254. Sternberg M., Etude crist. de l'anhydride "norfriedelènédioique" (2,4-dioxo-3-oxa-23-norfriedela-1(10)-ène). Bull. soc. chim. France 2, 362.
255. Struchkov Yu. T., Cr. str. of dibenzoylferrocene. Dokl. AN SSSR 110, 67.
256. Saito E., Uyeda N., Study of dimorphism a. cr. habit of Cu-phthalocyanine by e. microdiffrn. method. Proc. Japan Acad. 32, 182.
257. Sutor D. June, Isomorphous-replacement method applied to mols. containing like atoms. Acta Cryst. 9, 969.
258. Swaminathan S., Sivarajan S. R., Sundara Rao R. V. G., U. c. dims. a. sp. gr. of Cu ethyl sulphate. Curr Sci. 25, 81.
259. Sydow E. von., Normal fatty acids in solid state. Cr. str. investn. Arkiv. Kemi 9, 231.
260. Sydow E. von., On str. of cr. form A of lauric acid. Acta Chem. Scand. 10, 1.
261. Takeuchi Y., Pepinsky R., On sp. gr. a. mol. orientation of azulene. Science 124, 3212, 126.
262. T'ang Yu-ch'i, Hao Jun-yung, Chou Kung-tu., Cr. str. of addn. product of Na bisulfite and acrolein. Huchsüeh hsüehpao 22, 391 (Chinese; Eng. Summary).
263. Tomlin S. G., Worthington C. R., Low angle X-ray diffrn. pats. of collagen. Proc. Roy. Soc., Ser. A 235, 189.
264. Toussaint J., Etude radiocrist. de l'hétérocycle γ-pyrone. I. Str. mol. et cr. de la diméthyl-2-6-γ-thiopyrone. Bull. soc. chim. Belges 65, 213.
265. Tranter T. C., Cr. str. of glycyl-L-alanine hydrochloride. Nature 177, 37.
266. Traub, W., Cr. str. of biotin. Nature 178, 649.
267. Trillat J. J., Barbezat Mme. S., Jacquot Mme. A., Etude aux r. X des transformns du stéarate et du laurate de Pb en fonction de la temp. Compt. rend. 243, 71.
268. Truter M. R., Cox E. G., Stereochem. of sesquiethylenediaminetrimethylplatinic iodide, J. Chem. Soc., 3476.
269. Tsoucaris G., La str. de la β-phényl-éthylamine. Bull. soc. franc. mineral. et crist. 79, LVII.
270. Turley J. W., Pepinsky R., Cr. str. of cycloserine hydrochloride. Acta Cryst. 9, 948.

271. Turner T. E., Ilonic J. A., Detn. of mol. strs. from rotational spectra measrts. J. Chem. Phys. 25, 826.
272. Ubbelohde A. R., Parry G. S., Therm. expan. of p-nitroaniline. Acta Cryst. 9, 6.
273. Viswamitra M. A., Sundara Rao R. V. G., U. c. a. sp. gr. of cupric ammonium s. potassium oxalates. Curr. Sci. 25, 115.
274. Volarovich M. P., Gusev K. F., X-ray str. investn. of peat bitumens and waxes. Kolloidnyi Zh. 18, 643.
275. Wallwork S. C., Powell H. M., Str. of mol. compds. Part XI, Cr. str. of addition complex of quinol a. methyl cyanide. J. Chem. Soc. 12, 4855.
276. Webster M. S., X-ray examn. of cr. str. of p-iodonitrosobenzene. J. Chem. Soc., 2841.
277. Weiss E., Fischer E. O., Über Atomstenkomplexe v. Metallen. II. Zur Kr. str. u. Molekelgestalt d. Di-benzol-chrom (0). Z. anorg. Chem. 286, 142.
278. Weiss E., Fischer E. O., Zur Kr.-str. v. Di-cyclopentadienyl-chrom (II). Z. anorg. Chem. 284, 69.
279. Welsh H. K., Cr. str. of 14-heptacosanol. Acta Cryst. 9, 89.
280. White, N. E., Clews C. J. B., Cr. a. mol. str. of 4,5 diamino-2-chloropyrimidine. Acta Cryst. 9, 586.
281. Wilson F. C., Shoemaker D. P., X-ray crystallogr. data for met. cyclopentadienyl carbonyl compds. Naturwiss. 43, 57.
282. Wolfe P. N., Microwave spectrum of chloroform. J. Chem. Phys. 25, 976.
283. Wood E. A., Guanidinium Al sulfate hexahydrate: crystallogr. data. Acta Cryst. 9, 618.
284. Woolfson M. M., Cr. str. of 5'-Br-3' : 5'-dideoxythymidine. Acta Cryst. 9, 974.
285. Wright W. B., Stereochem. of glutatione in cr. state. Chem. and Ind. (London) 20, 437.
286. Zeil W. D., Mikrowellenspektrum d. Trichloracetonitrils u. d. 1,1,1-Trichloräthans im Bereich v. 23500 bis 25500 MHz. Z. Electrochem. 60, 752.
287. Zaides A. L., Stoyanova I. G., Some details of e. diffm. investn. of high polymers. Dokl. AN SSSR 107, 711.
288. Zvonkova Z. V. Cr.-chem. investn. of the nature of the donor – acceptor bond in complex compds. of B. Kristallografiya 1, 73.
289. Zhdanov G. S., Umanskii M. M., Varfolomeeva L. A., Ezhkova Z. I., Zolina Z. K., X-ray diffm. detn. of u. cell and space gr. of piezoelectr. crs.: $KLiC_4H_4O_8 \cdot H_2O$, $NH_4LiC_4H_4O_8 \cdot H_2O$, $NaHC_4H_4O_8 \cdot H_2O$ and $(NH_4)_2C_4H_4O_8 \cdot H_2O$. Kristallografiya 1, 271.
290. Zhdanov G. S., Zvonkova Z. V., Rannev N. V., X-ray str. investn. of Pb diethyldithiocarbamate. Kristallografiya 1, 514.
291. Zhdanov G. S., Zvonkova Z. V., Vorontsova L. G., X-ray diffm. investn. of methylene blue dye. Kristallografiya 1, 61.

All abbreviations of periodicals in the above bibliography are letter-by-letter transliterations of the abbreviations as given in the original Russian journal. *Some or all of this periodical literature may well be available in English translation.* A complete list of the cover-to-cover English translations appears at the back of this issue.